SYNTHESIS AND CHARACTERIZATION OF SULFONATED POLYIMIDES AS PROTON EXCHANGE MEMBRANES FOR FUEL CELLS

by

Nazan Gunduz

Dissertation Submitted to the Faculty of the
Virginia Polytechnic Institute and State University
in partial fulfillment of the requirements for the degree of
DOCTOR OF PHILOSOPHY
in
Chemistry

APPROVED:

Dr. James E. McGrath
Dr. Allan R. Shultz
Dr. Judy S. Riffle
Dr. James P. Wightman
Dr. Timothy E. Long
Dr. James E. Wolfe

February 28, 2001
Blacksburg, VA

Keywords: Sulfonated polyimides, naphthalic polyimides, sulfonated diamines, fuel cells, ion-exchange capacity, conductivity

SYNTHESIS AND CHARACTERIZATION OF SULFONATED POLYIMIDES AS PROTON EXCHANGE MEMBRANES FOR FUEL CELLS

by

Nazan Gunduz

Committee Chairman: Dr. James E. McGrath

Department of Chemistry

(ABSTRACT)

Series of homo- and copolyimides containing controlled degrees of sulfonic acid ion conducting pendant groups have been synthesized from both phthalic (five-) and naphthalic (six-membered) dianhydrides and appropriate wholly aromatic diamines and heterocyclic analogues. The goal is to identify thermally and hydrolytically stable ion conducting polymers (ICP) suitable as proton exchange membranes, PEM, for fuel cells. The candidate ICP's have been synthesized and characterized for molecular weight, chemical composition, film forming properties, thermal transition behavior, boiling water stability, solvent solubility and water absorption and conductivity

Commercially available five-membered ring dianhydrides such as 6FDA, BPDA, and six-membered ring dianhydrides such as naphthalene tetracarboxylic dianhydride (NDA) have been used. High molecular weight five-membered ring polyimides were obtained from an equimolar ratio of diamines and dianhydride using a one-pot ester-acid procedure by initially converting the dianhydride to a diester-diacid derivative, followed by the reaction with sulfonated and unsulfonated aryl diamines. The sulfonated diamine monomer was allowed to oligomerize with the diester-diacid of the dianhydride for 2-3 hours, before unsulfonated diamine was charged into the reaction flask. The levels of sulfonation in the polymer backbones were controlled by varying the mole ratio of sulfonated diamine to unsulfonated diamine.

For the six-membered ring polyimides, phenolic solvents, e.g. m-cresol, have been used. In general, 4,4´-diamino-biphenyl-2,2´-disulfonic acid (DPS) has been

employed as the source of the sulfonated unit. The chemical compositions of both sulfonated and unsulfonated polyimides were obtained using ^{1}H-NMR and FT-IR. The sulfonic acid contents in both diamine monomers, as well as the sulfonated polyimides were also analyzed by acid-base potentiometric titration.

In all cases, high inherent viscosity values and good film forming ability of the polymers were the key indications of high molecular weight. The viscosity values increased with an increase of sulfonation degree in the polymers. This increase of viscosity in these ionomers can be attributed to the increase of polymer chain aggregation with their increasing ionic character.

Polymers were fabricated into membranes via solution casting or spin casting from DMAc or m-cresol in order to study film-forming properties. The solution cast dry films of the sulfonated polyimide membranes gave tough, ductile membranes and demonstrated moderate to high water absorption, which is necessary for PEM fuel cells. However, swollen films, in general, showed poor hydrolytic stability which resulted in brittle membranes.

The solution-cast membranes were thermally analyzed to study the effect of the degree of sulfonation on the thermal properties of sulfonated polymers. All the thermograms of the sulfonated polyimide films exhibited a two-step degradation behavior. The first weight loss, observed between 300-400 ^{o}C, corresponds to desulfonation in the sulfonated block, and the second weight loss, observed for a temperature around 500 ^{o}C or above, corresponds to the polymer backbone degradation. The TGA thermograms indicated that the initial weight losses were steeper for polymers with higher sulfonation degrees. Furthermore, the weight loss temperature of sulfonated polyimides decreased and broadened with increasing sulfonation levels. However, the onset temperature of the first weight loss was independent of the degree of sulfonation. Weight loss data in TGA curves of the sulfonated polymers were used to calculate the degree of sulfonation. Experimental and theoretical values were in good agreement with each other.

The sulfonated five-membered polyimide membranes were aged in an air-oven at increasing temperatures (30-220 ^{o}C) for 30 min and then titrated with TMAH using non-

aqueous potentiometric titration. All the films that were aged up to 220 ^{o}C were still completely soluble in DMAc. Moreover, the sulfonic acid groups were unchanged.

In addition, several new flexible sulfonated and unsulfonated diamines and bis(naphthalic anhydride) monomers containing phosphineoxide [P(O)] or sulfone [$S(O)_2$] moieties in their structure have been synthesized and characterized with various analytical techniques. The structural design of naphthalic polyimides by incorporating bis(naphthalic anhydrides) was one approach to give a better solubility and processability of their related products.

Development of an iterative approach for defining the optimum degree of sulfonation that will produce the highest ionic conductivity while still retaining other important properties such as flexibility, strength, hydrolytic stability has been a goal of this research and will be discussed in the thesis.

Dedicated to my loving husband, Irfan and dear daughter Erin

ACKNOWLEDGMENTS

I would like to thank Dr. James E. McGrath as my research advisor for his efforts and direction throughout my education at Virginia Tech. Through his wealth of knowledge, direction and leadership I have been able to expand my knowledge in many areas of polymer science.

I would also like sincerely to thank the members of my committee, Dr. Allan R. Shultz, Dr. Judy S. Riffle, Dr. James E. Wightman, Dr. Timothy E. Long and Dr. James P. Wolfe.

I was quite fortunate in having the opportunity to interact with all those students and postdoctoral associates of our great research group. I truly enjoyed the valuable discussions with Drs. Charles Tchatchoua, H.K. Shobha, M. Sankarapandian, Debi Dunson, Feng Wang, Yuseung Kim and Vinayak Bhanu, and fellow graduate students Jeff Mecham, William Harrison, Dave Polk, Mike Hickner, Kent Wiles, and Brian Einsla.

I particularly appreciate Mike Hickner for conductivity measurements, Dr. H.K. Shobha for GPC, Yuseung Kim for some thermal characterization tests, and technician Kerry O'Connor for intrinsic viscosity measurements. I would also like to acknowledge others in the chemistry department. Specifically, Mr. Tom Glass, NMR Spectroscopist for his assistance in using the NMR facilities, and Anna for her mass spectroscopy efforts.

I owe a particular word of thanks to our secretarial staff, Laurie Good, Esther Brann and Millie Ryan for their assistance and levity during my stay at VPI.

Nothing can be accomplished without family support. I would like to extend my special gratitude to my parents, Mr. and Mrs. Kenan and Huriye Kaptan for their never-ending love, support and encouragement from thousands of miles away.

Much thanks is due to my husband Irfan and my dear daughter Erin Ilge for accepting and understanding my long hours in the laboratories and lately in front of the computer while I am writing this dissertation. Much appreciation is also due to my husband for his help in assembling this thesis. Their support, encouragement and patience enables me to pursue my career, while at the same time enjoying a lifetime of happiness with them.

TABLE OF CONTENT

CHAPTER 1. INTRODUCTION.....1

CHAPTER 2. LITERATURE REVIEW.....4

2.1 INTRODUCTION 4

2.2 SYNTHESIS OF POLYIMIDES 5

2.2.1 Classical Two-Step Route 6

2.2.2 Additional Methods for Synthesizing Polyimides..... 44

2.3 POLYIMIDE PROPERTIES and APPLICATIONS 55

2.3.1 Characterization of Polyimides 56

2.3.2 Polyimide Applications 60

2.4 FUEL CELLS 75

2.4.1 Introduction and Historical Development..... 75

2.4.2 Technical Capabilities of Fuel Cells 75

2.4.3 Environmental Considerations..... 76

2.4.4 Types of Fuel Cells 77

2.4.5 Perfluorinated Membranes as Polymer Electrolyte Membrane Fuel Cells (PEMFC)..... 101

2.4.6 Review of Other Candidate Polymers for PEMFC..... 110

2.4.7 Use of polyphosphoric acids..... 113

CHAPTER 3. EXPERIMENTAL.....114

3.1 Purification of Solvents 114

3.2 Reagents and Commercially Available Dianhydrides and Diamines 118

3.2.1 General Reagents 118

3.2.2 Monomers 119

3.2.3 Monomer Synthesis 127

3.3 Polyimide Synthesis 146

3.3.1 Polyimide Synthesis by the Ester-Acid Route..... 147

3.3.2 Polyimide Synthesis via One-step High Temperature Direct Imidization Method 149

3.4 Characterization Methods..... 152

3.4.1 Nuclear Magnetic Resonance (NMR) Spectroscopy 152

3.4.2 High Performance Liquid Chromatography (HPLC)..... 152

3.4.3 Fourier Transform Infrared (FTIR) Spectroscopy..... 152

3.4.4 Gel Permeation Chromatography (GPC) or Size Exclusion Chromatography (SEC)..... 152

3.4.5 Intrinsic Viscosity (IV)..... 153

3.4.6 Thermogravimetric Analysis (TGA) 153

3.4.7 Differential Scanning Calorimetry (DSC) 153

3.4.8 Mass Spectroscopy (MS)..... 154

3.4.9 Thin Layer Spectroscopy (TLC)..... 154

3.4.10 Melting Point (m. p.) Measurements of Monomers by Capillary Method..... 154

3.4.11 Solubility Tests..... 154

3.4.12 Non-Aqueous Potentiometric Titration of Sulfonic Acids 155

3.4.13 Solvent-Cast Free Standing Films 155

3.4.14 Spin-Cast Films 156
3.4.15 Water Sorption 156
3.4.16 Conductivity Measurements 157

CHAPTER 4. RESULTS AND DISCUSSIONS.....158

4.1 Monomer Synthesis and Characterization.....159

4.1.1 Synthesis of Bis(3-aminophenyl)phenyl Phosphine Oxide (BAPPO)..... 159
4.1.2 Synthesis of Sulfonated Bis(4-fluorophenyl) Phenyl Phosphine Oxide 167
4.1.3 Sulfonated Bis(3-aminophenoxy)phenyl sulfone (s-BAPPO).. 170
4.1.4 Synthesis of Disulfonated 4,4'-dichlorodiphenyl sulfone (s-DCDPS)..... 175
4.1.5 Disulfonated 4,4'-bis(3-aminophenoxy)phenyl sulfone (s-DADPS)..... 178
4.1.6 Bis (4-hydroxyphenyl) phenyl phosphine oxide (BOHPPO) ... 181
4.1.7 4,4'-Bis(oxynaphthalic anhydride) phenyl phenyl phosphine oxide (NDA-PO)..... 183
4.1.8 4,4'-Bis(oxynaphthalic anhydride) phenyl sulfone (NDA-SO_2)186

4.2 Polyimide Synthesis.....189

4.2.1 Synthesis and Characterization of Sulfonated Phthalic Anhydride (Five-Membered Ring Polyimides)..... 189
4.2.2 Synthesis and Characterization of Sulfonated Six-Membered Ring Polyimides..... 253

CHAPTER 5. CONCLUSIONS.....308

VITA ……..…..312

LIST OF TABLES

Table 2.1 Electron Affinity and Log Rate Constant Values for Aromatic Dianhydrides Towards 4,4'-oxydianiline (4,4'-ODA)[0] 15

Table 2.2 Reactivity (Log Rate Constant) and Basicity pKa Values of Aromatic Diamines Towards 1,2,4,5-Benzenetetracarboxylic Dianhydride (PMDA). 16

Table 2.3 Infrared Absorption Bands of Imides and Related Compounds 27

Table 2.4 ^{1}H NMR Chemical Shifts (ppm), Ea (eV) and Relative Abundance of meta- and para-positions 42

Table 2.5 Curable Polyimides for Aerospace Applications 68

Table 2.6 Relative Advantages and Disadvantages of Different Types of Fuel Cells 102

Table 4.1.1 Advancement of starting materials and their reaction products in thin layer chromatography purification solvents; ethyl acetate (EtAC), methanol (MeOH) and their mixtures. 172

Table 4.2.1 Elemental Analysis Results of Sulfonated Polyimide Polyimides 196

Table 4.2.2 Chemical Structure and Molecular Weight Characterization of the Sulfonated 6FDA/m-PDA -based Polymers in NMP 201

Table 4.2.3 Chemical Structure and Molecular Weight Characterization of the Sulfonated 6FDA/DDS-based Polymers in NMP 202

Table 4.2.4 Theoretical and Experimental IEC Values of Selected Sulfonated 6FDA/m-PDA Based Polyimide Membranes. 210

Table 4.2.5 Theoretical and Experimental IEC Values of Selected Sulfonated 210
6FDA/DDS Based Polyimide Membranes. 210

Table 4.2.6 Film thicknesses and water uptakes [SW (%)] of the sulfonated 214
6FDA/m-PDA/p-PDA-SO_3H 214

Table 4.2.7 Film thickness and water uptakes [SW (%)] of the sulfonated 215
6FDA/m-PDA/p-PDA-SO_3H 215

Table 4.2.8 Molecular Weight Characterization of the Sulfonated BPDA/FDA- Based Polymers 222

Table 4.2.9 Molecular Weight Characterization of the Sulfonated BPDA/APB-Based Polymers 223

Table 4.2.10 Ion Exchange Capacity of Sulfonated BPDA/FDA-Based Polyimides228
Table 4.2.11 Ion Exchange Capacity of Sulfonated BPDA/APB-Based Polyimides 228
Table 4.2.12 Effect of Thermal Aging on Experimental IEC Values for 40 % and 60 % Sulfonated BPDA/FDA/BDA Polyimide Membranes 230
Table 4.2.13 Effect of Thermal Aging on Intrinsic Viscosity for 40 % and 60 % Sulfonated BPDA/FDA/BDA Polyimide Membranes (Intrinsic viscosity at RT in NMP solvent using a Ubbelohde viscometer) 230
Table 4.2.14 Water Uptakes [SW (%)] of the Sulfonated BPDA/FDA/BDA Polyimides..... 232
Table 4.2.15 Water Uptakes [SW (%)] of the Sulfonated BPDA/FDA/BDA Polyimides..... 232
Table 4.2.1.3.1 Intrinsic Viscosity and Thermal Analysis of BPSDA/FDA/BDA-Based Sulfonated Polyimides 242
Table 4.2.1.3.2 Intrinsic Viscosity and Thermal Analysis of BPSDA/APB/BDA-Based Sulfonated Polyimides 243
Table 4.2.1.3.3 Theoretical and Experimental IEC Values for Sulfonated Polyimides of BPSDA/FDA/BDA 245
Table 4.2.1.3.4 Theoretical and Experimental IEC Values for Sulfonated Polyimides of BPSDA/APB/BDA 245
Table 4.2.1.3.5 Theoretical and Experimental IEC Values of Aged Films of Sulfonated Polyimides of BPSDA/FDA/BDA..... 247
Table 4.2.1.3.6 Theoretical and Experimental IEC Values of Aged Films of Sulfonated Polyimides of BPSDA/APB/BDA..... 247
Table 4.2.1.3.7 Water Uptake and Ion Exchange Capacity Values of Sulfonated BPSDA/FDA/BDA Polyimide Membranes..... 250
Table 4.2.1.3.8 Water Uptake and Ion Exchange Capacity Values of Sulfonated BPSDA/APB/BDA Polyimide Membranes 251
Table 4.2.2.1 The repeat unit and inherent viscosities of sulfonated NDA/FDA based polyimides 263
Table 4.2.2.2 The repeat unit and inherent viscosities of sulfonated NDA/APB based

polyimides 264
Table 4.2.2.3 Thermal Characterization of Sulfonated NDA/FDA/BDA Polyimides by dynamic TGA in air 271
Table 4.2.2.4 Thermal Characterization of Sulfonated NDA/APB/BDA Polyimides by dynamic TGA in air 272
Table 4.2.2.5 Water Uptake and Ion Exchange Capacity Values of Sulfonated NDA/FDA/BDA Polyimide Membranes 275
Table 4.2.2.6 Water Uptake and Ion Exchange Capacity Values of Sulfonated NDA/APB/BDA Polyimide Membranes 276
Table 4.2.3.1 Inherent Viscosity and Thermal Analysis of BPDA/s-DADPS/APB-Based Sulfonated Polyimides 297
Table 4.2.3.2 Inherent Viscosity and Thermal Analysis of BPDA/s-DADPS/APB-Based Sulfonated Polyimides 297
Table 4.2.3.3 Calculated and observed (TGA; 10 ^{o}C/min in air) weight losses for BPDA/s-DADPS/APB Polyimides in the $-SO_3H$ decomposition region. . 298
Table 4.2.3.4 Calculated and observed (TGA; 10 ^{o}C/min in air) weight losses for BPDA/s-DADPPO/APB Polyimides in the $-SO_3H$ decomposition region. 299
Table 4.2.3.5 Water Uptake and Ion Exchange Capacity Values of Sulfonated BPDA/s-DADPS/APB Polyimide Membranes 305
Table 4.2.3.6 Water Uptake and Ion Exchange Capacity Values of Sulfonated BPDA/s-DADPPO/APB Polyimide Membranes 306

LIST OF FIGURES

I**Figure 2.1** General structure of a polyimide 4

Figure 2.2 Kapton® Polyimide produced by DuPont 6

Figure 2.3 Commonly used dianhydrides and diamines 14

Figure 2.4 A Model for 4:1 ratio of NMP complexation with a di(amic) acid repeat unit 19

Figure 2.5 The repeat unit structure of Kapton-H™ Polyimide formed from PMDA and ODA 22

Figure 2.6 Conformations of poly(amic) acid during cyclodehydration..... 23

Figure 2.7 Three Common Routes to Facilitate to Conversion of Polyamide Acids to Polyimides..... 24

Figure 2.9 ^{1}H-NMR Spectrum of 4,4'-ODA/ODPA poly(amic) acid/imide at different imidization stages (180 ^{o}C) 37

Figure 2.10 Dianhydrides for Methanolysis Reaction..... 41

Figure 2.11 Intramolecular poly(amic) acid salt from aliphatic amino group 44

Figure 2.12 Delocalization of Negative Charge in Meisenheimer Transition State in an Imide System..... 47

Figure 2.13 Proposed 7-membered cyclic intermediate in the reaction of isocyanate with anhydride..... 51

Figure 2.14 Common Dianhydrides and Diamines to increase the solubility of polyimides 60

Figure 2.15 The coefficient of thermal expansion of various metals, ceramics and organic polymers..... 62

Figure 2.16 Typical Negative Imaging Photosensitive Polyimide 64

Figure 2.17 Flip-chip Configuration with Waveguide 66

Figure 2.18 Effect of Adhesion Viscosity on Interfacial Contact 70

Figure 2.19 Spontaneously Adsorbed Layers of on a Metal Surface..... 71

Figure 2.20 Adhesion Properties of Polyimide-Isoindoloquinazolinedione (PIQ) to SiO_2 with and without Adhesion promoter (aminosilane)..... 74

Figure 2.21 Operation of an Alkaline Fuel Cell 79
Figure 2.22 Principles of Operation of a Phosphoric Acid Fuel Cell 82
Figure 2.23 Schematic of a Molten Carbonate Fuel Cell 84
Figure 2.25 A single fuel cell assembly 89
Figure 2.26 Terminal voltage vs. current density of Ballard Technologies Corporation's SPEFC 90
Figure 2.27 Comparison of DuPont's Nafion® and Dow perfluorosulfonate ionomer membranes 92
Figure 2.28 Schematic of a direct methanol fuel cell 94
Figure 2.29 H_2/air PEFC polarization curves showing the effects of CO contamination for a 0.14 mg of Pt/cm^2 thin film anode at 80 ^oC. 99
Figure 2.30 H_2/air PEFC polarization curves showing the effects of CO_2 contamination for a 0.12 mg of Pt/cm^2 thin film anode at 80 ^oC. 100
Figure 2.31 Cluster network model for Nafion® perfluorosulfonic membrane. 105
Figure 2.32 The variation of the cluster diameter (O) and the number of ion exchange sites (Ä) per cluster with water content in Nafion® 1200 EW polymer. 106
Figure 2.33 Redistribution of ion exchange sites occurring during dehydration of the polymer 107
Figure 3.1 Distillation apparatus 117
Figure 3.3 Conductivity Cell 157
Figure 4.1.1 ^{31}P NMR spectrum of BNPPO 163
Figure 4.1.2 ^{1}H NMR spectrum of BNPPO 164
Figure 4.1.3 ^{1}P NMR spectrum of BAPPO 165
Figure 4.1.5 Mass spectrum of DAPPO 166
Figure 4.1.6 ^{1}H NMR spectrum of s-BFPPO *(solvent: DMSO-d_6)* 168
Figure 4.1.7 ^{31}P NMR spectrum of s-BFPPO *(solvent: DMSO-d_6)* 168
Figure 4.1.8 Elemental analysis data and Mass spectrum of s-BFPPO 169
Figure 4.1.9 TLC of the purified diamine, DA (sBAPPO) and the starting materials, ... 171
Figure 4.1.10 ^{1}H NMR of s-BAPPO in *d*-DMSO 173
Figure 4.1.11 Elemental analysis and FAB$^+$ Mass Spectroscopy of s-BAPPO 174

Figure 4.1.12 ^{1}H and ^{13}C NMR spectra of s-DCDPS (solvent: DMSO-d6) 176
Figure 4.1.13 Elemental Analysis of s-DCDPS 177
Figure 4.1.14 Mass Spectrum of s-DCDPS 177
Figure 4.1.15 ^{1}H NMR of s-DADPS in DMSO-d6 179
Figure 4.1.16 Elemental Analysis Data and Mass Spectroscopy of s-DADPS 180
Figure 4.1.17 ^{1}H NMR of BOHPPO 182
Figure 4.1.18 ^{13}C NMR of BOHPPO 182
Figure 4.1.19 ^{1}H NMR Spectrum of NDA-PO 184
Figure 4.1.20 ^{31}P NMR Spectrum of NDA-PO 185
Figure 4.1.21 ^{1}H NMR Spectrum of NDA-SO_2 187
Figures 4.1.22 DSC thermogram of NDA-SO_2 (in nitrogen) 188
Figure 4.2.1 Monomers used for synthesis of sulfonated five-membered ring polyimides 192
Figure 4.2.2 FTIR of High Molecular Weight 50 % Sulfonated 6FDA/m-PDA/p-PDA-SO_3H Showing Absorptions Due to Cyclic Imide Functionalities. 199
Figure 4.2.3 Typical Raw GPC Chromatogram Obtained for a High Molecular Weight 50 % Sulfonated 6FDA/m-PDA/p-PDA-SO_3H Copolyimide. 200
Figure 4.2.4 Thermogravimetric analysis of sulfonated 6FDA-based polyimides in air. 204
Figure 4.2.5 DSC of (1) 6FDA/m-PDA homopolymer and (2) 10 % sulfonated 6FDA/m-PDA/m-PDA-SO_3H copolymer (in nitrogen, heating rate =10 ^{o}C/min) 206
Figure 4.2.6 FT-IR Spectra of Non-Substituted Polyimide Control(top spectrum) and 25% Sulfonated 6FDA/DDS/m-PDA-SO_3H polyimide (bottom spectrum) membranes 207
Figure 4.2.7.a Non-aqueous potentiometric titration of a 50 % sulfonated 6FDA/ DDS/ p-PDA-SO_3H polyimide membrane 209
Figure 4.2.7.b Swelling degree (%) vs. Sulfonation level (%) for 6FDA/m-PDA/p-PDA-SO_3H after 24 h immersion in water at R.T 216
Figure 4.2.8 Three Dimensional Models of BPDA and 6FDA 218
Figure 4.2.9 Three Dimensional Projection of Disubstituted BDA 219

Figure 4.2.10 TGA of BDA in air at a heating rate of 2 ^{o}C/min from 40 to 150 ^{o}C and 10 ^{o}C/min from 150 to 700 ^{o}C 219
Figure 4.2.11 Chemical structures of sulfonated (1) BPDA/FDA/BDA and (2) BPDA/ DDS/BDA polyimides 221
Figure 4.2.12 FTIR Spectra of (1) BPDA/FDA homopolymer (2) BPDA/FDA/BDA copolymer 225
Figure 4.2.13 Degree of sulfonation calculated from BPDA/FDA/BDA polyimides. 226
Figure 4.2.14 IEC (meq/g) *vs*. Water uptake (SW %) of sulfonated BPDA/FDA/BDA membranes at 25 ^{o}C (2), and at 80 ^{o}C (1). 233
Figure 4.2.15 Water uptake (SW %) *vs*. $t^{1/2}$ (square root of time, min) 234
Figure 4.2.16 Chemical structures of BPSDA-based sulfonated polyimides 236
Figure 4.2.17 ^{1}H NMR spectroscopy of 50 % sulfonated random copolyimide of BPSDA/FDA/BDA. 238
Figure 4.2.18 Infrared Spectrum of BPSDA/APB/BDA-Based Polyimide with APB:DAB 239
Figure 4.2.19 Plot of the degree of sulfonation data obtained from FTIR measurements (A_{SO3H}/ $A_{C=O}$) against theoretical ion exchange capacity (IEC, meq/g) of BSDA/APB/BDA-based sulfonated polymers. 240
Figure 4.2.20 TGA thermograms of BSDA/APB/BDA polyimides 241
Figure 4.2.21 The number of water molecules absorbed per ionic group) plotted versus the theoretical IEC for BPSDA-based sulfonated polyimides. 252
Figure 4.2.2.1 Monomers utilized for the syntheses of sulfonated six-membered polyimides 255
Figure 4.2.2.2 Formation of tertiary amine-sulfonate in m-cresol 257
Figure 4.2.2.3 FTIR spectra of (1) 40 %, (2) 60 %, (3) 75 %, (4) 100 % sulfonated NDA/APB/BDA polyimide membranes 261
Figure 4.2.2.4 The inherent viscosity plotted against concentration for a 25% sulfonated NDA/FDA/BDA solution in m-cresol at 25 ^{o}C 265
Figure 4.2.2.5 Inherent viscosity (concentration of 0.1 g dl^{-1} in m-cresol at 25 ^{o}C) and theoretical IEC (meq/g) plotted against % sulfonation for sulfonated (25-100%) for NDA/FDA/BDA polymers 265

Figure 4.2.2.7 TGA Thermograms of Sulfonated NDA/FDA/BDA Polyimide Membranes..... 269
Figure 4.2.2.8 TGA and dTGA Thermograms of a 40 %Sulfonated NDA/APB/BDAPolyimide Membrane..... 270
Figure 4.2.2.9 λ (H_2O molecules/SO_3^-) vs. IEC (meq/g) for NDA/FDA/BDA and NDA/APB/BDA polyimide membranes..... 278
Figure 4.2.2.10 Tapping mode, 1 ìm wide height and phase images of a dry 75 %sulfonated NDA/FDA/BDA film..... 280
Figure 4.2.2.11 Tapping mode, 1 ìm wide phase images of 40 % sulfonated dry and wet NDA/FDA/BDA films (a) dried at 120 ^oC overnight (b) soaked in water(25 ^oC) for 24 hours (Z range = 30^o). 281
Figure 4.2.2.12 Tapping mode, 1 ìm wide phase images of 75 % sulfonated dry and wet NDA/FDA/BDA films (a) dried at 120 ^oC overnight (b) soaked in water (25 ^oC) for 24 hours (Z range = 50^o). 282
Figure 4.2.3.1 H-Bonding in (O=S=O) and (P=O) Containing Sulfonated PIs..... 283
Figure 4.2.3.2 ^1H NMR spectrum of 40 % sulfonated random copolyimide of BPDA/s-DADPS/APB in DMSO-d_6..... 287
Figure 4.2.3.3 FTIR spectra showing the effect of level of sulfonation on relative peak intensities of BPDA/s-DADPS/APB polyimides..... 288
Figure 4.2.3.4 Repeat Units of Sulfonated PBDA/s-DADPS/APB and BPDA/s-DADPPO/APB Polyimides..... 289
Figure 4.2.3.5 Plots of mol % Sulfonation (theory) vs mol % Sulfonation (FTIR) (▲); % Sulfonation (theory) vs IEC (theory)..... 290
Figure 4.2.3.6 Plots of mol % Sulfonation (theory) vs mol % Sulfonation..... 291
Figure 4.2.3.7 The effect of IEC (meq/g) on η_{inh} of (1) BPDA/s-DADPS/ APB and (2) BPDA/s-DADPPO/ APB polymers..... 293
Figure 4.2.3.8 Thermogravimetric curves (TGA and dTGA) for (a) Control BPDA/APB polyimide (b) 40% sulfonated BPDA/s-DADPS/APB polyimide. 296
Figure 4.2.3.9 Weight loss by due to sulfonic acid group decomposition for BPDA/s-DADPS/APB Polyimides (TGA in air, 10 ^oC/min)..... 300

Figure 4.2.3.10 Weight loss due to sulfonic acid decomposition for BPDA/s-DADPPO/APB Polyimides (TGA in air, 10 ^{o}C/min) 301
Figure 4.2.3.11 DSC of BPDA/s-DADPS/APB polyimides, ... 302
Figure 4.2.3.12 Effect of Sulfonation on Glass Transition Temperature [Tg (^{o}C)] for 303
Figure 4.2.3.13 Effect of IEC (meq/g) on conductivity (S/cm) for 307

LIST OF SCHEMES

Scheme 2.1 Polyimide synthesis via the classical two-step route (*the bracketed x and y unit structures represent different configurational isomers*) 9

Scheme 2.2 Mechanism for isomeric poly(amic) acid formation via nucleophilic substitution at an anhydride carbonyl 10

Scheme 2.3 A Possible Mechanism for the Hydrolytic Degradation of poly(amic) acid 20

Scheme 2.4 Mechanism of chemical imidization..... 28

Scheme 2.5 Synthesis of m-BAPPO Based Polyimides via Solution Imidization. ... 31

Scheme 2.6 Ultem™, high temperature solution imidization 32

Scheme 2.7 Mechanism of high-temperature solution imidization. 35

Scheme 2.8.a Synthesis of Polyimides via Ester-Acid Solution Imidization Route 39

Scheme 2.8.b Synthesis of the Three Isomers of Diester-Diacids Prepared from Bridged Dianhydrides 42

Scheme 2.9 Mechanism of anhydride formation during ester-acid solution imidization route to polyimides 43

Scheme 2.10 Reaction of activated nitrobisimide monomer with bisphenoxide 46

Scheme 2.11 Mechanism of water-catalyzed reaction of diisocyanates and dianhydrides..... 50

Scheme 2.12 Preparation of a Polyimide from a Dianhydride and Diisocyanate with Bulky Substituents 50

Scheme 2.13 Imide-amine interchange or transimidization reaction..... 52

Scheme 2.14 PMR-15 Resin Chemistry..... 72

Scheme 3.2.1. Synthesis of Bis(3-nitrophenyl)phenyl phosphine oxide (BNPPO) ... 128

Scheme 3.2.2 Synthesis of Bis(3-aminophenyl)phenyl Phosphine Oxide (BAPPO). 130

Scheme 3.2.3 Synthesis and Purification of s-BFPPO[223] 133

Scheme 3.2.4 Procedure for synthesis of sulfonated diamine monomer [Bis(3-aminophenyl) phenylphosphine oxide (s-BAPPO)] and its elemental analysis data 135

Scheme 3.2.5 Synthesis and isolation of s-DCDPS..... 137

Scheme 3.2.6 Synthetic procedure for disulfonated DADPS diamine monomer..... 139

Scheme 3.2.7 Synthesis of BOHPPO 141
Scheme 3.2.8 Synthesis of NDA-PO 143
Scheme 3.2.9 Synthesis of NDA-SO_2 145
Scheme 4.1.1 Synthesis of Bis(3-aminophenyl)phenyl Phosphine Oxide (BAPPO)..... 160
Scheme 4.1.2 Possible sequential nitration reactions of triphenyl phosphine oxide .. 161
Scheme 4.2.1 Ester-acid route for sulfonated BPDA based polyimides 193
Scheme 4.2.2.1 One-step high temperature solution imidization of sulfonated NDA/FDA/BDA polyimides 258

CHAPTER 1. INTRODUCTION

Rapidly developing branches of the twenty first century's modern technology put forward ever-increasing requirements[1] for thermally and chemically resistant aromatic polymers, *e.g.* polyheteroarylenes. During the last two-decades, including work in our research group[2], particular interest has been devoted to the synthesis of polyimides based on phthalic anhydrides or naphthalic anhydrides due to the their high thermal, fire, radiation and chemical resistance and excellent mechanical properties. They are currently applied in many areas such as microelectronics, aerospace, automotive and gas separation industries as high-temperature coatings, films, structural adhesives, interlayer dielectrics, wire insulation and semipermeable membranes.

Further development of new polyimide systems and modification of existing systems is an ongoing task to further enhance their desirable properties and applications[3]. One area, which has received extensive attention in the last several years, is development of solid polymer electrolyte proton exchange membranes (PEM) for fuel cells that are known to be promising energy conversion technologies. These efficient, nonpolluting and low-noise electrical generators can be viable in a number of areas, including transportation, residential (stationary) power, and lap top computers and cell phones (portable power).

The current materials used for these cells are the poly(perfluorosulfonic acid) statistical copolymers produced by DuPont under the trade name, Nafion®. Although

1. A. Rusanov, Advances in Polymer Science, Vol.111, **1994**, Springer-Verlag Berlin Heidelberg, Ed. K.Dušek
2. Moy, T.M., DePorter, C.D. McGrath, J.E. Polymer, **1993**, 34(4), 819; Meyer, G.W., McGrath, J.E. US Patent, 5,493,002 (to VPI and State University), **1996**; Meyer, G.W., Pak, S.J., Lee, Y.J., and McGrath, J.E. Polymer **1995** 36(11), 2303; Summers, J.D., Arnold, C.A., Chen, Y.P. and McGrath, J.E. Polym. Prepr. 27 (2), **1986**, 403; Johnson, B.L., Tran, C., Yilgor, I., Igbal, M., Wightman, J.P., Lloyd, D.R. and McGrath, J.E., ACS Polym. Prepr., **1983**, 24 (2), 31;
3. Farr, I.V., Ph.D. Thesis, July **1999**, Virginia Tech.

they have good chemical and physical properties for use as a PEM in fuel cells, they are recognized to have some significant technical deficiencies such as reduction in conductivity at low humidity or high temperatures, high methanol permeability and high cost[4].

Therefore, the development of new ionomeric membranes that will provide improved and economical proton exchange membranes for fuel cell applications is an urgent need. In these generators, new proton exchange membranes must exhibit several important characteristics, including good film formation and highly hydrophilic character to allow adequate ionic conductivity, but while maintaining good mechanical stability and durability for long times at temperatures at or above 100 ^{o}C.

The research in this dissertation has focused on the synthesis and characterization of linear high molecular weight, soluble aromatic polyimides by utilizing wholly aromatic five- and six-membered ring polyimides containing pendant sulfonic acid functional groups that are of interest for solid polymer electrolyte membrane fuel cells. The six-membered ring polyimides (based on naphthalic anhydrides) were of interest due to their better chemical and thermal stability compared with the analogous systems derived from five-membered ring systems (based on phthalic anhydrides)[5]. The primary interest was to design polymer repeat units which would yield soluble, film forming, hydrolytically and thermally stable polyimides containing controlled degrees of pendant sulfonic acid groups in repeat units. Monomer selection was initially based on literature observations.

Since polyimides based on bis(naphthalic anhydrides) display poor solubility and low processability in common solvents, and give soluble products with only a limited number of diamines, structural design of the six-membered ring polyimides was one approach to give a better solubility and processability of their related products. This thesis will also describe synthesis and characterization of phosphine oxide and sulfone based sulfonated and unsulfonated diamine monomers and their five-membered ring polymers for potential proton exchange membranes for fuel cells.

4. Miyatake, K., Iyotani, H., Yamamoto, K., and Tsuchida, E., *Macromolecules*, **1996**, 29, 6969.
5. Faure, S., Mercier, R., Aldebert, P., Pineri, M. and Sillion, B., *French Patent* 9 605 707 (**1996**).

Although several sulfonated and unsulfonated new diamines have been prepared in this research, the incorporation of these monomers into six-membered polyimide backbones has been left as future work.

CHAPTER 2. LITERATURE REVIEW

2.1 INTRODUCTION

Polyimides are step or condensation polymers that have heterocyclic imide functionalities in their repeat unit, as shown in Figure 2.1. They are generally derived from the reaction of organic diamines and organic tetracarboxylic acids or derivatives thereof [6,7].

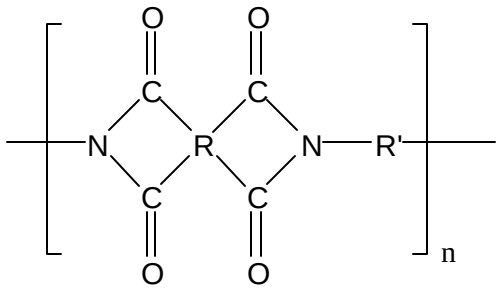

R = cycloaliphatic, aromatic

R' = aliphatic, aromatic

Figure 2.1 General structure of a polyimide

Polyimides are both scientifically and commercially important, because of their excellent thermal stability and mechanical strength. Proper design of polyimides has led to their use in aerospace, microelectronics, automotive and packaging industries.

The discussion comprising this chapter will provide a background to the experimental section that follows, and emphasizes the most recent developments in polyimide synthesis and structure/property modifications as revealed in the literature. Section 2.2 will discuss the common synthetic methods used to prepare polyimides, while the next section deals with the structure-property relationship of thermoplastic polyimides and also in briefly, for the sake of comparison, thermosetting polyimides. The last two

6. Bower, G.M. and Frost, L.W., *J. Polym. Sci*., A1, 3135 (**1963**).

7. Kreuz, J.A. et.al., *J. Polym. Sci*., A1, 4, 2607 (**1966**).

sections review fuel cells, sulfonated polymers and their applications for solid polymer electrolyte membranes in fuel cells.

2.2 SYNTHESIS OF POLYIMIDES

Aromatic polyimides, in general, consist of five- or six-membered heterocyclic imide units and aromatic rings. This cyclic chain structure of polyimides generally makes them insoluble/intractable and not applicable to traditional solution/melt condensation reactions.

The first report of a polyimide in the literature arose from the work of Bogert and Renshaw[8]. They discovered that 4-aminophthalic anhydride self-condensed to give an intractable polymeric material. Similarly Brandt found that upon reduction of 4-nitrophthalic anhydride, an oligomeric substance was formed by the reaction of the nitro compound with the amine reduction product[9]. Despite this early work, it was many years before the efforts of Edwards and Robinson suggested that polyimides could be developed into viable commercial materials[10,11]. Their research focused on the reaction of aliphatic diamines with pyromellitic dianhydride (PMDA) using nylon-salt type chemistry to form insoluble, but yet melt processable polyimides. The subsequent attempts made at DuPont R & D in the 1950's utilizing the direct reaction of dianhydrides and aromatic diamines in melt or in solution resulted in precipitation of intractable low molecular weight polyimides[12]. However, by mid-1950's, Dr. A. Endrey at DuPont had successfully pioneered the invention of obtaining polyimides through

8. Bogert, T.M. and Renshaw, R.R., *J. Am. Chem. Soc*., 30, **1908**, 1135.
9. Brandt, S. *J. Prakt. Chem*., 4, **1958**, 163.
10. Edwards, W.M., Robinson, I.M., *US Patent* 2710853, **1955**.
11. Edwards, W.M., Robinson, I.M., *US Patent* 2867609, **1959**.
12. Ghosh, M.K., Mittal, K.L. (eds.) *Polyimides: Fundamentals and Applications*; Marcel Dekker: **1996**.
13. Endrey, A.L., *Can. Patent* 659,328 (**1962**); Endrey, A.L., *US Patent* 3,179,631 (**1965**); Endrey, A.L., *US Patent* 3,179,633 (**1965**).

reaction of soluble/processable intermediates known as poly(amic acid)s. The first commercially produced polyimide was then introduced by DuPont[13] with the tradename of Kapton® (Figure 2.2) over three decades ago. Since that time, extensive research has been reported to provide a better understanding of the synthesis, characterization, and structure property behavior of polyimides.

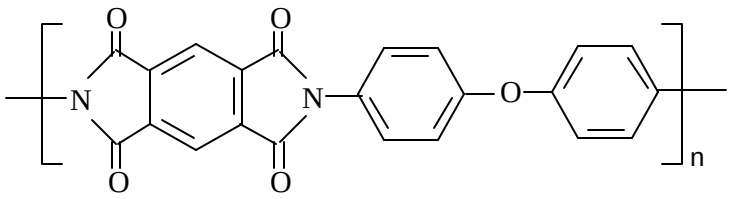

Figure 2.2 Kapton® Polyimide produced by DuPont

The number of versatile synthetic methods for the formation of polyimides has facilitated their range of utility in high performance applications[14]. The prominent synthetic methods, as well as some more novel routes to polyimide formation will be reviewed in this section of the thesis.

2.2.1 Classical Two-Step Route

The most common method of preparing aromatic polyimides involves the reaction of an aromatic tetracarboxylic acid anhydride with an aromatic diamine. The initial step consists of preparing a solution of the aromatic diamine in a polar aprotic solvent, such as

14. Mittal, K.L. (ed) *Polyimides: Synthesis, Characterization and Applications*, 1&2. Plenum, NY, **1984**; Feger, C., Khojasteh, M.M., McGrath, J.E.(eds) *Polyimides: Materials, Chemistry and Characterization*. Elsevier, Amsterdam, **1989**; Wilson, D., Stenzenberger, H.D., Hergenrother, P.M. (eds) *Polyimides* Blackie Glasgow, **1990**; Lupinski, J.H. and Moore, R.S. (eds) *Polymeric Materials for Electronics Packaging and Interconnections*, ACS Symposium Series 407, ACS, Washington, DC, **1989**; Takekoshi, T. *Adv. Poly. Sci*. 94, 1 **1990**; Cassidy, P.C. and Fawcet, N.C. In: Grayson, M.E. (ed) *Encylodedia of Chemical Technology*, Wiley, NY, 18, 704 **1982**; Verbicky, J.W. In: Mark, H.F., Bikales, N.M., Overberger, C.G., Menges, G.(eds.*); Encyclopedia of Polymer Science and Engineering, 2nd ed*., Wiley, NY, 12, 364 **1988**; Sato, M. *Polyimides, Plast. Eng. 41* (Handbook of Thermoplastics, Marcel Dekker) 665, **1997**.

N-methylpyrrolidone (NMP), dimethylacetamide (DMAc) or dimethylsulfoxide (DMSO), to which is added a tetracarboxylic dianhydride, which forms a soluble, processable poly(amic) acid intermediate at ambient temperature (Scheme 2.1). The high molecular weight isomeric poly(amic)acid formation is completed within 24 hours or less, depending on monomer reactivity. Since it is fully soluble in the reaction solvent, the solution may be cast into a film on a suitable substrate. The second step in this synthetic method is the cyclodehydration reaction (imidization) that is accomplished by thermal (heating to elevated temperatures), chemical (incorporating a chemical dehydration agent) or by azeotropic solution imidization. This method is representative of the initial work on aromatic polyimides[15] and remains the most practical way to synthesize high performance polyimides. The reason for this two-step method is that many of the resulting polyimides (e.g., Kapton®) are insoluble and infusible due to their rigid aromatic repeat unit. On the other hand, the soluble and processable poly(amic) acid intermediates that are heated to elevated temperatures also facilitate the generation of fully cyclized films via spin casting coating procedures. The overall reaction scheme for the two-step method is depicted in Scheme 2.1.

2.2.1.1 Poly(amic) acid Formation

In the classical two-step reaction of poly(amic) acid formation, any aliphatic, cyclo- aliphatic or aromatic dianhydride can, in principle be used with a suitable diamine. The poly(amic) acid is generally formed when a difunctional amine and a difunctional dianhydride mutually react in a polar aprotic solvent. This proceeds by a reversible nucleophilic acyl substitution when the nitrogen of the diamine, having an unshared pair of electrons, attacks either of the carbonyl carbons of an anhydride moiety comprising the tetracarboxylic acid anhydride, then displaces the carboxylate functionality, which is followed by proton transfer.

An accepted reaction mechanism for poly(amic) acid formation is given in Scheme 2.2. Bonding between the carbonyl carbon and the nitrogen results in formation

15. Bender, M.L., Chow, Y.L. and Chloupek, F.J., *J. Am. Chem. Soc*., 80, 5380 (**1958**); Kolegov, V.I., *Polym. Sci*. USSR, A18, 1929 (1976); Dine-Hart, R.A. and Wright, W.W., *J. Polym. Sci*., 11, 609 (**1967**).

of cyclic intermediate, **1**, with the pi electrons shifted onto the oxygen. This intermediate is short lived because the displayed electron pair shifts back to reform the carbonyl double bond and simultaneous bond-breaking occurs between the carbon and a "leaving group". The bond that must break in this ejection step to give linear amide-acid releases the central oxygen of the cyclic intermediate, **1**, and therefore gives a carboxylate leaving group. However, if instead the bond breaks between the nitrogen and developing sp^2 carbon, the reaction is reversed to give starting species; free amine and anhydride species. The rate of the forward reaction must be faster than the reverse reaction to obtain high molecular weight poly(amic) acid. Since the carboxylate group is chemically bonded, it cannot be systematically removed to drive the equilibrium in the forward direction. However, it can be deactivated through hydrogen bonding with a basic-aprotic solvent such as NMP[16].

The reactivity and concentration (kinetic 2^{nd} order progress) of each of the monomeric units and the nature of the solvent is very important in determining the rate of poly(amic) acid formation and successfully producing high molecular weight poly(amic) acid. Typical requirements for step-growth polycondensation reactions[17] to obtain high molecular weight linear poly(amic) acid are summarized below:

(1) Monomers must be highly pure (>99.9 %).

(2) Monomers must be difunctional and reactive groups must be mutually accessible.

(3) One-to-one stoichiometry of A-A, B-B monomers must be employed.

(4) Length of reaction time must be sufficient for high conversion.

(5) Side reaction must be minimal or absent.

---

16. Koton, M.M., Kudryavtsev, V.V., Adrova, N.A., Kalnin'sh, K.K., Dubnova, A.M.,Svetlichnyi, V.M., *Poym. Sci*. USSR **1974**, 16(9), 2411; Solomin, V.A., Kardash, I.YE., Snagovskii, Yu.S., Messerle, P.E., Zhubanov, B.A., Pravednikov, A.N., Dokl. Akad. Nauk SSSR (Engl. Transl.) **1977**, 236(1), 510; Pravednikov, A.N., Kardash, I.YE., Glukhoyedovv, N.P., Ardashnikov, A.YA.Polym. Sci. USSR **1973**, 15(2), 399; Solomin, V.A., Kardash, I.YE., Snagovskii, Yu.S., Messerle, P.E., Zhubanov, B.A.

17 . McGrath, J.E. "*Polymers, Synthesis"* Encyclopedia of Physical Science and Technology, Vol. 13; Academic Press: **1992**.

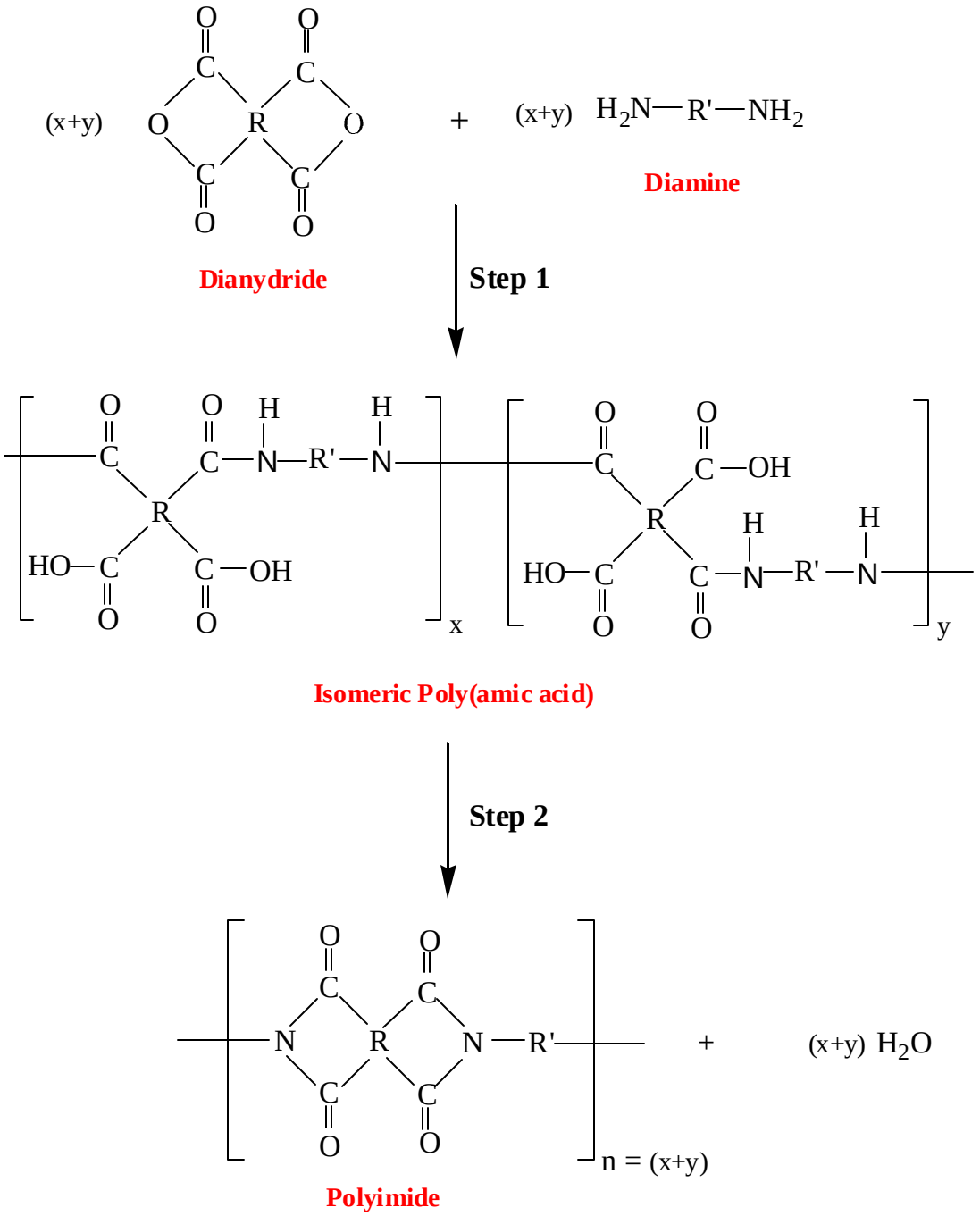

R = cycloaliphatic, or aromatic residue
R'= aromatic residue

Scheme 2.1 Polyimide synthesis via the classical two-step route (*the bracketed x and y unit structures represent different configurational isomers*)

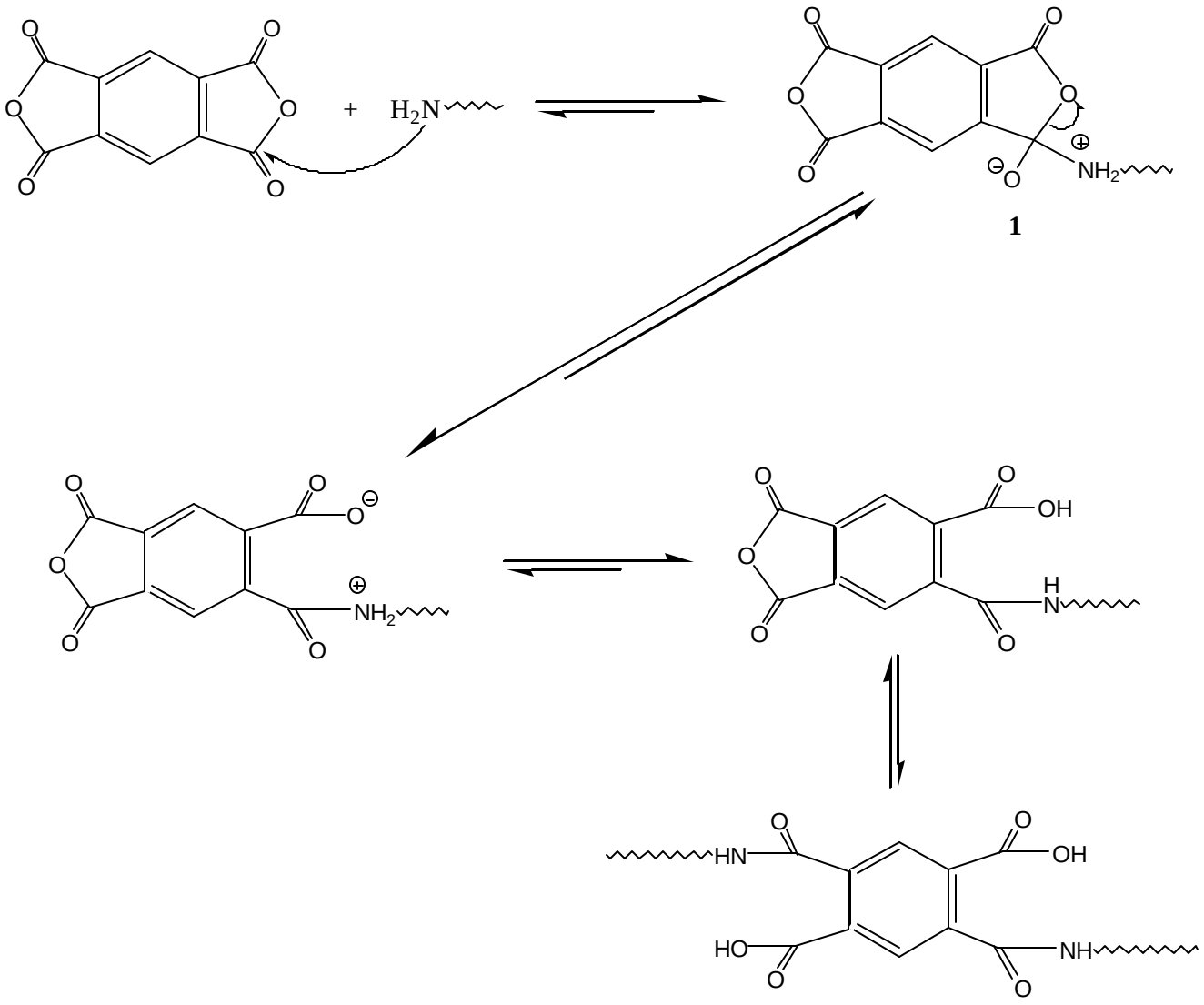

Scheme 2.2 Mechanism for isomeric poly(amic) acid formation via nucleophilic substitution at an anhydride carbonyl

Many studies have explained reaction rate and how it is affected by various factors such as monomer structure, reaction temperature, solvent composition and side reactions. Some typical dianhydrides and diamines, their structures and acronyms are shown in Figure 2.3. The five-membered phthalic anhydride groups which comprise aromatic tetracarboxylic acid anhydrides are highly electrophilic acylation agents toward diamines[18]. The enhanced electrophilicity results from strong electron-withdrawing effects exerted by the ortho-placement of the carbonyl groups[19]. However, almost all tetracarboxylic acid anhydrides contain bridging groups between two phthalic anyhdride units that one way or another affect the electron-accepting ability of the carbonyl carbons. Dianhydride reactivity, the ability to accept an incoming electron pair from a nucleophile, was found to best correlate with the electron affinity (E_a) of the dianhydride. Table 2.1 demonstrates the correlation between E_a, measured for a series of aromatic dianhydrides, and log of the reaction constant (log k_r) for acylation of ODA[20]. The dianhydride with the greatest electrophilicty, i.e. the highest electron affinity, will react first with a given nucleophile. In Table 2.1, PMDA is clearly much more reactive than the other anhydrides . The reason for the high reactivity of PMDA and the range of dianhydride E_a's observed is electronic in nature and can easily be illustrated with BTDA, DSDA, BPDA, and ODPA. BTDA and DSDA are bridged by electron-withdrawing carbonyl and sulfone groups respectively. By decreasing the electron density of the anhydride carbonyl carbon by delocalization of electrons through pi-orbitals, the anhydride carbons experience a greater positive environment that facilitates their addition to a nucleophile. ODPA on the other hand, has rings linked by an oxygen atom, which is able to donate electrons into the rings, and thereby serves to reduce the anhydride carbons affinity for more electrons made available by a nucleophile. In the case of BPDA, where no bridging functionality is present to withdraw or donate electron density, an intermediate value between BTDA and

18. Carey, F.A.; Sundberg, R.J. *Advanced Organic Chemistry, 3rd Ed., Part A: Structures and Mechanisms*; Plenum Press: **1993**.

19. Ghosh, M.K., Mittal, K.L. (eds.) *Polyimides: Fundamentals and Applications*; Marcel Decker: **1996**.

20. Svetlichnyi, V.M., Kalnins, K., Kudryavtsev, V.V., Koton, M.M. *Dokl. Akad Nauk SSSR (Engl. Transl.)* **1977**, 237(3), 693.

ODPA is observed. Electron withdrawing and donating bridges attached to the anhydride functionality will have a greater effect on the para- or ortho- anhydride carbonyls.

Diamine reactivity towards phthalic anhydride has been found to correlate with its basicity pK_a, *e.g.* an amine with a greater basicity will react faster. Early studies demonstrated the direct relationship between pK_a values and the rate constants (k_r) determined for a series of diamines reacted with PMDA (Table 2.2)[21]. The more basic diamines, such as p-PDA and ODA, showed relatively higher reaction rates. The electron-withdrawing nature of the bridging units was also shown to affect the acylation rate of diamines. Both the pKa and acylation rate of 4,4'-diaminobenzophenone was relatively low due to the electron-withdrawing carbonyl groups.

Monomer reactivity is important in controlling equilibrium to favor the formation of poly(amic) acid. When diamines and dianhydrides of low reactivity are used for PAA formation, a lower molecular weight would be expected when compared to a highly reactive diamine/ dianhydride system[22], since X_n is directly dependent on 1/ (1-p), where p is the extent of reaction. High molecular weight poly(amic) acid is obtained when the electron affinity of the dianhydride and basicity of the diamine are both high.

From the discussion above, it is already apparent that the rate of PAA formation is largely dependent on basicity and electron affinity of the monomers, but it is also dependent on the reaction temperature and the solvent used. It has been reported that higher molecular weight poly(amic) acids are obtained at lower temperatures[23-24]. These results are not surprising considering the exothermic nature of poly(amic) acid formation ($-\Delta H_{rxn}$). The effect of equilibration temperature on molecular weight was systematically tested [24]. This was accomplished by preparing a poly(amic) acid at room temperature

21 . Zubkov, V.A., Koton, M.M. Kudtyavtsev, V.V., Svetlichnyi, V.M. Zh. Org. Khim. (Engl. Transl.) 1981, 17(8), 1501.

22. Takekoshi, T., Synthesis of Polyimides, Polyimides: Fundamentals and Applications, Ghosh, M.K. and Mittal, K.L. (Editors), Wiley and Sons, **1996**.

23. Sroog, C.E., Endret, A.L., Abramo,S.V., Berr, C.E. Edwards, W.M., Oliver, K.L. *J. Polym. Sci.* Part A **1965**, 3, 1373; Bower, G.M., Frost, L. *J. Polym. Sci*. **1963**, A1, 3135.

24. Kaas, R.L. *J. Polym. Sci.: Polym. Chem. Ed*. **1981**, 19, 2255. SAME WITH 44.

and removing aliquots for equilibrating individually at a given temperature. After a fixed equilibration time, the individual samples were chemically imidized and isolated for molecular weight characterization by GPC. Comparison of the data showed a corresponding decrease in M_w with increasing temperature. However, since M_w was used as the basis for comparison, another factor must be taken into consideration: the dissolution of solid dianhydride in the reaction solution is slower at lower temperatures. This means that polymerization can occur at the solid-liquid interface more extensively at lower temperatures. Thus, high molecular weight poly(amic) acid can be rapidly attained by this interfacial type reaction before all of the dianhydride has dissolved and stoichiometric balance is achieved[25]. The result is higher M_w and a broad molecular weight distribution.

25. Wilson, D., Stenzenberger, H.D., Hegenrother, P.M. *Polyimides*; Chapman & Hall: **1990**.

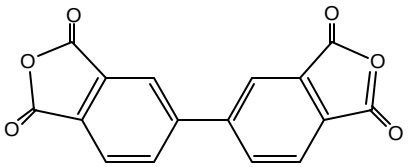

s-biphenyl tetracarboxylic dianhydride (**BPDA**)

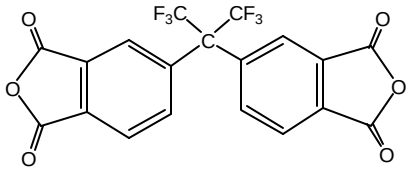

2,2-bis(3,4-dicarboxyphenyl)hexafluoropropane dianhydride (**6FDA**)

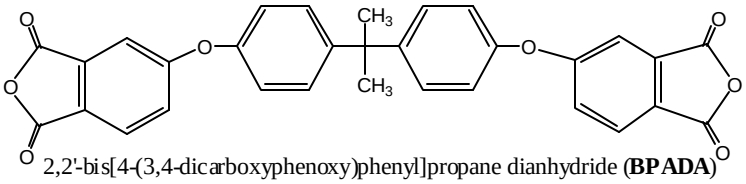

2,2'-bis[4-(3,4-dicarboxyphenoxy)phenyl]propane dianhydride (**BPADA**)

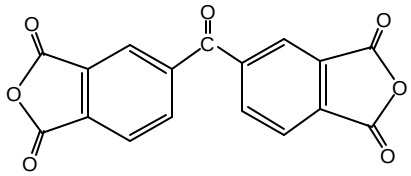

3,3',4,4'-benzophenonetetracarboxylic dianhydride (**BTDA**)

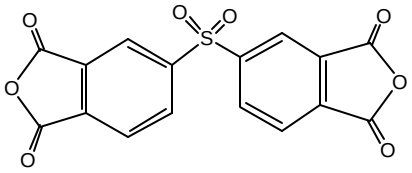

4,4',5,5'-sulfonyldiphthalic anhydride (**DSDA**)

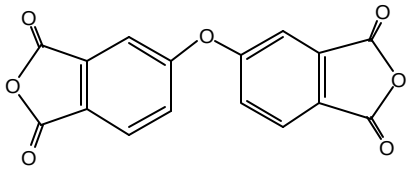

3,3',4,4'-oxydiphthalic anhydride (**ODPA**)

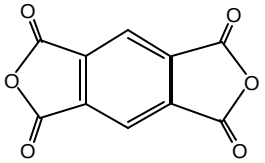

pyromellitic dianhydride (**PMDA**)

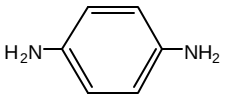

p-phenylene diamine (**p-PDA**)

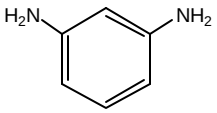

m-phenylene diamine (**m-PDA**)

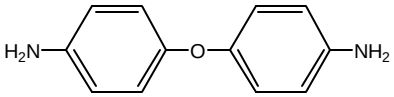

4,4'-oxydianyline (**4,4'-ODA**)

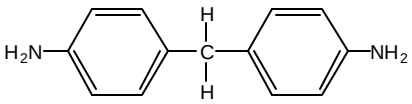

methylene dianiline (**MDA**)

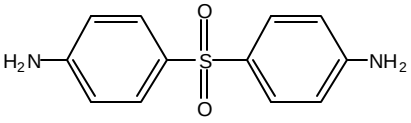

4,4'-diaminodiphenyl sulfone (**4,4'-DDS**)

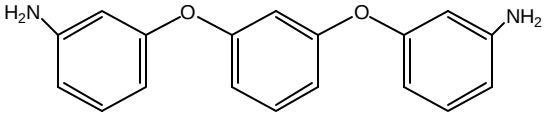

1,3-Bis(3-aminophenoxy) benzene (**APB**)

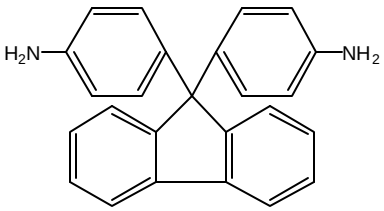

4,4'-(9-Fluorenylidene) dianyline (**FDA**)

Figure 2.3 Commonly used dianhydrides and diamines

Table 2.1 Electron Affinity and Log Rate Constant Values for Aromatic Dianhydrides Towards 4,4'-oxydianiline (4,4'-ODA)[20]

Dianhydrides	E_a , eV	Log k_r
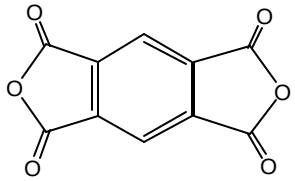 **(PMDA)**	0.85	0.78
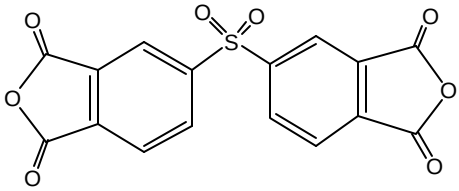 **(DSDA)**	0.52	1.05
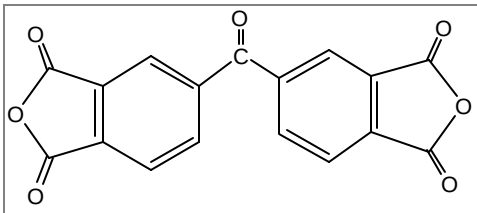 **(BTDA)**	0.48	0.49
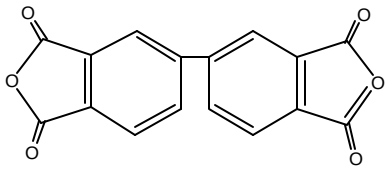 **(BPDA)**	0.21	0.13
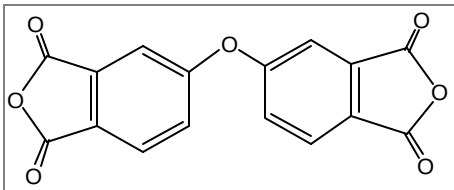 **(ODPA)**	0.18	-0.06

20. Svetlichnyi, V.M., Kalnins, K., Kudryavtsev, V.V., Koton, M.M. *Dokl. Akad Nauk SSSR (Engl. Transl.)* **1977**, 237(3), 693.

Table 2.2 Reactivity (Log Rate Constant) and Basicity pKa Values of Aromatic Diamines Towards 1,2,4,5-Benzenetetracarboxylic Dianhydride (PMDA)[20].

Diamines	pK_a	Log k_r
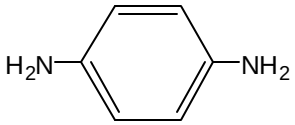 **(p-PDA)**	6.08	2.12
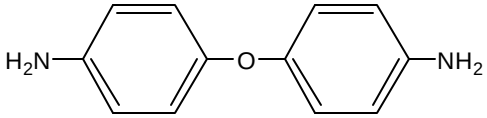 **(4,4'-ODA)**	5.20	0.78
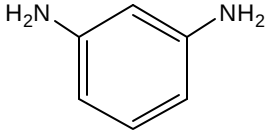 **(m-PDA)**	4.80	0
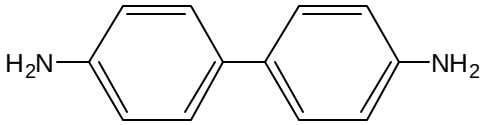	4.60	0.37
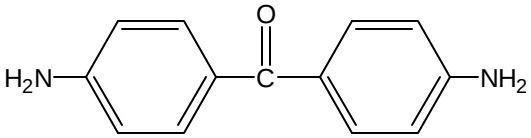	3.10	-2.15

20. Svetlichnyi, V.M., Kalnins, K., Kudryavtsev, V.V., Koton, M.M. *Dokl. Akad Nauk SSSR (Engl. Transl.)* **1977**, 237(3), 693.

The basicity of the reaction solvent has been found to influence the reaction rate and molecular weight of the product obtained during poly(amic) acid formation [16]. The overall reaction involves a relatively weak base reacting with a non-protic anhydride to yield a strong protic acid. In general, the use of dipolar aprotic amide solvents, such as DMAc and NMP, increases the rate of the forward reaction due to the hydrogen bonding of the o-carboxyamide group with the solvent. This reaction is favored when a more basic aprotic solvent is utilized (NMP>DMAc>Acetonitrile>THF)[26] due to its favorable interaction with the strong acid. As suggested earlier, the acid- base interaction prevents dissociation of the carboxyl proton, which can reverse the reaction. It has been also discussed in some papers that the ratio of DMAc: NMP in 4:1 vol/vol complexes with each di(amic) acid repeat unit[27, 28] (Figure 2.4), which could be a driving force for PAA formation. However, if the aprotic solvent is not basic enough it is possible that the strong acid formed may autoaccelerate the reaction and also shift the equilibrium away from high molecular weight PAA[24].

Ether solvents, which are less polar and basic than the amines, lack the ability to form tight H-bonded complexes with the carboxyl group. Thus, the reaction rate is slower than in THF. However, it has been suggested that the free carboxyl proton also participates in catalyzing the forward reaction by protonation of the carbonyl group of the dianhydride[24]. It has been reported that diamines which are weak bases, such as 4,4'-diaminodiphenylsulfone, react slowly with BTDA in DMAc, but high molecular weights are rapidly achieved in THF[29]. This may be due to a specific interaction between the amine and THF, which increases its basicity and/or may be due to a not basic enough

26 . Solomin, V.A., Kardash, I.YE., Snagovskii, Yu.S., Messerle, P.E., Zhubanov, B.A., Pravednikov, A.N., *Dokl. Akad. Nauk* SSSR 236(1), 139 1977; (Engl. Transl.), 236(1), 510, **1977**.

27. Kreuz, J.A., Endrey, A.L., Gay, F.P., Sroog, C.E. *J. Polym. Sci*. **1966**, A-1(4), 2607.

28. Brekner, M.J., Feger, C. *J. Polym. Sci. Part A: Polym. Chem*. **1987**, 25, 2005.

29. Egli, A.H. and St. Clair, T.L., *Recent Advances in Polyimide Science and Technology* (Weber, W.D. and Gupta, M.R. (Eds.), Soc. Plast. Eng., Brookfield, CT, 57, (**1985**).

characteristic of THF to deprotonate the acid to form the carboxylate, thus driving the reverse reaction[30].

The most deleterious side reaction in PAA formation is hydrolysis, which upsets the equilibrium balance of anhydride and amine endgroups and, consequently, amide-acid linkages degrade to reform them (Scheme 2.3). The o-dicarboxylic acid is unreactive with aromatic diamines under the conditions of poly(amic) acid synthesis (eg. 25 ^{o}C) and, therefore, the molecular weight is limited. Therefore, it is imperative to strictly remove water either in the monomers or in the reaction solvents in order to form the PAA and maintain constant molecular weight. This is usually achieved by carefully drying the monomers and distilling the solvents. Consideration of PAA cyclization to the polyimide makes it apparent that water will be generated, which will also facilitate chain hydrolysis, if it is not removed. Low molecular weight PAA formation due to hydrolysis also affects/reduces the film-forming ability of the poly(amic) acid when cast from solution and thermally imidized[31]. When sufficient heat is applied to the bulk film, o-dicarboxylic acid groups cyclodehydrate to form anhydride and these can acylate neighboring free amine endgroups to increase the molecular weight[20, 25]. However, the water librated during subsequent imidization cannot be quickly removed from the bulk film and could cause the deleterious hydrolysis cycle once again[32].

30. Adrova, N.A., Bessonov, M.I., Laius, L.A. and Rudakov, A.P., Polyimides: A New Class of Thermally Stable Polymers, Technomic, Conn. (**1970**).

31. Volksen, W. *Adv. Polym. Sci*. **1994**, 117, 111.

32. Bell, V.L., Stump, B.L. and Gafer, H., J. Polym. Sci. Polym. Chem. Ed., 14, 2275, (**1976**).

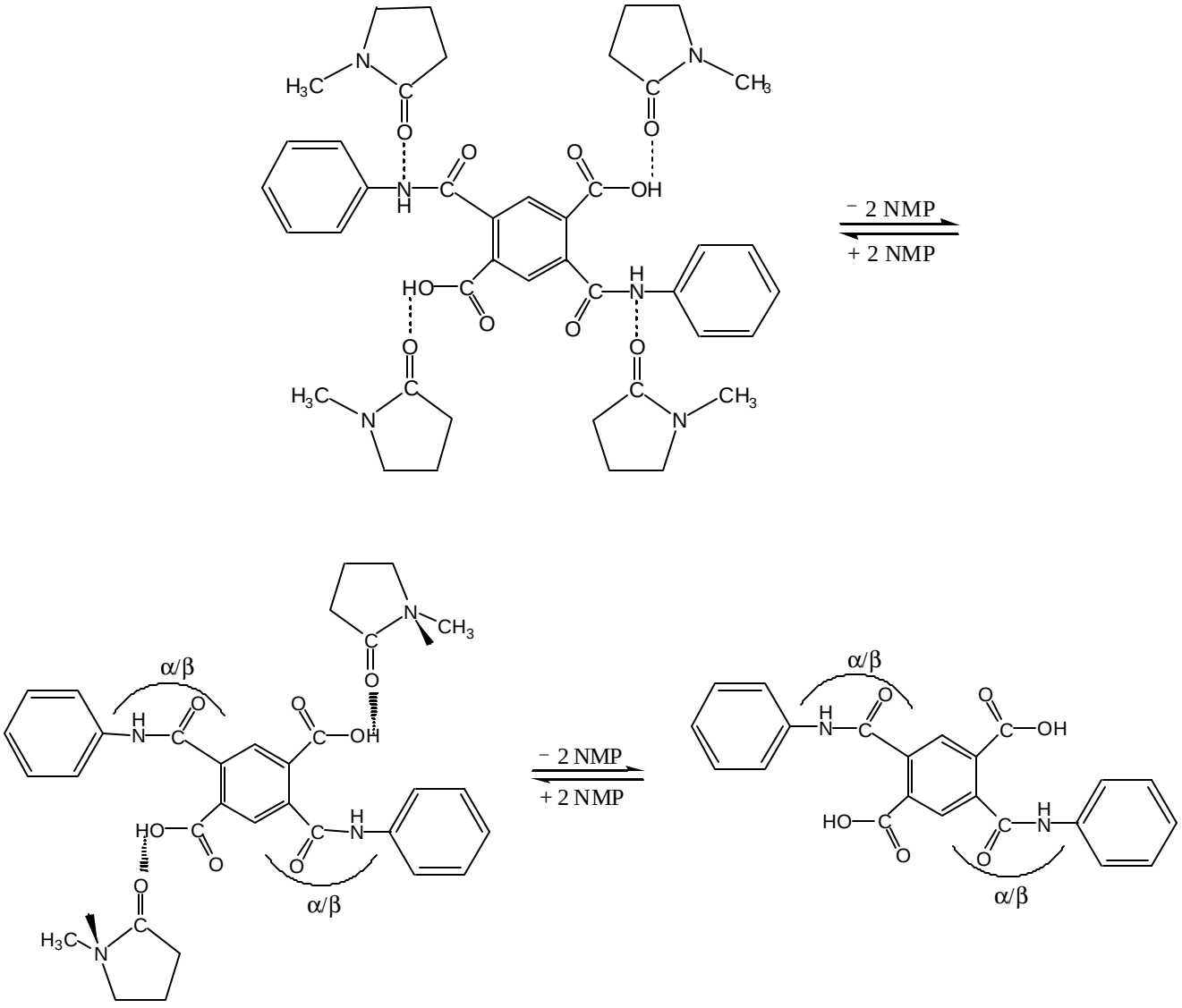

Figure 2.4 A Model for 4:1 ratio of NMP complexation with a di(amic) acid repeat unit[34]

34. Brekner, M.J., Feger, C. *J. Polym. Sci. Part A: Polym. Chem.* **1987**, 25, 2005.

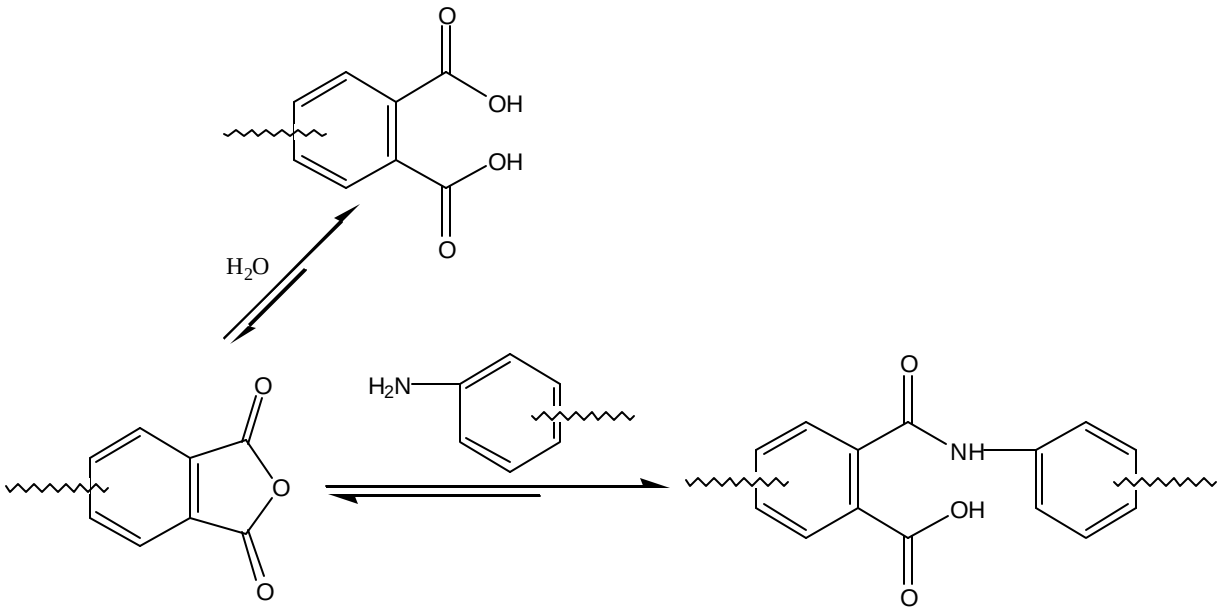

Scheme 2.3 A Possible Mechanism for the Hydrolytic Degradation of poly(amic) acid

2.2.1.2 Thermal (Bulk) Imidization

Thermal imidization method can be used for poly (amic) acids, which may precipitate upon cyclization because of the increase in chain rigidity. It consists of casting a poly(amic) acid solution onto a suitable substrate, followed by gradual heating in a programmed time and temperature cycle to affect solvent removal and the cyclodehydration reaction to form polyimide in a film form. This method is also known as "bulk imidization". A widely employed laboratory thermal cycle, under vacuum or nitrogen atmosphere to remove all traces of water and solvent, and prepare bubble-free films is believed to have been developed at NASA Langley, is given below[35]. 25 ^{o}C for 1 hour, heat to 100 ^{o}C within 1 hour,

1) 100 ^{o}C for 1 hour, heat to 200 ^{o}C within 1 hour,
2) 200 ^{o}C for 1 hour, heat to 300 ^{o}C within 1 hour,
3) 300 ^{o}C for 1 hour, then
4) One-half to one hour at a temperature just above T_g.
5) Cool to 25 ^{o}C.

This is the most common method used with insoluble polyimides to cast films from poly(amic) acid solution because it is relatively low cost and can be readily instituted and easily controlled in an industrial setting[36,37, 27]. One commercial example of a polyimide produced by the thermal imidization pathway is the Kapton polyimide from DuPont (Figure 2.5).

Some important features of the solid-state imidization reaction are not completely understood, including the influence of decreased molecular mobility and the effect of residual solvent[38]. Although its complete mechanism is not well understood, it is

---

35. Synder, R.W., Thomson, B., Bartges, B., Czerniwski, D. and Painter, P.C., *Macromolecules*, 22, 4166 (**1989**).
36. Saini, A.K., Carlin, C.M. and Patterson, H.H., *J. Polym. Sci.:* Part A, 30, 419 (**1922**).
37. 37 Lavrov, S.V., Talankina, O.B., Vorobyev, V.D., Izyumnikov, A.L., Kardash, I.Y., Pravednikov, A.N., *Polym. Sci. USSR*., 22(8), 2069 **1980**.
38. Farr, I.V. *Ph.D Thesis*, Virginia Tech. **1999**.

believed to proceed by a nucleophilic substitution reaction involving the amide nitrogen and ortho-carboxylic acid[39].

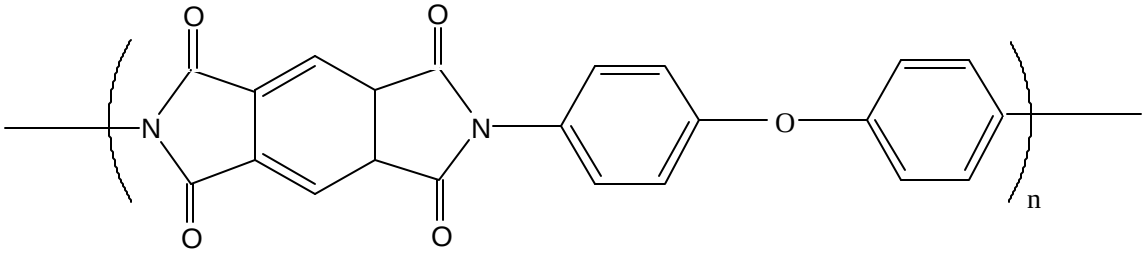

Figure 2.5 The repeat unit structure of Kapton-H™ Polyimide formed from PMDA and ODA

The product of this reaction, water, is then thermally removed. The bulk reaction is known to be promoted by residual solvent. Much of the solvent is removed produced during heating ranging from ambient temperature to approximately 150 ^{o}C. Both solvent evaporation and maximum evolution of water from imidization take place between 150 ^{o}C and 250 ^{o}C, while solvent removal and final imidization are completed at 250 ^{o}C and higher.

Since the solvent removal and maximum imidization occur simultaneously, there is tremendous shrinkage which results in maximum stress in the film[40-42]. Release of volatiles, especially water, which cause degradation, voids and film shrinkage is one important negative effect of bulk thermal imidization[25, 15].

As the rigid cyclic imide structure is formed during cyclodehydration, the glass transition temperature,T_g, increases dramatically and can rise above the reaction temperature[19]. The resulting decrease in chain mobility markedly hinders attainment of

39. Volksen, W. in Weber, W.D. and Gupta, M.R. (eds.) *Recent Advances in Polyimides and Technology*, Mid-Hudson Section of Soc. Of Plast. Eng., New York, 102 (**1987**).

40. Brink, M.H., Ph.D. Thesis, Virginia Tech (1994).

41. Lin, T., Stickney, K.W., Rogers, M., Riffle, J.S., McGrath, J.E., Marand, H., Yu, T.H. and Davis, R.M. *Polymer*, 34, 772 (**1993**).

42. Kim, Y.J., *Ph.D. Thesis*, Virginia Tech (**1992**).

the intramolecular conformation favoring the cyclodehydration reaction[25, 27]. (Figure 2.6, Structure I)[19].

Conformations unfavorable to imide formation, such as Structure II in Figure 2.6, due to the decreased entropy, remain rigidly fixed and cause the decrease in the rate of cyclization[27]. In the glassy state, residual solvent molecules, such as NMP, may also hinder attainment of imidization-favoring conformations by forming intermolecular hydrogen bonds with the reactive groups[43]. Therefore, the final polyimide film may contain residual uncyclized amic-acid structures, which are hydrolytically unstable and which may ultimately cause chain degradation[44].

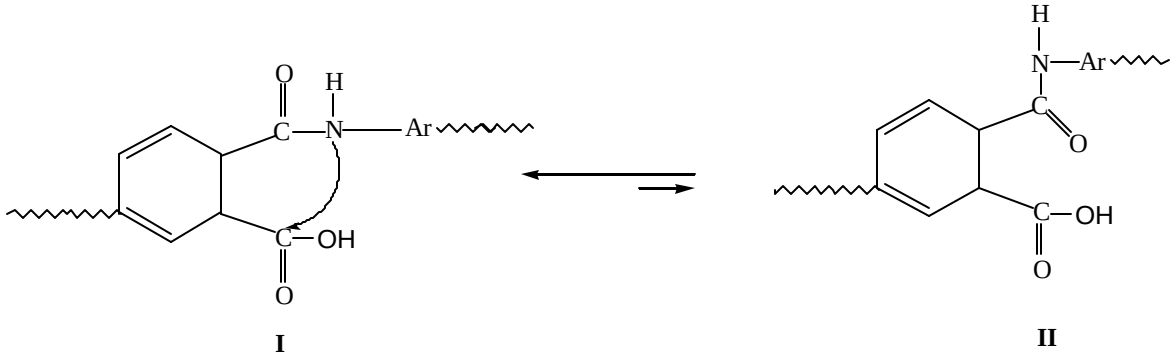

Figure 2.6 Conformations of poly(amic) acid during cyclodehydration

In thermal imidization, not only does solvent plasticize the polymer film, which allows greater chain mobility, but it also favors the appropriate conformation needed for cyclization to occur[27]. An increase in chain mobility is required to fully cyclize the polyamic acid. Chain mobility can also be achieved above the glass transition temperature of the polyimide.

Since the degree of imidization affects the stability and physical properties of the polyimide film during use[44], several analytical techniques have been developed for determining the quantity of residual amic-acid groups. However, the methods are limited by the often insoluble nature of the polyimide films.

43. Brekner, M.J., Feger, C. *J. Polym. Sci. Part A: Polym. Chem*. **1987**, 25, 2005.

44. Sroog, C.E. Prog. Polym. Sci. 1991, 16, 561., A.P. *Polyimides*: *A New Class Of Thermally Stable Polymers*; Technomic: **1970**.

Infrared spectroscopy[19,27,45,46] has been the most commonly used to determine residual amide-acid groups in insoluble polyimides. Table 2.3 shows several of the absorption bands used for quantitative and qualitative analysis of polyimides and poly(amic) acids. Since during cyclodehydration of poly(amic) acid, the imide absorption bands grow in intensity, the degree of imidization can be determined by comparing the imide band intensities (I) in a reacted sample to those in the spectrum of a fully imidized "standard" film (I^o). A normalization factor is used to correct variations in film thickness. This is obtained by means of a band in the spectrum whose intensity remains constant throughout the imidization process, such as the aromatic absorption band at 1500 cm^{-1}.

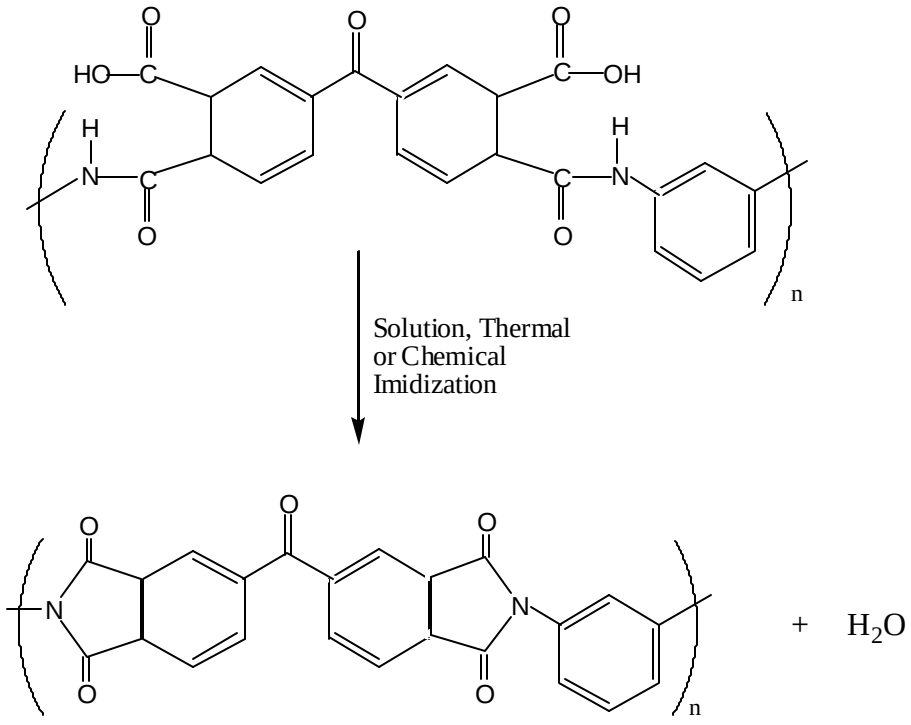

Figure 2.7 Three Common Routes to Facilitate to Conversion of Polyamide Acids to Polyimides

45. Frost, L.W., Kesse, I. *J. Appl. Polym. Sci*. **1964**.

46. Adrova, N.A., Bessonov, M.I., Laius, L.A., *Rudakov mers*; Technomic: **1970**; Koton, M.M., Meleshko, T.K., Kudryavtsev, V.V., Nechayev, P.P., Kamzolkina, Ye.V., Bogorad, N.N. *Poym. Sci. USSR* **1982**, A24(4), 791; Pyrde, C.A. *J. Polym. Sci. Part A* **1989**, 27, 711; Pyrde, C.A. *J. Polym. Sci. Part A* **1993**, 31, 1045.

The degree of imidization is given by the following equation:

$$P = \frac{\mathbf{I}(\text{imide}) / \mathbf{I}(\text{ref})}{\mathbf{I^0}(\text{imide}) / \mathbf{I^0}(\text{ref})}$$

Although this method is widely used in determining residual amide-acid groups in insoluble polyimide films, there are some drawbacks[47] to utilizing this method for quantitative analysis, such as:

(a) Accuracy of the true extent of imidization of the "standard" film.

(b) Imide absorbances at 1780 and 720 cm^{-1} can be affected by overlapping anhydride absorptions and by anisotropy.

(c) Low sensitivity

(d) H-bonding with solvent

2.2.1.3 Chemical Imidization

Although used much less frequently than the conventional thermal method, this approach can be utilized for imidization when the polyimide product is insoluble. The chemical imidization of poly(amic) acid is accomplished by using chemical reagents as catalysts for cyclodehydration at room temperature or below the temperature at which thermal imidization occurs[48-50]. Various combinations of chemical reagents have been used to effect this conversion. The reagent combination most widely used is an equimolar mixture of pyridine and acetic anhydride[51-53] The preferred product of the reaction, either a polyimide or polyisoimide, will be determined by the chemical reagent selection,

47. Dunson, D., *Ph.D Dissertation*, May **2000**, Virginia Tech, Blacksburg, VA.

48. Vinogradova, S.V. et al., Polym. Sci. USSR., 22(8), **1980**, 2069.

49. Endrey, A.L., US Patent 3,242,136, **1966** (to DuPont Co).

50. Meyer, G.W., Heidbrink, J.L., Franchina, J.G., Davis, R.M., Gardner, S., Vasudevan, V., Glass, T.E., McGrath, J.E. *Polymer*, 37 **1996**, 5077.

51. Searl, M.E., *US Patent* 2,444,536 (**1958**).

52. Roderick, W.R., *J. Am. Chem. Soc*., 79, 1710 (**1957**).

53. Cotter, R.J., Sauers, C.K. and Whelan, J.M., *J. Org. Chem*., 26, 10 (**1961**).

e.g. a combination of pyridine and trifluoroacetic anhydride favor isoimide formation[54]. Using pyridine or triethylamine as the base catalyst, the amic acid reacts with acetic anhydride to form a mixed anhydride (Scheme 2.4). The formation of the mixed anhydride intermediate leads to resonance structure **1** and **2**[55,56]. Pathway **A**, it should be pointed out, is thermodynamically favorable. However, for kinetically favorable isoimidization products, it is also possible for the isoimide to isomerize to the thermodynamically more stable imide form. The latter is supported by the fact that stronger amines, such as triethylamine, promote acetate formation and therefore increase the back reaction leading to exclusive imide formation.

As mentioned above, polyisoimides can be thermally converted to the polyimide or they can serve as reactive intermediates[57]. Post-reactions on polyisoimides with amines, alcohols, thiols or hydazoic acid results in poly(amide-imide), poly(amide-ester), poly(amide-thioester) and polytetrazole acid, respectively. A number of polyisoimide oligomers having thermally curable endgroups were prepared by Landis *et al.*[58]. The results indicated that polyisoimides are more soluble than their related polyimide structures. In fact, the increase in solubility/processability compared to polyimides is the most significant feature of polyisoimides.

Chemical imidization is less attractive for the manufacture of commercial polyimides due to the need for additional reactants and the complexity of the process. However, since water is not released during this type of imidization, this approach eliminates the potential of hydrolytic molecular weight degradation during thermal consolidation. Wallach[59] prepared a PMDA/ODA system in the late 60's via both chemical imidization and thermal imdization. The results showed that this particular polymer showed better elongation-at-break values for the polymer resulting from chemical imidization than those resulting from thermal imidization.

---

54. Koton, M.M.., et al., *Vysokomol. Soedin*. Ser. A, 26(12), **1984**, 2534.

55. Kailani, M.H., Sung, C.S.P. *Macromolecules*, **1998**, 31, 5771.

56. Kailani, M.H., Sung, C.S.P. *Macromolecules*, **1998**, 31, 5779.

57. Angelo, R.J., Golike, R.C., Tatum, W.E., Kreuz, J.A., *Proc. 2nd Int. Con. on Polyimides*, 67, Ellenville, NY (Oct-30-Nov.1, **1985**.

Landis, A.L., US Patent 4,496,711 (1985) (Hughes Aircraft Co).

59. Wallach, M.L., *J. Polym. Sci*., A-2, 953 (**1968**).

Without any doubt, this is valuable information that could possibly offer a potential pathway to toughen otherwise brittle polyimides.

Table 2.3 Infrared Absorption Bands of Imides and Related Compounds[19,27,45,46,3]

	Absorption Band (cm^{-1})	**Intensity**	**Origin**
Aromatic Imides	1780	s	C═ O asymmetric stretch
	1720	vs	C ═ O symmetric stretch
	1380	s	C— N stretch
	725		C═ O bending
Amic Acids	2900-3200	m	COOH and NH_2
	1710	s	C ═O (COOH)
	1660 amideI	s	C ═ O (CONH)
	1550 amide II	m	C ─ NH
Anhydrides	1820	m	C ═ O
	1780	s	C═ O
	720	s	C ═ O
Amines	~3200		NH_2 symmetrical structure
	two bands	w	NH_2 asymmetrical structure

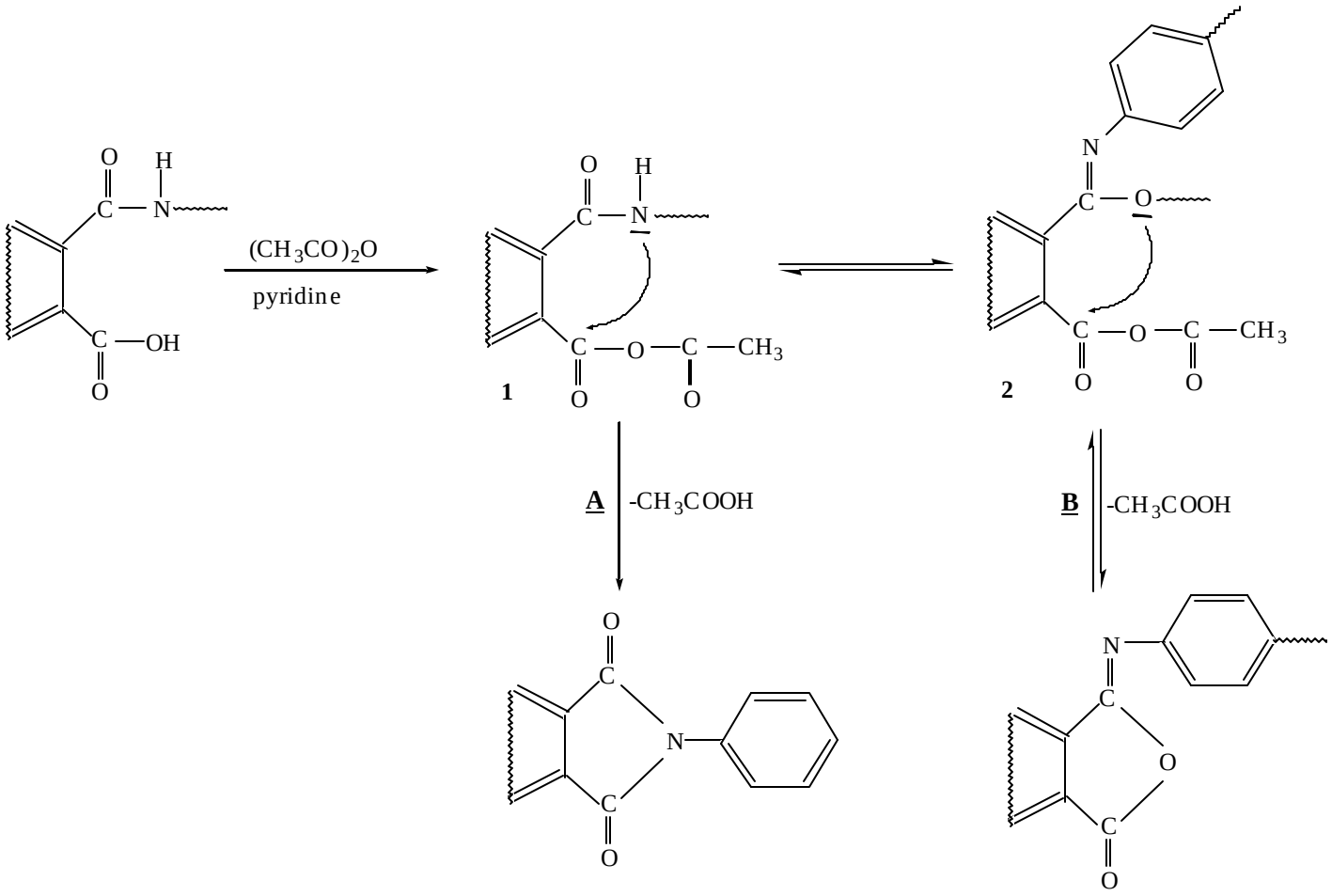

Scheme 2.4 Mechanism of chemical imidization[55,56]

2.2.1.4 Solution Imidization

The development of soluble fully-cyclized polyimides has become important as a result of the difficulties in processing and handling of poly(amic acid)s. When the cyclized form of poly(amic acid)s remain soluble in organic solvents, it is possible to react dianhydrides and diamines, and obtain fully imidized, high molecular weight, high T_g polymers via thermal imidization without using any catalyst(s) in a homogeneous reaction solution at temperatures above 170 ^oC. Alternatively, a solution of poly(amic) acid which has been allowed to equilibrate in a suitable solvent can be subsequently heated to efffect cyclodehydration to soluble polyimides[3,47,60-64]. This is known as a "one-pot, one-step, high temperature procedure in which polycondensation and imidization occur in the homogenous solution and differs from the classic two-stage method because the polyimide is fully soluble in the solvents employed. A typical solvent combination and temperature profile is shown in Scheme 2.5.

Although there are variations in the one-pot procedure, the most common one involves the synthesis from dianhydride and diamine in NMP, as the reaction solvent. An azeotropic solvent is typically used in order to remove the water formed during the reaction to drive the reaction to completion. The solvent choice needs to be capable of transporting the water from the reaction medium. Typical azeotropic solvents are: o-dichlorobenzene (o-DCB), cyclohexylpyrrolidone (CHP), toluene or xylene. In this procedure, the reaction is heated to high temperatures (160-190 ^oC) over several hours, which allows the water generated by imidization to azeotropically distill into a Dean-Stark trap. A widely known example of a commercial polyimide prepared by the one-pot

60. Waldbauer, R.O., Rogers, M.E., Arnold, C.A., York, G.A., McGrath, J.E. *35th Int. SAMPE Symp*. **1990**, 97.

61. McGrath, J.E., Rogers, M.E., Arnold, C.A., Kim, Y.J., Hedrick, J.C. *Makromol. Chem., Makromol. Symp*. **1991**, 51, 103; Rogers, M.E., Grubbs, H., Brennan, H. Rodrigues, D., Lin, T., Marand, H., Wilkes, G.L., McGrath, J.E. *37th Int. SAMPE Symp*. **1992**, 717.

62. Yagci, H., Ostrowski, C., Mathias, L.J. *J. Polym. Sci. Part A: Polym. Chem*. **1999**, 37, 1189.

63. Ayala, D., Lozano, A.E., de Abajo, J., de la Campa, J.G. *J. Polym. Sci. Part A: Polym. Chem*. **1999**, 37, 805.

64. Yang, C.-P., Tang, S.-Y. *J. Polym. Sci. Part A: Polym. Chem*, **1999**, 37, 455.

procedure is General Electric's Ultem™, obtained by reacting diamines and dianhydrides in o-DCB as shown in Scheme 2.6.

A procedural modification developed for less reactive diamines involves dissolving the reactants in m-cresol and heating the solution for several hours at temperatures ~ 200 ^{o}C. Due to the high temperature, the water evolved during the imidization can be removed easily by distillation into the trap, or by passing an inert gas stream through the system. Nitrobenzene or other chlorinated solvents, including ortho- / para-dicholoro phenol and α-chloronaphthalene, can also be used in these reactions.

Harris and coworkers have done extensive work using the one-step method[65-73], which primarily involved the development and use of phenylated monomers. The reactivity of these monomers at lower temperature is insufficient for successful polymerization, but the one-step process allows high molecular weight polyimides to be synthesized.

65. Harris, F.W. and Hsu, S.L.C., *High Perform. Polym*., 1, **1989**, 3.

66. Harris, F.W., Feld, W.A. and Lanier, L.H. in *Applied Polymer Symposium* No. 26, N. Platzer (ed.), Wiley, New York, **1975**, 421.

67. Harris, F.W., Norris, S.O., Lanier, L.H., Reinhardt, B.A., Case, R.D., Varaprath, S., Padaki, S.M., Torres, M. and Feld, W.A. in *Polyimides: Synthesis, Characterization, and Applications*, Mittal, K.L. (ed.), Plenum, New York, 1, **1984**, 3.

68. Cheng, S.Z.D., Arnold, F.E., Zhang, A., Shen, D., Park, J.Y., Lee, C.J. and Harris, F.W. *Polymer Prepr*., 33, **1992**, 313.

69. Cheng, S.Z.D., Wu, Z., Eashoo, M., Hsu, S.L. and Harris, F.W. *Polymer*, 32, **1991**, 1803.

70. Tomikawa, M., Cheng, S.Z.D. and Harris, F.W. *Polym. Prep*. 36(1) **1995**, 707.

71. Harris, F.W., Sakaguchi, Y., Shibata, M. and Cheng, S.Z.D. *High Perform. Polym*., 9(3), **1997**, 251.

72. Harris, F.W., Li, F., Lin, S.H., Chen, J. and Cheng, S.Z.D. *Macromol. Symp*., 122, **1997**, 33.

73. Lin, S.H., Li, F., Cheng, S.Z.D and Harris, F.W. *Macromolecules*, 31(7), **1998**, 2080.

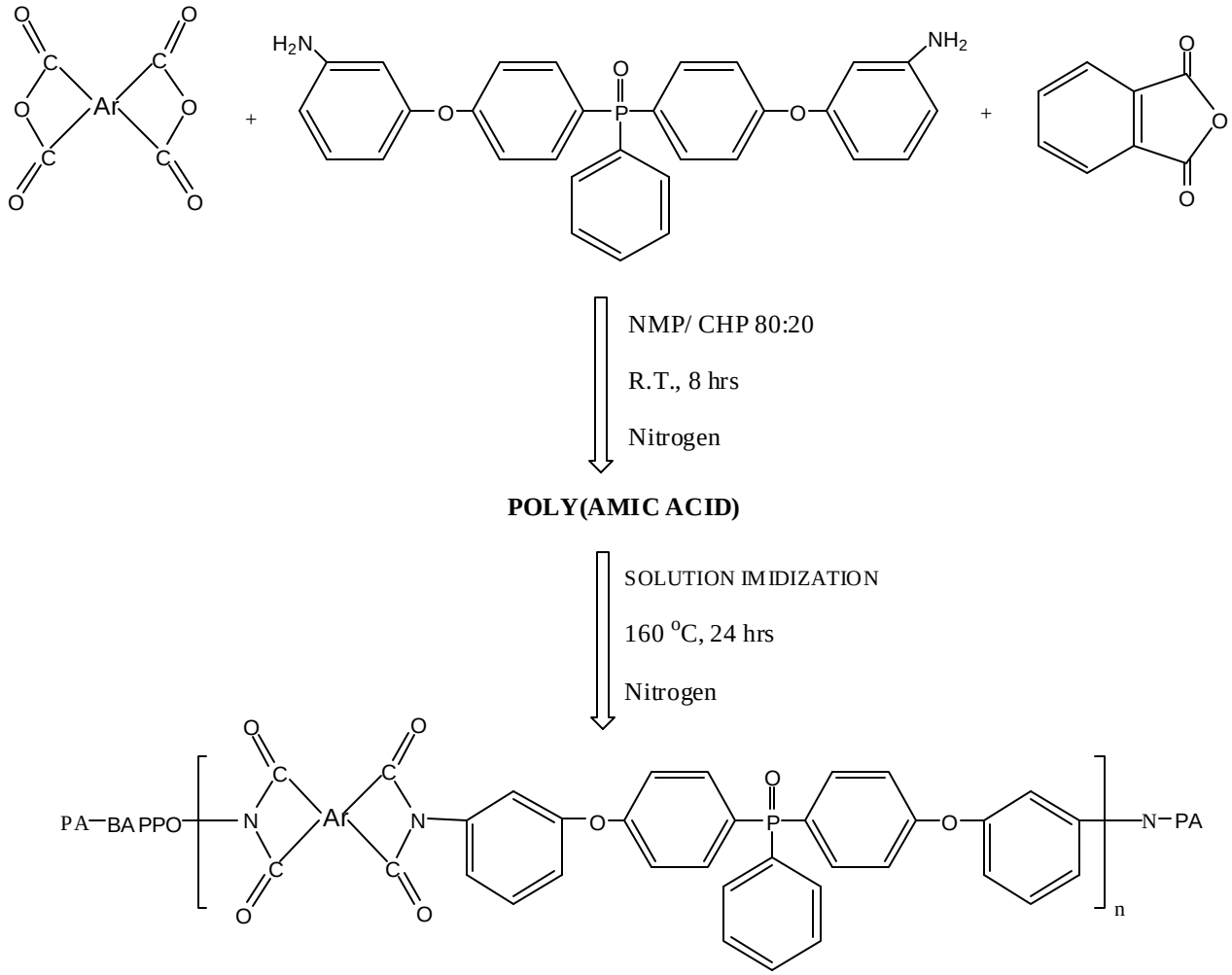

Ar = BPDA, BTDA, ODPA, PMDA, and 6FDA

Scheme 2.5 Synthesis of m-BAPPO Based Polyimides via Solution Imidization[74].

74. Lee, Y.J., Gungor, A., Yoon, T.H., McGrath, J.E., *J. Adhesion*, 55, **1995**, 165.

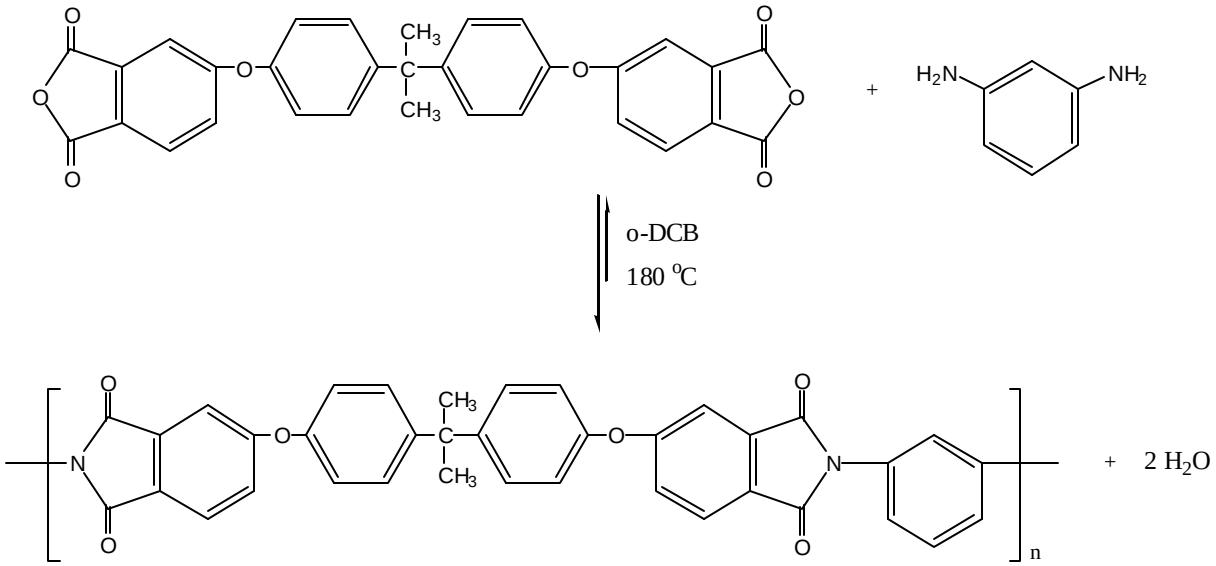

Scheme 2.6 Ultem™, high temperature solution imidization[47]

To prepare soluble, fully cyclized polyimides containing aryl groups, the rigid-rod structure must be modified to reduce stiffness and interchain ordering. Several strategies that have been developed to make soluble amorphous polyimides without sacrificing the excellent physical properties[44,75,76] are briefly outlined below:

(a) Incorporating flexible bridging units between aryl groups, such as –O–, $-CH_2-$, $-SO_2-$, –C(=O) –, $-C(CF_3)_2-$, –S–, and –P(=O)–

(b) Utilizing "kinked" or isomeric (*eg*. indane) linkages such as meta- or ortho-catenation between rings.

(c) Introduction of asymmetrical and cardo (loop) structures along the backbone.

75. Huang, S.J., Hoyt, A.E. *TRIP* **1995**, 3, 262.

76. **(a)** Sato, M. *Polyimides*; In *Plast. Eng.: Handbook of Thermoplastics*, V. 41; Marcel Dekker: **1997**; **(b)** Farr, I.V., Kratzner, D., Glass, T.E., Dunson, D., Ji, Q., McGrath, J.E., J. Polym. Sci.:Part A: Polym. Chem., Vol. 38 (**2000**), 2840-2854.

(d) Incorporating bulky pendant groups along the chain.

(e) Controlling molecular weight and endcapping with monofunctional endcappers.

Molecular weight must be sufficiently high to attain good mechanical properties, but it must not be so high that it leads to solubility/processing problems. Therefore, the reactive amine or anhydride endgroups can be capped to prevent further reaction and buildup of extremely long chains.

The effects of using one or several of these strategies on polyimide physical properties will be discussed in a separate section entitled "Structures and Properties".

The advantages of a soluble amorphous polyimide include the following:

(1) The reaction requires only one step: homogenous solution imidization.

(2) Usually fever than 1% of the amic-acid groups remain unimidized.

(3) Polyimides are hydrolytically stable compared to poly(amic) acids and, therefore, may be stored at ambient conditions for long periods of time.

(4) Polyimide solids may be re-dissolved in polar solvents suitable for spin casting or solution casting films.

(5) When the films are being heat processed, there is no release of water to form voids and cause shrinkage.

(6) Amorphous polyimides are transparent and usually exhibit isotropic physical properties.

Kinetic and Mechanistic Aspects of High-Temperature Solution Imidization

During thermal imidization of solid poly(amic)acid films there is an increase in T_g and simultaneous decrease in molecular motion which prevents complete conversion to imide. In contrast, the increased entropy of high-temperature solution imidization provides adequate chain mobility throughout the reaction. Homogenous solution conditions and elevated temperatures are believed to facilitate the rapid exchange of kinetically non-equivalent conformations[77]. In this case, the kinetics would be governed by the chemical reactivity of the amide-acid groups and not by the limited mutual accessibility of reacting groups resulting from unfavorable conformations.

77. Kim, Y.J., Glass, T.E., Lyle, G. D., McGrath, J.E. *Macromolecules* **1993**, 26, 1344

Kim *et al.* conducted extensive studies on the kinetics of high-temperature solution imidization and proposed a reaction mechanism for the imidization of homogenous systems in solution[77] (Scheme 2.7). The percentage of unreacted acid groups was followed as a function of reaction time by non-aqueous potentiometric titrations using a standardized weak base, tetramethylammonium hydroxide. The degree of imidization was calculated and provided a linear fit when utilized in a second-order kinetic equation. Second-order kinetics with respect to the PAA links were also confirmed by demonstrating that the rate of imidization depended on the initial amic-acid concentration. Additionally, reaction rates were found to increase after introducing small amounts of monofunctional acid catalyst. This information led to the proposed reaction mechanism as shown in Scheme 2.7, which was consistent with a second-order, auto-catalyzed nucleophilic acyl substitution. Indeed, the nucleophilicity of the amide nitrogen was found to influence the reaction rate; electron-donating bridging units, incorporated from relatively more basic diamines such as ODA, resulted in faster rates.

The rate-determining step in this process, which is second order with respect to PAA and acid catalyzed, was recently confirmed by Furukawa et al.[78]. Kim et al.[77] monitored the imidization by monitoring residual amic-acid content and intrinsic viscosities as functions of imidization time at a given temperature. The results revealed the effects of temperature and time in obtaining fully-cyclized high molecular weight polyimides (Figure 2.8). During the initial stages of imidization, the intrinsic viscosity was observed to decrease drastically. This was attributed to chain-scission of the amic-acid. The degradation was confirmed by ^{1}H NMR where the appearance of the new peaks at 6.67 and 6.85 was attributed to aromatic protons adjacent to terminal amino groups (Figure 2.9). The gradual disappearance of those extra new peaks, as well as the increase in the intrinsic viscosity with increasing reaction time indicated re-formation of the chains. The extent of the re-formation and subsequent imidization reactions was shown to be a function of the reaction temperature at a given time: higher temperatures resulted in fewer residual amic-acid functionalities and higher intrinsic viscosities. For example, complete backbone cyclization shown in Figure 2.9 occurred at 180 ^{o}C within 12 hours.

78. Furukawa, N., Yuasa, M., Kimura, Y., *J. Polym. Sci.: Part A: Polym. Chem*., 36, **1998**, 2237

At lower temperatures, e.g. 140 ^{o}C and 150 ^{o}C, however, even after 24 hours, incomplete imidization was evident.

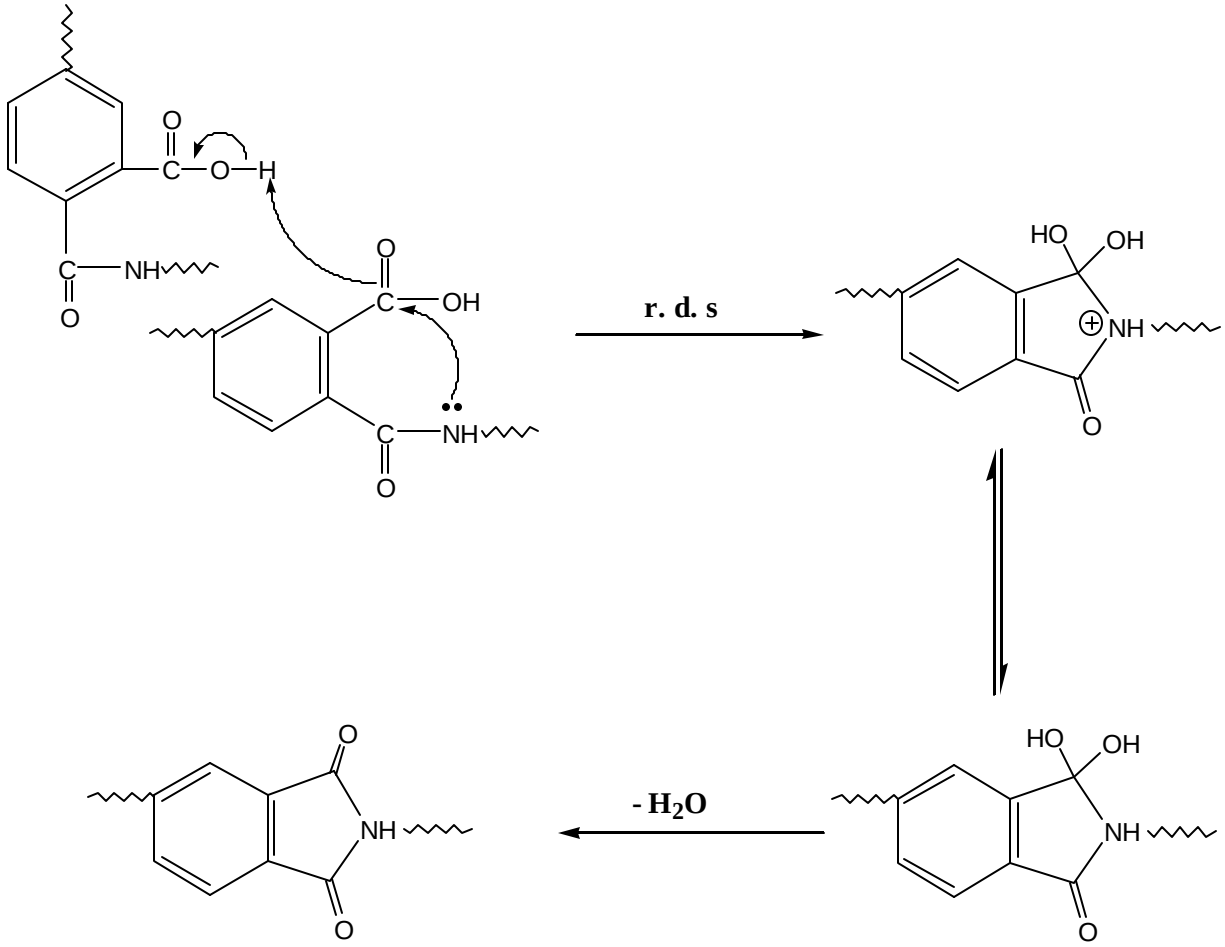

(r.d.s ≡ rate determining step)

Scheme 2.7 Mechanism of high-temperature solution imidization[77].

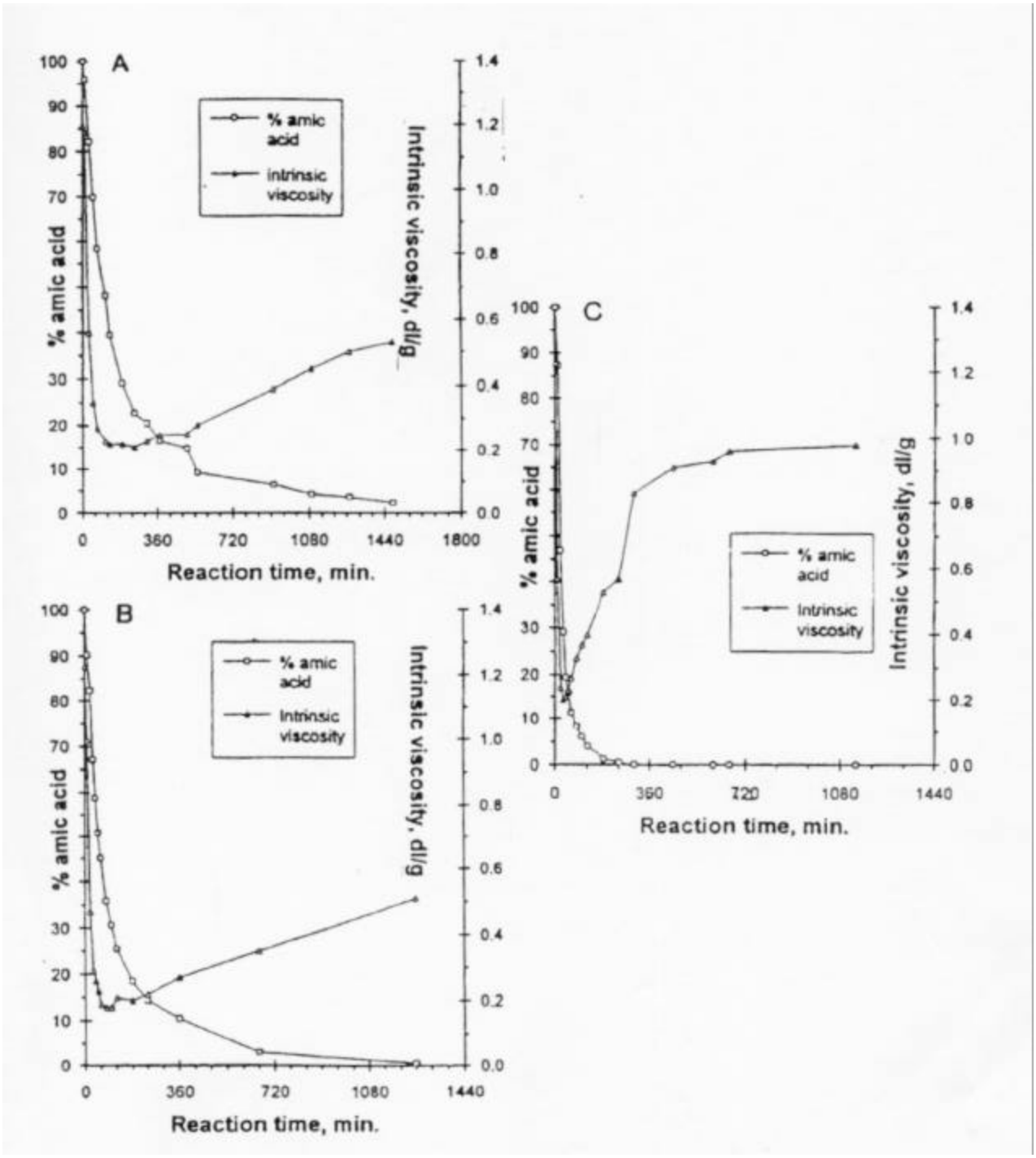

Figure 2.8 Remaining amic-acid content and intrinsic viscosity as a function of reaction time: (A) at 140 ^{o}C; (B) at 150 ^{o}C; (C) at 180 ^{o}C[77].

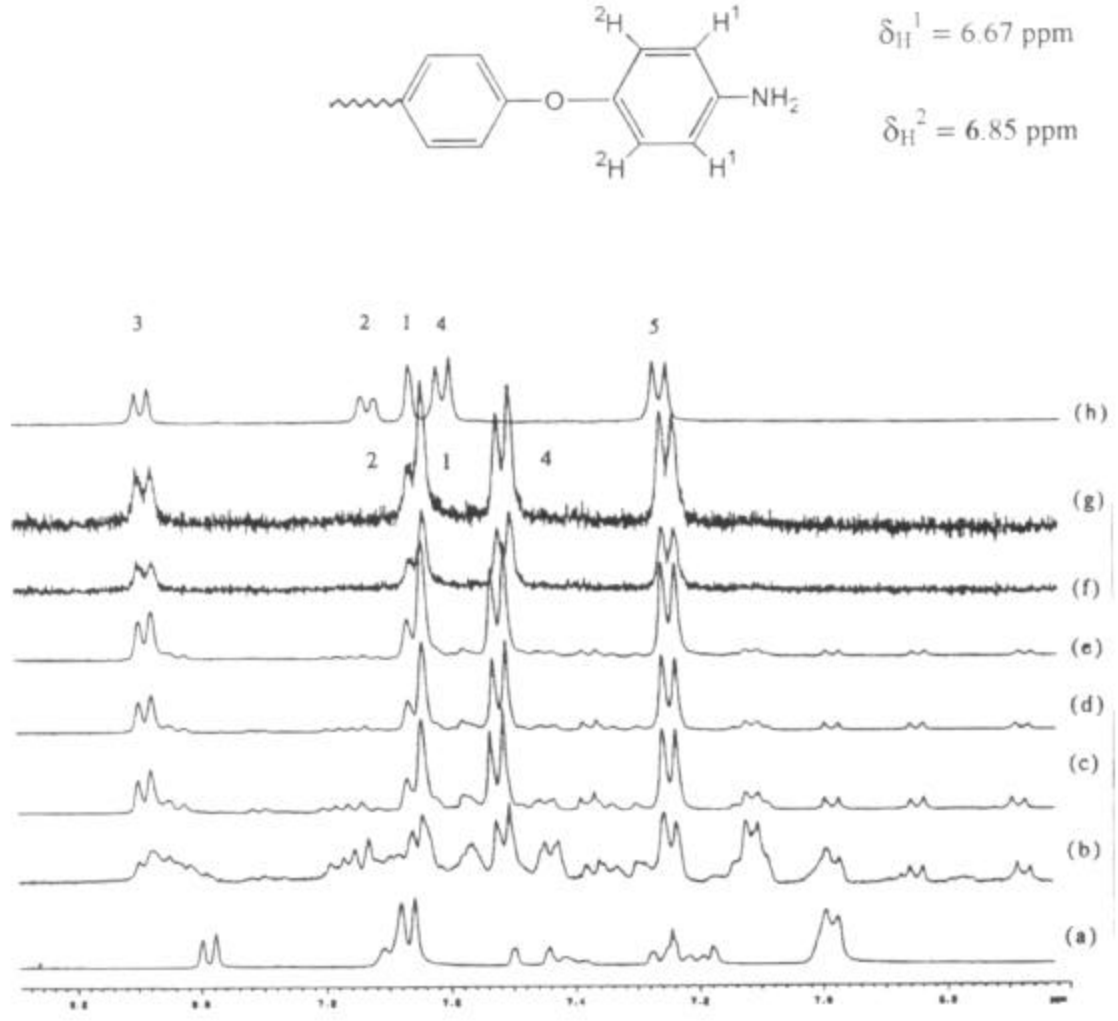

Figure 2.9 ^{1}H-NMR Spectrum of 4,4'-ODA/ODPA poly(amic) acid/imide at different imidization stages (180 ^{o}C): (a) 0 h, poly(amic) acid; (b) 0.33 h; (c) 0.66 h; (d) 1.0 h; (e) 1.66 h; (f) 3 h; (g) 11 h diluted with dry NMP.

These results imply that proper conditions must be employed during high-temperature solution imidization to achieve complete cyclization and maintain high molecular weight, as incomplete imidization will affect the end-use properties. It is well known that o-carboxylic acids significantly promote hydrolysis of amide linkages.

2.2.1.5 Synthesis of Polyimides Via the Ester-Acid Route

During the 1970's, NASA modified the reactivity of dianhydrides by preparing diester-diacid derivatives using aliphatic alcohols[79]. The modified structure imparted hydrolytic stability, thereby improving handling. Additionally, the dicarboxylic acid diesters were unreactive when combined with diamines at ambient temperatures. This allowed the formulation of stable solutions containing both monomers, which were used to impregnate carbon fiber composites. A staged heating process was applied to effect *in situ* polycondensation and imidization. Thermosetting resins, called PMR-15, were prepared by incorporating an endcapping group for crosslinking via addition polymerization during post-cure[78-80]. Advantages of this method included prolonged shelf life and low viscosities at high monomer concentrations. The thermal and mechanical properties of the cured resins were comparable to those of control polyimides prepared by the classical method.

The chemistry of tetracarboxylic diesters has led to an alternative high temperature solution imidization route for preparing soluble polyimides[38,81-84]. In this one-pot synthetic route, the monomeric dianhydride is pre-reacted with an aliphatic alcohol, such as methanol or ethanol, in the presence of a tertiary amine catalyst, eg. triethylamine, to form the o-ester-acid of the dianhydride (Scheme 2.8.a)[85] Excess

79. Serafini, T.T. Delvigs, P., Lightsey, G.R. *J. Appl. Polym. Sci*. **1972**, 16, 905.
80. Vannucci, R.D. Proc. *32nd Intnl. SAMPE Symp*. **1987**, 602.
81. Moy, T.M. *Ph.D Thesis*, Virginia Tech., **1993**.
82. Moy, T.M., DePorter, C.D. McGrath, J.E. *Polymer*, **1993**, 34(4), 819.
83. Tan, B. *Ph.D. Thesis*, Virginia Tech, **1997**.
84. Tan, B., Tchatchoua, C.N., Dong, L., McGrath, J.E. Polym. Adv. Technol. **1997**, 9, 84.
85. Farr, I.V., Glass, T.E., Ji, Q., McGrath, J.E. *High Perf. Polym*. **1997**, 9, 345.

alcohol, used as a solvent, was subsequently distilled from the reaction flask leaving a viscous mixture of dialkylester-diacid. The next step in this procedure involved the addition of diamine with a solvent such as NMP, which contained an azeotroping agent. When the solution was heated to high temperature (170-185 ^{o}C), the monomers reacted to form poly(amic) acid with evolution of alcohol. Due to the high temperature and the effective removal of water as azeotrope, both chain growth and imidization could proceed to high levels in the homogenous solution.

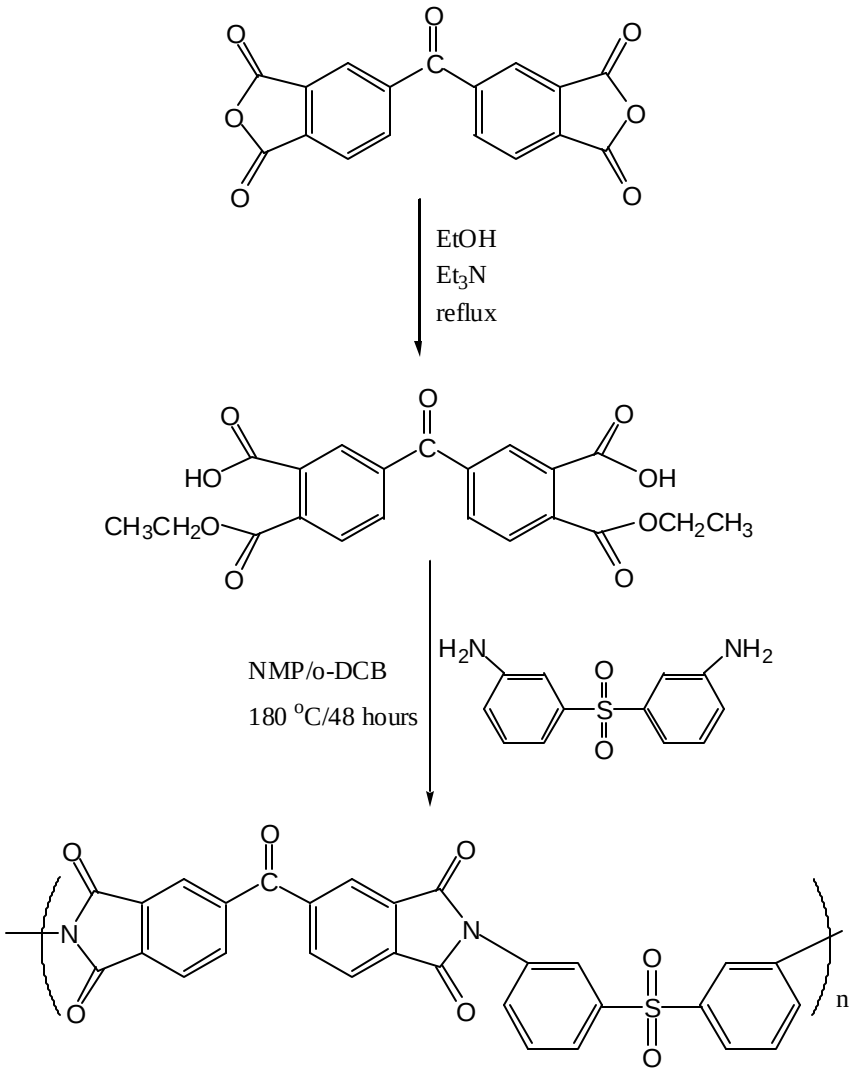

Scheme 2.8.a Synthesis of Polyimides via Ester-Acid Solution Imidization Route[81]

Huang et al. recently reported on the ring opening selectivity of various dianhydrides towards alcohols (Figure 2.10). The isomeric ratios were found to be independent of alcohol structure but quantitatively correlated with the electron affinities of the different bridging groups (Scheme 2.8.b and Table 2.4)[86]. Thus, not only does the derivative possess superior hydrolytic stability, but it is also more soluble than the dianhydride. The ester-acid route is more versatile than classic amic acid synthesis due to the following reasons:

(1) Eliminates the necessity for drying the solvents or apparatus
(2) Monomers are readily dissolved which prevents interfacial-type interactions
(3) Imidization is performed in a one-pot process

During early studies utilizing FTIR, the formation of poly(amic) acid was not detected as a reaction intermediate using diester-diacids and aromatic diamines[87]. Therefore, the acylation of the diamine by the ester functionality appeared to be negligible. Instead, it was noticed that significant amounts of anhydride appeared which did not arise from hydrolytic degradation. Moy et al. showed in their FTIR studies that the diester-diacid derivative of BTDA readily formed the dianhydride during heating in NMP/o-DCB to 120-140 ^{o}C[82]. Model reactions showed that acylation of aniline did not happen under the same conditions using either diethyl phthalate or benzoic acid. However, when the monoester of phthalic acid was refluxed in toluene, the corresponding phthalimide was obtained.

86. Huang, W., Tong, Y., Xu, J., Ding, M. *J. Polym. Sci. Part A: Polym. Chem*. **1997**, 35, 143.

87. Johston, J.C., Meador, M.A.B., Alston, W.B. J. Polym. Sci. Part A: Polym. Chem. 1987, 25, 2175.

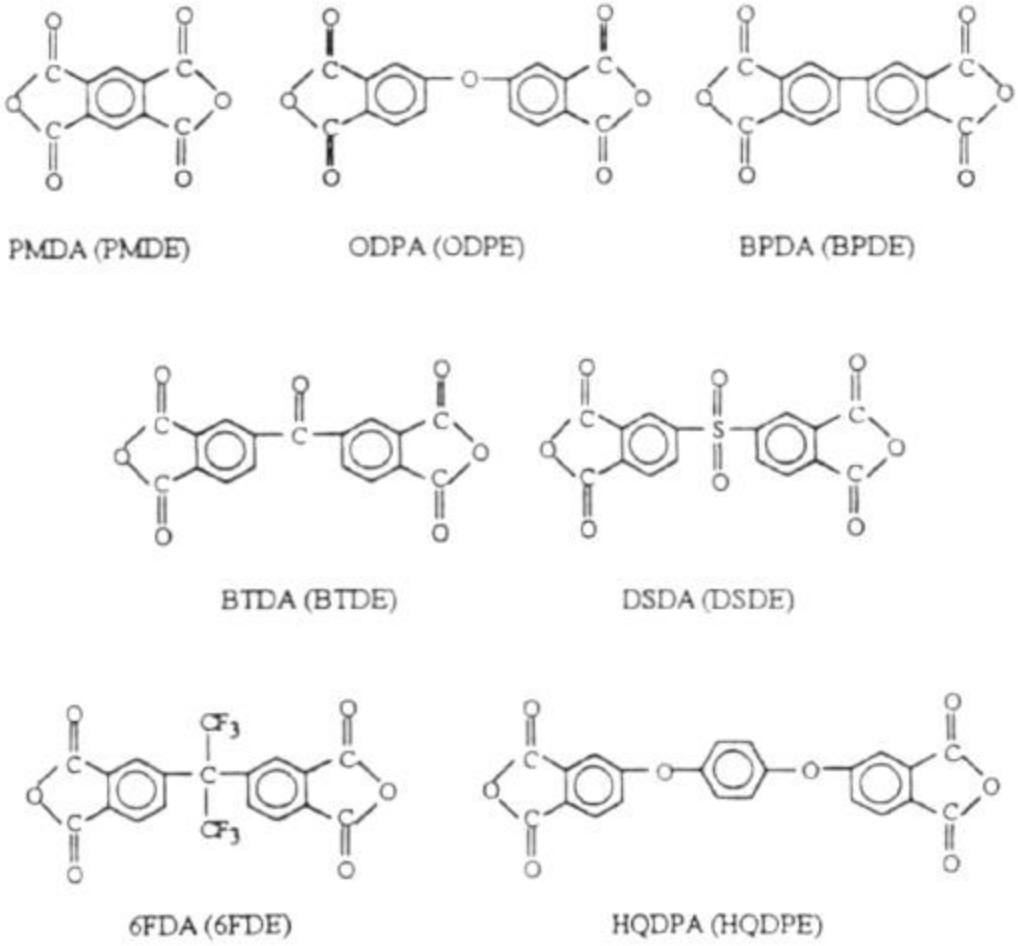

Figure 2.10 Dianhydrides for Methanolysis Reaction[86]

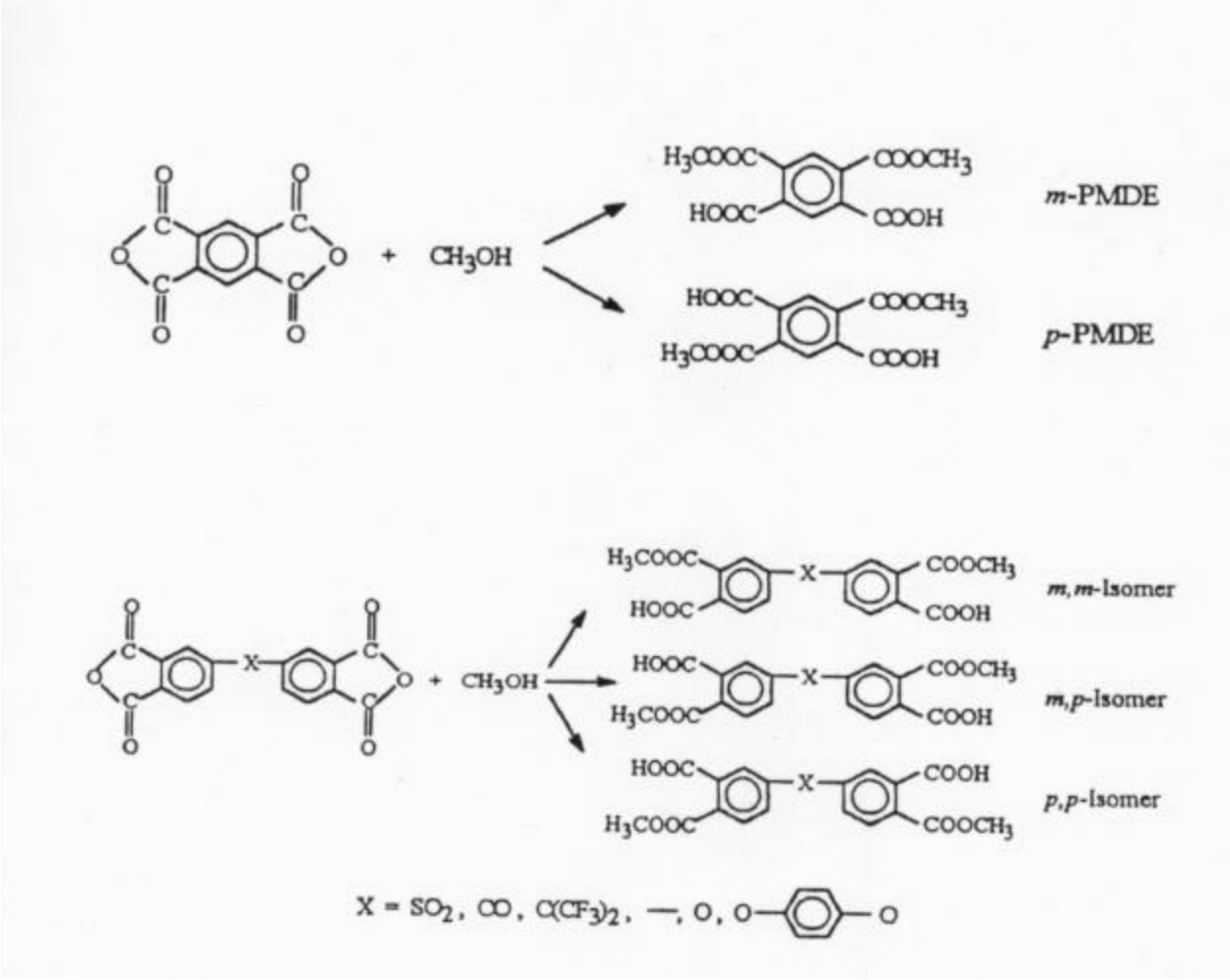

Scheme 2.8.b Synthesis of the Three Isomers of Diester-Diacids Prepared from Bridged Dianhydrides[86]

Table 2.4 ^{1}H NMR Chemical Shifts (ppm), Ea (eV) and Relative Abundance of meta- and para-positions[86]

Diester-Diacids	Ea	Relative Abundance para	meta
DSDE	1.57	0.62	0.38
BTDE	1.55	0.57	0.43
6FDE	–	0.52	0.48
BPDE	1.38	0.43	0.57
QDP E	1.30	0.34	0.66
HQDPE	1.19	0.26	0.74

This suggested that the mechanism of ester-acid solution imidization involved in-situ generation of anhydride, which became the acylation agent for the aromatic diamine (Scheme 2.9)[87]. Since amic-acid is an intermediate in this case, it seems reasonable to conjecture that its lifetime is extremely short and that immediate cyclization to imide occurs. The low concentration would render corresponding amic-acid vibrations in the FTIR below the detection limits.

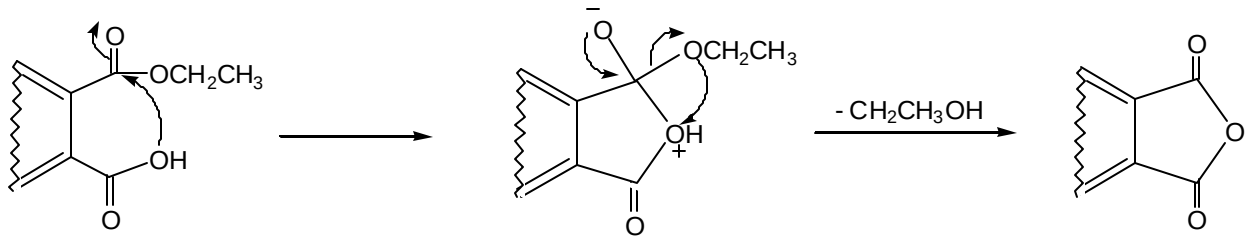

Scheme 2.9 Mechanism of anhydride formation during ester-acid solution imidization route to polyimides

The ester-acid route is found to be further advantageous when one of the monomers is an aliphatic diamine. During classic amide-acid synthesis, the higher basicity of aliphatic diamines was found to cause intra- and inter-molecular salt formation by extraction of carbonyl protons by amino endgroups (Figure 2.11)[88,89]. The amic-acid salts were found to have low reactivity under normal conditions at room temperature and, therefore, only low molecular weight amic-acids could be obtained. On the other hand, when the ester-acid method was employed, high molecular weight polyimides were obtained using aliphatic diamines[87]. It has been surmised that the intermediate consists of an amide-ester, which lacks the highly acidic carboxyl protons. Since they are relatively more basic, it is plausible that aliphatic diamines are sufficiently nucleophilic to effect acyl substitution at the carbonyl carbon.

88. Kreuz, J.A., Hsiao, B.S., Renner, C.A., Goff, D.L. *Macromolecules*, **1995**, 28, 926.

89. Seino, H. *J. Polym. Sci. Part A: Polym. Chem*. **1999**, 37, 3584.

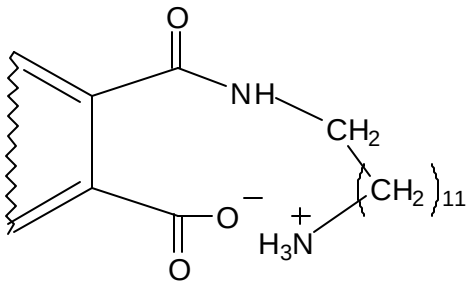

Figure 2.11 Intramolecular poly(amic) acid salt from aliphatic amino group

2.2.2 Additional Methods for Synthesizing Polyimides

The methods of synthesizing polyimides that have been described thus far can be utilized for both soluble and insoluble systems. However, there are numerous other ways to produce polyimides, but many are limited to soluble polyimides or are restricted in some other manner.

2.2.2.1 Synthesis of Polyimides via Derivatives of Poly(amic acid)s

During classical poly(amic) acid synthesis, proton transfer by the o-carboxylic acid group initiates reversal of the polycondensation reaction. Derivatization has been utilized to convert the acid to a species such as an ester, incapable of releasing an acidic proton, under the standard reaction conditions. Ester-amide derivatives have been successfully prepared by utilizing diester-diacyl chloride monomers in solution polycondensation reaction with diamines[31,86,90-91]. These derivatized polymers have been found to be useful as photosensitive polyimide precursors[85] in electronics applications and as thin film dielectrics[92]. The improved hydrolytic stability and solubility of the poly(ester-

90. Stoffel, N.C., Kramer, E.J., Volksen, W., Russell, T.P. *Polymer* **1993**, 34(21), 4524.

91. Carter, K.R., Srinivasan, S.A., Hedrick, J.L., Miller, R.D., Lee, V.Y., DiPietro, R.A., Nguyen, T. In *Advances in Polyimides and Low Dielectric Polymers*, Sachdev, H.S., Khojasteh, M.M., Feger, C. (eds), Soc. Plast. Eng., **1997**.

92. Yoda, N., Hiramoto, H.J. *Macromol. Sci. Chem*. **1984**, A21(13&14), 1641

amide) precursors allow for the isolated product to be stored and then reformulated in suitable solvents as needed for spin casting[91].

Imidization processing of the films is similar to that of poly(amic) acids: (1) thermal, which requires somewhat higher temperatures than used for amide-acids, and (2) chemical, using a base such as triethylamine to remove the amide proton[31]. FTIR studies indicated that chain scission side reactions involving decomposition of ester-amide to anhydride and amine groups are absent during thermal imidization of poly(amide ester)s[93]. This results in retention of high molecular weight and hydrolytic stability of the films.

2.2.2.2 Aromatic Nucleophilic Displacement Polymerization

It was recognized in the early 1970s that the insertion of ether linkages into the polyimide main chain provided increased flexibility, which greatly enhanced the solubility and processing characteristics[94]. As described above concerning production of G.E.'s Ultem, it is possible to synthesize soluble polyetherimides by direct solution polymerization of ether-containing dianhydrides and diamines. However, during the early development of Ultem, G.E.'s chemists performed a new type of synthesis involving nucleophilic aromatic substitution reactions. This involved the development of new bisnitroimide monomers, which were capable of undergoing nucleophilic displacement reactions with bisphenolates in dipolar aprotic solvents (Scheme 2.10).

Bisnitroimide monomers have been obtained in high yields by reaction of either 3- or 4-nitrophthalic anhydride with aromatic diamines, such as m-PDA, in acetic acid solvent. Utilization of reflux temperatures and azeotropic agents afforded fully imidized monomers[95]. Bisphenoxide monomer preparation consisted of heating a bisphenol,

93. Stoffel, N.C., Kramer, E.J., Volksen, W., Russell, T.P., *J. Polym. Sci. Part B:Polym. Phys*. **1998**, 36, 2247.

94. Takekoshi, T., Kochanowski, J.E., Manello, J.S., Webber, M.J. *J. Polym. Sci. Polym Symp*. **1986**, 74, 93.

95. White, D.M., Takekoshi, T., Williams, F.J., Relles, H.M., Donahue, P.E., Klopher, H.J., Loucks, G.R., Manello, J.S., Matthews, R.O., Schluemz, R.W. *J. Polym. Sci. Polym. Chem. Ed*. **1981**, 19, 1635

dissolved in DMSO, with an aqueous sodium hydroxide solution in the presence of toluene to azeotropically dehydrate the product[96].

During polymerization of these monomers, attack of the phenoxide at the nitro-substituted aryl carbon resulted in a resonance stabilized Meisenheimer transition state (Figure 2.12)[12]. The reaction was favored with strongly nucleophilic bisphenoxides giving high molecular weight polyimides[96]. When the phenolate salts of benzenediols were utilized, such as resorcinol and hydroquinone, a competing redox side reaction occurred, which resulted in lower molecular weight polymers[95].

In the presence of water, only low molecular weight polyimides were obtained[96]. Hydrolytic ring opening of the imide caused bisphenoxide to become inactivated due to its ready acceptance of carbonyl protons from amide-acid groups.

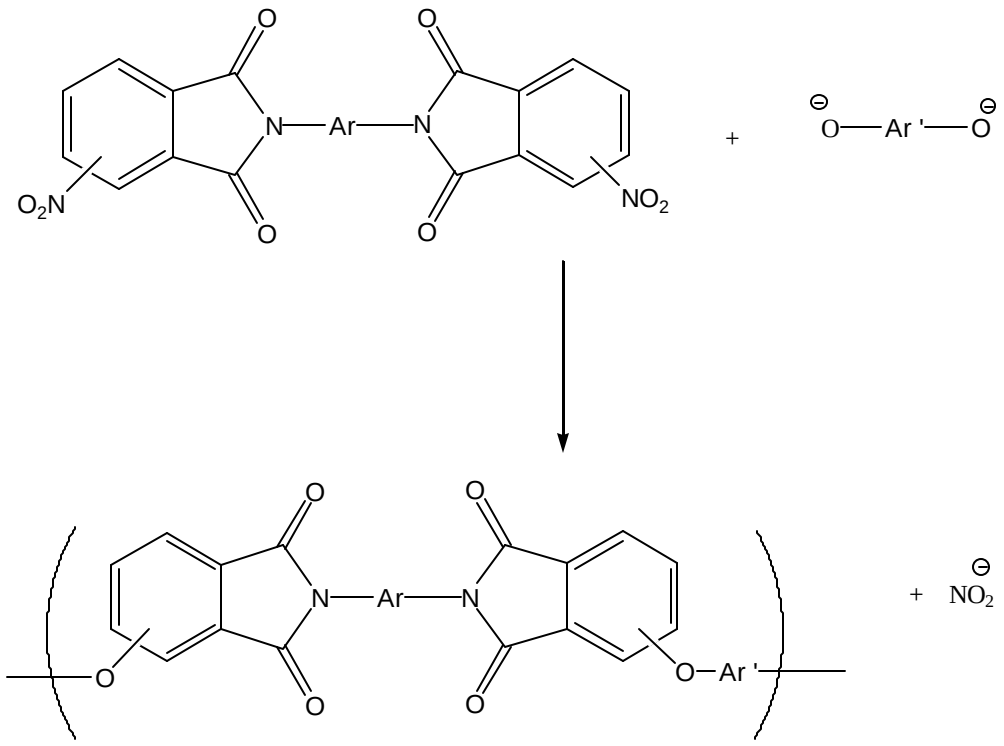

Scheme 2.10 Reaction of activated nitrobisimide monomer with bisphenoxide

96. Takekoshi, T., Wirth, J.G., Heath, D.R., Kochanowski, J.E., Manello, J.S., Webber, M.J. *J. Polym. Sci. Polym. Chem Ed*. **1980**, 18, 3069.

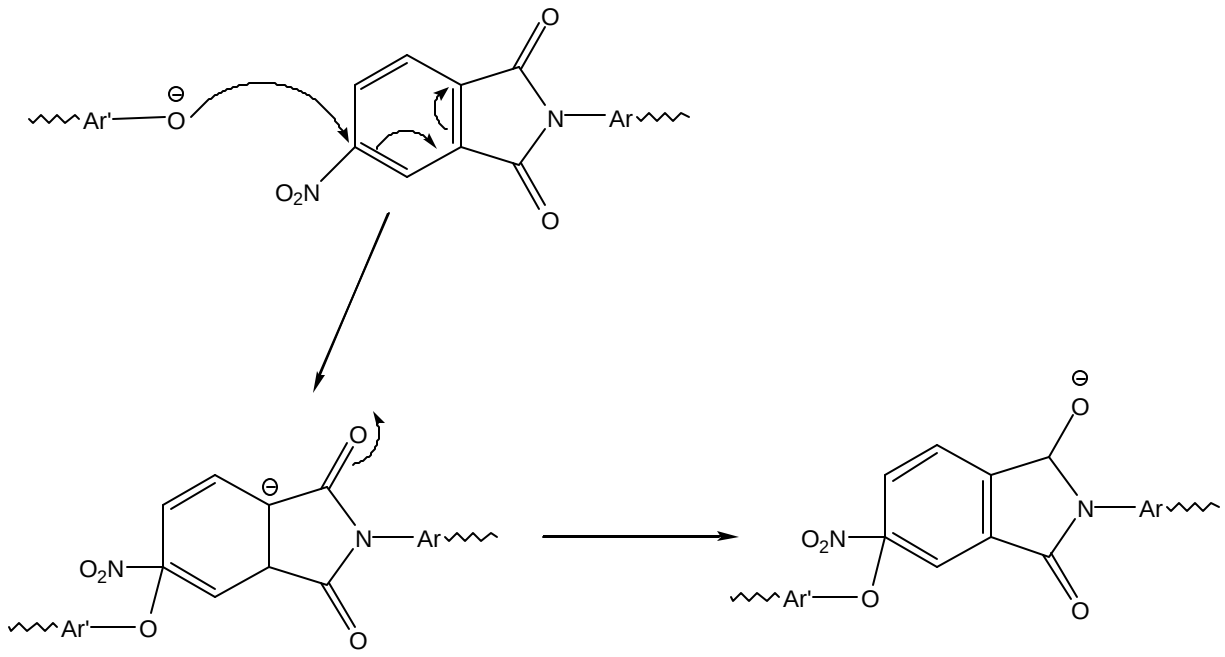

Figure 2.12 Delocalization of Negative Charge in Meisenheimer Transition State in an Imide System[12]

2.2.2.3 Polymerization of Diisocyanates and Dianhydrides

The reaction of aromatic diisocyanates with dianhydrides has been utilized to synthesize polyimides with a biproduct of carbon dioxide[97-103]. The chemistry, developed during the late 1960s, was subsequently investigated to elucidate the reaction mechanism and the effect of conditions on product yields. It was found that the imidization path depended on the reaction conditions.

Although the mechanism is still vague, it has been observed that the reaction proceeds at relatively moderate temperatures (at ~ 40 ^{o}C) in dipolar aprotic solvents, in the presence of alcohols, water or tertiary amines.

In the case of alcohol, it was proposed that a urethane, formed by the reaction of alcohol and isocyanate, underwent slow reaction with anhydride to form imide[99]. Consequently, regeneration of alcohol and evolution of carbon dioxide occurred as a result.

The mechanism with water as a catalyst, on the other hand, has been thought to proceed through the hydrolysis-reaction product of isocyanates, urea, which decomposes to amine and carbon dioxide[98]. In this case, the amine reacts with anhydride to give amic-acid, which subsequently imidizes by releasing water.

It was also reported that high molecular weight polyimides were obtained using mixtures of anhydrides and their corresponding tetracarboxylic acids with diisocyanates in the presence of tertiary amines[99]. Although, the mechanistic role for carboxylic acid groups in the reaction of diisocyanates with dianhydrides has not been understood very well, high molecular weights have been obtained, suggesting that the stoichiometry was

97. Farrissey, W.J., Rose, J.S., Carleton, P.S. *J. Appl. Polym. Sci*. **1970**, 14,1093.
98. Carleton, P.S., Farrissey, W.J., Rose, J.S. *J. Appl. Polym. Sci*. **1972**, 16, 2983.
99. Alvino, W.M., Edelman, L.E., *J. Appl. Polym. Sci*. **1975**, 19, 2961.
100. Alvino, W.M., Edelman, L.E., *J. Appl. Polym. Sci*. **1978**, 22, 1983.
101. Ghatge, N.D., Mulik, U.P., *J. Polym. Sci., Polym. Chem. Ed*. **1980**, 18, 1905.
102. Shinde, B.M., Ghatge, N.D., Patil, N.J. *J. Appl. Polym. Sci.* **1985**, 30, 3505.
103. Wenzel, M., Ballauff, M., Wegner, G. *Macromol. Chem.* **1987**, 188, 2865.

not upset by the presence of hydrolyzed anhydrides as it would have been in classic polyimide synthesis via amic-acids.

In Volksen's review, a mechanism has been proposed to address the role of the hydrolyzed species (Scheme 2.11)[31]. In the presence of water, the anhydride and isocyanate hydrolyze simultaneously to dicarboxylic and carbamic acids, respectively (reactions 1 and 2). Some of the carbamic acid reacts with isocyanate to form urea (reaction 3). It has been suggested that the urea is capable of reacting slowly with anhydride to form imide[98], so the presence of urea would not limit the molecular weight. Additionally, either product of the hydrolysis, carbamic acid or diacid, is capable of reacting to form a mixed carbamic carboxylic anhydride (reactions 4 and 5, respectively). Subsequent heating causes the mixed dianhydride to cyclize generating imide with the loss of carbon dioxide and water. Kakimoto et al. has recently formed soluble polyimides in benzonitrile using bulky diisocyanates[104] (Scheme 2.12)

Furthermore, a cyclic seven-membered intermediate has been proposed for uncatalyzed reactions in the melt or in anhydrous solutions, which is directly formed by anhydride and isocyanate groups (Figure 2.13)[31,105]. This intermediate is believed to split out carbon dioxide when heated to form five-membered imide rings.

The lack of understanding of the precise conditions required for quantitative conversion of diisocyanates and dianhydrides to polyimides has delayed wider application and potential commercialization of this synthetic method. The potential for side reactions is an important drawback to this preparation method. For example, isocyanates can undergo dimerization, cyclotrimerization, and even polymerization to form Nylon-1[106].

104. Kakimoto, M., Akiyama, R., Negi, S., Imai, Y., *J. Polym. Sci., Part A: Poly. Chem*. 26 **1988**, 99.

105. Avadhani, C.V., Wadgaonkar, P.P., Vernekar, S.P. *J. Polym. Sci. Part A: Polym. Chem*. **1990**, 28, 1681.

106. Takekoshi, T., Webb, J.L., Anderson, P.P., Olsen, C.E. *IUPAC Abstracts: 32nd Intnl. Symp. on Macromol*. **1988**, 464.

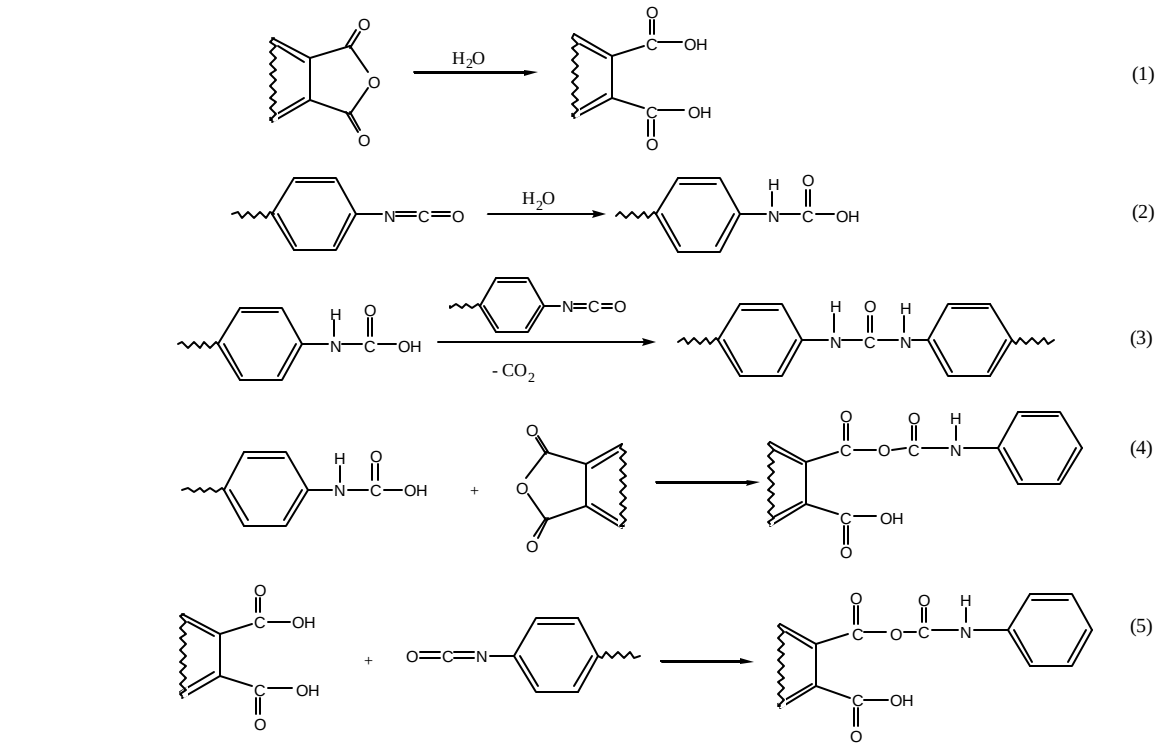

Scheme 2.11 Mechanism of water-catalyzed reaction of diisocyanates and dianhydrides

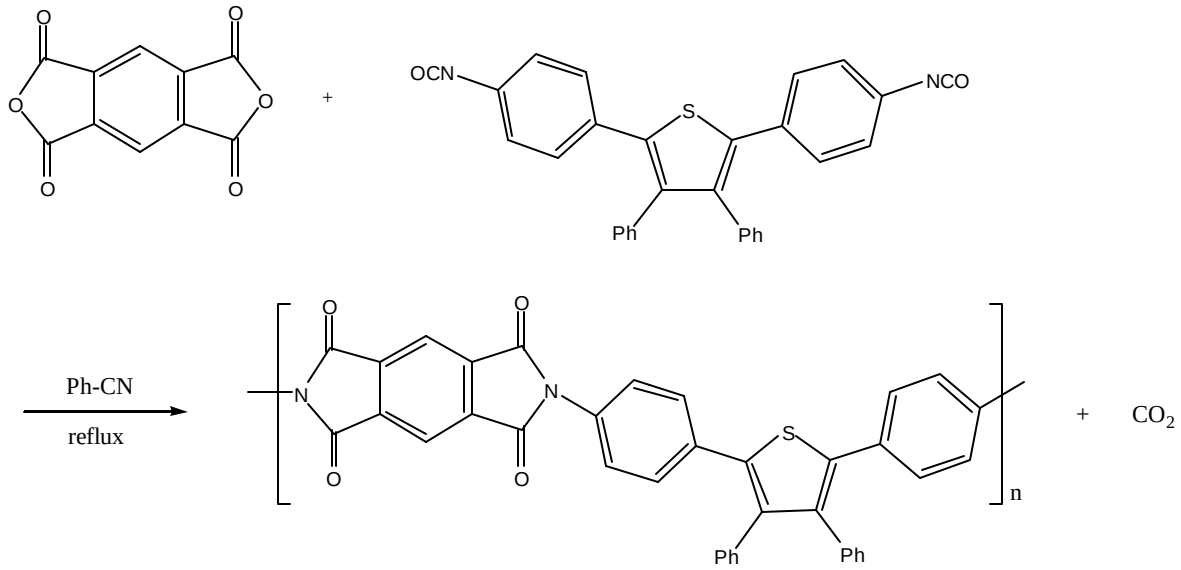

Scheme 2.12 Preparation of a Polyimide from a Dianhydride and Diisocyanate with Bulky Substituents[104]

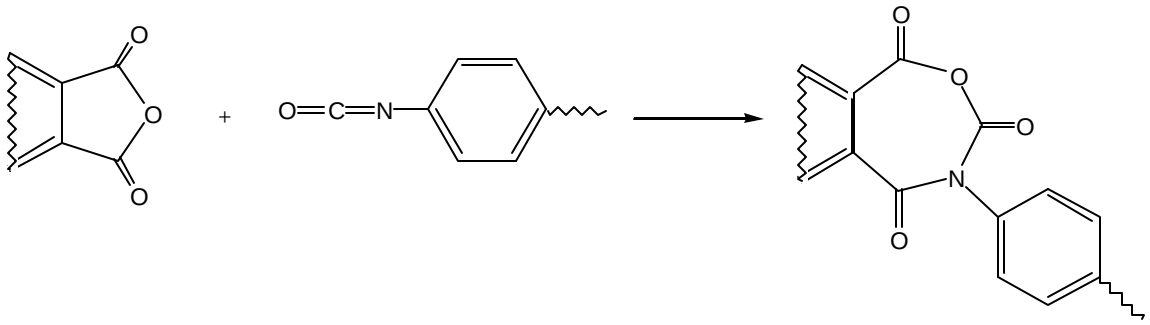

Figure 2.13 Proposed 7-membered cyclic intermediate in the reaction of isocyanate with anhydride[31,105]

2.2.2.4 Synthesis of Polyimides by Transimidization

High molecular weight homo- and co-polyimides can be prepared via a transimidization reaction involving an amine-imide exchange with either aromatic or aliphatic amines including aminofunctional siloxane oligomers (Scheme 2.13). This one-step method is used for soluble/tractable polyimides, which polymerize in solution or in the melt.

At high temperatures, N,N'-substituted bisimide monomers can undergo nucleophilic attack by diamines at the imide carbonyl carbon. This generates an amic-amide intermediate, which can re-cyclize to form imide. The ejection of a monoamine leaving-group during cyclization provides polymer chain growth. However, since this is an equilibrium process, the leaving group can also consist of the diamine.

Distillation of the volatile monoamine from the reaction assists in polymer formation by driving equilibrium to the right. Another driving force is the reduction in basicity/nucleophilicty of the mono-amine leaving group. Bisimides derived from heteroaromatic diamines such as 2-aminopyridine, readily undergo exchange reactions with aromatic diamines[106]. When the transimidization reaction involves aromatic amines

of similar nucleophilicity, organo-metallic catalysts containing zinc, lead, or cadmium can be utilized[107].

Compared to the conventional amic-acid route, the primary advantage of this method is the lack of water evolution during cyclization. Therefore, this technique can be employed with monomers containing groups that are easily hydrolyzed, such as ester or siloxane groups. Rogers et al., for example, utilized the transimidization method to synthesize perfectly alternating polyimide-polydimethylsiloxane copolymers[108,109]. Polyimide oligomers, having N-(2-pyrimidyl)phthalimide endgroup, were reacted with aminopropyl terminated dimethyl siloxane) oligomers in polar solvents at relatively low temperatures. This afforded high molecular weight polymers containing sequentially alternating hard- and soft-segments.

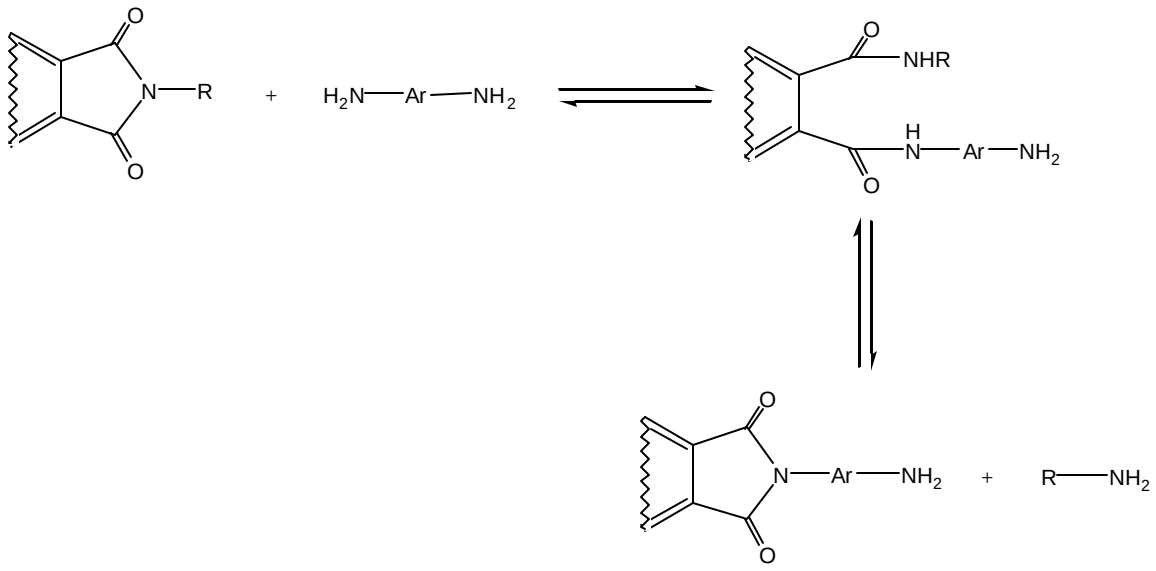

Scheme 2.13 Imide-amine interchange or transimidization reaction

107. Takekoshi, T., Kochanowski, E.J. *US Patent* 3,850855 (to General Electric), **1974**.

108. Rogers, M.E., McGrath, J.E. Polym. Prepr. 1993, 34(2), 1993.

109. Rogers, M.E., Glass, T.E., Mecham, S.J., Rodrigues, D., Wilkes, G.L., McGrath, J.E, *J. Polym. Sci. Part A: Polym. Chem.* **1994**, 32, 2663.

2.2.2.5 Polyimides by Nylon-Salt Method

As was mentioned earlier, initial efforts to make commercially viable polyimides involved the use of nylon-salt type of chemistry. However, this method gave some difficulties for aromatic diamines due to problems with low molecular weights, intractability, and processing. More recently, Imai and others have resumed the utilization of aliphatic diamines in high-pressure methods to produce high molecular weight crystalline polyimides by the salt method [109].

2.2.2.6 Polyimides by One-Step High Temperature Solution Imidization

Polyimides that are soluble in organic solvents are usually prepared by a so-called one- step solution polymerization route[110-1]. In this procedure, the dianhydride and diamine are stirred in a high boiling point solvent at 180-220 ^{o}C. Under these conditions, chain growth and imidization are believed to occur spontaneously. The water generated by imidization is usually allowed to distill from the reaction mixture.

The one-step method is especially useful in polymerization of unreactive dianhydrides and diamines. For example, it is known that rigid rod like polymers are insoluble and difficult to characterize, which limits their synthesis and applications. Phenylated dianhydrides cannot be used to prepare high molecular weight poly(amic acids). These sterically hindered monomers, however, react rapidly with diamines at elevated temperatures to give high molecular weight polymers[110-2]. Thus, one-step polyimidization in m-cresol by using a catalyst, usually isoquinoline, is a very useful method for the preparation of polyimides from especially unreactive dianhydrides and diamines which cannot form high molecular weight poly(amic acids) by the two-step method[14,25]. Besides m-cresol, nitrobenzene and α-chloronaphthalene containing isoquinoline are also mostly used for this imidization method.

---

109. Imai, Y. *Polym. Prep*. 35(1) **1994**, 399; Itoya, K., Kumagai, Y., Kakimoto, M. and Imai, Y. *Polym. Prep. Jpn*., 42, **1993**, 2109.

110. (1)-Beck & Co., French Pat. 1,373,383 (1964); Chem. Abst. 62 (1965) 10636; (2)-Harris, F., Feld, W.A. and Lanier, L.H., in Applied Polymer Symp. No. 26, (ed. Platzer, N.) Wiley, New York (1975), pp. 421-428.

Harris and coworkers have done extensive work using the one-step method[65-73], which was primarily involved in the development and use of phenylated monomers. The reactivity of these monomers at lower temperature is insufficient for successful polymerization, but the one-step process allowed high molecular weight polyimides to be synthesized.

The one-step imidization method can also yield a material with a higher degree of crystallinity than can be obtained from the two-step method. The excellent solvation of the polymer at high temperature may allow it to obtain a more favourable conformation for polymer chain packing[14].

Although it is believed that the mechanism of the one-step method is likely involves the formation of an amic acid intermediate, as in the two-step route, it appears that the amic acid is an extremely short-lived intermediate in the one-step imidization route. For example, the kinetic studies have shown that the rate-determining step in imide formation is the second order reaction between the anhydride and diamine. Therefore, imidization occurs either simultaneously with propagation, or very quickly afterwards. Evidence for the former is found in IR studies, which have not been abe to detect the presence of amic cid. The degree of imidization attained is essentially 100%. However, one research group claimed that they have determined two distinct rate constants, one for propagation and one for imidization. They also found that the initial rate constant remains constant only in the initial stages of the reaction.

2.3 POLYIMIDE PROPERTIES and APPLICATIONS

Polyimides are generally regarded as materials possessing high levels of thermal stability as well as excellent mechanical and electrical properties[12,14]. If designed properly, this class of polymers can exhibit high performance under a variety of environments such as short and long-term exposures to extreme temperatures, stresses, chemicals, and atmospheres. Since the commercialization of Kapton polyimide by DuPont, a large effort has been spent in developing other processable polyimides with even greater performance capabilities.

The expansive body of literature devoted to polyimides has resulted in a number of generalities concerning the structure-property relationships of these particular polymers[111]. For example, thermal stability is greater in wholly aromatic polyimides than those containing aliphatic moieties. Within the polyimide chain, larger amounts of internal mobility will equate to lower thermal transition temperatures and increased solubility. More energy is required for more rigid systems to induce mobility, leading to higher transition temperatures.

Semi-crystalline order in polyimides is the result of close packing of the polymer chains, which is primarily achieved in fairly rigid structures with a high degree of regular ordering. However, many material applications necessitate the absence of crystallinity, and consequently, modifications are made in molecular design to accomplish this goal. Flexible linkages are often utilized to eliminate such ordering. Also, the presence of asymmetry along the polyimide backbone can in some cases hinder polyimide crystallization. In addition, pendant side moieties such as alkyl groups can be incorporated in polyimide chains to disrupt possible crystallinity.

As with all polymers, molecular weight plays an important role with polyimides. Higher molecular weights result in more polymer entanglement, which may in turn leads to higher glass transition temperatures. A lower concentration of chain ends results in higher Tg. Higher molecular weights can also diminish the level of crystallinity in a polyimide due to the lack of mobility associated with high polymer viscosity. This subject will be covered in more detail in the following section.

111. Sroog, C.E., *Applications of High Temperature Polymers*, R.R. Luise (ed.), CRC Press, Boca Raton, 99, **1997**

2.3.1 Characterization of Polyimides

2.3.1.1 Molecular Weight and Endgroup Analysis

The molecular weight of a polyimide is a critical factor, because this paramater often dictates the physical properties, processability and film forming properties of these materials. Therein, the polymer molecular weight impacts not only the end use of the material, but also the means by which processing is conducted. It is well documented that polymers, in general, exhibit an increase in properties such as tensile strength, modulus, density, and glass transition temperature with increasing molecular weight[112]. Specifically, some of these properties are optimized upon reaching the onset of the entanglement molecular weight of the polymer, which is usually in excess of 10,000 grams per mole. Therefore, it is not surprising that a majority of commercially available thermoplastic condensation polymers report number average molecular weight values of 15,000 to 30,000 grams per mole.

Solubility is a must requirement for determining the molecular weight of a polymer with solution techniques. Soluble polyimides are characterized very easily. However, many polyimides are insoluble due to crystallinity, chain rigidity or network formation. Although poly(amic acid) (PAA) precursors of these polyimides are soluble, careful procedures need to be followed to correctly assess their molecular weight, due to the hydrolytic instability of the o-carboxylic amide linkages.

Among several solution techniques, solution viscosity is one easy method to indirectly investigate polymer viscosity average molecular weight. It is also a very useful technique, especially, if the empirical Mark-Houwink constants have been determined. However, the molecular weight distribution cannot be assessed thereby and it is often necessary to utilize additional techniques to better define the system.

The most used technique to determine the molecular weight and molecular weight distribution of a polymer is gel permeation chromatography (GPC), which is also known as size exclusion chromatography (SEC). Properly calibrated GPC allows the number, viscosity, weight and "z" average molecular weight to be determined. Moreover,

112. Rudin, A., *The Elements of Polymer Science and Engineering*, Academic Press, Orlando, 1982; Bilmeyer, Jr. F.W. Textbook of Polymer Science, 3rd ed., Wiley, New York, **1984**.

polymer-solvent pair intrinsic viscosity/molecular weight constants, K and a, and also the radius of gyration R_g can be determined.

It is common to use several monodisperse polystyrene samples of varying molar mass to generate a calibration curve for GPC. In the literature, thus, molecular weights relative to polystyrene molecular weights are often reported. In most cases, the actual molecular weight values are different. However, if GPC is coupled with a viscosity detector, the absolute molecular weight can be determined via the Universal Calibration method.

Several solvents including chloroform, tetrahydrofuran, and N-methylpyrrolidone (NMP) with 0.06 M LiBr, or NMP, strirred over P_2O_5 before use, served as good mobile phases for polyimides. The additiono of LiBr and P2O5 eliminates spurious high molecular weight peaks and is thought to suppress interactions between a polymer and the NMP solvent, and/or the stationary phase due to the polyelectrolyte or other "less defined"[3,112] effects.

Endgroup analysis via potentiometric titration experiments is a valuable and complementary technique to GPC[3]. Titration experiments may also be conducted to determine particular reactive functional group concentrations. The degree of polymerization via percent residual carboxylic acids as well as the number average molecular weight of polymers based on reactive difunctional endgroups can be calculated. Correlation of reactive group concentrations from titration and spectroscopic endgroup analysis with molecular weight data from GPC helps establish well-defined polyimide systems.

Membrane osmometry (for M_n), light scattering (for M_w), and low angle laser light scattering (LALLS) (for M_w) are among other well-established techniques to determine the molecular weight of a polymer.

112. Konas, M., Moy, T.M., Rogers, M.E., Shultz, A.R., Ward, T.C. and McGrath, J.E., *J. Polym. Sci., Part B: Polym. Phys.*, 33, 1429 (**1995**); Konas, M., Moy, T.M., Rogers, M.E., Shultz, A.R., Ward, T.C. and McGrath, J.E., *J. Polym. Sci., Part B: Polym. Phys.*, 33, 1441 (**1995**).

2.3.1.2 Structural Characterization

A number of structural changes occur when poly(amic acid)s are formed and subsequently imidized. Several spectroscopic methods play an important role to understand these chemical transformations. These are: Fourier Transform Infrared (FTIR), Raman, UV, and ^{1}H, ^{13}C, ^{15}N and ^{19}F NMR spectroscopies.

Functional groups are conveniently determined by FTIR. Characteristic absorptions are observed for the imide, anhydride, amine, isoimide and amic acid moieties. (Table 2.3). Although a great deal of structural information can be found in the later stages of imidization, FTIR cannot detect small amounts of uncyclized amic acid groups due to its insensivity. However, it can give semiquantitative data on the imidization process [113].

NMR spectroscopy is an often used method to the monitor imidization process. Imide conversion can be monitored from the ^{1}H NMR signal intensities of –COOH protons. ^{13}C NMR spectroscopy has been utilized to monitor thermal and chemical imidization as well as depolymerization[114]. ^{19}F NMR has also been conducted on fluorine-containing polyimides is in agreement with carbon-fluorine coupling constants[115].

2.3.1.3 Insolubility/Infusibility

Insolubility and infusibility of some polyimides have been rationalized to be due to crosslinks formed during the imidization process. Although, this is true in some cases, there are other possible explanations such as charge transfer complexes[116] and semi-crystallinity[117].

Insolubility which is probably due to the rigid macromolecular chain structure, can be reduced by incorporating several groups into the polymer backbone.

---

113. Moriyuki, S. Plast. Eng., Handbook of Thermoplastics, New York, 41 (1997).
114. Ando, S., Matsuura, T., Nishi, S., *Polymer*, 33, 2934 (**1992**).
115. Smith, C.D., Mercier, R., Watson, H., Sillion, B., *Polymer* 34, 4852 (**1993**).
116. Viallat, A., Bom, R.P., Cohen-Addad, J.P., *Polymer*, 35, 2730 (**1994**).
117. Muellerleile, J.T., Risch, B., Rodrigues, D.E., Wilkes, G.L., Jones, D.M., *Polymer*, 34, 789 (**1993**).

For example:

(a) Polar groups are placed either pendant to or along the backbone,

(b) Bulky groups are employed either pendant to or bridging,

(c) Chain flexibility is promoted by *ortho* and *meta* catenation versus *para* catenation,

(d) Chain flexibility is promoted by linking groups with greater rotational freedom, such as, -O-, -CH_2-, -SO_2-, -$(CH_3)_2$- and –$C(CF_3)_2$-.

Some of the monomers[3] that may increase the solubility when incorporated into the polymer backbone were given in Figure 2.14.

2.3.1.4 Glass Transition Temperature

The glass transition temperature (T_g) is the temperature at which a polymer undergoes extensive cooperative segmental motion along the backbone. The T_g may also be termed as the relaxation point, which occurs between glassy and rubbery plateaus. A number of intra- and intermolecular interactions may affect the T_g including, electrostatic and ionic interactions, hydrogen bonding, chain packing efficiency and chain stiffness. The last one affects the T_g to a great extent[3]. T_g increases with increasing chain stiffness. Incorporation of pendant ionic groups such as –SO_3H groups into the polymer backbone also results in an increase of T_g due to ionic interactions.

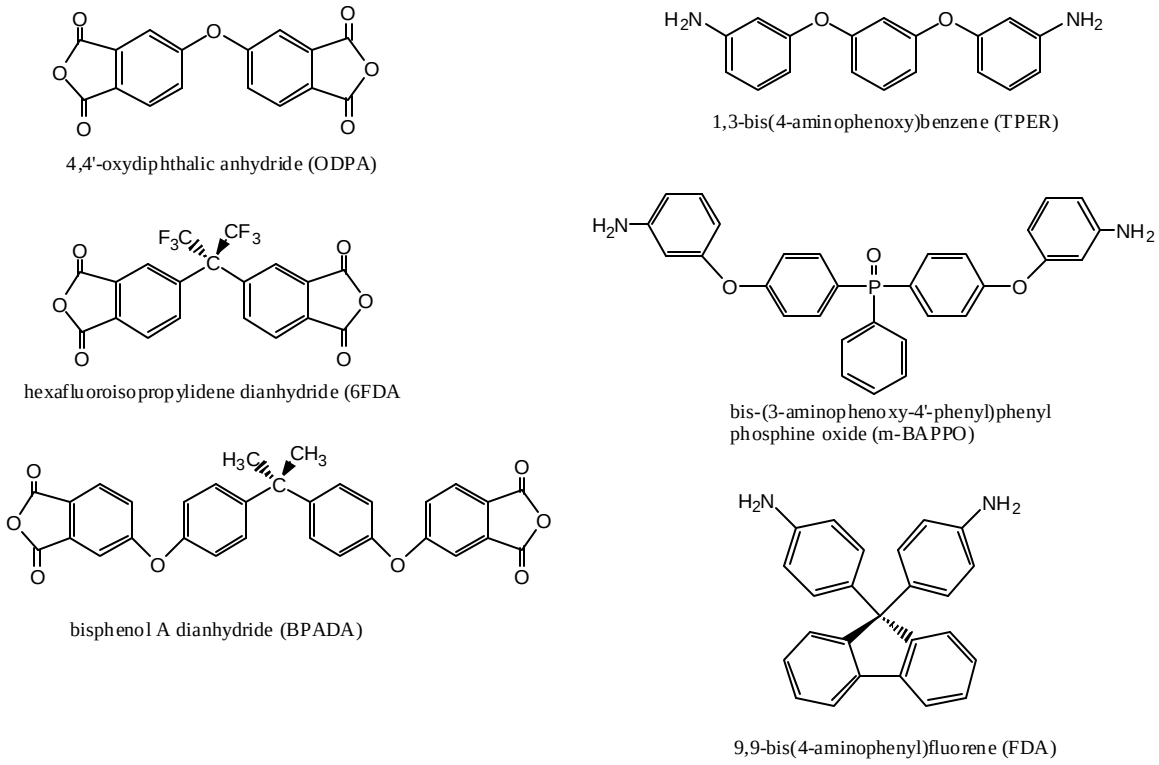

Figure 2.14 Common Dianhydrides and Diamines to increase the solubility of polyimides[3]

2.3.2 Polyimide Applications

2.3.2.1 Polyimides in Electronics

Polymers are widely used in the electronics field in areas such as adhesion, wafer fabrication, chip packaging and assembly[118]. Polyimides have found great utility in wafer fabrication as photoresists and dielectrics due to their excellent elevated temperature performance, corrosion resistance, and their ability to be spin coated onto substrates.

118. Wong, C.P., *Mater. Chem. And Phys*., 42, 25 (**1995**); Bluestein, S.D., Bramono, D.P.Y., Miaoulis, I.N., Wong, P.Y., *Mater. Res. Soc. Symp. Proc*., 445, 185 (**1997**); Malba, V., Liberman, V., Berhardt, J., Vac. *Sci. Technol. A* 15(3), 844 (**1997**); Reichmanis, E., MacDonald, S.A., Iwayanagi, T. (eds.), *Polymers in Microlithography: Materials and Processes*, ACS Symp. Ser. (**1989**).

They also serve as insulators, which prevent "cross-talk" between conducting vias, and as adhesives between polymer-polymer and polymer-metal interfaces. They may also be designed to more nearly match the coefficient of thermal expansion (CTE) of the supporting substrate, which is generally metal or ceramic (Figure 2.15)[119]. By more nearly matching the CTE of the metal, the polyimide-metal interface reduces the stress associated with thermal cycling, which otherwise may cause premature failing.

Photosensitive polyimides are used in electrical devices where a submicron pattern is needed to route electric current. They also greatly simplify the complex, multistep processing used in the high-resolution photolithography process needed for nonphotosensitive materials. The properties of a photosensitive polyimide are changed upon exposure to light. The exposed portion of the polyimide undergoes scission or crosslinking chemical changes that either promote or inhibit solubility. If light exposure prevents solubility, the polymer is said to be negatively-imaged[120,121]. However, if light exposure promotes solubility, the resin is said to respond positively[121].

119. Sillion, B. and Verdet, L., *Heat Resistant Polymers for Electronics Applications, in Polyimides and Other High Temperature Polymers*, Abadie, M.J.M. and Sillion, B. (eds.), 363 (**1991**).

120. Ueda, M. and Nakayama, T., *Macromolecules* 29, 6427 (**1996**).

121. Omoto, T., *Photosensitive Polyimides: Molecular Design and Synthesis, in Polyimides: Fundamentals and Applications*, Ghosh, M.K. and Mittal, K.L. (eds.), Marcel Dekker Inc. 121 (**1996**).

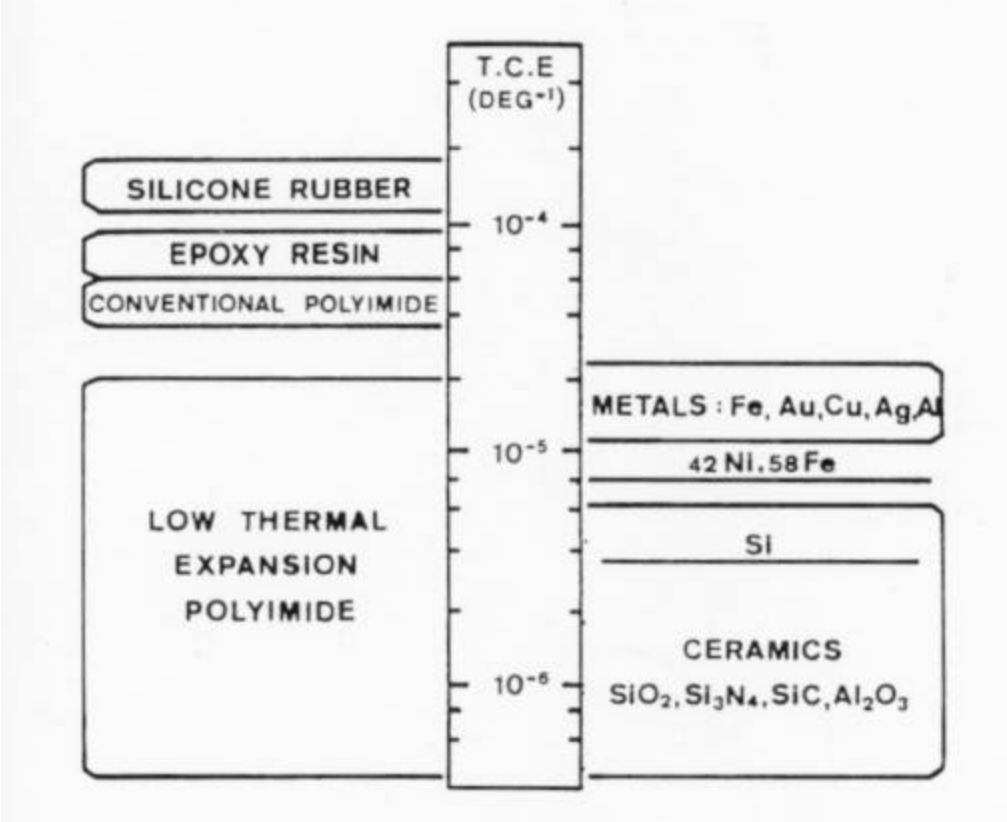

Figure 2.15 The coefficient of thermal expansion of various metals, ceramics and organic polymers[119]

Figure 2.16 shows a typical negative imaging photosensitive polyimide[121]. Upon exposure to light, the derivatized polyamic acid undergoes crosslinking, which renders it insoluble. The unexposed region, which is still relatively soluble, can be removed by solvent development. The final curing step causes the cleavage and volatilization of the crosslink while simultaneously forming the heterocyclic imide structure. A negative-image response can also be promoted through a polyimide in-chain functionality, which is photo-excitable. One of the most widely known polyimides of this type contains a photosensitive benzophenone carbonyl and labile benzylic or methylene protons, which can be abstracted by the excited carbonyl moiety. An interchain bond is formed when two carbon radicals combine to form a carbon-carbon bond. These materials have the advantage of being fully cyclized before the exposure, which allows the shrinkage upon curing to be greatly reduced.

Positive photoresist polyimides[122-125] become more soluble when exposed to the correct wavelength of light. An increase in solubility is observed when the backbone undergoes either cleavage or the side groups' polarity changes. Ho *et al.*[123] recently reported silylating a hydroxyl group in a polyimide backbone. The trimethoxysilane bond was found to undergo hydrolysis in the presence of a photoacid-generating molecule. The solubility differential between the silylated and non-silylated polyimide allowed them to be selectively developed.

2.3.2.2 Polyimides as Optical Waveguides

The function of an optoelectronic device is to convert electrical signals to optical signals, transport the signals through space, and reconvert them back to electrical signals. Optical wave-guides are reflective channels, which allow information in the form of light to be transported through a medium by internal reflection [126]. Optical wave-guides have the advantage of being able to transport multiple signals simultaneously without affecting each other and show immunity to electromagnetic interference and experience noninteraction when signals cross[127]. The prevailing method for communication relies heavily on optoelectronic devices.

122. Feng, K., Matsumoto, T., Kurosaki, T. , *Chem. Mater*., 9(6), 1362 (**1997**).

123. Ho, B., Chen,J., Perng, W., Lin, C. and Chen, L., *J. Appl. Polym. Sci*., 67, 1313 (**1998**).

124. Oba, M. and Kawamonzen, Y., *J. Appl. Polym. Sci*., 58, 1535 (**1995**).

125. Ho, B., Lin, Y., Lee, Y., *J. Appl. Polym. Sci*., 58, 1513 (**1994**).

126. Hornak, L.A. (ed.) *Polymers for Lightwave and Integrated Optics: Technology and Applications*, Marcel Dekker Inc. (**1992**).

127. Feger, C. and Franke, H., *Polyimides in High-Performance Electronics Packaging and Optoelectronics Applications, in Polyimides: Fundamentals and Applications*, Ghosh, M.K. and Mittal, K.L. (eds.), Marcel Dekker Inc., 759 (**1992**).

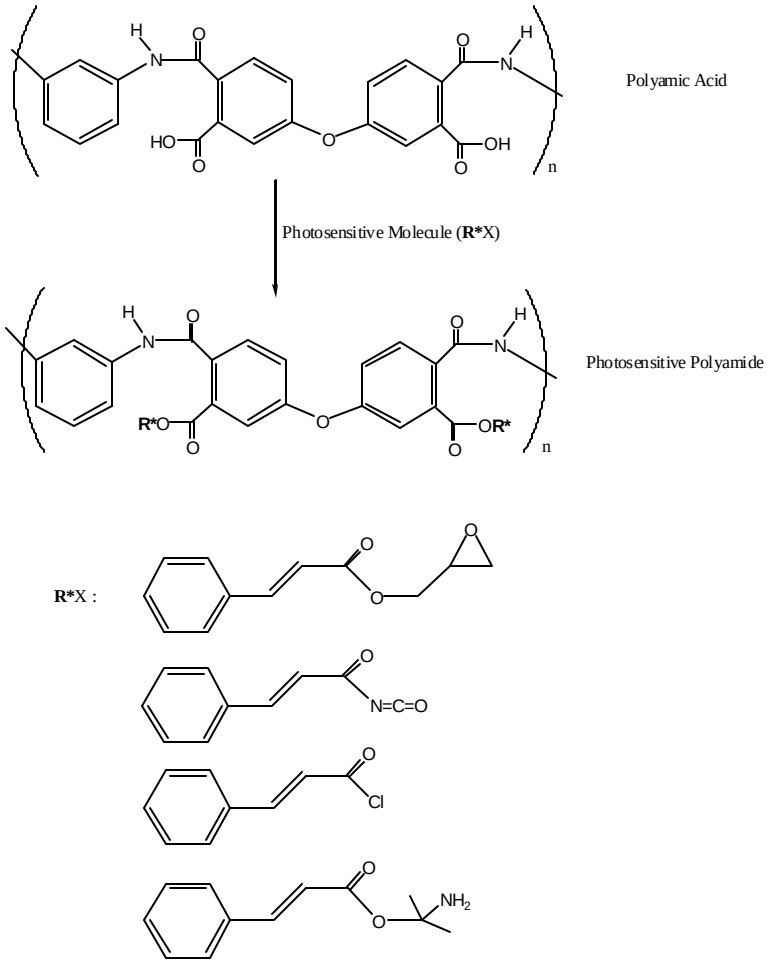

Figure 2.16 Typical Negative Imaging Photosensitive Polyimide[127]

Both freestanding and embedded waveguides are well known[127]. The former consists of a polymeric material coated onto a substrate that is patterned by photolithography, laser ablation, or ion beam etching techniques. The pattern allows the transmission of light through the remaining polymer structure. Embedded waveguides use UV lithography to record a pattern onto a polymeric material by altering its chemical structure, thereby facilitating selective ion diffusion. Selective ion-diffusion of dye molecules can change the refractive index of the material.

The process requirements for waveguide materials exceed those found in many thermoplastics. A typical flip-chip configuration, in which the active chip area faces the substrate, is shown in Figure 2.17[128]. Materials used in this configuration need to withstand chip joining temperatures up to 360 ^{o}C, must be patternable to fit between C4 connections, need to allow signal detection by transmitting the information through the beveled plane reflector, and must be influenced by organic solvents. Polyimides, which are well known for their excellent thermal stability, good dimensional stability, and high decomposition temperatures, can satisfy these material requirements[127].

Polyimides that are thermally imidized from the poly(amic) acid were found to show a large optical loss, which is not suitable for the wavequide application. Upon poly(amic) acid cyclization to the polyimide and solvent removal, it was found microvoids formed causing density fluctuations and light scattering leading to an optical loss in the material. On the other hand, fully imidized polyimides show a significant reduction in optical loss. By introducing bulky side groups, such as 6F and 3F, the polyimide can be generated in the fully cyclized form[129]. 6F and 3F groups also promote solubility, hinder chain ordering and chain transfer complexes, and give high T_g materials, all of which are favorable for this application[127].

128. Feger, C. and Perutz, S., Reuter, R., McGrath, J.E., Osterfeld, M. and Franke, H., in *Materials for Microelectronic Applications*, Ito, H., Tagawa, S. and Horie, K. (eds.) ACS Symp. Ser. 579, 272 (**1994**).

129. Feger, C., Reuter, R. and Franke, H., *Polym. Prep*. (ACS Div. Polym. Chem.), 29(2), 242 (**1998**).

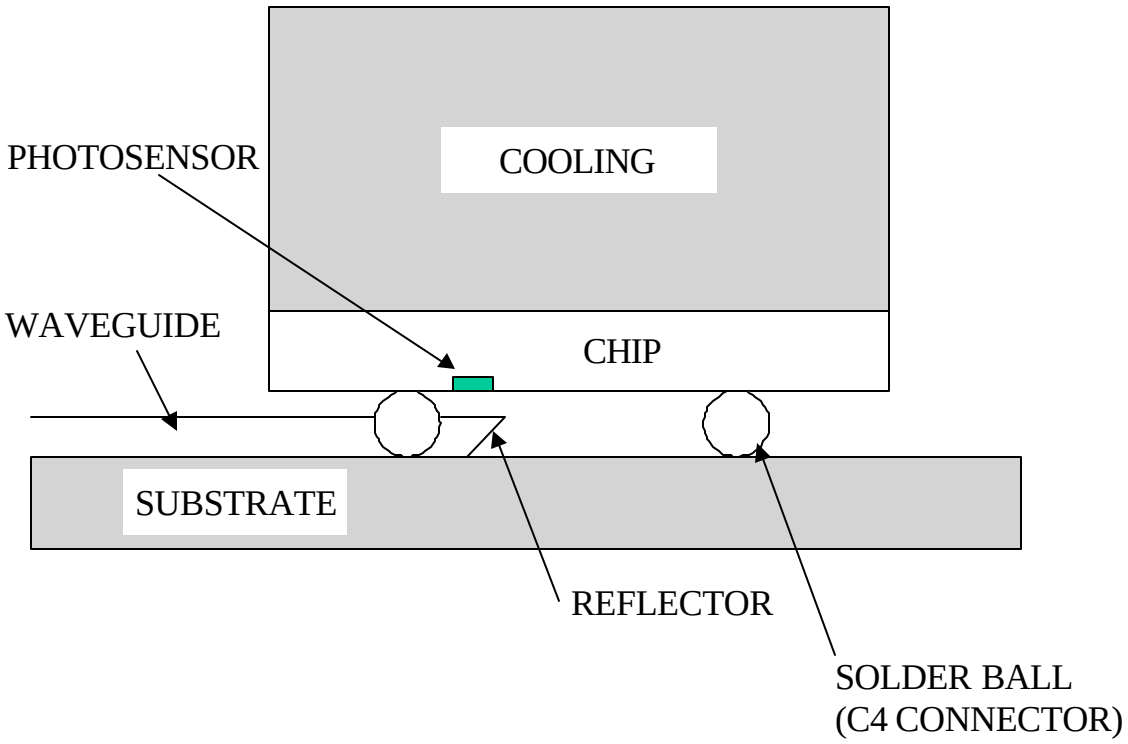

Figure 2.17 Flip-chip Configuration with Waveguide[128]

2.3.2.3 Polyimides in Aerospace Applications

A number of structurally modified polyimides have been developed to meet the increasing demand of our societie's growing technology. The aerospace industry is one of these areas which continues to require more from the materials it consumes. Researchers have met this challenge primarily with polyimides, which can be modified to meet processing conditions while maintaining several of their advantageous properties.

Polyimides[129-131] are known to have excellent heat and chemical resistance, excellent adhesion to a number of substrates, and superior mechanical properties, such as

129. Butkus, L.M., Mathern, P.D. and Johnson, W.S., J. Adhesion 66, 251 (1998).
130. J.E. McGrath, Tan, B., Vasudevan, V., Meyer, G.W. and Loos, A.C., Bullions, T. *Int. SAMPE Tech. Conf.*, 28, 29 (**1996**).

high flexural modulus and compressive strength. Polyimides are also known to possess outstanding dimensional stability under loads, which allows their use in high temperature environments. The addition of phosphorus substituents is known to impart fire retardancy as evidenced by high TGA char yields in air. Lee *et al.*[132] found that incorporation of bis(m-amino phenoxy) triphenylphosphine oxide not only improved fire retardancy but also solubility and adhesive strength to titanium.

Polyimide composites surpass mechanically fastened assemblies in terms of fatigue and corrosion resistance, aerodynamic properties, manufacturing costs, and repairs [129]. Due to these outstanding properties and economical advantages, polyimides are used in the aerospace industry as struts, brackets, composites, and structural adhesives[129-131].

Composite applications, such as those found in aerospace, require the resin material to thoroughly wet the matrix, such as carbon fibers. In order to promote good wettability, the polyimide can be introduced as an oligomer. Oligomers, capped with reactive endgroups, exhibit lower viscosities and can undergo crosslinking at elevated temperatures. Some of the commercial examples of these systems are shown in Table 2.5[133]. PMR-15 contains low molecular weight oligomers end-capped with nadic anhydride which undergoes crosslinking at 250-300 ^{o}C. The important drawback of the PMR-15 is the volume of the solvent removed such as methanol, water and cyclopentadiene, which produce voids in the final laminate. High temperature, void-free systems can be achieved with acetylene, phenylacetylene, and phenylethynyl terminated oligomers[134-137, 83].

---

131. Morgan, R.J., Shin, E.E., Lincoln, J.E., *Int. SAMPE Tech. Conf.*, 28, 213 (**1996**).

132. Lee, Y.J., Gungor, A., Yoon, T.H., McGrath, J.E., *Adhesion* 55, 165 (**1995**).

133. Verbicky Jr., J.W. *Polyimides, in Polymers: High Performance Polymers and Composites*, Kroschwitz, J.I. (ed.), John Wiley and Sons, Inc., 7777 (**1991**).

134. Tan, B., Vasudevan, V., Lee, Y.J., Gardner, S., Davis, R.M., Bullions, T., Loos, A.C., Paravatareddy, H., Dillard, D.A., McGrath, J.E., Cella, J., *J. Polym. Sci.:Part A: Polym. Chem*., 35, 2943 (**1997**).

135. Zhuang, H., *Ph.D. Thesis*, Virginia Tech, **1998**.

136. Meyer, G., Ph.D. Thesis, Virginia Tech, **1995**.

137. Meyer, G.W., Tan, B. and McGrath, J.E., *High Performance Polymers* 6(4), 423 (**1994**).

Table 2.5 Curable Polyimides for Aerospace Applications[133, 138]

Monomers	Unsaturated End Cap	Examples
methylenedianiline, benzophenone dianhydride	nadic imide	PMR-15 LARC-13
methylenedianiline, maleic anhydride	maleimide	Kerimid 601
methylenedianiline benzophenone	acetylene	ATPI Thermid
m-phenylene, bisphenol A dianhydride	phenylethynyl [134,137]	

2.3.2.4 Polyimide Adhesives in Aerospace and Microelectronics

A number of variables are involved in defining specific chemical interactions, which lead to an adhesive bond. Several scientists have developed theories to explain and predict these interactions. The generally accepted theories of adhesion[139-141] are given below:

(a) Mechanical interlocking: the adhesion due to tortuous path of fracture

(b) Surface energetics: good wetting is required for good adhesion (Figure 2.18)[142]

(b) Diffusion Theory: interpenetrating network formation across the interface to form an interphase region

(c) Acid-Base Theory: strength of the acid-base interaction

138. Hergenrother, P.M. and Smith Jr., J.G., *Polymer*, 35, 4857, **1994**.

139. Kinloch, A.J., in Durability of Structural Adhesives, Kinloch, A.J. (ed.), Appl. Sci.Publ. LTD 1 (**1998**).

140. Buschwalter, L.P., in *Polyimides: Durability and Applications*, Ghosh, M.K. and Mittal, K.L. (eds.) Marcel Dekker, Inc., 587 (**1996**).

141. Sharpe, L.H., J. *Adhesion* 67, 277 (**1998**).

142. Minford, J.D., in *Durability of Structural Adhesives*, Kinloch, A.J. (ed.),. *Appl. Sci.Publ*. LTD 135 (**1983**).

(d) Chemical Bonding: physical bond formation leading to adhesive strength

(e) Weak Boundary Layer Mechanism: explains poor adhesion relating to cohesive failure in the interfacial region

It is impossible to completely explain adhesion by any of these mechanisms, although one mode of adhesion may be predominant and lead to the majority of the observed adhesive strength[143-144]. The most desired interaction at the polymer/substrate is often proposed as a chemical bond[145,146]. Unlike Van der Waals forces and hydrogen bonding, chemical bonds are much less likely to be disturbed by heat, water and exposure to chemicals.

Surface contaminants will play a significant role in chemical interactions and bond durability and complicate the matter of adhesion. Figure 2.19 pictures a typical surface with a number of adsorbed contaminants. It is essential to properly prepare a surface which has a number of adsorbed contaminants. This can be done in a number of ways ranging from a pumice scrubber and heat treatments to reactive ion-etching and chemical modification[147].

Polyimide adhesives fall into one of three classes based on their adhesion characteristics[148]. The first class is amorphous polyimides, which self-adhere and bond well with metals such as Cu, Cr and Al. Semicrystalline polyimides form the second class of polyimide adherents. This class adheres well to reactive metals such as Al and Cr, but not to unreactive metals such as Cu. Presumably, this is due to hindered molecular mobility within the more ordered regions. Some semicrystalline polyimides also exhibit marginal self-adhesion.

---

143. Buchwalter J., *Adhesion Sci. Technol*. 4, 697 (**1990**).

144. Van Ooji, W. J., in Physiochemical Aspects of Polymer Surface, Mittal, K.L. (ed.). Plenum Press, N.Y., 2, 1035 (1983).

145. Lacombe, R.H., Buchwalter, L.P. and Holloway, K., *J. Adhesion Sci. Technol*., 7, 1293 (**1993**).

146. Gledhill, R.A., Kinloch, A.J., Shaw, S.J., *J. Adhesion* 11, 3 (**1980**).

147. Ho, P.S., in *Principles of Electronic Packaging*, D.P. Seraphim, Lasky, R. and Li, C.-Y. (eds.), McGraw Hill, NY, 809 (**1989**).

148. Feger, C. and Franke, H., in *Polyimide: Fundamentals and Applications*, Ghosh, M.K. and Mittal, K.L. (eds.), Marcel Dekker Inc., 759 (**1996**); Browden, M.J. and Turner, S.R. (eds.), *Polymers for High Technology: Electronics and Photonics*, ACS Symp. Ser. 346 (**1996**).

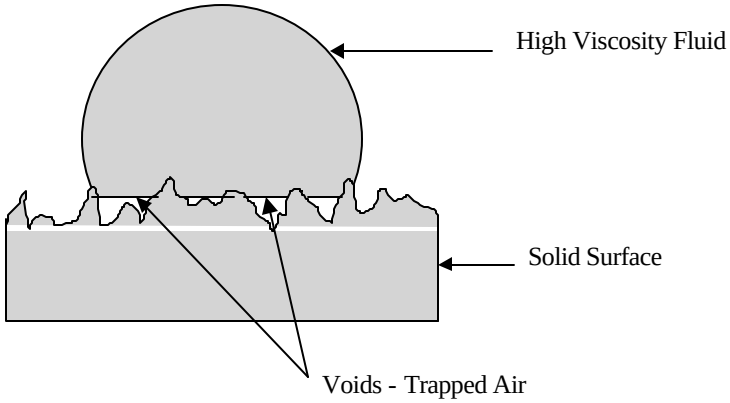

LOW AREAS OF INTERFACIAL CONTACT RESULTING FROM HIGH VISCOSITY OF FLUIDS

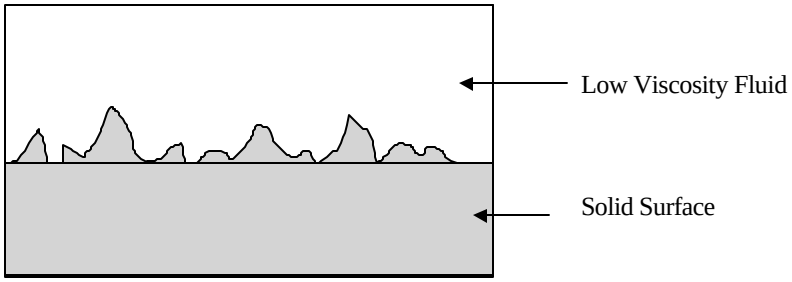

LACK OF VOIDS AND HIGH AREA OF INTERFACIAL CONTACT RESULTING FROM LOW VISCOSITY OF FLUIDS

Figure 2.18 Effect of Adhesion Viscosity on Interfacial Contact[142]

Brown *et al.*[149] explained that, polyimide/polyimide adhesion is influenced by the cure temperature before adhesive bond formation. The bond strength between two fully cured (400 ^{o}C) polyimides (ODA/PMDA) was weak whereas the bond strength between one fully cured polyimide with an incompletely cured polyimide (200 ^{o}C) was good. The interdiffusion region between each set of polymer films was higher for the fully cured/incompletely cured laminent than it was for the fully cured/fully cured laminent (47 nm vs. 30 nm)[149].

149. Brown, H.R., Yang, A.C.M., Russel, T.P., Volksen, W. and Kramer, E.J., *Polymer* 29, 1807 (**1988**).

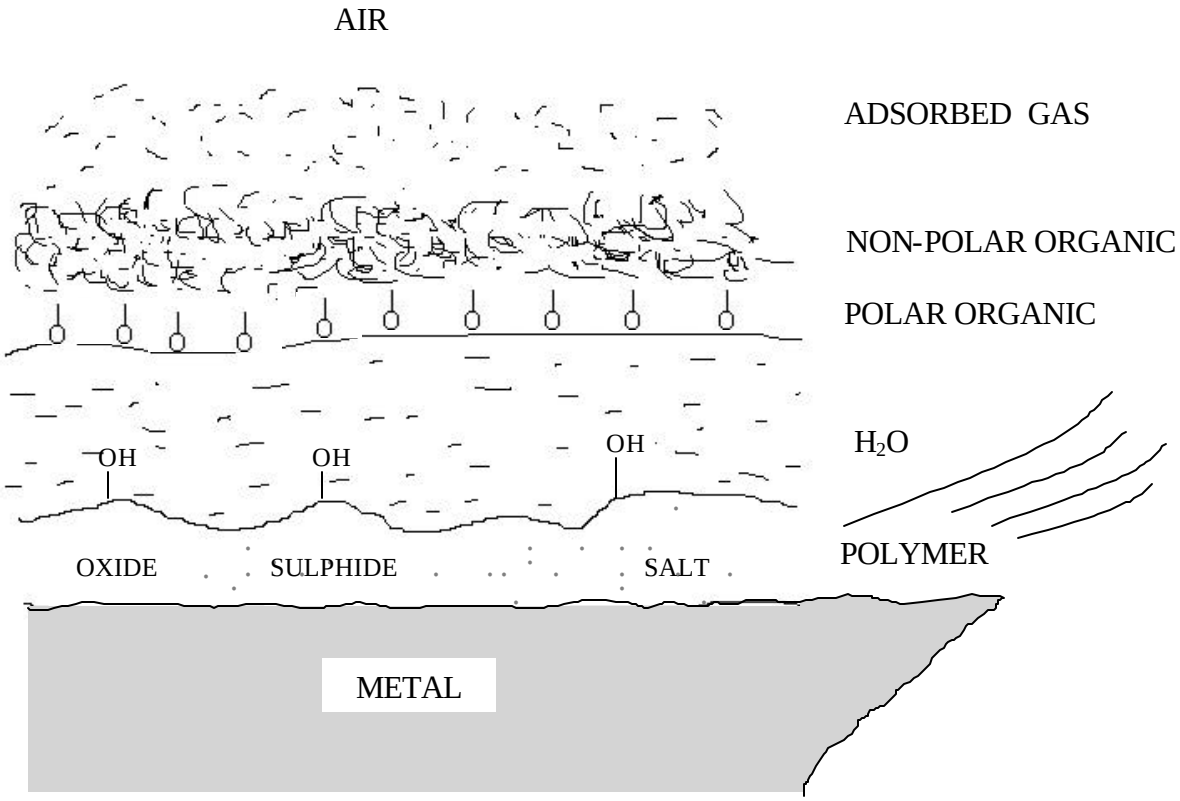

Figure 2.19 Spontaneously Adsorbed Layers of on a Metal Surface

Thermosetting resins represent a third class of polyimide adherents. Low molecular weight polyimides with curable endgroups allow for good wetting and adhere well to metals, ceramics and to themselves, if one of the layers remains uncured prior to adhesive bond formation[148].

Polyimides are leading candidates for aerospace applications[149] due to their excellent thermooxidative stability, good adhesion to metals and good mechanical properties over a wide range of temperatures. PMR-type chemistry (polymerization of monomeric reactants) that employs nadic anhydride endgroups, as shown in Scheme 2.14, is a leading resin for this application.

149. Lupinski, J.H. and Moore, R.S. (eds) *Polymeric Materials for Electronic Packaging and Interconnections*, ACS Symp., Ser., 407, ACS, Washington DC (**1989**).

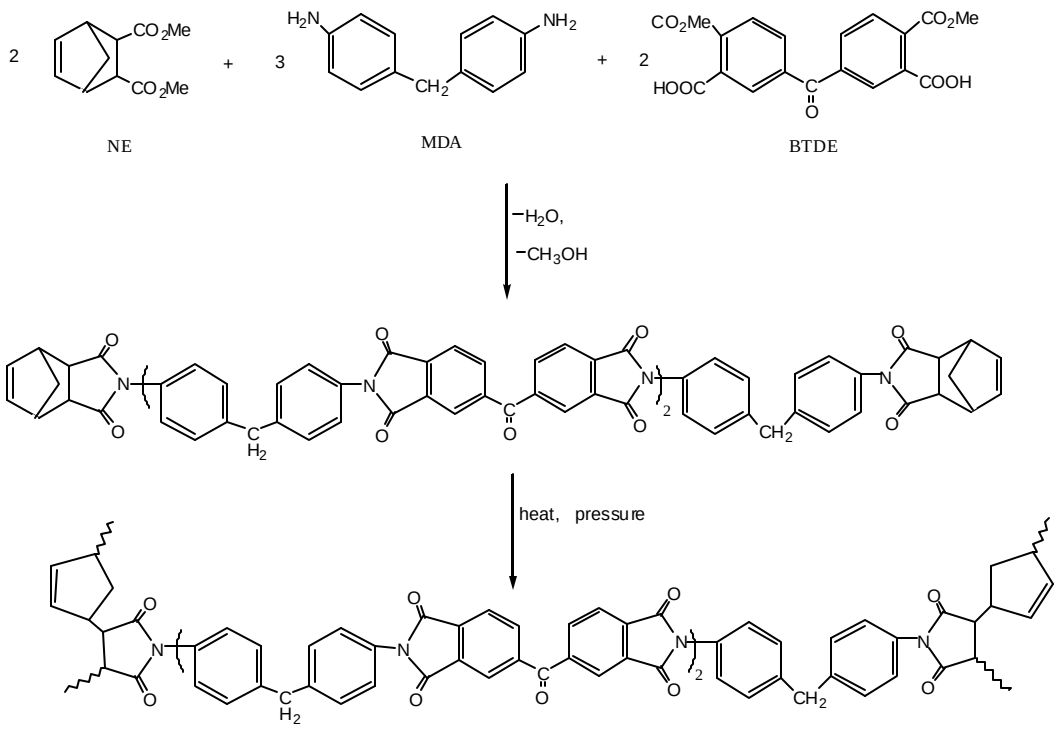

Scheme 2.14 PMR-15 Resin Chemistry[150]

A potential drawback to this material is the evolution of cyclopentadiene upon thermal crosslinking. Evolution of volatiles may produce a significant number of voids in the bondline[142], which will reduce long-term adhesion.

The polyimide oligomers terminated with acetylene[135,151], phenylacetylene[152,134,137], phenylmaleimide[144,153] or phenylethynyl[134,137] reactive endcaps are alternatives to PMR-type chemistry. These materials, which may be fully cyclized, do not emit volatiles when thermally crosslinked at elevated temperatures and

150. Serafini, T.T., Delvigs, P. and Lightsey, G.R., *J. Appl. Polym. Sci*., 16, 905 (**1972**).

151. Landis, A.L., Bilow, N., Boschan, R.H., Lawrence, R.E. and Aponyi, T.J. *Polym. Prep*. 15(2), 537 (**1974**); Hergenrother, P.M., *Polym. Prep*. 21, 81 (**1980**); St. Clair, A.K. and St. Clair, T.L., *Polym. Eng. Sci*., 22, 9 (**1982**).

152. Paul, C.W., Shultz, R.A. and Fenelli, S.P., *Advances in Polyimide Sci. Tech*., Feger, C., Khojasteh, M.M. and Htoo, M.S. (eds)., Technomic Publ. Co., Lancaster, PA 220 (**1993**).

153. Meyer, G.W., Heidbrink, J.L., Franchina, J.G., Davis, R.M., Gardner, S., Vasudevan, V., Glass, T.E. and McGrath, J.E., *Polymer* 37(22) 5077 (**1996**).

possess good adhesion to metals. They also have excellent shelf-life, low crosslink density, excellent solvent resistance when cured, and a wide processing window between the glass transition temperature and the cure exotherm[134].

Microelectronic devices such as printed circuit boards and multiple packages also rely on good adhesion between polyimide-polyimide and polyimide-metal interfaces. For this application, polyimide precursors, either poly(amic) acid (PAA) or poly(amic) ester (PAE), are generally applied to the desired substrate from solution to form a thin polymer layer, which can be imidized at elevated temperatures. This process involves a number of chemical and physical changes, many of which have not been sufficiently addressed due to the complexity of the adhesive behavior.

Imidization of the PAA and PAE thin films results in loss of water, water and alcohol residual solvent and other volatile components present in the film. Because of the loss of volatiles and differences in the thermal coefficient of expansion between the film and substrate, the films experience residual stress build-up[154]. Residual stress may lead to premature adhesive failure. The surrounding environment, such as humidity and temperature, of the operating device will also affect the stress build-up[155] and bond stability[156]. Polyimides are known to absorb various amounts of water from their surroundings, which may disrupt adhesion. This is illustrated by the common laboratory practice of applying water to remove polyimide films from glass substrates. Interfacial adhesion characteristics may be improved with coupling agents such as aminosilanes and aluminum chelates (Figure 2.20)[157].

Ozowa and coworkers[158] reported data on a series of fully cyclized Probimide® photoimagable polyimides and compared them with PAA precursors of Kapton.

---

154. Noe, S.C., Pan J.Y. and Senturia, S.D. Soc. of Plast. Eng. ANTEC, Montreal, May 1598 (**1991**); Galopeau, D.W. Vetelino, J.F. and Feger, C. Adv. in *Polyimide Sci. and Tech*. Feger, C., Khojasteh, M.M. and Htoo, M.S. (eds.) 540 (**1993**).

155. Pan J.Y. and Senturia, S.D. *Soc. of Plastic. Eng.* ANTEC, Montreal, May 1618 (**1991**).

156. Furman, B.K., Clearfield, H.M., Purushothaman *Soc. of Plast. Eng.* ANTEC, Montreal, May 552 (**1991**).

157. Satoo, J., Suzuki, H. and Makino, D. *Polyimides for Semiconductor Applications in Polyimides*, Wilson, D., Stenzenberger, H.D. and Hergenrother P.M. (eds.), Chapman and Hall, NY 227 (**1990**).

158. Ozowa, T., Sorimachi, H., Izumi, K. Yoneda, Y., "*Thin Film Hybrid Interconnects*", ISHM 1991 Proceedings p.6 (**1991**).

The authors applied a typical cure schedule used in photolithography to each polymer, namely, 30 minutes at 110 ^{o}C (soft bake) followed by 2-14 hours at 350 ^{o}C (hard bake). Shrinkage of the poly(amic) acid materials ranged from 30-60% due to cyclization, which produces water, and residual solvent removal. The refractive index of the PAA's also changes dramatically upon conversion to the polyimide. On the other hand, the cyclized Probimide® series showed minimal shrinkage as well as constant refractive indices. Polymers, which maintain constant refractive indices and UV spectra over a wide range of baking conditions, are useful for fabricating multilayered structures such as multichip modules(159).

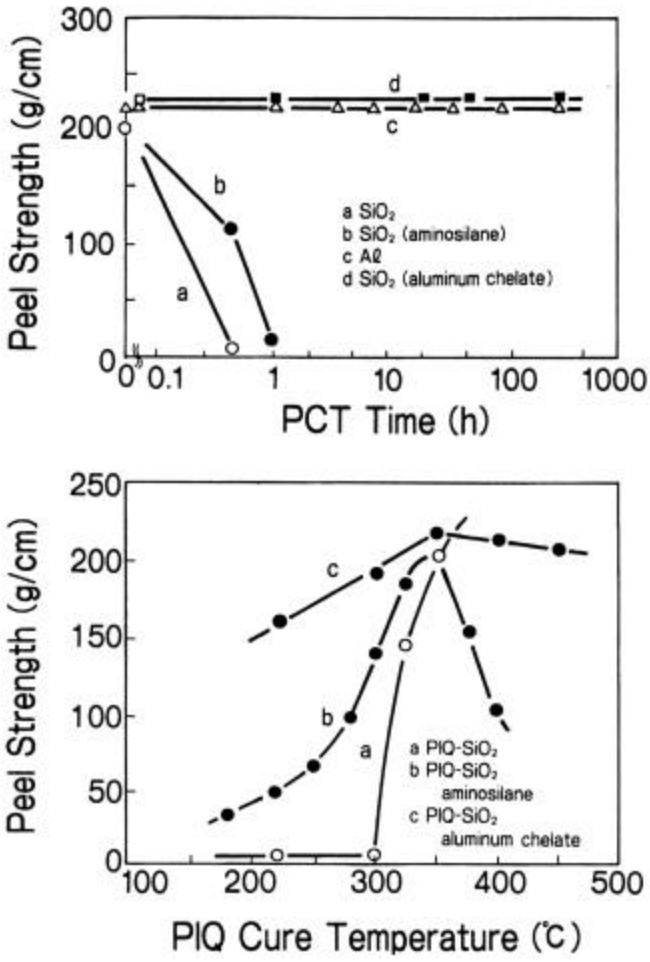

Figure 2.20 Adhesion Properties of Polyimide-Isoindoloquinazolinedione (PIQ) to SiO_2 with and without Adhesion promoter (aminosilane)(157)

159. Saiki, A. and Harada, S. *J. Electrochem. Soc*. 129, 2278 (**1982**).

2.4 FUEL CELLS

2.4.1 Introduction and Historical Development

A fuel cell is an electrochemical device that combines a hydrogen-rich gas with air and converts the chemical energy of this mixture into electricity directly with no intermediate combustion step[158]. Although, its construction is similar to the dry-cell battery, unlike a battery, a fuel cell does not undergo a material change or run down, does not require recharging, and operates as long as fuel and air supplied to the electrodes. This concept was first introduced in 1839 by Sir W. R. Grove and direct conversion of chemical to electrical energy in a hydrogen/oxygen fuel cell was demonstrated[159].

A typical fuel cell produces a high current and low voltage. Practical voltages are obtained by connecting many individual cells into a cell stack (0.9 Volt/cell). A fuel cell produces direct current, which usually requires an inverter to convert the output to alternating current. Depending on the type of fuel that is to be used, a fuel cell system may also require a reformer, a fuel-reforming unit, to convert the input into a hydrogen-rich gas. Since a fuel cell transforms fuel directly to electricity without an intermediate conversion to heat, less waste heat is produced, and very high conversion efficiencies, *e.g*. 40-60 % are achieved[158]. Additionally, in the case of the constant temperature operation of a fuel cell, the heat generated by the electrochemical reaction can be used for space heating, water heating or industrial heat. When a fuel cell is used in this cogeneration mode, producing both power and heat, overall efficiencies can reach as high as 80 percent[158].

2.4.2 Technical Capabilities of Fuel Cells

Besides their high fuel efficiencies and possible environmental advantages, fuel cells promise to offer several technical advantages. One technical advantage is fuel flexibility. Since a fuel cell employs a hydrogen rich gas to produce electricity, it can, in principle

158. Appleby, A.J., Fuel Cells: Trends in Research and Applications, **1987**.

159. Kua, Jeremy and Goddard III, W. A., J. Am. Chem. Soc. 121, **1999**, 10928-10941.

use any fuel source including petroleum, naphtha, natural gas, and methanol that will supply this gas. Additionally, where hydrogen storage is feasible, renewable power sources could drive an electrolysis process to produce hydrogen during off-peak periods that can be used to operate fuel cells during peak demands[160].

One of the fuel cell's most important characteristics is its ability to operate efficiently and to respond rapidly to sudden increases or decreases in power demand. The fuel cell's ability to increase output quickly (known as its spinning reserve capability), and its ability to decrease output quickly (known as its load-following capability) makes fuel cells attractive as peak-load facilities.

Another technical capability of a fuel cell is its compact design that enables it to be added in small, discrete increments of capacity, which allows better matching capacity to expected load growth[158]. A fuel cell's small size also enables it to be located close to the load, which can reduce the energy losses, costs associated with transmission and distribution equipment, and the likelihood of system blackouts. Finally fuel cells show high performance reliability and their construction facilitates repair when they need maintenance.

2.4.3 Environmental Considerations

2.4.3.1 Environmental Advantages

Air Quality: Since fuel cells do not rely on a fuel-burning process, their air pollution emissions are projected to be al least 1000 times smaller than those of fossil-fueled plants. Due to their fuel cells' low emission, they can be sited close to the load in highly crowded cities of poor air quality. The expected reduction in sulfur and nitrogen oxides could also enable fuel cells to reduce acid rain[158], which is an important environmental issue of our days.

Water quality: The use of fuel cells is also expected to provide significant benefits related to water use and water quality. Since water is produced as a by-product during the

160. Hawaii Natural Energy Institute, *International Symposium on Hydrogen Produced from Renewable Energy*, Honolulu, HI, May 25, **1984**.

electrochemical reaction of the fuel cell, only a small amount of external water is required for its operation. They may also reduce or eliminate water quality problems created by conventional plants' thermal discharges and disposal of residues from air pollution control equipment[158].

Noise Reduction: The quiet electrochemical conversion process of fuel cells enables them to sit close to the load featuring reduced community concerns associated with conventional steam power plants.

2.4.3.2 Environmental Disadvantages

In some respects, fuel cells will likely have some undesirable impacts on the environment. Many of the fuels employed by fuel cells are inflammable, explosive and may contain organic components that are toxic and use of these fuels create environmental and safety concerns. These concerns are especially important because fuel cells are most likely located in residential, commercial and industrial areas.

2.4.4 Types of Fuel Cells

Electrochemical cells such as electrolysers, batteries and fuel cells, require separators or electrolytes, which allow a flow of specific ionic charges but prevent the transfer of chemical species, which stay either in the cathodic or anodic compartment. Among the various separators of electrochemical cells, the type of electrolyte, conductive material, used for the chemical conversion process, characterizes fuel cells. The discussion comprising this part of the chapter will provide types of fuel cell revealed in the literature. The types of fuel cells can be given as follows:

(1) Alkaline fuel cells
(2) Phosphoric Acid Fuel Cells
(3) Molten Carbonate Fuel Cells
(4) Solid Oxide Fuel Cells
(5) Solid Polymer Electrolyte Fuel Cells

2.4.4.1 Alkaline Fuel Cells

The first alkaline fuel cell was developed in the early 1930's by Dr. Francis T. Bacon[161]. It is an attractive power source if pure hydrogen is available as a fuel. One of the main differences between alkaline and hydrogen-oxygen fuel cell systems is the use of non-noble metal electrocatalysts. In his fuel cell, Bacon used a nickel electrocatalyst for the anode and lithiated nickel oxide (lithium improves the electronic conductivity and the corrosion resistance of nickel oxide) for the cathode. The cell electrolyte was 30 % KOH and the cell operating temperature and pressure were 200 ^{o}C and 50 atm, respectively. Figure 2.21 illustrates the operating principle of an alkaline fuel cell. The equations presented below illustrate its half reactions.

Anode $\quad H_2 + 2OH^- \longrightarrow 2H_2O + 2e^-$ Equation 2.2.1

Cathode $\quad O_2 + 2H_2O + 4e^- \longrightarrow 4OH^-$ Equation 2.2.2

Potassium hydroxide, which is the most conducting of all alkaline hydroxides, has always been chosen as the electrolyte in which the hydroxyl ions are the conducting species. Water is produced at the anode, and some of this water migrates to the cathode. Hence, product water exits the cell from both the anode (~) and cathode (~) compartments.

The main advantage of an alkaline electrolyte fuel cell over an acid one is that noble metal electrocatalysts are not necessary for the former[162]. In addition, even with the non- noble metal or oxide electrocatalysts, the oxygen electrode performance is found to be very good. Fuel cells have been developed with platinum electrocatalysts as well. Recently, it was shown that a heat-treated cobalt tetraphenyl porphyrin deposited on high-surface-area carbon exhibits the highest activity ever reported for oxygen

161. Adams, A.M., Bacon, F.T., and Watson, G.H., in *Fuel Cells* (W. Mitchell, ed.) (Academic Press, New York, (**1963**).

162. Srinivisan, S., Dav , B., Murugesamoorthi, K.A., Parthasarathy, A., and Apleby, A.J., *Fuel Cell Systems* (Blomen, L.J.M.J. and Mugerwa, M.N., eds) (Plenum Press, New York, **1993**).

reduction[163,164]. The reason for this is that anion adsorption is minimum from alkaline electrolytes.

Alkaline fuel cells generally operate between 60-80 ^{o}C. Most often the operating pressure is atmospheric pressure; in some cases, it is a few atmosphere. In these fuel cells, the methods for product water and heat removal are critical, particularly because the alkaline fuel cell operates at less than 100 ^{o}C. However, several manufacturers of alkaline fuel cells have resolved these problems and manufactured them for NASA in the Apollo missions (1960s and early 1970s).

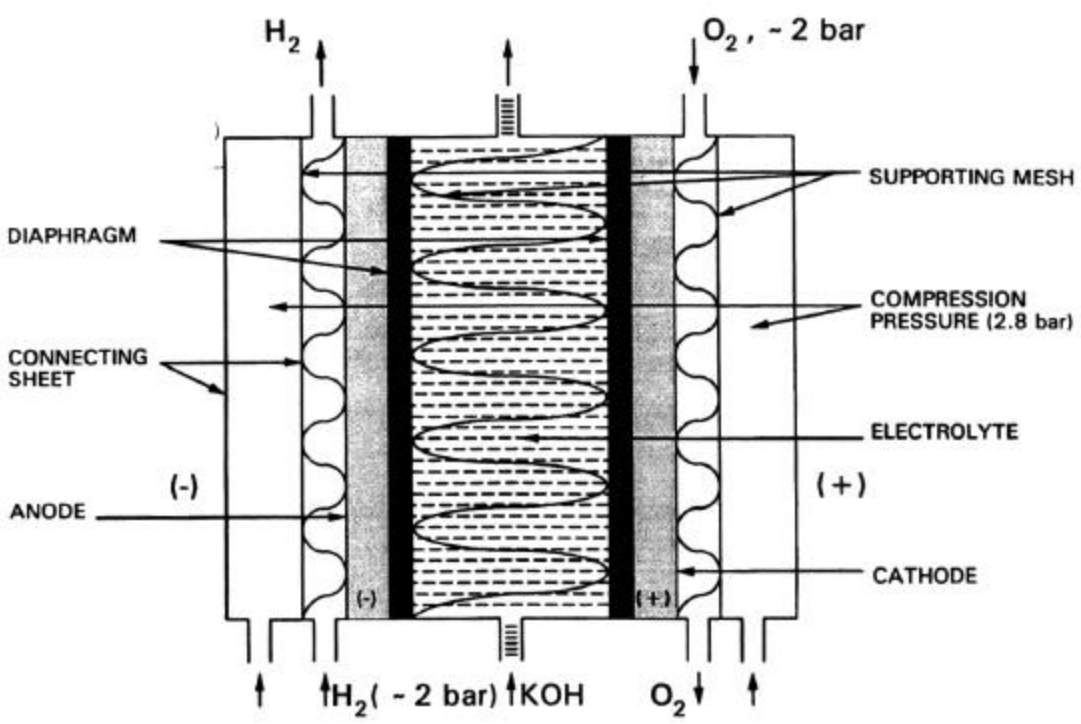

Figure 2.21 Operation of an Alkaline Fuel Cell[162]

163. Yeager, E., *Presentation at DOE Contractors Meeting* (Technology Base Research Project), Cleveland, OH, April 14-15, **1986**.

164. Solomon, F., Ext. Abstracts, *Electrochemical Society Spring Meeting*, Toronto, Canada, **1985**.

The alkaline fuel cell system is the most efficient of all fuel cells, but the major challenge is the complete removal of CO_2 from the anodic and cathodic gas streams before they enter into the electrochemical cell stack. Even the small level of CO_2 in the air (350 ppm) is sufficient to carbonate the electrolyte and form solid deposits in the porous electrode.

The alkaline fuel cell system, using pure H_2 and O_2 as reactants, has established its space application. This system can be coupled with an alkaline or a solid polymer electrolyte water electrolyzer. The challenges are to economically remove CO_2 from these reactants and to develop safe, lightweight methods of transportation and storing of gaseous hydrogen. Another application of alkaline fuel cell systems is for standby power, for example, for telephone companies[162].

2.4.4.2 Phosphoric Acid Fuel Cells

Phosphoric acid is the electrolyte of choice for these types of fuel cells, particularly with hydrogen produced by steam forming of organic fuels such as hydrocarbons (natural gas), and alcohols (methanol or ethanol) as the anodic reactant. The main characteristics of phosphoric acid fuel cells (PAFC) are:

(a) CO_2-rejection

(b) Toleration of 1-2% CO at the current operating temperature of 200 ^oC

(c) Utilization of the waste heat from the electrochemical cell stack efficiently for the endothermic steam-reforming reaction, as well as providing space heat or hot water.

The principles of operation of the cell are schematically illustrated in Figure 2.2.2. The reformed fuel and oxidant enter the anode and cathode gas chambers, dissolve in the electrolyte, and diffuse to the electrocatalyst sites in the porous gas-diffusion electrodes. The anodic and cathodic reactions and the transport of hydrogen ions from the anode to the cathode are also indicated in Figure 2.22. The attractive features of PAFCs are:

(1) stability in the electrochemical environment at temperatures up to at least 225 ^oC,

(2) reasonably good electrolyte conductivity at temperatures above 150 ^oC,

(3) efficient rejection of product water and waste heat at the operating temperature.

The main drawback associated with PAFC was that the kinetics of oxygen reduction was considerably slower than in other acids, such as sulfuric or perchloric[162]. However, increasing the operating temperature to above 150 ^{o}C allowed higher rates of oxygen reduction to be achieved. The reason for this slow kinetics below 150 ^{o}C has been explained to be due to the adsorption of the phosphoric acid molecule and/or anions of the acid which inhibits oxygen adsorption, an intermediate step in oxygen reduction. However, at >150 ^{o}C, phosphoric acid exist predominantly in the polymeric state, as polyphosphoric acid. The acid is strongly ionized and, probably due to the relatively large size of the anions ($H_3P_2O_7^-$) of the acid, the anion adsorption is minimal.

In PAFCs, carbon is the vital material for the electrochemical cell stack: high-surface area powder for the electrocatalyst support, porous carbon paper for the electrode support, and graphitic carbon for the bipolar plate. The essential components of an electrochemical cell stack are the porous gas-diffusion electrode, electrolyte matrix, and bipolar plate. The porous electrode consists of an electrocatalyst layer, which is carbon-supported platinum electrocatalyst bonded with Teflon and a carbon paper substrate. The state-of-the-art electrolyte matrix is Teflon- bonded silicon carbide. The matrix is microporous and is generally deposited on the cathode.

PAFC systems operate at 190-210 ^{o}C. Because of the relatively high operating temperature, compared with low-temperature fuel cell systems, such as alkaline and solid polymer electrolytes, water and heat rejection are relatively simpler.

The poisoning of the hydrogen electrode by CO and H_2S present in the reformed fuels was a problem encountered in the early years of PAFCs. Since the fuel processing includes steam reforming and shift conversion, CO levels were reduced to about 1-2 %. Furthermore, CO poisoning is greatly reduced at high operating temperatures. At an operating temperature above 180 ^{o}C, it has been found that the PAFC system is tolerant of CO to the extent of <1-2 %. In addition, the hydrogen sulfide level has been significantly reduced to a level of a few ppm using a hydrodesulfurizer.

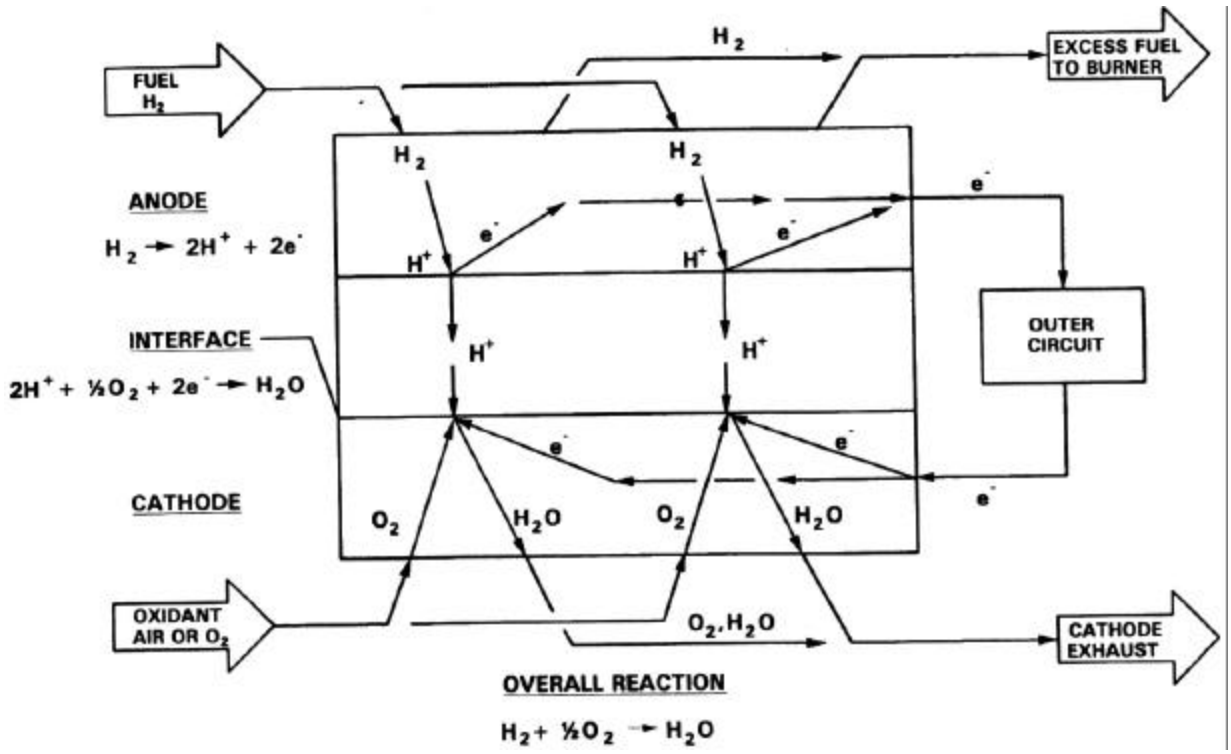

Figure 2.22 Principles of Operation of a Phosphoric Acid Fuel Cell[162]

2.4.4.3 Molten Carbonate Fuel Cells

Molten Carbonate Fuel Cells (MCFC) use a molten alkali carbonate mixture as an electrolyte (Figure 2.23). At the anode, made of lithiated NiO, oxygen reacts with carbon dioxide and electrons to form carbonate ions:

$$1/2\,O_2 + CO_2 + 2e^- \longrightarrow CO_3^{-2} \qquad \text{Equation 2.2.3}$$

The ionic current through the electrolyte matrix is carried by the carbonate ions from the cathode to anode. At the anode (Nickel with 10 % Cr), oxidation of hydrogen consumes the carbonate ions and forms water vapor and carbon dioxide releasing electrons to the external circuit:

$$H_2 + CO_3^{-2} \longrightarrow H_2O + CO_2 + 2e^- \qquad \text{Equation 2.2.4}$$

In a practical MCFC, carbon dioxide produced at the anode must be transferred to the cathode where it is consumed. MCFC systems operate at about 650 ^oC [165-167]. Thus, a power plant with cell stacks of this type has several favorable characteristics:

(1) due to the reduced polarization losses, they do not require expensive catalysts, as do low-temperature fuel cells, such as PAFC;

(2) the operating temperature is high enough to produce high-quality waste heat which can be further used for fuel processing and cogeneration, and internal reforming of methane.

MCFC does not have a problem of anode CO poisoning as in low temperature fuel cells, in fact CO in the anode gas is used as a fuel[158,168]. Anderson and his co-workers

---

165. Kinoshita, K., McLarnon, F.R. and Cairn, E.J., Fuel Cells: A Handbook (U.S. Department of Energy, Morgantown, WV, 1988), DOE/METC88/6096.
166. Appleby, A.J. and Foulkes, F.R., *Fuel Cell Handbook* (Van Nostrand Reinhold, New York, **1989**.
167. Selman, J.R., *Energy* 11, 153, **1986**.

discussed some of the contaminants of fuel gas, derived from fossil fuels, and their effects on a MCFC[168].

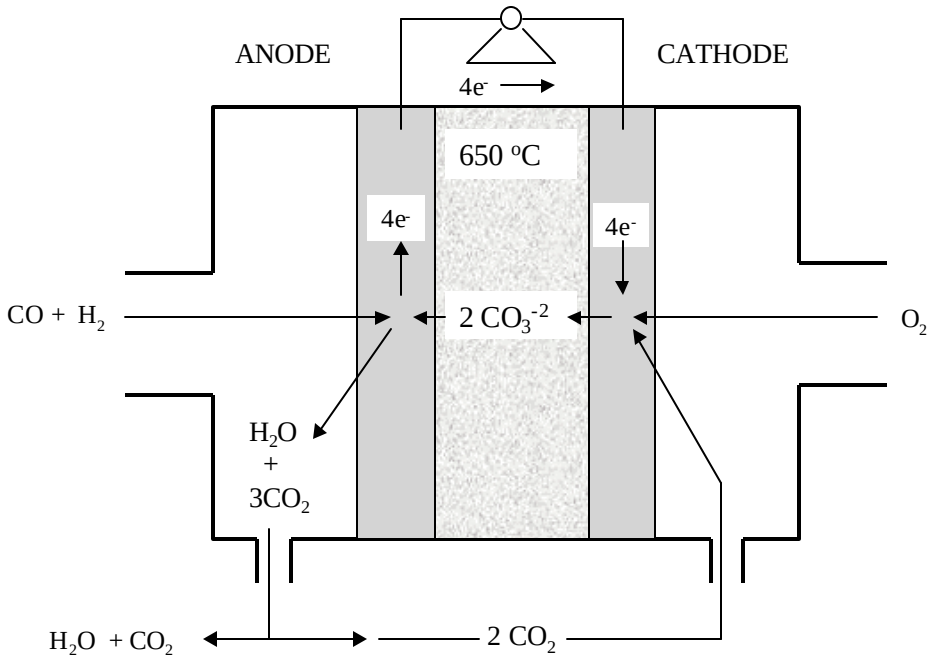

Figure 2.23 Schematic of a Molten Carbonate Fuel Cell

168. (a)Anderson, G.L. and Garrigan, P.C. in *Proceedings of the Symposium on Molten Carbonate Fuel Cell Technology* (Selman, R.J. and Claar, T.D., eds), the Electrochemical Society, Inc., Pennington, NJ, **1984**, Table 1, p. 299).

2.4.4.4 Solid Oxide Fuel Cells

The solid oxide fuel cell (SOFC) is an all solid-state power source that uses yttria-stabilized zirconia as the electrolyte layer[158]. The operating principle of SOFC is shown in Figure 2.24. At the anode, hydrogen reacts with oxide ions transported through the electrolyte to form water. This is accompanied by the release of electrons to the external circuit. The electrons from the external circuit react with oxygen at the cathode and produce oxide ions. The overall process is the reaction of oxygen with hydrogen to produce water. Carbon monoxide can also be used instead of hydrogen, and the corresponding reaction product will be carbon dioxide.

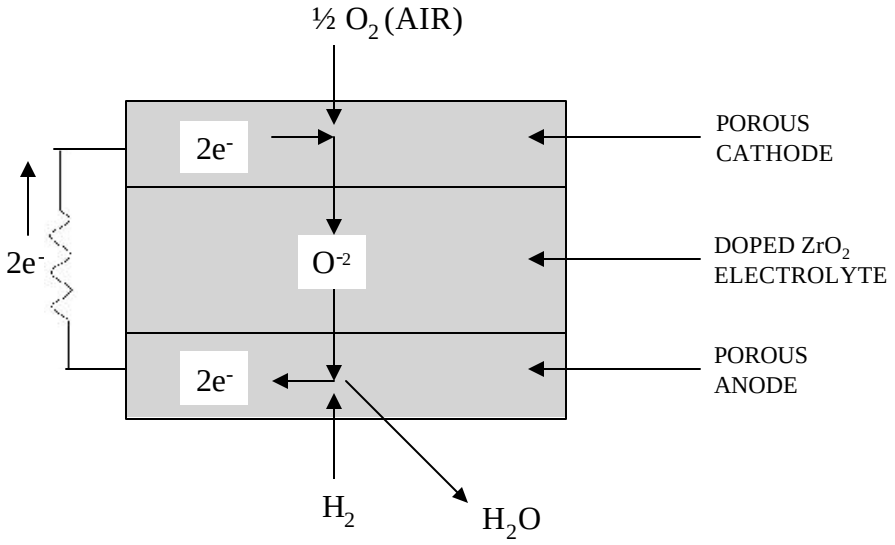

$$\text{CATHODE}: \quad 1/2\ O_2 + 2e^- \longrightarrow O^{2-} \qquad \text{Equation 2.2.5}$$

$$\text{ANODE}: \quad H_2 + O^{2-} \longrightarrow H_2O + 2e^- \qquad \text{Equation 2.2.6}$$

$$\text{CELL}: \quad H_2 + 1/2\ O_2 \longrightarrow H_2O \qquad \text{Equation 2.2.7}$$

$$(CO + 1/2\ O_2 \longrightarrow CO_2)$$

Figure 2.24 Principle of Operation High-Temperature Solid Oxide Electrolyte Fuel Cells[158]

These types of fuel cells operate equally well on dry or humidified hydrogen or carbon monoxide fuel or on their mixtures. Moreover, the high operating temperature considerably minimizes the catalyst poisoning. For example, a concentration of 50 ppm of hydrogen sulfide in the fuel lowers the operation cell potential by only 5 %. The sulfur tolerances are found to be about one to two orders of magnitude higher than for other types of fuel cells.

SOFCs are very attractive for electric utility and industrial applications. The high operating temperature and tolerance to impure fuel streams make SOFCs especially attractive for utilizing H_2 and CO from natural gas steam-reforming plants[158].

A major technical challenge in SOFC technology is the fabrication of the components of the electrochemical cell stacks. The cathode material must be stable to an oxidizing environment and should exhibit a good activity to oxygen reduction under the operating conditions. It should have some porosity and an electronic conductivity > 50 $Ù^{1}cm^{-1}$ [158]. Similarly, the anodic material must be stable in the reducing environment with a conductivity of more than 120 $Ù^{1}cm^{-1}$. The electrolyte layer for SOFCs must have high ionic conductivity and compared to other cell components, negligible electronic conductivities. This layer must also be very dense to prevent the crossover of reactants. In a SOFC stack, a mismatch of the thermal expansion coefficients of the cell components is a big issue and difficult to be minimized.

2.4.4.5 Solid Polymer Electrolyte Fuel Cells (SPEFC)

The solid polymer electrolyte fuel cells consist of a solid polymeric membrane which acts as an electrolyte. The membrane is sandwiched between two platinum catalyzed porous electrodes. A single cell assembly, shown in Figure 2.25, can be mechanically compressed. The fuel cell requires humidified gases, hydrogen as a fuel source and air as an oxygen source. The electrochemical reactions that occur at the platinum electrocatalyst sites can be written as follows[162,168b-c]:

168. (b) T. Zawodzinski, *Green Power*, *Los Alamos National. Lab*., 1999; (c) Savadoga, O. J. *New Materials For Electrochemical Systems* **1998**, Vol.1, No 1.

The overall fuel cell reaction is thus simply expressed by:

Anode : $H_2 \longrightarrow 2H^+ + 2\,e^-$ Equation 2.2.8

Cathode : $O_2 + 4\,H^+ + 4\,e^- \longrightarrow 2H_2O$ Equation 2.2.9

$$H_2 + 1/2\,O_2 \longrightarrow H_2O \qquad \text{Equation 2.2.10}$$

It is known that the oxygen reduction reaction is slower than the oxidation of hydrogen (the exchange current for oxygen reduction reaction is at least three orders of magnitude lower than that of hydrogen oxidation), therefore, one challenge is the enhancement of the electrocatalytic activity of this reaction. Several detailed studies of the electrode kinetic parameters at the platinum-isomer interface have been cited in the literature[169].

The functioning of a fuel cell depends on the formation of a stable three-phase boundary in the immediate vicinity of the electrocatalyst site. A thin film of the electrolyte layer may form on the electrocatalyst, and the reactant gas can dissolve in the electrolyte interface and then diffuse through the electrolyte film to the electrocatalyst.

In the SPEFC there is no liquid electrolyte and possibly a thin film forms on the electrocatalyst[158]. The presence of excess liquid water blocks the easy access of gas into the porous structure of the electrode, and the fuel cell's performance decreases due to mass transport limitations of the oxidant gas. This flooding situation is worsened by the ingress of water from the hydrogen side. The proton formed during hydrogen oxidation is usually strongly hydrated. This causes transport of water from anode to cathode. This phenomenon has further complications in that the loss of water causes drying out of the membrane and an increase in electrical resistance at the anode-membrane interface. It is

169. Srinivisan, S., Dav , B., Murugesamoorthi, K.A., Parthasarathy, A., and Appleby, A.J., *Fuel Cell Systems* (Blomen, L.J.M.J. and Mugerwa, M.N., eds) (Plenum Press, New York, **1993**) and Reference No's.49 and 50 therein.

therefore of greatest importance to be able to control the efficient addition of water to the hydrogen electrode and removal of water from the oxygen electrode.

Compared to the other types of fuel cells, including PAFC, MCFC, and SOFC, the solid polymer electrolyte fuel cells operate at a lower temperature. The thermal stability and conductivity characteristics of the polymeric membrane that is used as electrolyte limit the temperature at which the fuel cell operates.

For example, with Nafion®, it is best not to exceed an operating temperature of 85 ^{o}C. With the similar class of ionomers developed by Dow Chemical Company, this temperature can be increased by another 10-20 ^{o}C[158]. Operating pressures for oxygen can be atmospheric to 8 atm. Air pressures up to 8 atm have been used. Operation at higher pressure is necessary for attaining higher power densities, particularly with air as the cathodic reactant. In general, the pressure is maintained equally on either side of the membrane[169]. This minimizes gas crossover through the membrane. Gas crossover reduces the cell potential and also increases the risk of forming an explosive mixture of oxygen and hydrogen. Figure 2.26 shows the terminal voltage *vs*. current density plot for a SPEFC (with a loading of 4 mg/cm^2 Pt) that has been reported to be the best performance of its kind.

As mentioned earlier, the water management in the membrane and electrode assembly of the SPEFC is fairly complex and requires dynamic control to match the varying operating conditions of the fuel cell. Researchers at Los Alamos National Laboratory used a simple humidification scheme to disperse the gas through a ceramic frit immersed in a column of water. The disadvantage of this method is that the humidification depends greatly on the flow rate of the gases introduced into the fuel cell. High flow rate results in entrainment of the water as droplets in the gas stream. The flow rate is usually determined by stoichiometric flow requirements[158].

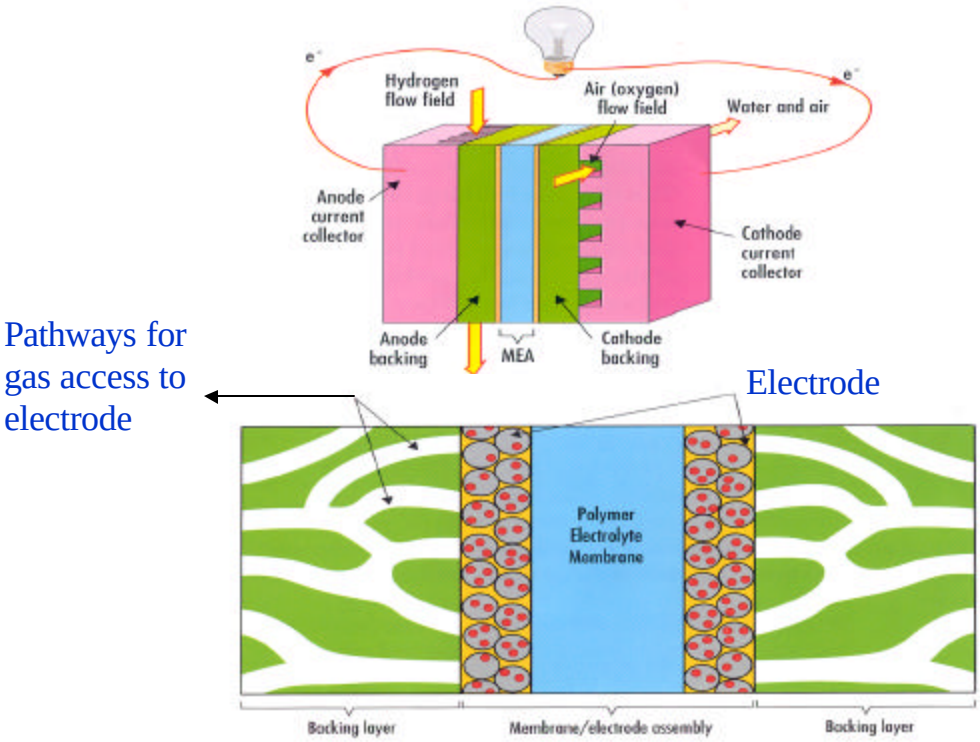

Figure 2.25 A single fuel cell assembly[168b]

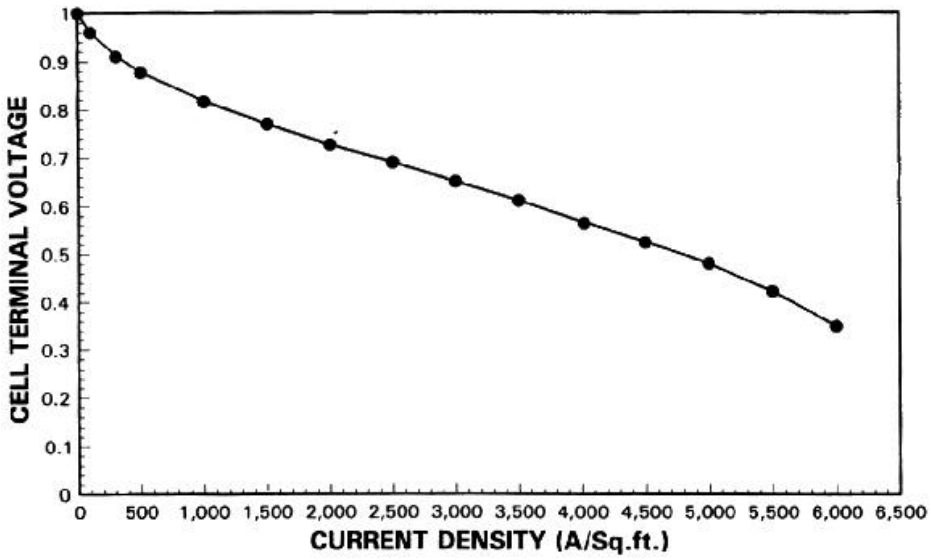

Figure 2.26 Terminal voltage vs. current density of Ballard Technologies Corporation's SPEFC[158]

2.4.4.5.1 Cell Materials

The solid polymer electrolyte fuel cells have made a great revival, mainly due to the success at DuPont and Dow Chemical Company in developing perfluorinated sulfonic acid membranes. It has been found that these polymers have high oxygen solubility, high proton conductivity, high chemical stability, low density, and high mechanical strength. As proton transport occurs from the anode to the cathode, a proton-conducting solid electrolyte is a must. The polymeric membranes developed by DuPont (Nafion®) and Dow have replaced conventional sulfonic acids of polydivinylbenzene-styrene based copolymers that have been discussed previously. The current state-of-the-art polymeric electrolyte used in the fuel cell produced by DuPont, is completely fluorinated and has a

poly(tetrafluoroethylene) backbone. The fluorocarbon chain is connected by means of a partial ether linkage to a sulfonic acid group. Although, the perfluorosulfonate ionomer from Dow is no longer commercially available, a comparison of DuPont's Nafion® and Dow perfluorosulfonate ionomer membranes is shown in Figure 2.27, for the sake of argument. These polymers have been synthesized over a wide range of equivalent weights (ratio of the weight of the polymer to the number of sulfonic acid groups). These polymers absorb a considerable amount of water into their molecular superstructure, which makes them fairly conductive over a wide range of temperature and pressure. Properties such as water content, oxygen solubility, conductivity, and thermal stability are closely related to the equivalent weight of the polymer and their exact interdependence is still being investigated.

The gas diffusion electrodes that have been used so far contain unsupported (2-10 mg/cm^2) or supported platinum (platinum supported on carbon; 0.4 mg/cm^2, 10% or 20% Pt on C) electrocatalysts[138]. The supported platinum electrode is essentially kept the same as that developed for phosphoric acid fuel cells (PAFC) and has not been optimized for the SPEFC. The electrodes have a carbon backing such as cloth or paper. A Nafion emulsion is used to bond the platinum particles (nm diameter) to the carbon layer. The active layer is deposited a few microns thick on the substrate layer (about 10 ìm for unsupported and 50 ìm for supported electrocatalysts). Studies at Los Alamos National Laboratory and at Texas A&M University have shown that the performance of electrodes with low platinum loading (0.4 mg/cm^2) is comparable to those with high platinum loading [170]. This was achieved by impregnating the active layer of the former type of electrode with a proton conductor[170].

The graphite support structures have gas flow paths to allow for laminar flow of gases across the electrode. Rectangular and circular flow paths in axial and concentric directions as well as flow-modeling studies on these electrodes have been attempted at several corporations and laboratories.

170. Srinivisan, S., Dav , B., Murugesamoorthi, K.A., Parthasarathy, A., and Apleby, A.J., *Fuel Cell Systems* (Blomen, L.J.M.J. and Mugerwa, M.N., eds) (Plenum Press, New York, **1993**) and Reference No. 54 therein.

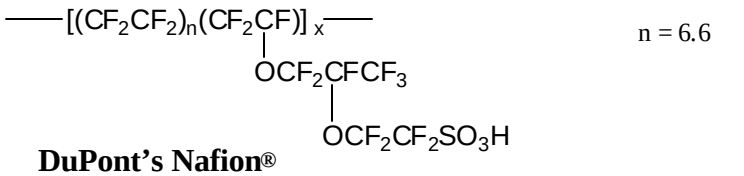

DuPont's Nafion®

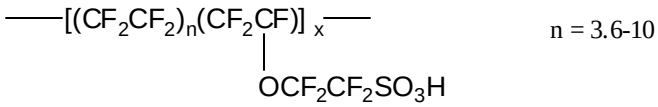

Dow Perfluorosulfonate Ionomers

Figure 2.27 Comparison of DuPont's Nafion® and Dow perfluorosulfonate ionomer membranes

2.4.4.5.2 Contamination Characteristics of SPEFC

Unlike the alkaline fuel cell, which is very sensitive to CO_2, the SPEFC is insensitive to CO_2 in the oxidant. This enables the possibility of using reformed gas directly as the oxidizer. The major contaminant, however, is carbon monoxide. It was proved that the performance of the fuel cell decreases dramatically when there is even 0.17 % carbon monoxide in the oxygen gas. It was demonstrated that the CO level can be significantly reduced from 1-2 % to 100 ppm by passing the reformed methanol and a small amount of oxygen (1-2 %) over a platinum-on-alumina catalyst[171]. An alloy catalyst, such as platinum-ruthenium, in the anode can tolerate this reduced level of CO. The following section discusses more about CO poisoning of polymer electrolyte membranes.

171 Srinivisan, S., Dav , B., Murugesamoorthi, K.A., Parthasarathy, A., and Apleby, A.J., *Fuel Cell Systems* (Blomen, L.J.M.J. and Mugerwa, M.N., eds) (Plenum Press, New York, **1993**) and Reference No. 53 therein

The high performance efficiency-power density of the SPEFC has made it an attractive candidate for both spaceships and terrestrial applications. Its performance evolution in space and on the oceans is already in progress. It shows promise for transportation applications because of the high power densities reported in hydrogen/oxygen fuel cells with low-platinum loading electrodes.

At present, one of the major challenges is economic, namely reducing the costs of the proton-conducting membranes and platinum-catalyzed electrodes. DuPont's Nafion® membrane cost about ($800/m^2) $60 - %200 per kilowatt.

2.4.4.6 Direct Methanol Fuel Cells

Although hydrogen/oxygen fuel cells are used in spaceships, wider applications in traction-based vehicles, e.g. electric cars, are limited by several continuing problems such as transport and transportation of hydrogen. Liquid fuels would solve this problem; however, a reformer is needed to extract molecular hydrogen from a liquid fuel. This, unfortunately, increases the overall cost of the cell and reduces the fuel conversion efficiency. An alternative to H_2 is the use of a liquid fuel such as methanol supplied directly to the anode and electrooxidized to CO_2. For the last few decades, the direct methanol fuel cell (DMFC) has been the dream of fuel cell researchers. Methanol is the simplest organic liquid fuel, which can most economically and efficiently be produced on a large scale from the fossil fuels, e.g. coal and natural gas. Furthermore, the steam reforming of methanol occurs at a relatively much lower temperature (200 ^{o}C versus 700 ^{o}C) than that of other organic fuels such as natural gas or ethanol.

A simple schematic of the DMFC is shown in Figure 2.28. The fuel, methanol and water are passed through the anode, and the oxidant, O_2 in air, flows through the cathode. The proton exchange membrane such as Nafion® separates the two electrodes. Again, platinum-based electrodes demonstrate the highest catalytic activity and cleanest combustion products. In methanol fuel cells, methanol reacts with water that is required for the overall conversion of fuel to carbon dioxide. The anodic reaction is:

$$H_2O + CH_3OH \longrightarrow CO_2 + 6H^+ + 6e^- \qquad \text{Equation 2.2.11}$$

Protons are again generated at the anode and move through the membrane to the cathode. With methanol fuel cells, the diffusion of methanol through the polymeric proton conductor is an important drawback that has to be into consideration[172].

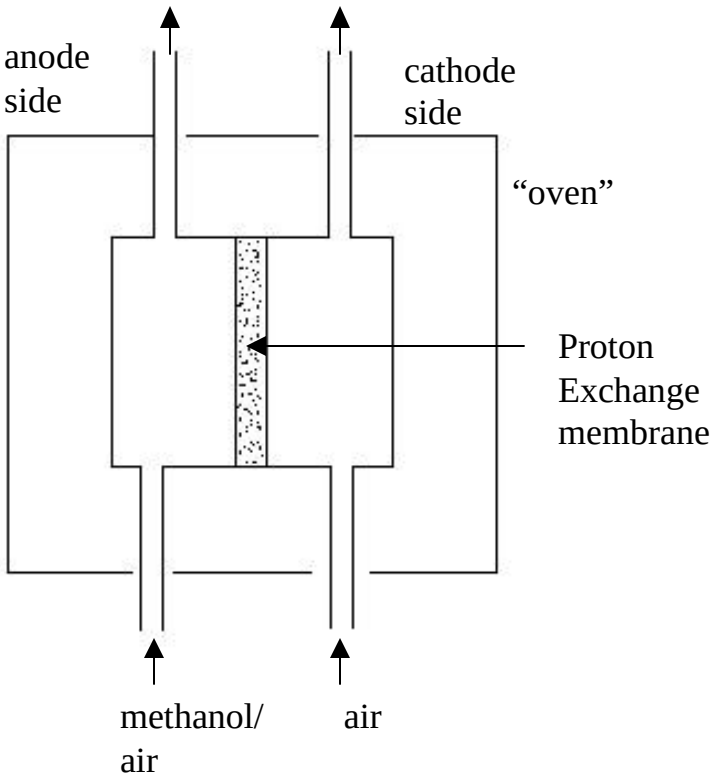

Figure 2.28 Schematic of a direct methanol fuel cell[173]

172. Verbrugge, M.W. *J. Electrochem. Soc*. 136 (**1989**) 417-83.

173. Kua, J. and Goddard III, W.A. *J. Am. Chem. Soc*. 121, **1999**, 10928-10941.

Another disadvantage associated with direct methanol fuel cells is a low power density[173]. High over-potentials at the anode catalyst combined with the low temperature use severely reduce the conversion efficiency. Thus, a high amount of noble metal loading is required to enhance the performance of the anode, thereby increasing costs. In addition, the membrane properties need to be improved with respect to water balance sensitivity (six protons at the anode produced per methanol molecule) and inhibition of methanol crossover. Diffusion of methanol across the membrane leads to depolarization of the cell and loss of activity.

Although the detailed reaction mechanism of DMFC's is not completely understood, relevant mechanistics were discussed by Leger and Lamy[174] and recently reviewed by Hamnett[175]. Several plausible pathways for the oxidation of methanol are discussed by Kua *et al.*[173] after examining the intermediates involved in the methanol oxidation in DMFCs on the several Group VIII transition metals. The overall reaction, which requires water for the conversion of methanol to carbondioxide as given in Equation 2.2.11 above, is considered in three stages: (1) dehydrogenation of methanol, (2) dehydrogenation of water, and (3) formation of a second C–O bond.

Methanol adsorbed on the electrode surface can undergo successive dehyrogenation, as shown in Equations 2.2.12-2.2.15. However, the exact structures of the adsorbed intermediates are unknown except for $(CO)_{ads}$, Kua *et al* said[173].

$$(CH_3OH)_{ads} \longrightarrow (CH_3O)_{ads} + H^+ + e^- \qquad \text{Equation 2.2.12}$$

$$(CH_3O)_{ads} \longrightarrow (CH_2O)_{ads} + H^+ + e^- \qquad \text{Equation 2.2.13}$$

$$(CH_2O)_{ads} \longrightarrow (CHO)_{ads} + H^+ + e^- \qquad \text{Equation 2.2.14}$$

$$(CHO)_{ads} \longrightarrow (CO)_{ads} + H^+ + e^- \qquad \text{Equation 2.2.15}$$

174. Leger, J.M. and Lammy, C. *Ber Bunsen-Ges. Phys. Chem*. **1990**, 94, 1021

175. Hamnett, A. *Catal. Today*, **1997**, 38, 445.

Their results also suggested that water may also dehydrogenate forming adsorbed OH and O atoms as shown in Equations 2.2.16 and 2.2.17, and $(CO)_{ads}$ is then removed from the surface with the formation of second C–O bond as in Equation 2.2.18.

$$(OH_2)_{ads} \longrightarrow (OH)_{ads} + H^+ + e^- \qquad \text{Equation 2.2.16}$$

$$(OH_2)_{ads} \longrightarrow (O)_{ads} + H^+ + e^- \qquad \text{Equation 2.2.17}$$

$$(CO)_{ads} + (O)_{ads} \longrightarrow CO_2 \qquad \text{Equation 2.2.18}$$

That last equation assumes complete dehydrogenation for both CH_3OH and H_2O takes place to form $[CO]_{ads}$ and $[O]_{ads}$ which then forms CO_2 that desorbs from the surface. Recombination followed by the dehydrogenation of adsorbed [CO] and [OH] species can also form CO_2 as shown in Equation 2.2.19.

$$(CO)_{ads} + (OH)_{ads} \longrightarrow (COOH)ads \longrightarrow CO_2 + H_{ads} \qquad \text{Equation 2.2.19}$$

A major concern of reformed fuels such as methanol is the potential need to remove large amounts of CO_2 from the H_2, as is necessary for CO (21). Reformed methanol, as seen in equations above, contains H_2, CO, CO_2 and H_2O, which undergo reactions on Pt electrodes. Stonehart and Ross explained that the electrooxidation of H_2 is a two-step reaction[175,176]. The first step (Equation 2.2.20), rate limiting, is dissociation of H_2 and requires two adjacent bare Pt sites.

$$H_2 + 2Pt \longleftrightarrow 2Pt\text{–}H \qquad \text{Equation 2.2.20}$$

$$Pt\text{–}H \longleftrightarrow Pt + H^+ + e^- \qquad \text{Equation 2.2.21}$$

175. Bellows, R.J., Marucchi-Soos, E.P. and Buckley, T.D., *Ind. Eng. Chem. Res*. **1996**, 35,1235.

176. Stonehart, P., Ross, P.N., Catal. Rev.-Sci. Eng. **1975**, 12, 1-35.

The second step (Equation 2.2.21) is the formation of free H^+ which is relatively fast on Pt. CO can adsorb directly onto either bare Pt sites (Equation 2.2.22) or Pt–H sites (Equation 2.2.23). When CO binds strongly to Pt sites, it blocks them for the dissociation of H_2 reaction (Equation 2.2.20)[176].

$$CO + Pt \longrightarrow Pt{=}CO \qquad \text{Equation 2.2.22}$$

$$2CO + 2Pt{-}H \longrightarrow 2Pt{=}CO + H_2 \qquad \text{Equation 2.2.23}$$

Acid electrolyte fuel cells were developed with the anticipation that the electrolyte would reject any CO_2 in the feed gases. Acid rejection of CO_2 appeared to give acid electrolyte fuel cells a major advantage over alkaline fuel cells in which CO_2 reacts with the electrolyte. Wilson et al. reported that CO_2 can polarize anode performance in PEFC [177]. At low potentials, CO_2 is electroreduced (Eq. 2.2.24) by Pt hydrides[178]. The Pt=CO, formed by reducing CO_2, polarizes H_2 electrooxidation in the same manner as Pt=CO formed by direct CO adsorption. Reduction (Eq. 2.2.24) can be considered the surface equivalent of the water-gas shift reaction[175].

Gilman explained that adsorbed CO from the above reactions (Eq's. 2.2.21-2.2.23) can be electrooxidized at higher electrode potentials via the reactant pair (Eq. 2.2.25) mechanism[179]. CO electrooxidation can be followed electrochemically from the current given off by the formation of fresh Pt oxides or hydroxides (Eq. 2.2.26).

$$CO_2 + 2Pt{-}H \longrightarrow Pt{=}CO + H_2O + Pt \qquad \text{Equation 2.2.24}$$

$$Pt{=}CO + Pt{=}O \longrightarrow CO_2 + 2Pt \qquad \text{Equation 2.2.25}$$

$$Pt + H_2O \longrightarrow Pt{=}O + 2H^+ + 2e^- \qquad \text{Equation 2.2.26}$$

177. Wilson, M.S., Derouin, C., Valerio, J., Gottesfeld, S. *Proc. 28th IECEC*, **1993**, 1, 1203.

178. Giner, J., Electrochim. Acta 1963, 8, 857.

179. Gilman, S., *J. Phys. Chem*. **1964**, 68, 70.

"CO tolerance" is usually defined as the ability to electrooxidize H_2 in the presence of CO at an acceptable polarization loss and is usually quantified at some current density in terms of the maximum CO concentration that can be tolerated. This is defined as nominal polarization loss (typically 20-100 mV) at the anode. Losses are referenced to performance on pure H_2. Various groups have reported a wide range of CO tolerance in acid fuel cells. The following paragraph will summarize several research results dealing with CO tolerance discussed in literature.

Wilson *et al.*[177], Simpson *et al.*[180] and Schmidt *et al.*[181] reported that on low Pt-loaded electrodes, CO must be reduced to only a few (2-5) ppm. Schmidt *et al.*[181] reported higher CO tolerances, between 10-100 ppm, for Pt-Ru electrodes. It was also reported that Pt is more "CO tolerant" during higher temperature (120 ^oC) operation[175].

Platinum is a very active electrocatalyst for H_2 and small amounts of CO in the H_2 can increase polarization losses to unacceptable levels. Figures 2.29 and 2.30 show the performance curves for PEFC electrodes with low Pt loadings as a function of added CO and CO_2 respectively[177].

The data showed little or no polarization at lower current densities. Polarization increased abruptly at higher current densities. For example, 5 ppm CO polarized performance was about 150 mV and 25 % CO_2 polarized performance was about 75 mV.
A few ppm CO caused more polarization than 25% CO_2. The relative poisoning by CO and CO_2 found is curious because, at equilibrium under PEFC operating conditions, the water gas shift reaction could produce about 100-200 ppm CO with a 75 % H_2 /25% CO_2 feed. CO at these equilibrium levels is a severe poison and would make it necessary to remove most of the CO_2 from the feed.

Earlier, it has been observed by many[173,182] that Pt-Ru alloy electrodes increase the electrocatalytic activity compared to pure Pt. Although methanol oxidation on platinum is known to be structure sensitive, the issue of size effects is still unresolved. One group

180. Simpson, S.F., Salinas, C.E., Cisar, A.J., Murphy, O.J., *Proton Conducting Membrane Fuel Cells* I, Gottesfeld, S., Halpert, G., Landgrebe, A., Eds.; The Electrochemical Society: Pennington, NJ, **1995**; pp 182-191.

181. Schmidt, V.M., Ianiello, R., Oetgen, H.F, Reger, H., Stimming, U., Trila, F., *Proton Conducting Membrane Fuel Cells I*, Gottesfeld, S., Halpert, G., Landgrebe, A., Eds.; The Electrochemical Society: Pennington, NJ, **1995**; pp 1-11].

182. Bockris, J.O.; Wroblowa, H., *J. Electroanal. Chem*. **1964**, 7, 428; Petry, O.A., Podlovchenko, B.I., Frumkin, A.N., Hira, L., *J. Electroanal. Chem*. **1965**, 10, 253.

suggested an optimum diameter of 2 nm[183], however, others did not find any evidence for size effects, even for particles as small as 1.4 nm [184].

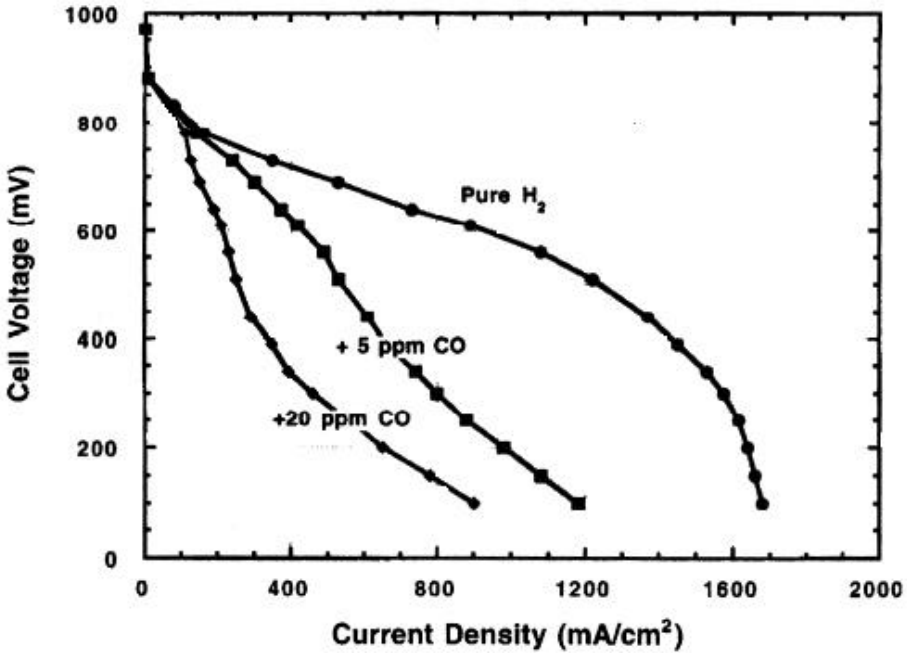

Figure 2.29 H_2/air PEFC polarization curves showing the effects of CO contamination for a 0.14 mg of Pt/cm^2 thin film anode at 80 ^oC[177].

183. Kennedy, B.J., Hamnett, A. *J. Electroanal. Chem*. **1990**, 283, 271.

184. Watanabe, M., Saegusa, S., Stonehart, P., *J. Electroanal. Chem*. **1989**, 271, 213.

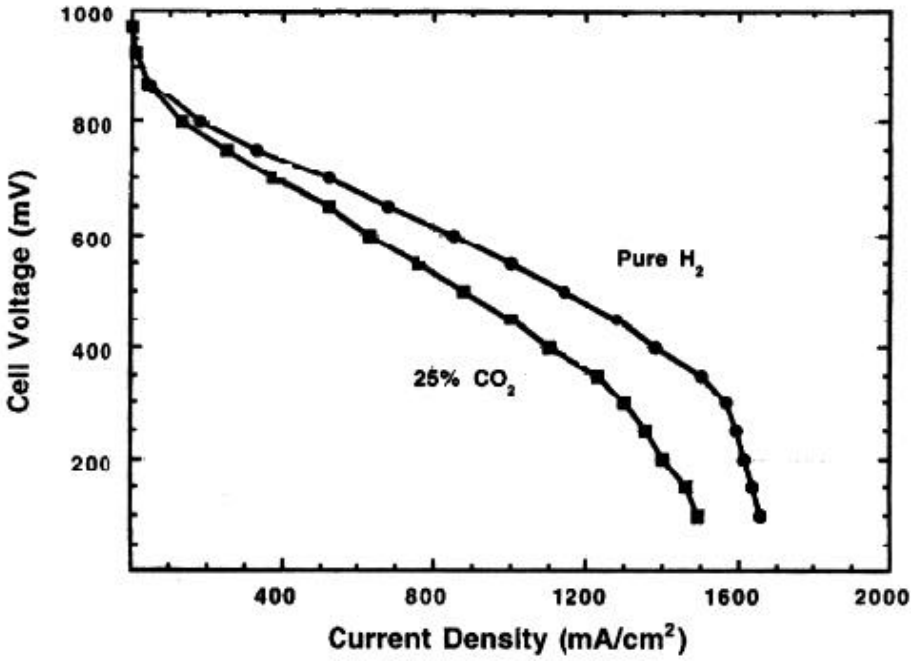

Figure 2.30 H_2/air PEFC polarization curves showing the effects of CO_2 contamination for a 0.12 mg of Pt/cm^2 thin film anode at 80 ^oC[177].

On the other hand, spectroscopic studies confirmed that only $(CO)_{ads}$ is the poisonous species [not $(COH)_{ads}$ or $(CHO)_{ads}$] for the electrode. Watanabe *et al*. presented a bifunctional mechanism of Pt-Ru. According to their mechanism, Pt is responsible for dehydrogenation of methanol[185]. On pure Pt, this reaction is poisoned because of the formation of $(CO)_{ads}$ after complete dehydrogenation of methanol. The removal of CO is facilitated by Ru, which may act by weakening the Pt-CO bond and/or by promoting the oxidation of CO to CO_2 via activation of water in an adjacent site to facilitate the formation of the second C–O bond. The onset potential of forming CO_2 on Pt-Ru (0.22 V vs RHS) is lower than that on Pt-black (0.325 V vs RHE). This has been attributed to the ability of Ru to adsorb OH at lower potentials. Pure Pt decomposes water at a high potential of 0.8 V vs RHE, whereas on pure Ru, the potential is required is only 0.2 V vs RHE [184,185].

185. Gateiger, H.A., Markovic, N., Ross, P.N., Jr, Cairns, E.J., *J. Electrochem. Soc*. **1994**, 98, 617; Lin, W.F., Wang, J.T., Savinell, R.F., *J. Electrochem. Soc*. **1997**, 144, 1917.

2.4.4.7 Relative Advantages and Disadvantages of Different Types of Fuel Cells

Much effort has been given to the development of highly efficient, emission free fuel cell power plants since the late 1950's for space and terrestrial applications. Fuel cells have been used in space applications for a long time compared to other applications. The main reason for that is that in space applications cost is of little consideration, while weight, volume, and reliability of cells are critical. Moreover, for space applications, cryogenic hydrogen and oxygen are the ideal fuels, in fact, they are the best fuels. However, for other applications of fuel cells, the cost is very critical as well as their durability, power efficiency, *etc*.

Table 2.6 summarizes the relative advantages and disadvantages of different types of fuel cells, assessed on a quantitative basis. Some of the factors taken into consideration are (1) fuel efficiency; (2) power density; (3) projected rated power level; (4) projected lifetime; (5) cost. This table also cites intended applications and the fuels which may be used in these fuel cells[162].

2.4.5 Perfluorinated Membranes as Polymer Electrolyte Membrane Fuel Cells (PEMFC)

Among the cation permeable membranes, the perfluorinated membranes which have been developed as separators for fuel cells as well as chlor-alkali electrolysers show the characteristic features of superselectivity, very high thermal stability and chemical resistance, which are not obtained by the other classes of polymeric ion permeable membranes. This section will provide the literature search on perfluorinated membranes including their historical development, synthesis, and their structural and proton conductivity characteristics.

Three commercial forms of cation permeable perfluorinated membranes have been proposed:

–the *Nafion*® monofunctional perfluorosulfonic membrane produced by Du Pont de Nemours,

– Dow® perfluorinated sulfonic acid ionomer membrane

–the *Flemion*® perfluorocarboxylic membrane produced by Asahi Glass,

–the Tokuyama Soda bifunctional membranes (both perfluorosulfonic and carboxylic)

Among them, only perfluorosulphonic membranes are proton conductors having high electrical conductivity combined with good mechanical properties, and a strong chemical resistance even in contact with oxidizing agent[186]. These membranes were first produced by Du Pont de Nemours (USA) under the registered trademark Nafion. To synthesize *Nafion®*, tetrafluoroethylene is reacted with SO_3 to form a cyclic sulfone. After rearrangement, the sulfone is then reacted with hexafluoropropylene epoxide to produce sulfonylfluoride adducts (m >1)[186].

Table 2.6 Relative Advantages and Disadvantages of Different Types of Fuel Cells

Type of fuel cell and of fuel	Fuel efficieny (%)		Power density (mW/cm^2)		Rated power-level projected (kW)	Lifetime projected (h)	Cost projected ($ / kW)		Applications, time frame
	Present	Projected	Present	Projected					
Alkaline H_2	40	50	100-200	>300	10-100	>10,000	>200	→	Space 1960- transportation 1996- standby power 1966-
Phosphoric Acid; CH_4, CH_3OH	40	45	200	250	100-5000	>40,000	1000-	→	Onsite integrated energy systems peak sharing 1992-
Molten carbonate CH_4; coal	45	50-60	100	200	1000-100,000	>40,000	1000	→	Base load and intermediate load power generation, cogeneration 1996-
Solid oxide Fuel cell CH_4; coal	45	50-60	240	300	100-100,000	>40,000	1500	→	Base load and intermediate load power generation, cogeneration 1996-
Solid polymer H_2; CH_3OH	45	50	350	>600	1-1000	>40,000	>200	→	Space 1960- Transportation 1996- Standby power 1992- Underwater 1996-
Direct Methanol $CH_3O + 1$	30	40	40	>100	1-100	>10,000	>200	→	Transportation 2010- Remote power 2000-

186. Colomban, P., *Proton Conductors: Solids, Membranes and Gel Materials and Devices*, Cambridge University Press, **1992**.

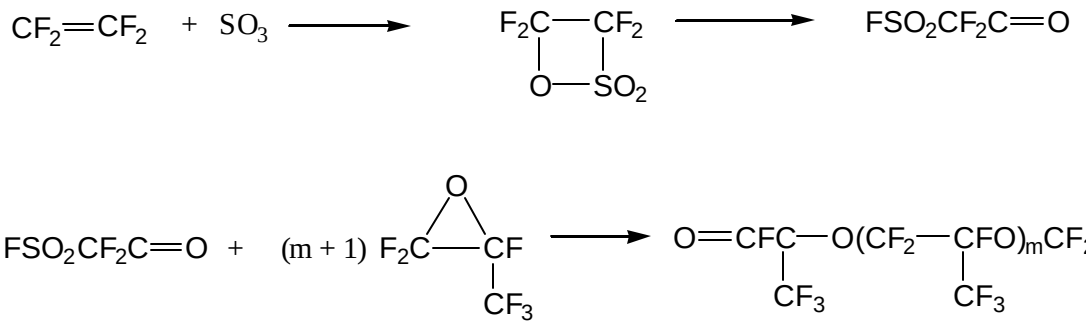

When these adducts are heated with sodium carbonate, a sulfonyl fluoride vinyl ether is formed. In the third step, this vinyl ether is copolymerized with tetrafluoroethylene to form XR resin.

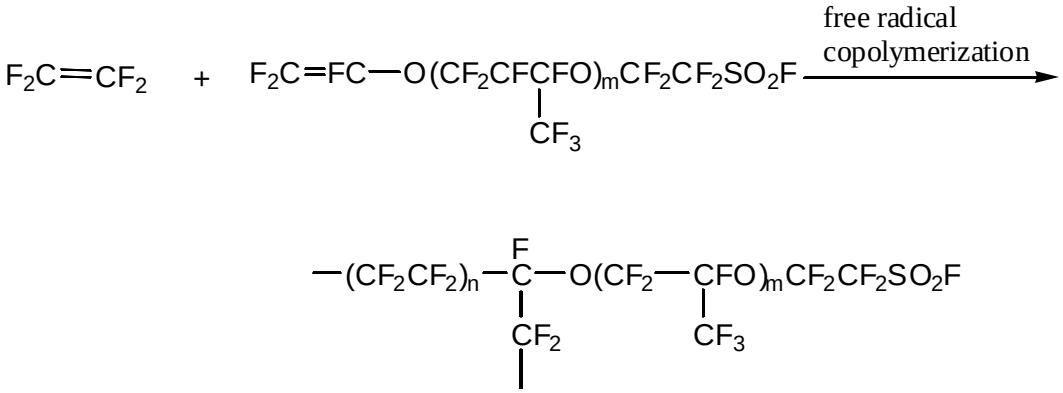

XR resin

This high molecular weight polymer is melt fabricable and can be processed into various forms, such as sheets or tubes. Finally, *Nafion*® perfluorosulfonic membrane is obtained by hydrolyzing the resin[186].

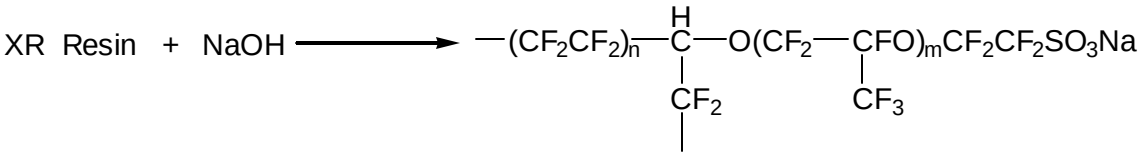

Nafion®

In this ion exchange membrane, the sodium-counter ion can be easily exchanged with other cations by soaking the polymer in an appropriate aqueous electrolyte solution.

To be able to conduct the proton, this membrane should be in its acid form (H^+ counter ion). For commercial materials, *m* is usually equal to 1 and *n* varies between 5 and 11. This generates an equivalent weight ranging from about 1000 to 1500 g of polymer in its dry hydrogen form per mole of exchange site. These membranes reveal a high permselectivity to cations and their water content can vary over a large range. It is widely accepted that sizeable ionic clusters scattered in a surrounding organic hydrophobic medium can exist in the polymer. A number of techniques including NMR, IR, mechanical and dielectric relaxation, electron microscopy and X-ray studies have suggested ion clustering in Nafion®. Gierke[187] proposed a cluster network model assuming that both the ions and sorbed solutions are all in clusters. Assuming the clusters to be spherical, their sizes have been calculated from solvent adsorption data obtained on various polymers of different equivalent weight. The calculated cluster diameters range between 3 and 5 nm for a 1200 equivalent weight polymer containing an average 70 ion exchange sites and 1000 water molecules[188]. In this model, the counter-ions, the fixed sites and the swelling water phase separate from the fluorocarbon matrix into approximately spherical domains interconnected by short narrow channels (Figure 2.31).

The fixed sites are embedded in the water phase near to the water fluorocarbon interface. This structure is essentially that of an inverted micelle. Lee and Meisel[189] using fluorescence spectroscopy, followed the diffusion of heavy cations in the membranes and have confirmed the inverted micellar structure. In the cluster network model, the diameter of the channels estimated from hydraulic permeability data is about 1 nm. Assuming that the the Bragg spacing (near 5 nm from SAXS data) represents the distance between clusters, they correlated the variations of cluster diameter and the number of ion exchange sites per cluster with water as shown in Figure 2.32, and established that the pore diameter decreases when the equivalent weight increases. Gierke

187. Gierke, T.D., *J. Electrochem. Soc*. 124 (**1977**) 319c.

188. Hsu, W.Y. and Gierke, T.D., *J. Membrane Sci*. 13 (**1983**) 307-26.

189. Lee, P.C. and Meisel, D., *J. Am. Chem. Soc*. 102 (**1980**) 5477-81.

et al.[190] established the existence of clusters even in the dry polymer. The increase in the number of exchange sites per cluster with increasing water content led them to suppose that a reorganization of the cluster network occurs during dehydration (Figure 2.33)

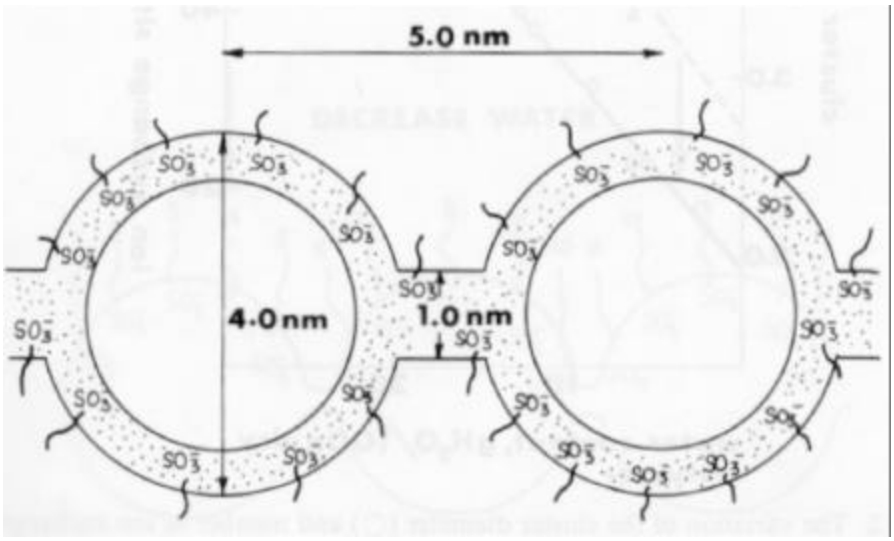

Figure 2.31 Cluster network model for Nafion® perfluorosulfonic membrane[188].

190. Gierke, T.D., Munn, G.E. and Wilson, F.C. *J. Polym. Sci. Polym. Phys. Ed.* 19 (**1981**) 1687-704.

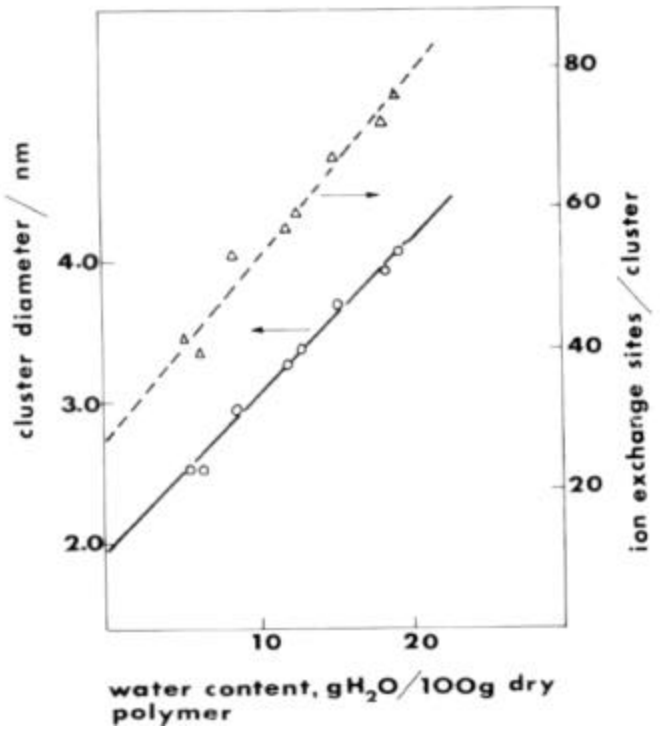

Figure 2.32 The variation of the cluster diameter (O) and the number of ion exchange sites (Ä) per cluster with water content in Nafion® 1200 EW polymer[188].

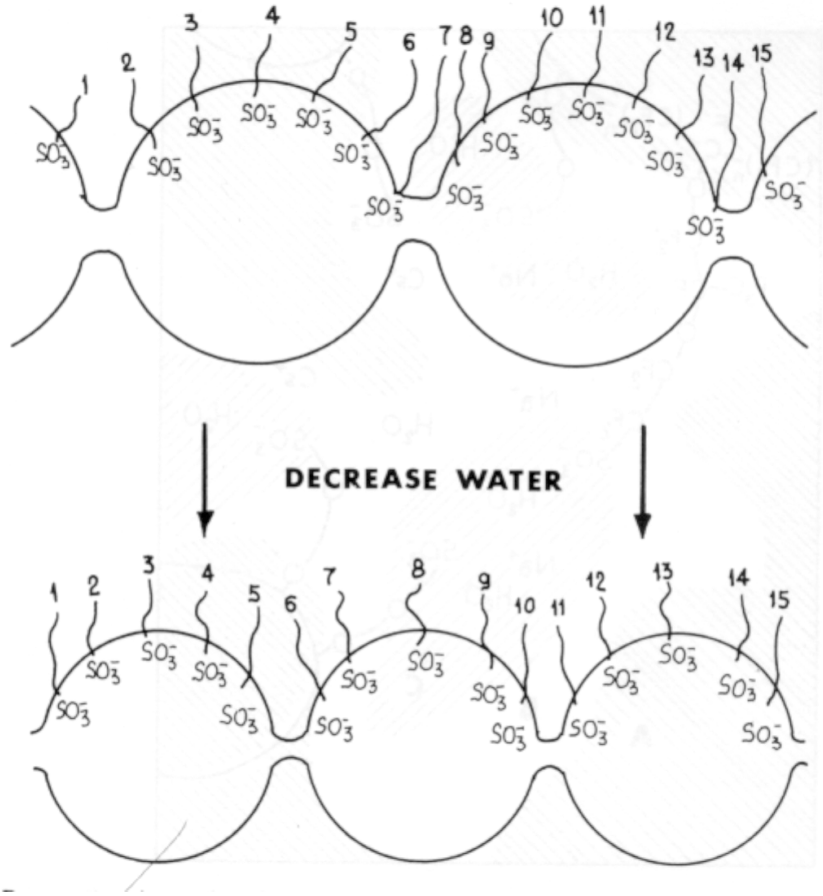

Figure 2.33 Redistribution of ion exchange sites occurring during dehydration of the polymer[190]

Using small angle (SAXS) and wide angle (WAXS) X-ray spectroscopy, Hashimota *et al.* established that ionic clusters affect the physical properties of the membranes[191]. The size of the ionic clusters was shown to depend on the equivalent weight, the nature of the cation and of the fixed sites, and also on temperature.

The perfluorinated ionomer membranes, with no crosslinking, rely upon their crystalline domains to inhibit dissolution[186]. The crystalline domains originating from

191. Hashimoto, T., Fujimara, M. and Hawai, H. in *Perfluorinated Ionomer Membranes*. Eisenberg, A. and Yeager, H.L.(eds) A.C.S. Symposium Series, no. 180 (**1982**) 217.

the tetrafluoroethylene material act as crosslinked points. The degree of crystallinity decreases with increasing equivalent weight (EW)[193].

Perfluorosulfonate polymers with EW less than 1000 are soluble[194] primarily due to the lack of crystallinity.

2.4.5.1 Proton Transport in Perfluorosulfonic Membranes

The transport properties of perfluorosulfonic membranes are largely dependent on the water content of the membrane, particularly when the membrane is in the acid form. In the dry state, the Nafion® ion-conductive membrane behaves like an insulator but, when hydrated, the membrane becomes conductive. The water content necessary for conduction has been established to be a minimum of about six to seven molecules of water per sulfonic site[195].

Because of the strong acidity of the sulfonic acid groups, the membrane is highly conductive to protons. Yeo *et al.*[196] have reported that the conductivity of Nafion® in concentrated acid electrolytes is one order of magnitude smaller than the electrolyte conductivity. In the case of very dilute electrolytes, the membrane conductivity is higher than that of the electrolyte because its intrinsic conductivity becomes important[197].

Among the polymer containing acid groups which all have high but similar intrinsic conductivities, the activation energy of proton conduction of Nafion® is low compared to that in other polymers[195]. This low activation energy of proton conduction may be due to the state of the water in the membrane phase.

In a fuel cell using proton exchange membranes, the water content of the membrane has been monitored by steady-state contact of humidified gas streams at each membrane interface. Under these conditions, Rieke and Vanderborgh have shown that the proton conductivity reaches a maximum over a temperature range of 55-70 ^{o}C even though the

193. Starkweather Jr, H. W. *Macromolecules* 15 (**1982**) 320.

194. Grot, W.T. *US Patent*, 4433082 (**1984**).

195. Yeo, R.S. *J.Electrochem.Soc.* 130 (**1983**) 533.

196. Yeo, R.S. and Chin, D.T. *J. Electrochem. Soc.*127 (**1980**) 549-55.

197. Yeo, R.S. and McBreen, J.C. *J. Electrochem. Soc*. 126 (10) (**1979**) 1682-6.

water content is lowest in this domain[198]. They have established that, in the temperature range of 25-50 ^{o}C, a variation in water content is less significant than a temperature increase. Consequently, temperature plays also an important role in the kinetics of proton motion in the polymeric membrane. Outside these two temperature ranges, the conductivity decreases due to a deionization of sulfonic acid groups and perhaps also due to a change of the hopping distance between cluster zones.

The mobility of protons in Nafion® perfluorosulfonic membranes is strongly associated with the water content of the membrane phase. This mobility is directly related to the molality of fixed charged sulfonic sites. By IR measurements, the protonated form of sulfonic sites was observed for low water contents in these membranes[186].

The conductivity of Nafion® membranes depends on the equivalent weight of the ion exchange polymer and its water content, these two parameters being closely related. On the other hand, the conductivity has been found to be affected strongly by the pretreatment of the membrane[195,196]. At room temperature, the maximum conductivity reaches 0.078 Ù^{1} cm^{-1} for a Nafion® 1100 EW without sorbed acid and 0.098 Ù^{1} cm^{-1} for a Nafion® 1200 EW when HBr is present in the membrane phase[197].

Nafion® materials, and more generally perfluorinated ionomers, are particularly suitable for water and brine electrolysis. Numerous groups have worked to develop alternatives to these expensive pefluorinated sulfonic acid membranes for Solid Polymer Electrolyte Membranes (SPEM). The dissolution of Nafion® membranes allows the preparation of materials with high porosity and high electroactive area. Such structures are required for the development of high power density SPEM fuel cells. Aldebert *et al*. have presented different methods for the preparation of SPEM electrocatalyst composites. One of the remaining problems of these composites is the optimization of the permeability of perfluorinated ionomer to H_2 and O_2 gas[199].

Polymers having both electronic and ionic conductivities are of interest due to the applications of composite materials in polymeric electrodes or in electrochemical catalysis. Electronic and ionic conductive polymer composites have been synthesized by

198. Rieke, P.C and Vanderborgh, N.E. *J. Membr. Sci.* 32 (**1987**) 313-28.

199. Aldebert, P., Novel, Castin, F., Pineri, M., Millet, P. Doumain, C. and Durand, R., *Solid State Ionics* 35 (**1985**) 3-9.

electropolymerization using pyrrole, bithiophene or aniline trifluoromethane with an hydrophobic ionomer gel of the Nafion® type[200].

Because of the great industrial importance of the perfluorinated cation exchange membrane, the research effort devoted to this membrane during the past 20 years has greatly exceeded that devoted to any other single ion exchange membrane. Their remarkable chemical stability, their high permselectivity to cations, particularly to protons, associated with a low electrical resistance and very good mechanical properties make them very good materials in an aggressive environment like fuel cell operation conditions. Concerning their structure, in addition to a small amount of crystallinity leading to cohesion of the material, two distinct non-crystalline regions exist. These regions are the hydrophobic fluorocarbon phase and the hydrophilic ionic area, comprised of aqueous clusters forming an inverted micellar-like structure. As a result of spectroscopic studies, it has been shown that interactions between the mobile cations and the anionic fixed sites are highly sensitive to the degree of hydration of the membrane. The relatively high cost of these perfluorinated ionomer membranes requires us to develop better knowledge of the relationship between the unusual ion cluster morphology and the transport properties. Such knowledge will lead to materials having similar or in some aspects better properties at lower cost.

2.4.6 Review of Other Candidate Polymers for PEMFC

The high electro-osmotic water flows, high methanol crossover rates and high cost of perfluorinated ionomer membranes have stimulated research into alternative proton-ion conducting polymer electrolyte membranes (PEM) for H_2/O_2 and/or direct methanol fuel cell applications. These are high temperature or engineering polymers that are almost always aromatic polymers linked together either in a single chain or in a ladder or step-ladder arrangement[201] and specifically modified to conduct protons. The high temperature-engineering polymers studied so far as a potential candidate for PEMs contain pendant ionic groups that are almost exclusively sulfonic acid moieties. Some of

200. Gebel, G., Aldebert, P. and Pineri, M., *Macromolecules* 20 (**1987**) 1425-8.

201. Robert William Kopitzke, *Ph.D Dissertation*, Florida Institute of Technology, **1999**, Melbourne, FL.

these polymers are: polyether(ether)ketones (PEEK), poly(p-phenylene) (PPP), polyethersulfones (PES), poly(sulfide)sulfones (PSS), poly(phenylene sulfide) (PPS), poly(aryl)ethers (PAE), polybenzimidazoles (PBI), polyimides (PI) and some block copolymers including sulfonated styrene-ethylene/butylenes-styrene triblock copolymer[202]. Of these, the sulfonated polyetherketones were first prepared in 1984[203]. Bailly *et al*. sulfonated the polymer by dissolving it as a powder in concentrated sulfuric acid solution and then precipitating it into water [204]. With this method, the degree of sulfonation could not be controlled. Several other studies have reported variations of this procedure with the focus being controlling the degree of sulfonation[205]. This polymer has been extensively characterized in terms of its molecular weight[206], water uptake[204] and glass transition temperature versus degree of sulfonation/cation type (H^+, Na^+, Zn^{2+})[205].

Bailly *et al*. also investigated the effect of sulfonation level on the crystallinity as well as on the microstructure of the polymer[204]. Finally, thermogravimetric analysis of these polymers containing different cations and degrees of sulfonation has been done under nitrogen atmosphere[205]. Very recently, Mikhailenko *et al*.[206] prepared polymer blends of sulfonated polyether ether ketone (SPEEK) with polyether imide (PEI) and studied the influence of blending and then doping with HCl and H_3PO_4 on the properties [207]. Blending with PEI resulted in decrease in membrane swelling at PEI concentrations greater than 5 %. Doping with acids, especially with HCl, greatly enhanced the conductivity.

---

202. Wnek, G.E., Rider, J.N., Serpico, J.M., Einset, A.G., Ehrenberg, S.G. and Raboin, L.A., in: Gottesfeld, S., Halpert, G., Landgrebe, A. (Eds.) *Proton Conducting Membrane Fuel Cells I*, PV 95-23, The Electrochemical Society Proceedings Series, Pennington, NJ, **1995**, pp.193-201.

203. Lee, J. and Marvel, C.S., *J. Polym. Sci. Poly. Chem*. Ed. 22, 295 (**1984**).

204. Bailly, C., Williams, D.J., Karasz, F.E. and MacKnight, W.J., *Polymer*, 28, 1009, **1987**.

205. Jin, X., Bishop, M.T., Ellis, T.S. and Karasz, F.E. *Brit. Poly.J*., 17, 4, **1985**.

206. Devaux, J., Delimov,D., Daousti, D., Legras, R., Mercier, J.P., Strazielle, C. and Nield, E., *Polymer*, 26 1994 **1985**.

207. Mikhailenko, S.D., Zaidi, S.M.J., Kaliaguine, S., *J. of Polym. Sci.: Part B: Polymer Physics*, 38, 1386-1395 **2000**.

Sulfonated polyethersulfones have been made by polymerization of sulfonated monomers[208,209] and by derivatization of the polymer with chlorosulfonic acid[210] with sulfur trioxide[211], and with sulfur trioxide complexed with triethylphosphate (SO_3-TEP)[212]. Thermal characterization of these polymers has included measurement of the glass transition temperature as well as thermo-mechanical and thermo-gravimetric analysis[208]. Nolte and his co-workers studied the membrane characteristics of the polymer including water uptake, permselectivity, resistance, and current-voltage behavior at room temperature[211]. Feng *et al*. prepared[209] a series of sulfonated poly(phenylene sulfide sulfone)s and poly(arylene ether sulfone)s via direct polymerization using A-A or A-B type difunctional monomers. Film forming membranes with up to 60 % of the sulfonated activated halide structure were obtained.

Sulfonated polybenzimidazoles (S-PBI) have been prepared by conventional polymerization of a tetraamine with sulfonated terephthalic acid[213]. In addition, S-PBI can be made by soaking PBI in dilute sulfuric acid solution to form the ammonium hydrogen sulfate salt followed by heating at 400 to 500 ^{o}C for several minutes to form the covalently bonded sulfonic acid[214]. The latter "soak and bake" process is used by Hoechst Celanese to produce sulfonated PBI fiber commercially. Thermogravimetric analysis coupled with mass spectroscopy studies of this polymer showed the decompostion producing SO_2 beginning at around 320 ^{o}C and peaking at approximately 475 ^{o}C. Conductivity measurements have also been made on S-PBI films[215].

---

208. Ueda, M., Toyata, H., Ouchi, T., Sugiyama, J., Yonetake, K., Masuka, T. and Teramoto, T., *J. Polym. Sci. Poly. Chem. Ed*. 31, 853 **1993**.

209. Wang, F., Mecham, J., Harrison, W. and McGrath, J.E., *Polym. Prep***. 2000**, 41(2), 1401; Wang, F., Ji, Q., Harrison, W., Mecham, J., Formato, R., Kovar, R., Osenar, P., McGrath, J.E., *Polym. Prep***. 2000**, 41(1), 237.

210. Quentin, J.P., *U.S. Patent* 3,709,841, Rhone Poulenc, **1973**.

211. Nolte, R., Ledjeff, K., Bauer, M. and Mulhaupt, R., *J. Memb. Sci*., 33, 211, **1993**.

212. Johnson, B.C., Yilgor, I., Tran, C., Igbal, M., Wightman, J.P., Lloyd, D.R. and McGrath, J.E., *J. Poly. Sci. Poly. Chem. Ed*., 22, 721, **1984**.

213. Dang, T.D., Chen, J.C. and Arnold, F.E. in *Hybrid Organic-Inorganic Composites*, ACS Symp. Ser., 585, 280, **1985**.

214. Kudor, J.E. and Chen, J.C., *U.S. Patent*, 4,634,530, **1987**.

215. Powers, E.J. and Serad, G.A. in *High Performance Polymers: Their Origin and Develop*ment, 355, **1986**.

Guo and his co-workers prepared sulfonated and crosslinked polyphosphazane proton-exchange membranes. The base polymer was first sulfonated with SO_3 and then solution cast to prepare its thin film. Dissolving benzophenone photoinitiator in the membrane casting solution and then exposing the resulting films after solvent evaporation to UV light achived out polymer crosslinking. Sulfonated and crosslinked polyphosphazane films showed no signs of mechanical failure up to 173 ^{o}C and exhibited low water and methanol diffusities[216].

2.4.7 Use of polyphosphoric acids

Several groups have studied the heteropoly acids (HPA) as proton-conducting electrolytes in the low-temperature fuel cells. In these studies, the HPAs have been used both, in crystalline form [217], or as concentrated aqueous solutions[218,219].

In these studies, composite membranes containing HPA anchored to a support, have been prepared. Preliminary conductivity tests performed on membranes prepared by introducing directly the HPAs into a polybenzimidazole (PBI) dispersion gave very poor proton conductivity. Similar results on conductivity of PBI films doped with phosphotungstic acid (PWA) solutions were also obtained by Xing and Savadogo(69). The low conductivity was explained in terms of lack of interaction between the PWA and polymer that does not allow the acid to remain fixed in the membrane. However, higher conductivites were recently obtained by Staiti *et al*. on samples that were prepared by the adsorption of HPAs on silica followed by the introduction into the PBI dispersion [221].

216. Guo, Q., Pintauro, P.N., Tang, H. and O'Connor, S., *J. Membrane Science* 154 (**1999**) 175-181.
217. Staiti, P., Hocevar, S. and Giordano, N., Journal of Hydrogen Energy 22 (**1997**) 809.
218. Giordano, N., Staiti, P., Hocevar, S. and Aricü, A.S. *Electrochim. Acta* 41 (**1996**) 397.
219. Staiti, P, Aricü, A.S, Hocevar, V. and Antonucci, J., *New Mater. Electrochem. Syst.* 1 (**1998**).
221. Staiti, P., Minutoli, M. and Hocevar, S., *Journal of Power Sources* 90 (**2000**) 231-235.

CHAPTER 3. EXPERIMENTAL

Pure reagents, solvents and monomers are important in the synthesis of monomers which can afford high molecular weight polymers. Therefore, monomers and reagents used in this research were carefully purified and dried prior to use. Solvents for polymerizations as well as monomer preparations were generally distilled from drying agents, such as calcium hydride, CaH_2, and phosphorus pentaoxide, P_2O_5, using the apparatus shown in Figure 3.1. This allowed reduced pressure distillations and refluxing over drying agents prior to solvent collection. The distilled solvents were collected in round bottom flasks and sealed under a dry nitrogen atmosphere with a rubber septum and parafilm. The solvent was transferred to reaction vessels using syringe techniques to minimize moisture exposure.

3.1 Purification of Solvents

Chloroform $CHCl_3$, (Fisher Scientific) was received as a HPLC grade solvent and used without purification (b.p. 61-62 ^oC / 760mmHg).

Ethanol, C_2H_5OH, (Aldrich, absolute) was used as received (b.p. 78.5 ^oC / 760mmHg).

o-Dichlorobenzene (o-DCB, Aldrich) was dried over calcium hydride for at least 12 hours and distilled under reduced pressure (b.p. 180 ^oC / 760mmHg).

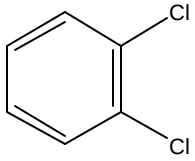

N,N-Dimethylacetamide (DMAc, Fisher Scientific) was dried over calcium hydride for at least 12 hours and distilled under reduced pressure (b.p. 163-165 ^oC / 760mmHg).

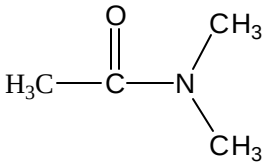

Acetic anhydride (Ac_2O, Fisher Scientific) was used as received (b.p. 138 ^oC).

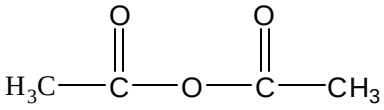

Diethyl Ether (Mallinckrodt) was used as received (b.p. 34.6 ^oC / 760mmHg).

Methanol (Fisher Scientific) was received as HPLC grade solvent and used without purification (b.p. 64.7 ^oC / 760mmHg).

1-Methyl-2-Pyrrolidone (NMP, Fisher Scientific) was dried over phosphorus pentoxide for at least 12 hours and distilled under reduced pressure (b.p. 205 ^oC / 760mmHg).

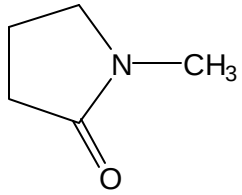

Toluene (Fisher Scientific) was used as received (b.p. 110.6 ^oC / 760mmHg).

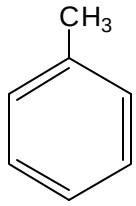

Triethylamine (Fisher Scientific) was dried over sodium for at least 12 hours and distilled under reduced pressure (b.p. 88.8 ^oC / 760mmHg).

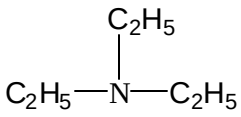

m-Cresol (Aldrich) was dried over phosphorus pentaoxide for at least 12 hours and distilled under reduced pressure (b.p. 205 ^{o}C / 760mmHg).

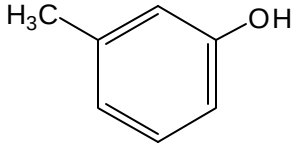

Methyl Ethyl Ketone (Fisher Scientific) was used as received (b.p. /760 mmHg)

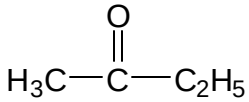

Deuterated Chloroform ($CDCl_3$, Cambridge Isotope Laboratories) was used as received (b.p. 61 ^{o}C / 760mmHg).

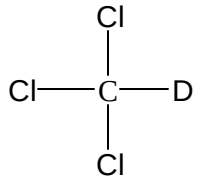

Deuterated Dimethyl Sulfoxide (DMSO-d6, Cambridge Isotope Laboratories) was dried over molecular sieves for at least 24 hours (b.p. 55 ^{o}C / 760mmHg).

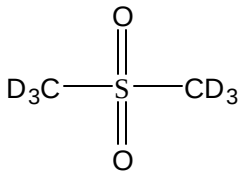

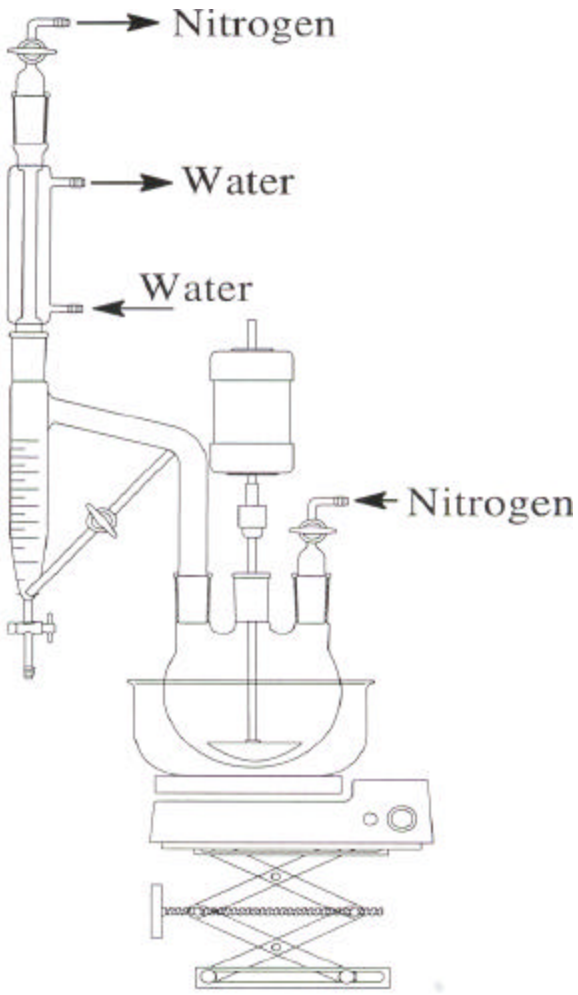

Figure 3.1 Distillation apparatus

3.2 Reagents and Commercially Available Dianhydrides and Diamines

3.2.1 General Reagents

Fuming Sulfuric Acid

Supplier:	Aldrich
Empirical Formula:	$H_2SO_4\ xSO_3$
Molecular Weight (g/mole):	98.08
Boiling Point (^{o}C):	120 ^{o}C
Purification:	used as received

Fuming Nitric Acid

Supplier:	Aldrich
Empirical Formula:	$HNO_3 \bullet xSO_3$
Molecular Weight (g/mole):	63.01
Boiling Point (^{o}C):	120 ^{o}C
Purification:	used as received

Hydrazine monohydrate

Supplier:	Acros
Empirical Formula:	$NH_2NH_2.H_2O$
Molecular Weight (g/mole):	50.07
Boiling Point (^{o}C):	120 ^{o}C
Purification:	used as received

Potassium carbonate

Supplier:	Fisher
Empirical Formula:	K_2CO_3
Molecular Weight (g/mole):	138.21
Melting Point (^{o}C):	891 ^{o}C
Purification:	used as received

Palladium on carbon (Pd/C)

Supplier: Aldrich

Empirical Formula: 10% Pd/C

Purification used as received

Isoquinoline

Supplier: Aldrich

Empirical Formula: C_9H_7N

Molecular Weight (g/mole): 129.16

Melting Point (^{o}C): 25-27 ^{o}C

Purification: used as received

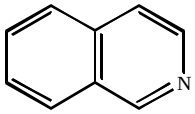

3.2.2 Monomers

3.2.2.1 3,4,3',4'-Biphenyltetracarboxylic dianhydride (BPDA)

Supplier: Aldrich Chemical Company

Empirical Formula: $C_{16}H_6O_6$

Molecular Weight (g/mole): 294

Melting Point (^{o}C): 300

Purification: Polymer grade BPDA was used after drying at 180 ^{o}C under vacuum for at least 12 hours.

Structure:

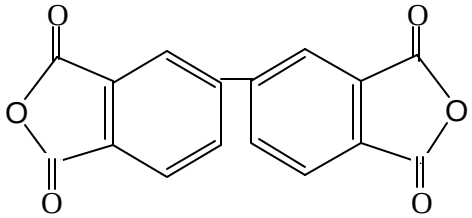

3.2.2.2 5,5'-[2,2,2-Trifluoro-1-(trifluoromethyl) ethylidene] bis-1,3-isobenzo-furandione (6FDA)

Supplier: Hoechst Celanese Corporation

Empirical Formula: $C_{19}H_6F_6O_6$

Molecular Weight (g/mole): 444.8

Melting Point (^oC): 247

Purification: Polymer grade 6FDA was used after drying at 180 ^oC under vacuum for at least 12 hours prior to use.

Structure:

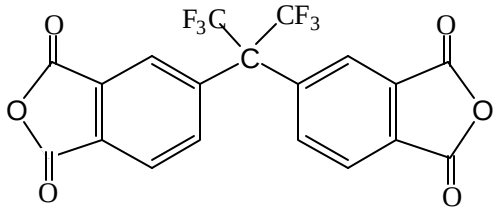

3.2.2.3 3,3',4,4'-Biphenyl sulfone tetracarboxylic dianhydride (BPSDA)

Supplier: Aldrich Chemical Company

Empirical Formula: $C_{16}H_6O_8S$

Molecular Weight (g/mole): 358.28

Melting Point (^oC): 292.1

Purification: Polymer grade BPSDA was used after drying at 180 ^oC under vacuum for at least 12 hours.

Structure

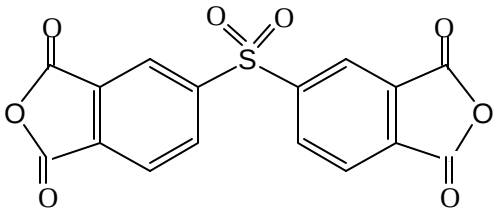

3.2.2.4 Napthalene tetracarboxylic dianhydride(NDA)

Supplier: Aldrich Chemical Company

Empirical Formula: $C_{14}H_4O_6$

Molecular Weight (g/mole): 268.18

Melting Point (^{o}C): >300

Purification: Polymer grade NDA was used after drying at 180 ^{o}C under vacuum for at least 12 hours prior to use.

Structure:

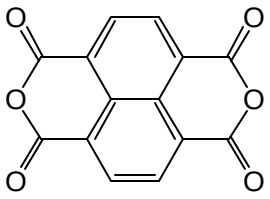

3.2.2.5 1,3-Phenylenediamine (mPDA)

Supplier: Acros Organics

Empirical Formula: $C_6H_8N_2$

Molecular Weight (g/mole): 108.12

Melting Point (^{o}C): 66

Purification: mPDA was sublimed under vacuum (~5 torr) at ~60 ^{o}C. This monomer oxidizes readily in air and must be used soon after sublimation. To prevent oxidation, it must be stored in the dark under vacuum.

Structure

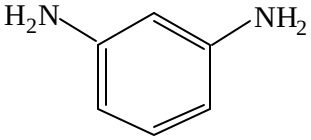

3.2.2.6 4,4 ¢-Oxydianiline (4,4 ¢-ODA)

Supplier: Kennedy and Kim

Empirical Formula: $C_{12}H_{12}N_2O$

Molecular Weight (g/mole): 200.24

Melting Point (^{o}C): 192

Purification: 4,4'-ODA was sublimed under vacuum (~5 torr) at ~170 ^{o}C.

Structure:

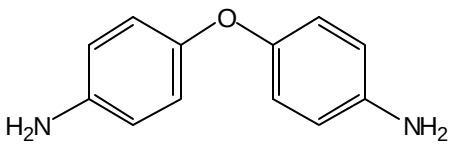

3.2.2.7 3,3'-Diaminodiphenyl Sulfone (pDDS)

Supplier: Aldrich Chemical Company

Empirical Formula: $C_{12}H_{12}N_2O_2S$

Molecular Weight (g/mole): 248.3

Melting Point (^{o}C): 173

Purification: pDDS was received at 97% purity and was recrystallized once from methanol. PDDS was then dried at ~110 ^{o}C for 24 hours.

Structure:

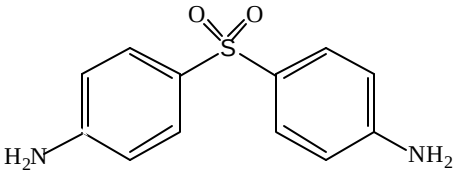

3.2.2.8 1,3-Bis(3-aminophenoxy) benzene (APB)

Supplier: Ken Seika

Empirical Formula: $C_{18}H_{16}N_2O_2$

Molecular Weight (g/mole): 292.34

Melting Point (^{o}C): 116-118

Purification: APB was recrystallized once from isopropanol and dried at ~90 ^{o}C for 24 hours prior to use.

Structure:

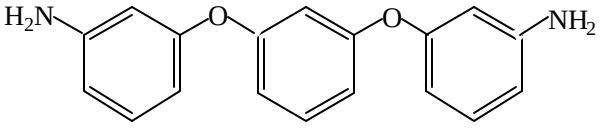

3.2.2.9 4,4'-(9-Fluorenylidene) dianiline (FDA)

Supplier: Aldrich Chemical Company

Empirical Formula: $C_{25}H_{20}N_2$

Molecular Weight (g/mole): 348.45

Melting Point (^oC): 237-239

Purification: FDA was dried at ~90 ^oC for at least 12 hours prior to use.

Structure:

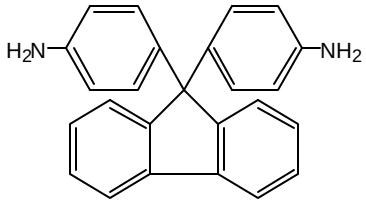

3.2.2.10 1,4-Diaminobenzene sulfonic acid (pPDA-SO_3H)

Supplier: Aldrich Chemical Company

Empirical Formula: $C_6H_8N_4O_3S$

Molecular Weight (g/mole): 188.21

Melting Point (^oC): -

Purification: pPDA-SO_3H was purified by refluxing in water for several hours. Carbon black was used as a de-colorization agent. The monomer was filtered and then dried at ~110 ^oC for at least 24 hours prior to use.

Structure:

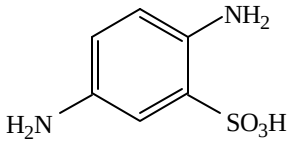

3.2.2.11 4,4'-diamino-2,2'-biphenyldisulfonic acid

Supplier: Alfa Aesar

Empirical Formula: $C_{12}H_{12}N_2O_6S_2$

Molecular Weight (g/mole): 344.37

Melting Point (^oC): -

Purification: BDA was purified by refluxing in water for several hours. The monomer was filtered and then dried at ~110 ^{o}C for at least 24 hours prior to use.

Structure:

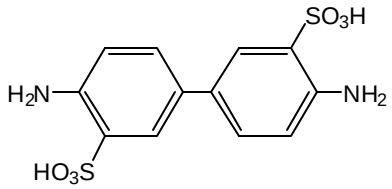

3.2.2.12 4,4'-Thiobisbenzenethiol (TBT)

Supplier: Aldrich

Empirical Formula: $C_{12}H_{10}S_3$

Molecular Weight (g/mole): 250.41

Melting Point (^{o}C): 112-114

Purification: TBT needed no further purification except for drying at 110 ^{o}C for 12 hours under vacuum prior to use. If needed, this reagent can be sublimed.

Structure:

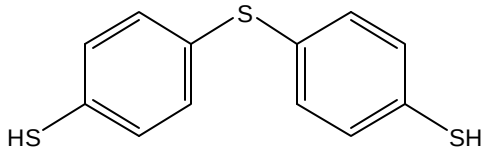

3.2.2.13 4,4'-Sulfonyldiphenol

Supplier: Aldrich Chemical Company

Empirical Formula: $C_{12}H_8O_4S$

Molecular Weight (g/mole): 250.27

Melting Point (^{o}C): 245-247

Purification: SDP needed no further purification except for drying at 110 ^{o}C for 12 hours under vacuum prior to use.

Structure:

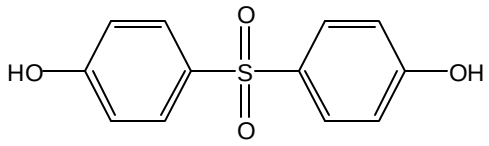

3.2.2.14 4-Bromo-1,8-naphthalic anhydride

Supplier: Aldrich Chemical Company

Empirical Formula: $C_{12}H_8O_4S$

Molecular Weight (g/mole): 275.94

Melting Point (^{o}C): 217-219

Purification: Dried at 120 ^{o}C for 12 hours before use. If needed this starting material can be sublimed at 160 ^{o}C under reduced pressure.

Structure:

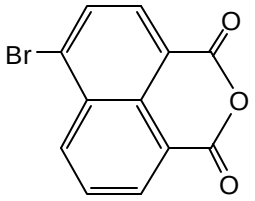

3.2.2.15 4,4'-Dichlorodiphenyl sulfone

Supplier: BP-Amoco

Empirical Formula: $C_{12}H_8Cl_2O_2S$

Molecular Weight (g/mole): 287.16

Melting Point (^{o}C): 148-150

Purification: Dried at 100 ^{o}C prior to use

Structure:

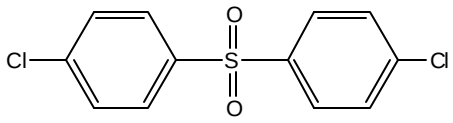

3.2.2.16 Triphenylphosphine Oxide (TPPO)

Supplier: BASF

Empirical Formula: $C_{18}H_{15}OP$

Molecular Weight (g/mole): 278.28

Melting Point (^{o}C): 156-158

Purification: Used as received

Structure:

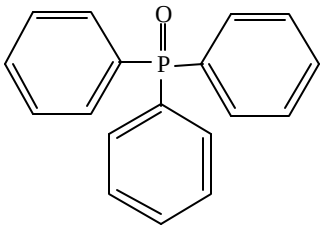

3.2.2.17 4,4'-Bisfluorophenyl phosphine oxide (BFPPO)

Supplier: Zeneca

Empirical Formula: $C_{18}H_{15}O_1P$

Molecular Weight (g/mole): 314.28

Melting Point (^{o}C): 162

Purification: Used as received

Structure:

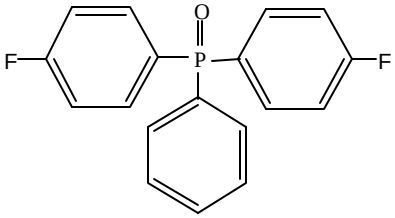

3.2.2.18 3-Aminophenol (mAP)

Supplier: Acros

Empirical Formula: C_6H_7NO

Molecular Weight (g/mole): 109.19

Melting Point (^{o}C): 124-126

Purification: Sublimed under reduced pressure at 120 ^{o}C prior to use

Structure:

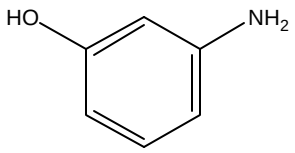

3.2.3 Monomer Synthesis

3.2.3.1 Bis(3-nitrophenyl) phenyl phosphine oxide (BNPPO)

Supplier: Synthesized in house by author

Empirical Formula: $C_{18}H_{13}N_2O_3P$

Molecular Weight (g/mole): 368.28

Melting Point (^{o}C): 141-142

Purification: Crude product was recrystallized many times from ethanol/water mixture in various ratios

Structure:

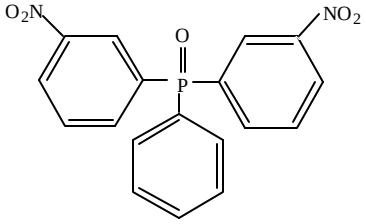

Synthetic Procedure:

Bis(3-nitrophenyl)phenyl phosphine oxide (BNPPO) was synthesized according to the reference[222] established by Dr. Charles Tchaoutcha. as shown in Scheme 3.2.1.

Triphenyl phosphine oxide (TPPO) (500 g, 1.8 mole) was charged into a 5 L round bottom flask equipped with an overhead mechanical stirrer, a reflux condenser and an additional funnel. The flask was placed in an ice-salt water bath (*subsequent temp. < 0 ^{o}C*) and concentrated sulfuric acid (1167 ml) was carefully added to the content of the

222. Charles Tchaoutcha, *Ph.D Dissertation*, Virginia Tech, May **2000**.

flask. The mixture was stirred for about 30 minutes until the starting material dissolved. In a separate ice bath, a 2-liter erlenmeyer flask containing nitric acid (327 g, 3,6 mole) was cooled and to it was slowly added 650 ml of concentrated sulfuric acid. The number of moles of nitric acid was 2 times excess than that of triphenyl phosphine oxide and the total amount of sulfuric acid was 10 times of nitric acid by weight.

The acid mixture was cooled to 0-5 ^{o}C and transferred to the addition funnel of the reaction apparatus. Slow dropwise addition of the acid mixture was employed and the ice bath temperature was maintained at between –10 to –5 ^{o}C. Once the addition had been completed, the reaction was allowed to continue for 2 hours at ~ 0 ^{o}C and 3 hours at room temperature. At the end of the five hours of stirring, the reaction mixture was precipitated by slow addition onto ice. The precipitate was dissolved in chloroform, and washed with dilute sodium hydroxide solution and water until the solution was neutral. During this time, the compound, BNPPO turned progressively yellowish green. The solvent, chloroform was then evaporated to afford a crude product containing about 10% of each mono- and trinitro and about 80% dinitro compound as determined by ^{31}P NMR. The product was purified after rigorous crystallization, using various ratios of ethanol/water mixtures (3/0 - 1/2 v/v). A detailed discussion of the synthesis and purification of the monomer will be given in Section 4.1.1 in Chapter 4.

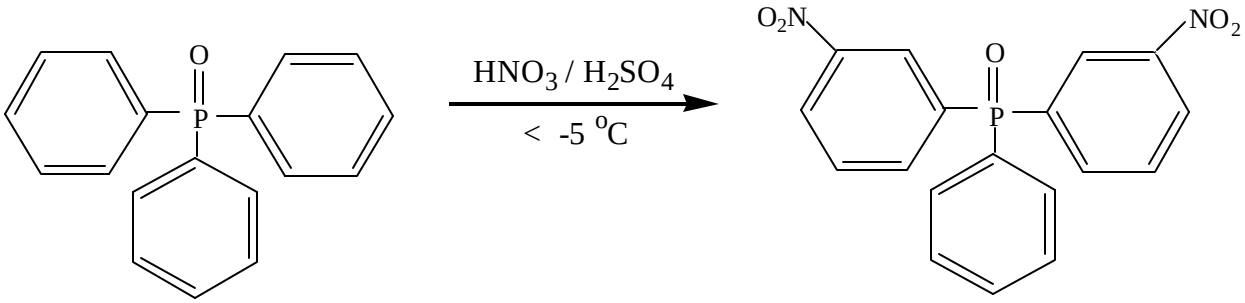

Scheme 3.2.1. Synthesis of Bis(3-nitrophenyl)phenyl phosphine oxide (BNPPO)

3.2.3.2 Bis(3-aminophenyl) phenyl phosphine oxide (BAPPO)

Supplier: Synthesized by reduction of the dinitro precursor by author

Empirical Formula: $C_{18}H_{17}N_2OP$

Molecular Weight (g/mole): 264.41

Melting Point (^oC): 212

Purification: See Section 4.1.1 in Chapter 4.

Structure:

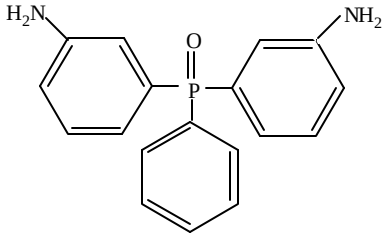

Synthetic Procedure

The dinitro compound was reduced to the diamine with hydrazine, as illustrated in following procedure[(222)] and Scheme 3.2.2.

Bis(3-nitrophenyl)phenyl phosphine oxide (BNPPO) (18.85 g, 0.051 mole) was charged into a 1 liter 3 neck round bottom flask equipped with an overhead stirrer, an additional funnel, and a reflux condenser. Absolute ethanol, (200 ml), was then added and heated to about to 50 ^oC while being purged with nitrogen. A small amount of catalyst Pd/C (~0.1 g) was added and then hydrazine monohydrate (66.8 g, 64.8 ml, 1.33 mole, 9 times excess of stoichiometry) was added drop-wise from an additional funnel. Evolution of gas from the reaction mixture indicated the occurrence of the reaction. No heating was needed at this stage because the reaction was exothermic. When the reaction rate decreased as indicated by the amount of evolving gas, a second portion of the catalyst, Pd/C, was added and the reaction was heated to reflux for two hours. The completion of the reduction was demonstrated by TLC.

About 2 g of decoloring activated carbon was then added to the solution and a gentle reflux was allowed to continue for an additional hour. The black solution was then cooled under nitrogen purge and subsequently filtered through celite on a Buchner funnel to afford a clear light yellow solution. The solvent was evaporated under vacuum

immediately. The product was then washed with water and dried in a vacuum oven at 100 ^{o}C. The pure product showed a melting point of 212 ^{o}C by DSC and no impurities were detected by HPLC (inverse phase, absolute methanol as mobile phase). ^{31}P NMR (500 MHz, DMSO-d_6) showed a single peak (27.3 ppm). ^{1}H NMR (400 MHz, DMSO-d_6) showed a matching chemical shift and integrations (Figures 4.1.1 and 4.1.2). Elemental analysis results for $C_{18}H_{17}N_2OP$: Calculated: C: 70.02%, H: 5.56 %, N: 9.09 %, P: 10.05% ; Found: C: 69.47%, H: 5.78 %, N: 8.88 %, P: 9.62 %.

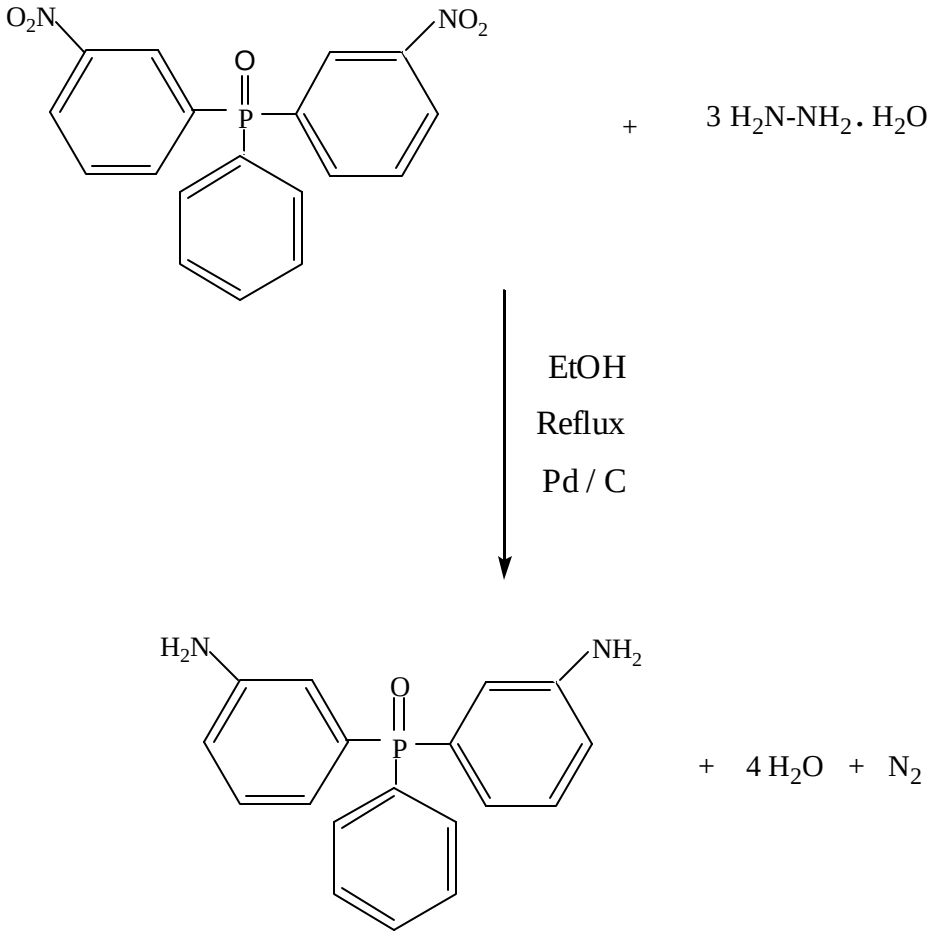

Scheme 3.2.2 Synthesis of Bis(3-aminophenyl)phenyl Phosphine Oxide (BAPPO)

3.2.3.4 Sulfonated Bis(4-fluorophenyl) Phenyl Phosphine Oxide (S-BFPPO)

Supplier: Synthesized in house by author.

Empirical Formula: $C_{18}H_{17}N_2OP$

Molecular Weight (g/mole): 416.33

Melting Point (^oC): -

Purification: See Section 4.1.2 in Chapter 4.

Structure:

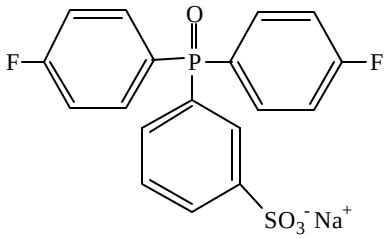

Synthetic Procedure

The synthesis of sulfonated bis(4-fluorophenyl) phenyl phosphine oxide (SBAPPO) is reported elsewhere[223].

In a three-neck flask, equipped with a nitrogen inlet, a thermometer, a mechanical stirrer, a Dean-Stark trap, and a condenser, 28.38 g (0.068 mol) of BFPPO and 53.9 ml 28% fuming sulfuric acid were added and the reaction solution was heated to 90 ^oC with stirring for 4 hours, under a slow nitrogen flow (Scheme 3.2.3). When BFPPO was first mixed with the fuming sulfuric acid, a light green color was observed. As the starting material dissolved in the reaction solution with stirring and heating, first the color turned to dark green and then to light brown.

At the end of four hours, the reaction mixture was cooled to room temperature and slowly added into ice water. The resulting sulfonic acid oiled out at the bottom of the beaker on saturation with a large amount of NaCl overnight. Large amounts of NaCl addition were necessary to extract any remaining product from the water phase.

223. Shobha H.K., Smalley, G.R., Sankarapandian, M. and McGrath, J.E. *ACS Div. Polym. Chem., Polym. Preprs.* **2000**, 41(1), 180

The upper part (water phase) was decanted to another flask and then the oily phase as well as the water phase were extracted separately with methyl ethyl ketone (MEK). Combined organic MEK solution was washed several times with saturated NaCl solution and then the solvent was evaporated under vacuum giving a light yellow product. After the removal of MEK, the sulfonic acid was neutralized with NaOH solution that was added dropwise into the solution of sBFPPO in water until pH~8. Neutralized sBFPPO solution was again extracted with MEK and washed with saturated NaCl solution three times. After the solvent was removed, the product was dried at 130 ^{o}C in a vacuum for 6 hours.

From TLC, it was seen that there was some un-reacted starting material, BFPPO (Figure 3.2). The product was then purified through a silica gel column using a methanol / ethyl acetate mixture as an eluent (BFPPO is soluble in ethyl acetate however, s-BFPPO is not soluble.). The pure product was then obtained with 79% yield after removal of the solvent mixture and drying overnight at 130 ^{o}C under vacuum. The purity of the product was confirmed with TLC, ^{1}H, ^{13}C, and ^{31}P NMR spectroscopy, FAB mass spectroscopy and HPLC.

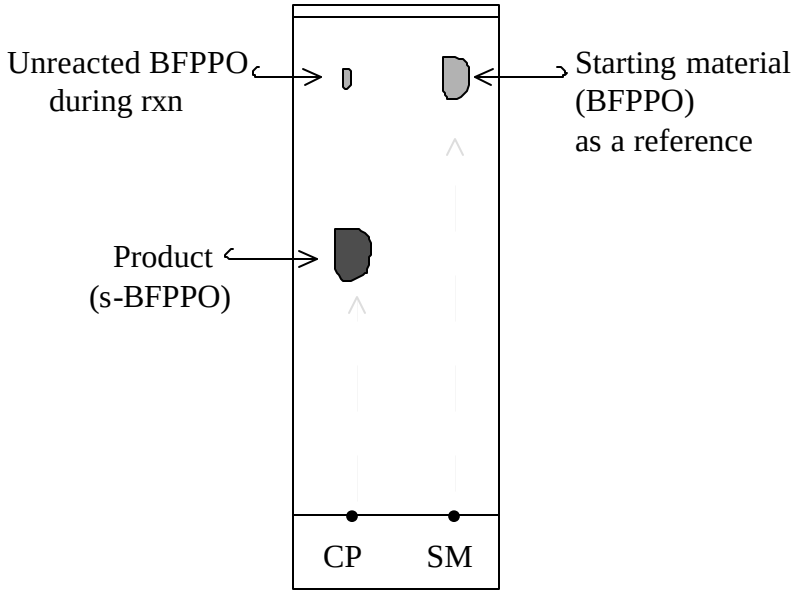

Figure 3.2 TLC of the crude product, CP (SBFPPO) dissolved in chloroform and the starting material, SM (BFPPO) in 25/75 (v/v) methanol/ethyl acetate mixture as an eluent.

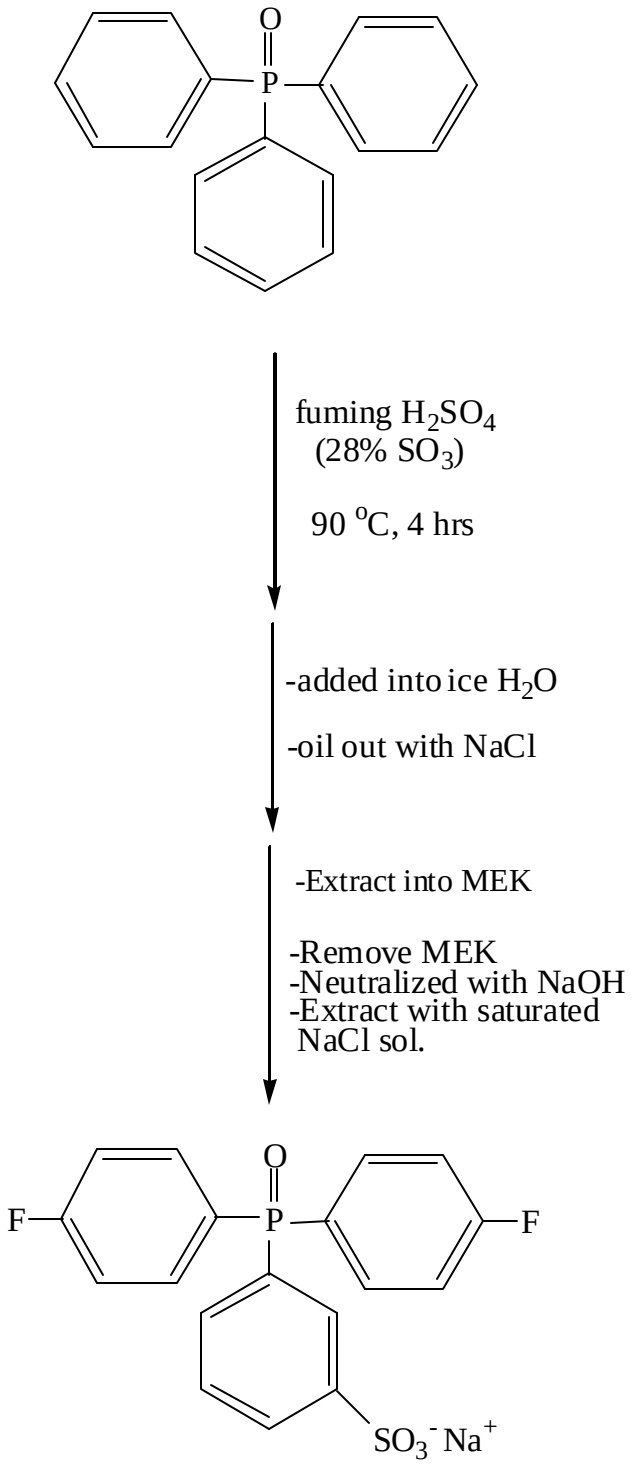

Scheme 3.2.3 Synthesis and Purification of s-BFPPO[223]

3.2.3.5 Sulfonated Bis(3-aminophenoxy)phenyl phosphine oxide (s-BAPPO)

Supplier: Synthesized in house by author.

Empirical Formula: $C_{30}H_{24}N_2NaO_6PS$

Molecular Weight (g/mole): 594.55

Melting Point (^oC): -

Purification: by column chromatography and/or dissolving in minimum amount of methanol and re-precipitating in ethyl acetate

Structure:

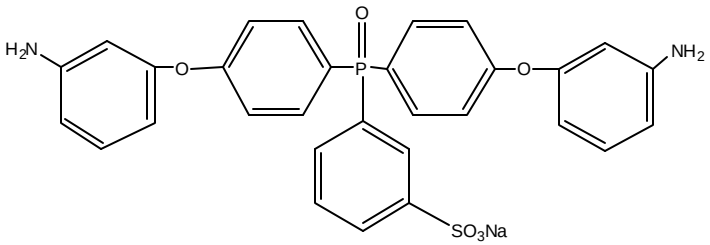

Synthetic Procedure

Synthesized sulfonated bis(4-fluorophenoxy) phenyl phosphine oxide (s-BFPPO) was used as a precursor in this reaction to obtain a sulfonated diamine monomer for polyimide synthesis.

In a three-neck flask, equipped with a nitrogen inlet, mechanical stirrer, a Dean-Stark trap, and a condensor, 5.254 g (47.96 mmol) of m-aminophenol (purified via sublimation) and 5.44 g (50.35 mmol) of dry K_2CO_3 were taken. Dried and distilled DMAc was used as a solvent and toluene as an azeotropic solvent (Scheme 3.2.4). The solution was allowed to reflux at 145 ^oC while toluene azeotropically removed water. The toluene was removed after 6 hours, and then 10.00 g (23.98 mmol) of s-BFPPO was added into the reaction medium and the reaction mixture was heated with stirring at 170 ^oC for 16 hours. The resulting solution was filtered to remove the salt and then precipitated in ethylacetate resulting in tan color powder. The resulting solid was re-dissolved in methanol, filtered and precipitated in ethylacetate. The product was purified through silica gel column using methanol/ethyl acetate mixture as eluent and the dried product yield about 72 %.

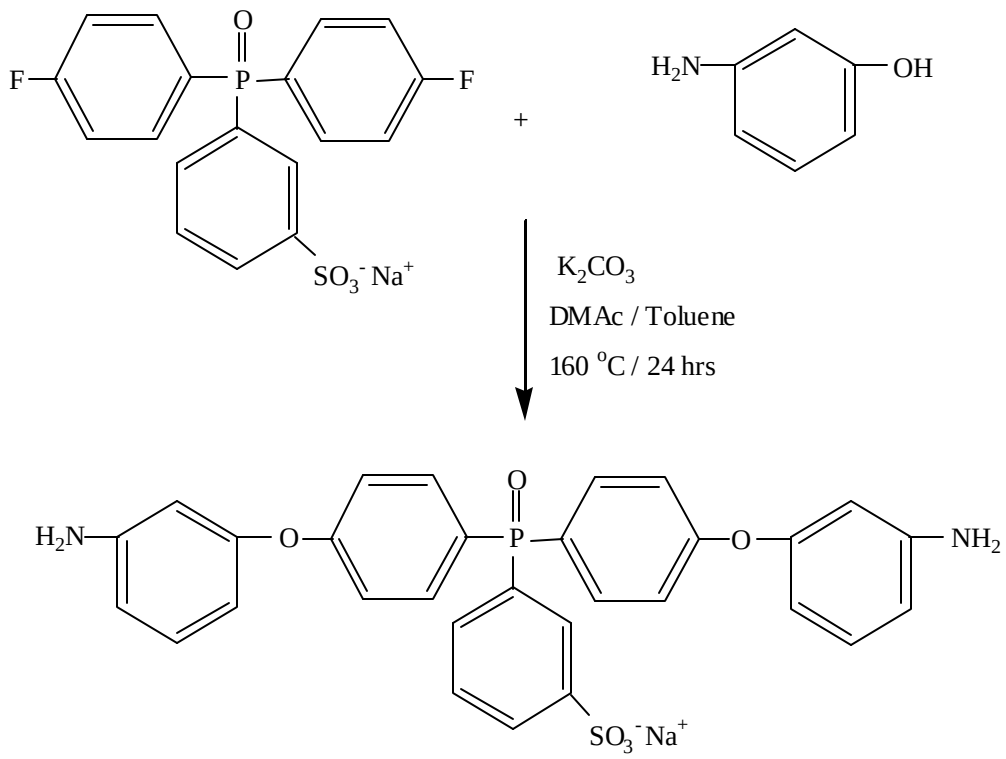

$C_{30}H_{24}N_2NaO_6PS$
Mol. Wt.: 594.55

Theoretical: C, 60.60 %; H, 4.07 %; N, 4.71 %; Na, 3.87 %; P, 5.21 %; S, 5.39 %

Experimental: C, 61.18 %; H, 3.83 %; N, 4.45 %; Na, 4.00 %; P, 4.82 %; S, 5.01 %

Scheme 3.2.4 Procedure for synthesis of sulfonated diamine monomer[223] [Bis(3-aminophenyl) phenylphosphine oxide (s-BAPPO)] and its elemental analysis data

3.2.3.5 Synthesis of Disulfonated 4,4'-dichlorodiphenyl sulfone (s-DCDPS)

Supplier: Synthesized in house by author.

Empirical Formula: $C_{12}H_6Cl_2Na_2O_8S_2$

Molecular Weight (g/mole): 491.25

Melting Point (^oC): -

Purification: See Section 4.1.3 in Chapter 4.

Structure:

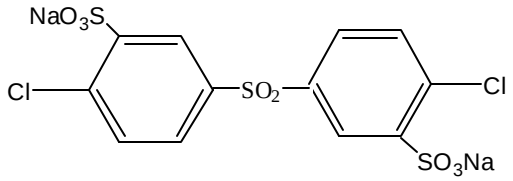

Synthetic Procedure

Ueda et al. reported general reaction conditions for sulfonation of DCDPS[224]. The reported straightforward electrophilic substitution reaction procedure formed the sulfonated monomer, which is then changed from the free acid form to its sodium salt form during neutralization and isolation, by "salting out", with excess of sodium chloride. A modified procedure of s-DCDPS reported by our research group[225] provides more characterization details of the monomer's synthetic scheme. A detailed reaction procedure of s-DCDPS was provided below in Scheme 3.2.5.

A mixture of 4,4'-dicholorodiphenyl sulfone (87 mmol, 25 g) and fuming sulfuric acid (28% SO_3) (191.4 mmol, 56 ml) was charged into a three neck 250 ml round bottom flask equipped with a mechanical stirrer, nitrogen inlet and a condenser attached with a outlet. Then, reaction solution was stirred at 110 ^oC for 6 hours yielding the opaque white crude product. After that time, the mixture was cooled to room temperature and slowly added into 500 ml of ice water in which the product was dissolved (brown clear solution).

Off-white fine precipitates were obtained upon addition of excess NaCl (150 g). The over-saturated salt solution, which was necessary to increase the yield by isolating the product as solid from water, was left overnight.

224. M. Udea, H. Toyota, T. Ochi, J. Sugiyama, K. Yonetake, T. Masuko and T. Teremoto, *J. Polym. Sci., Poly. Chem. Ed*., 31, 85 (**1993**).

225. F. Wang, J. Mecham, W. Harrison and J.E. McGrath, *Am. Chem. Soc. Polym. Prepr*. **2000**, 41(2), 1401

Next day, the fine crude product was filtered, dried and re-dissolved in 500 ml of deionized water and neutralized at room temperature by 2 N NaOH solution to a pH ~ 8. An off-white solid was isolated again with excess of NaCl, filtered and vacuum dried at 120 ^{o}C for 20 hours. The monomer grade sodium form of the sulfonated monomer (s-DCDPS) was generated by recrystallization from a mixture of 6/1 isopropanol / deionized water in a yield of 89% (MW=491.248 g/mol). Section 4.1.3 discusses the basic characterization results of this sulfonated DCDPS intermediate monomer in detail.

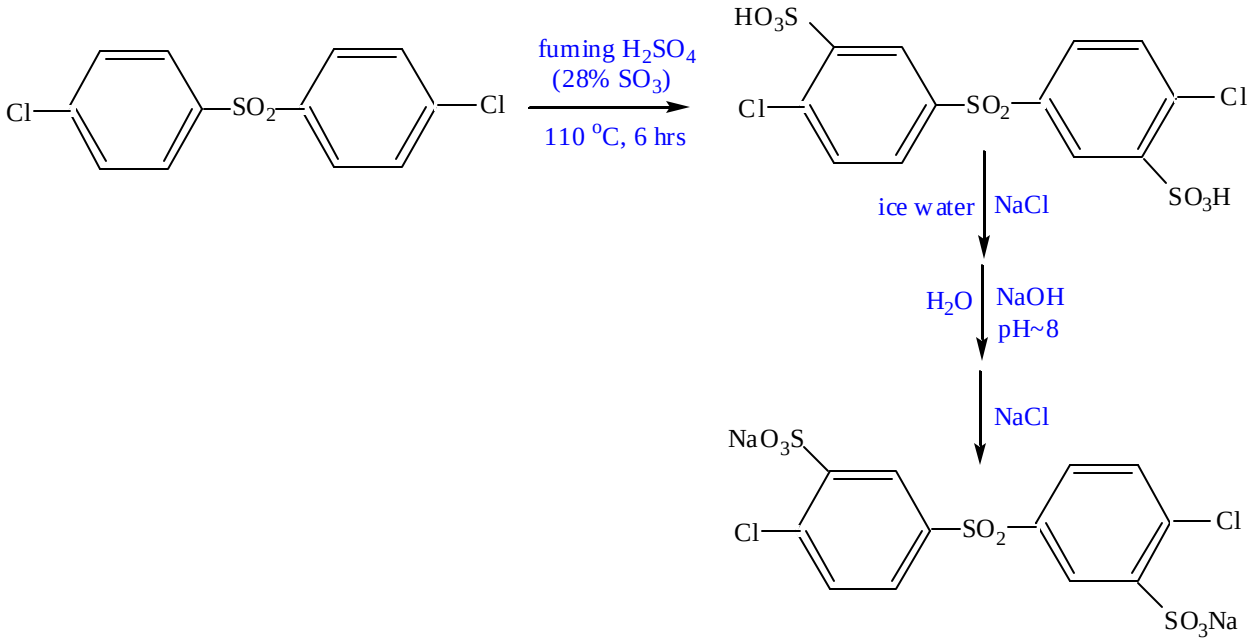

Scheme 3.2.5 Synthesis and isolation of s-DCDPS[225]

3.2.3.6 Disulfonated 4,4'-bis(3-aminophenoxy)phenyl sulfone (s-DADPS)

Supplier: Synthesized in house by author.

Empirical Formula: $C_{24}H_{18}Na_2O_{10}S_3$

Molecular Weight (g/mole): 636.58

Melting Point (^oC): -

Purification: Stirred in ethylacetate overnight at R.T

Structure:

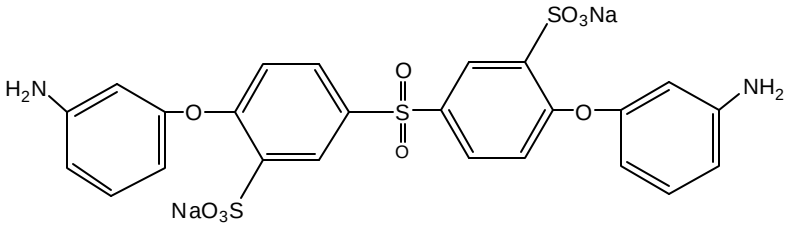

Synthetic Procedure:

Synthetic procedure of disulfonated diamine monomer was somewhat similar to that of s-DAPPO diamine monomer given in Section 3.2.3.5.

First, into a three neck 250 ml round bottom flask equipped with a mechanical stirrer, a nitrogen inlet-outlet and a Dean-Stark trap fitted with a condenser, freshly sublimed 3-amino phenol (6.65 g, 60.09 mmol) and dry K_2CO_3 (9.27 g, 67.1 mmol) were charged along with 90 ml of dry DMAc as a solvent and 37.5 ml of toluene as a azeotropic agent. The reaction mixture was stirred by refluxing at 145 ^oC for 5-6 hours, during this time toluene azeotropically removed water. Finally, the azeotropic solvent was completely removed after six hours, and then s-DCDPS (15 g, 30.53 mmol) was added into the reaction flask along with 15 ml of more DMAc and the reaction mixture was stirred by heating at 170 ^oC for 20 hours (Scheme 3.2.6). The reaction solution was then hot filtered to remove the salt and then cooled down to room temperature. The product, s-DADPS was isolated by precipitating in ethyl acetate solution resulting in very light brown solid. The sulfonated diamine product was finally obtained with very high purity (>99.5 %) and very high yield (92 %) in tan color after stirring the solid in ethyl acetate overnight to remove any un-reacted m-aminophenol. TLC also gave a single spot indicating s-DADPS was our only product obtained from this reaction.

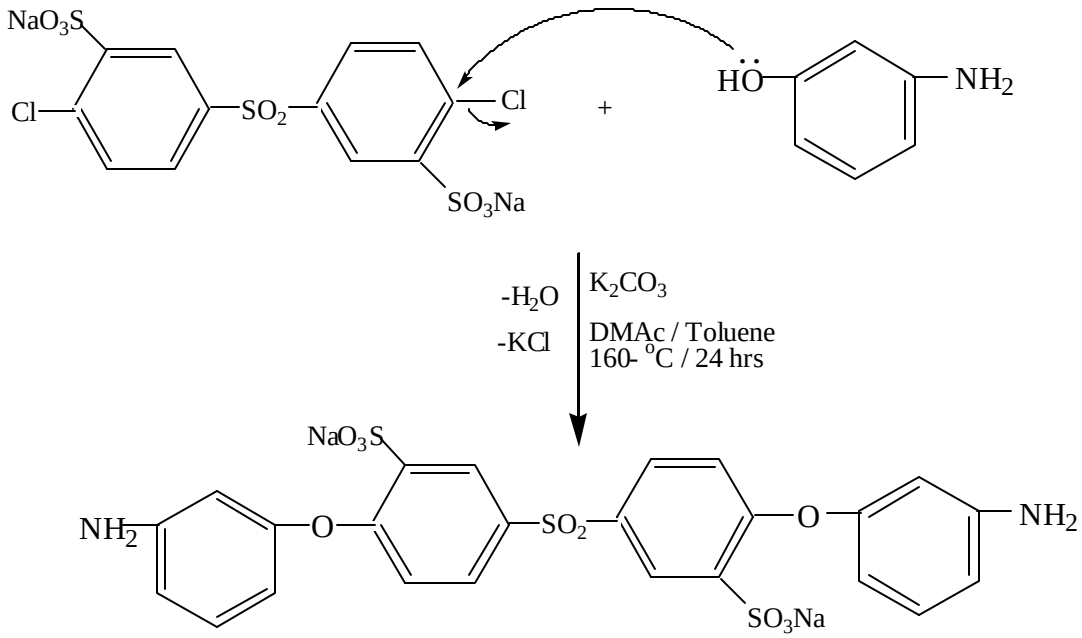

Scheme 3.2.6 Synthetic procedure for disulfonated DADPS diamine monomer

3.2.3.7 Bis (4-hydroxyphenyl) phenyl phosphine oxide (BOHPPO)

Supplier: Synthesized in house by author.

Empirical Formula: $C_{18}H_{15}O_3P$

Molecular Weight (g/mole): 310.29

Melting Point (^oC): 237

Purification: recrystallized from 1:5 methanol:water mixture.

Structure:

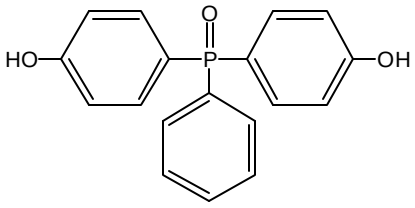

Synthetic Procedure

BOHPPO was synthesized using previously published chemistry[226]. BOHPPO was obtained by hydrolyzing 4,4'-Bisfluorophenyl phosphine oxide (BFPPO) using 5 moles of potassium hydroxide (KOH) in DMSO (Scheme 3.2.7). For example, 50 g (159.1 moles) of BFPPO and 250 ml of DMSO (Aldrich, 99 %) were added into a 500 ml 3-neck round bottom flask equipped with a mechanical stirrer, nitrogen inlet, and a condenser. To the solution was added a 15 N solution of 60 g (60/56 moles) of potassium hydroxide (Mallinckrodt, 88 %) in water. The solution was then raised to reflux at approximately 135 ^oC and allowed react for 10 hours. The completion of reaction was checked with TLC using 3/7 (vol/vol) methanol/chloroform mixture as eluent.

At the end of reaction, the solution was acidified by precipitating drop-wise into a 1/5 (vol/vol) concentrated HCl/water mixture. The reaction product was filtered, washed with excess of water to remove remaining salt and acid and then subsequently recrystallized from 1:5 methanol/water mixture.

The resulting material was monomer grade with a melting point of 237 ^oC. The reaction yield was greater than 96 % after purification. Elemental analysis for $C_{18}H_{15}O_3P$: C, 69.7 %; H, 4,9 %; P, 10 %. Found: C, 70.5 %; H, 5.3 %; P, 9.2 %.

226. Daniel. J. Riley, *Ph.D Thesis*, Virginia Tech, **1997**.

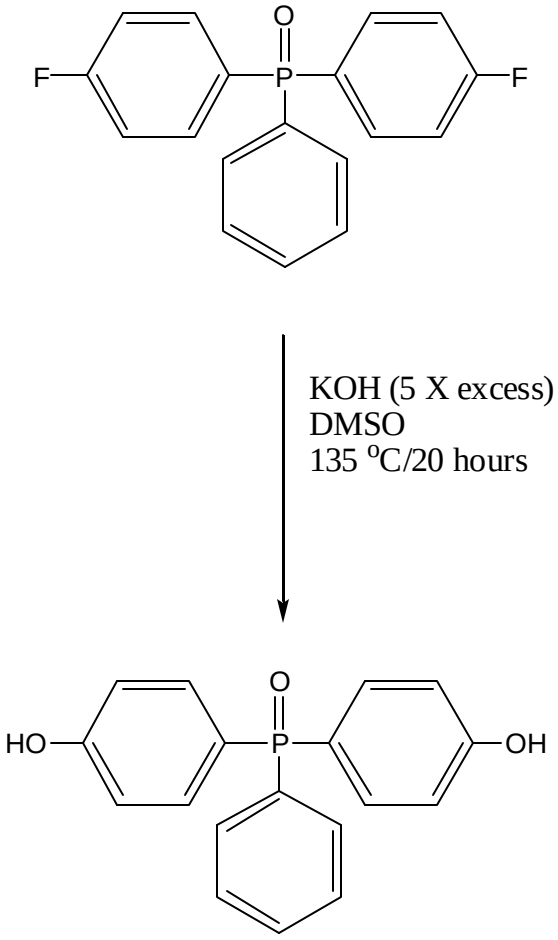

Scheme 3.2.7 Synthesis of BOHPPO[226]

3.2.3.8 4,4'-Bis(oxynaphthalic anhydride) phenyl phenyl phosphine oxide (NDA-PO)

Supplier: Synthesized in house by author.

Empirical Formula: $C_{42}H_{23}O_9P$

Molecular Weight (g/mole): 702.6

Melting Point (^oC): 238

Purification: See Section 4.1.6 in Chapter 4.

Structure

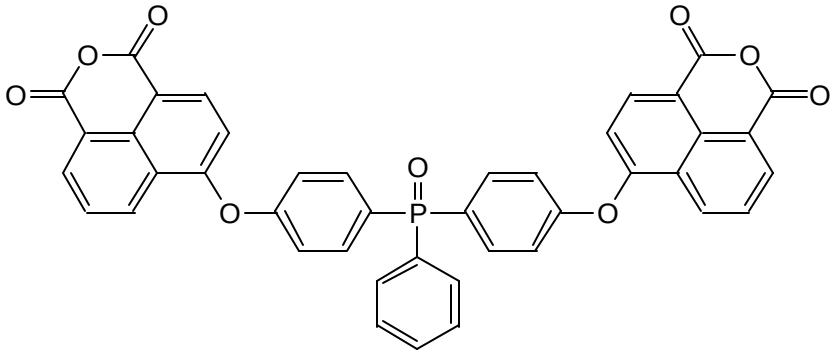

Synthetic Procedure

The synthesis of NDA-PO dianhydride is depicted in Scheme 3.1.8. In a typical experiment, 7.6 g of bis(4-hydroxyphenyl) phenyl phosphine oxide (BOHPPO) (0.024 moles), 2.34 g of NaOH (0.059 moles), 50 ml of dry DMAc as a solvent and 40 ml of toluene as an azeotropic agent were placed in a three neck, 250 ml round bottom flask equipped with a magnetic stirrer, reflux condenser, nitrogen inlet and thermometer. The reaction solution was stirred by heating at 130 ^oC for 6 hours, during which time, phenate (Na-salt of BOHPPO) formation was observed by watching removal of water azeotropically with toluene. Finally, the azeotropic solvent was completely removed after six hours, and 15.7 g Br-NDA (0.054 moles) was added into the flask by washing with 50 ml of more DMAc. The reaction solution was stirred while heating at refluxing temperature (~164 ^oC) for 24 hours (Scheme 3.2.8).

The reaction solution was then hot filtered to remove the salt and then cooled down to room temperature. The crude product, NDA-PO was obtained after precipitating

drop-wise in distilled water, filtration, and drying at 150 ^{o}C under vacuum overnight. The obtaining material was redissolved in 5 % NaOH solution, filtered to remove unsoluble part, and then precipitated with 5 % HCl solution. The green color solid was filtered again and washed with excess of water to remove remaining acid until obtaining a neutral wash water (pH=6-7 with pH paper), first air dried and then vacuum dried at 170 ^{o}C to remove any remaining solvent and fully cyclize the anhydride. The product was subsequently further recrystallized several times from very concentrated Toluene solution. The product yield was ~ 63 % after recrystallizations.

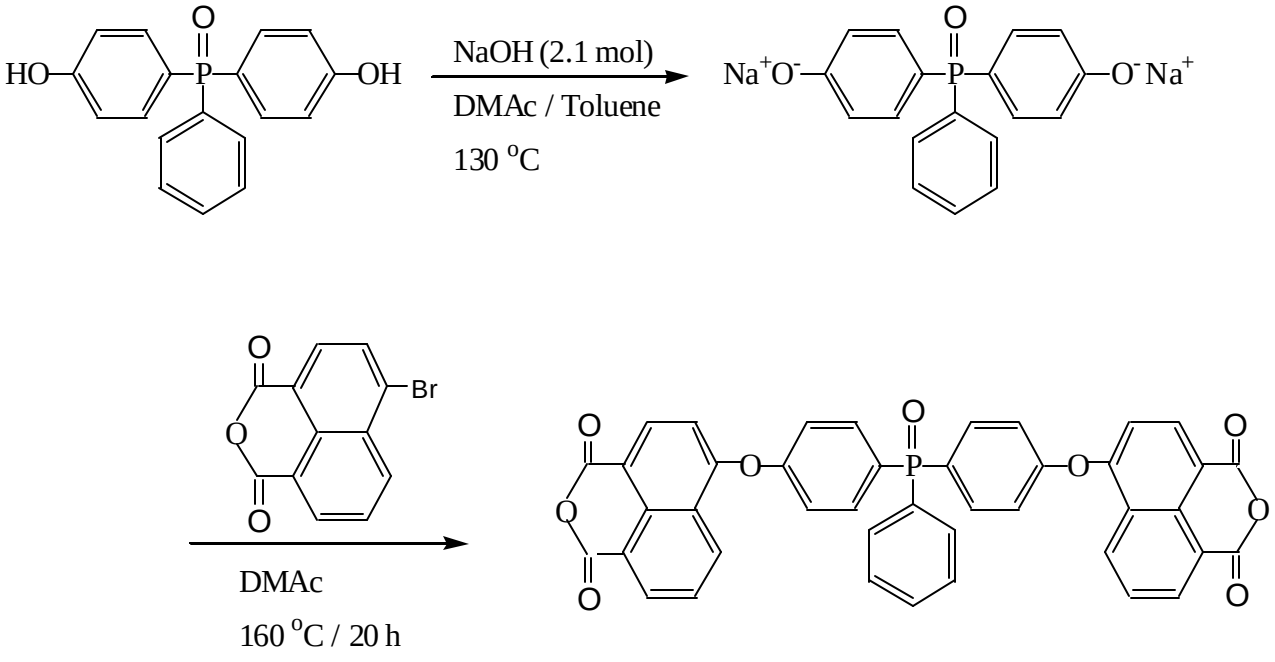

Scheme 3.2.8 Synthesis of NDA-PO

3.2.3.9 4,4'-Bis(oxynaphthalic anhydride) phenyl sulfone (NDA-SO_2)

Supplier: Synthesized in house by author.

Emprical Formula: $C_{36}H_{18}O_{10}S$

Molecular Weight (g/mole): 642.59

Melting Point (^oC): 250

Purification: See Section 3.2.7 in Chapter 4.

Structure

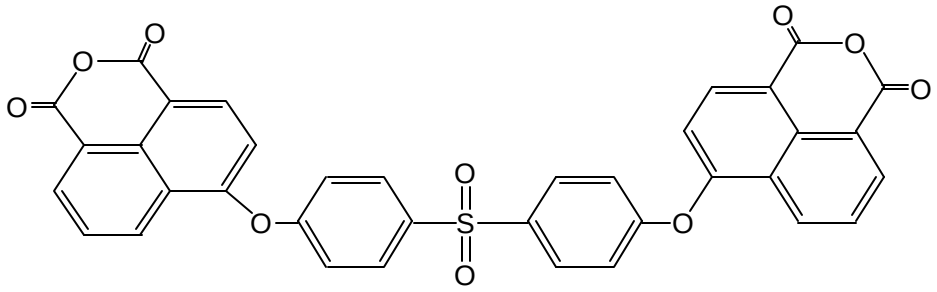

Synthetic Procedure

The synthesis and purification procedure of NDA-SO_2 dianhydride was similar to that of NDA-PO described in Section 3.2.3.8 and depicted in Scheme 3.2.9. In a typical experiment, 6.97 g of 4,4'-Sulfonyldiphenol (SDP) (0.028 moles), 2.67 g of NaOH (0.067 moles), 45 ml of dry DMAc as a solvent and 30 ml of toluene as an azeotropic agent were placed in a three neck, 250 ml round bottom flask equipped with a magnetic stirrer, reflux condenser, nitrogen inlet and thermometer. The reaction solution was stirred by heating at 130 ^oC for 6 hours, during which time, phenate (Na-salt of SDP) formation was observed by watching the removal of water azeotropically with toluene. Finally, the azeotropic solvent was completely removed after six hours, and 15.44 g Br-NDA (0.056 moles) was added into the flask by washing with 45 ml of more DMAc. The reaction solution was stirred while heating at refluxing temperature (~164 ^oC) for 24 hours (Scheme 3.2.9).

The reaction solution was then hot filtered to remove the salt and then cooled down to room temperature. The crude product, NDA-SO_2 was obtained after precipitating drop-wise in distilled water, filtration, and drying at 150 ^oC under vacuum overnight. The obtaining material was redissolved in 5 % NaOH solution, filtered to remove unsoluble

part, and then precipitated with 5 % HCl solution. The orange color solid was filtered again and washed with excess of water to remove remaining acid until obtaining a neutral wash water (pH=6-7 with pH paper), first air dried and then vacuum dried at 170 ^{o}C to remove any remaining solvent and fully cyclize the anhydride. The product was subsequently further recrystallized several times from very concentrated DMSO solution.

The product yield was ~ 67 % after recrystallizations.

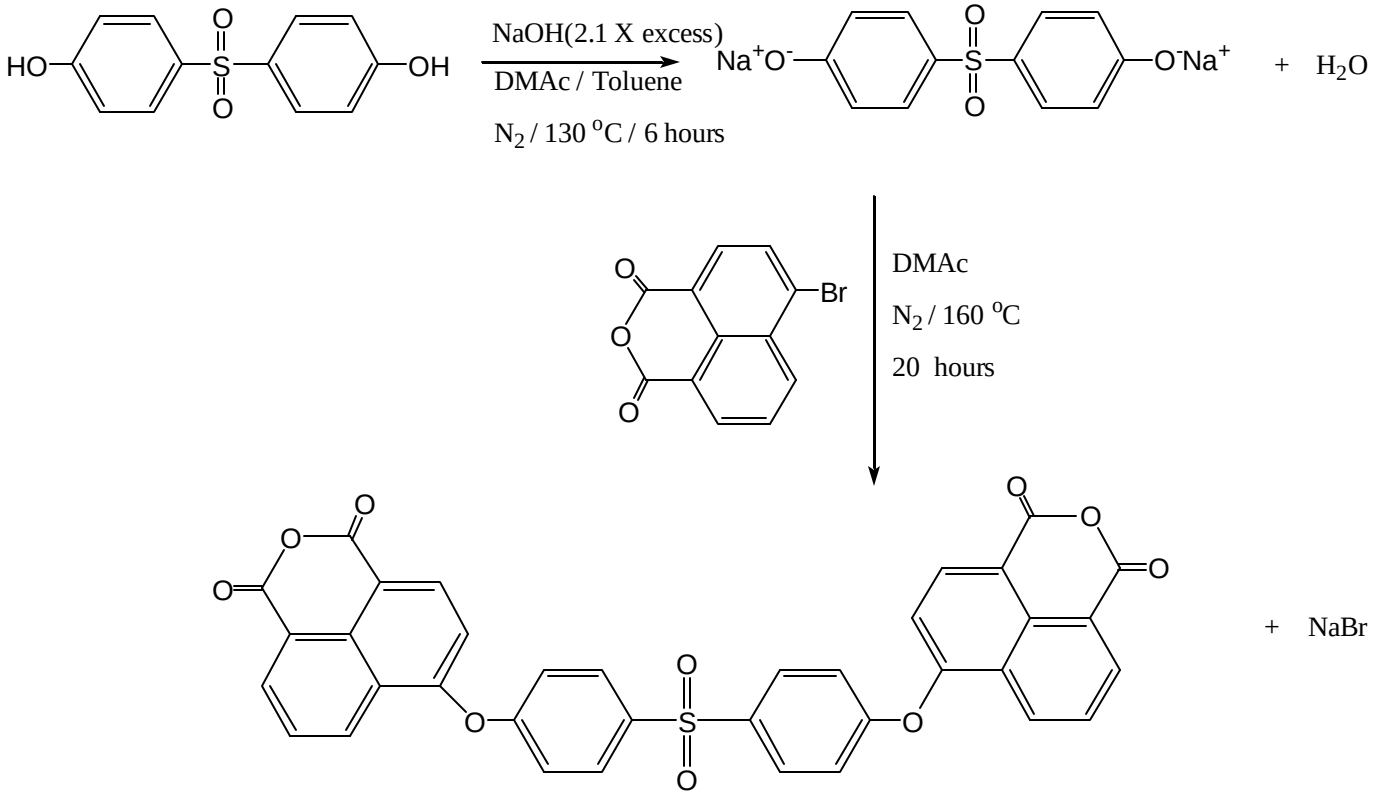

Scheme 3.2.9 Synthesis of NDA-SO_2

3.3 Polyimide Synthesis

Important prerequisites for obtaining polyimides having well-defined structures and good molecular weight control involve purification of the starting materials and control of stoichiometry.

Primarily, the two-step ester-acid route was used to synthesize high molecular weight five-membered polyimides using 1:1 stoichiometry of bifunctional dianhydrides and diamines. A one-step high temperature direct imidization method was used for six-membered-ring dianhydrides.

All of the five-membered-ring polymers were made in a three-neck, round bottom flask pictured in Figure 3.1.1. The size of the flask varied according to the amount of polymer being made. The flasks were fitted with a nitrogen gas inlet, a mechanical overhead stirrer and a reverse Dean-Stark trap to which a condenser was attached. The apparatus was flame dried prior to. A nitrogen purge was maintained through the flask while drying and during the polymerization. O-DCB was used as an azeotropic agent during imidization and the reverse Dean-Stark trap was also filled with o-DCB.

Six-membered dianhydrides were also made in a three-neck, round bottom flask fitted with a nitrogen gas inlet, a mechanical overhead stirrer and a condenser. One-step high temperature direct imidization in a phenolic solvent was the primary method to synthesize high molecular weight six-membered ring polymers due to the poor solubility of their related dianhydrides.

Synthetic procedures of the classic two-step route, ester-acid route and also the one-step direct imidization route will be outlined for the synthesis of sulfonated and unsulfonated homo- and copolyimides.

3.3.1 Polyimide Synthesis by the Ester-Acid Route

The ester-acid route for the synthesis of five-membered ring polyimides was the primary method used in this research. The synthesis requires two steps. The first step is to form the ester-acid intermediate by the reaction of the dianhydride with ethanol. The second step employs an elevated temperature reaction of the ester-acid intermediate with the diamine(s), in the presence of an azeotropic agent, which permits the formation of fully imidized amorphous polyimides. The reaction apparatus is shown in Figure 3.1. Both homo- and copolyimides can be synthesized by this procedure.

Example of Homopolyimide Synthesis

Polymerizations were conducted as follows for the synthesis of BPDA/FDA unsulfonated high molecular weight polymers using 1:1 stoichiometry of the dianhydride and diamine. Since the author did not attempt to control the molecular weight of the polymers no end capping monomer was used.

For example, 4.2 g (14.18 mmol) monomer grade dry BPDA were charged to a three-neck round-bottom flask equipped with a magnetic stirrer, nitrogen inlet, thermometer, reverse Dean-Stark trap and condenser. The flask was heated in a silicone oil bath. Absolute ethanol, 8-10 ml per gram of dianhydride, and ~3 ml of triethylamine catalyst were then introduced and the mixture was refluxed with stirring for about one hour until a clear solution was obtained. A clear solution in the reaction flask indicates the formation of the ester-acid intermediate. Meantime, the excess of the solvent and the catalyst were distilled off into the trap. When the distillation of ethanol ceased, the trap was filled with o-DCB and the diamine 4,4'-(9-Fluorenylidene) dianiline (FDA), 4.98 g (14.32 mmol) was added to the reaction vessel, followed by NMP (36 ml) and o-DCB (9 ml) (4:1 vol: vol) to provide a solids content of 20 % wt./vol. The reaction mixture was then heated to 175-185 ^{o}C for 24 hours, which was sufficient time to complete the reaction (e.g. the total fractional extent of the functional group conversion was >0.99). Then, the reaction mixture was cooled to room temperature and the polymer was coagulated by slowly dripping the mixture into isopropanol in a high- speed blender. The

polymer was collected by vacuum filtration and then washed with excess of methanol. It was air dried for several hours and then vacuum dried at ~160 ^{o}C for 24 hours.

Other homopolyimide systems synthesized by the same method include BPDA/APB, DSDA/FDA, DSDA/APB and 6-FDA/m-PDA

Example of Copolyimide Synthesis

Copolyimides were synthesized according to the procedure described above, except that where a mixture of dianhydrides and diamines (sulfonated/unsulfonated) were used instead of pure monomers (Scheme 3.3.1).

Polymerizations were conducted as follows for the synthesis of BPDA/FDA/BDA 50 %sulfonated high molecular weight polymers using 1:1 stoichiometry of the dianhydride and diamines.

As an example, 5.0 g (16.9 mmol) monomer grade dry BPDA were charged into a three-neck round-bottom flask equipped with a magnetic stirrer, nitrogen inlet, thermometer, reverse Dean-Stark trap and condenser, and was heated in a silicone oil bath. Absolute ethanol, 8-10 ml per gram of dianhydride, and ~3 ml of triethylamine catalyst were then introduced and the mixture was refluxed with stirring for about one hour until a clear solution was obtained. A clear solution in the reaction flask indicates the formation of the ester-acid intermediate. When the distillation of ethanol ceased, the trap was filled with o-DCB and the sulfonated diamine 4,4'-diamino-2,2'-biphenyldisulfonic acid (BDA), 2.97 g (8.62 mmol) was added to the reaction vessel, followed by NMP (22 ml) and o-DCB (5 ml) to pre-react with the dianhydride for oligomerization. A couple of hours later, the co-diamine, 4,4'-(9-fluorenylidene) dianiline (FDA), 3.02 g (8.62 mmol) was added to the reaction vessel, followed by more NMP (22 ml) and o-DCB (6 ml) (4:1 vol: vol) to provide total solids content of 20 % wt./vol. The reaction mixture was then heated to 175-185 ^{o}C for 24 hours, which was sufficient time to complete the reaction. Then, the reaction mixture was cooled to room temperature and the copolymide was coagulated by slowly dripping the mixture into isopropanol in a high-speed blender. The polymer was collected by vacuum filtration and then washed with excess of methanol It was air dried for several hours and then vacuum dried at ~160 ^{o}C for 24 hours.

Other high molecular weight five-membered copolyimide systems that will be discussed in Chapter 4 were also synthesized by the same procedure as described above.

3.3.2 Polyimide Synthesis via One-step High Temperature Direct Imidization Method

One-step high temperature direct imidization method was used for the synthesis of homo- and copolyimides of six membered dianhydrides due to the insolubility of the resulting polyimide oligomers (Scheme 3.3.2). Below is the synthetic procedure for 50 % sulfonated NDA/BDA/FDA copolyimides with 1:1 stoichiometry of reactants.

Direct polyimidizations to form sulfonated polyimide were conducted in a three-neck 500 ml round bottom flask equipped with a mechanical stirrer, nitrogen inlet/outlet, and a condenser. In a typical polymerization, 2.39 g (6.83 mmol) of sulfonated diamine, BDA were added to the flask along with 20 ml of dry m-cresol and 16 mmol of Et_3N as a solubilization agent and reacted at room temperature until a complete dissolution of the diamine. Then, 3.025 g (11.28 mmol) of NDA were added along with 28 mmol of isoquinoline as a catalyst and 34 ml of more m-cresol to afford a concentration of 10 percent solids. The reaction was heated to 200°C for several hours to oligomerize NDA and BDA. Lastly, 1.594 g (4.63 mmol) of 1,3-bis(3-aminophenoxy)benzene (APB) was added along with 16 ml of m-cresol as an unsulfonated diamine source to control the degree of sulfonation on the final polymer. The reaction solution was allowed to react for another 20 hours at 200 ^{o}C. At the end of this period, the reaction solution was diluted with more m-cresol and cooled down. The polymer was then isolated by precipitation into rapidly stirring 2 L isopropanol, filtered and dried for 6 hours at 100 ^{o}C and then for 24 hours at 150°C under vacuum. The polymer was finally kept in a large beaker with excess of water to remove any trace amount of m-cresol from the polymer and dried again at 150 ^{o}C for overnight.

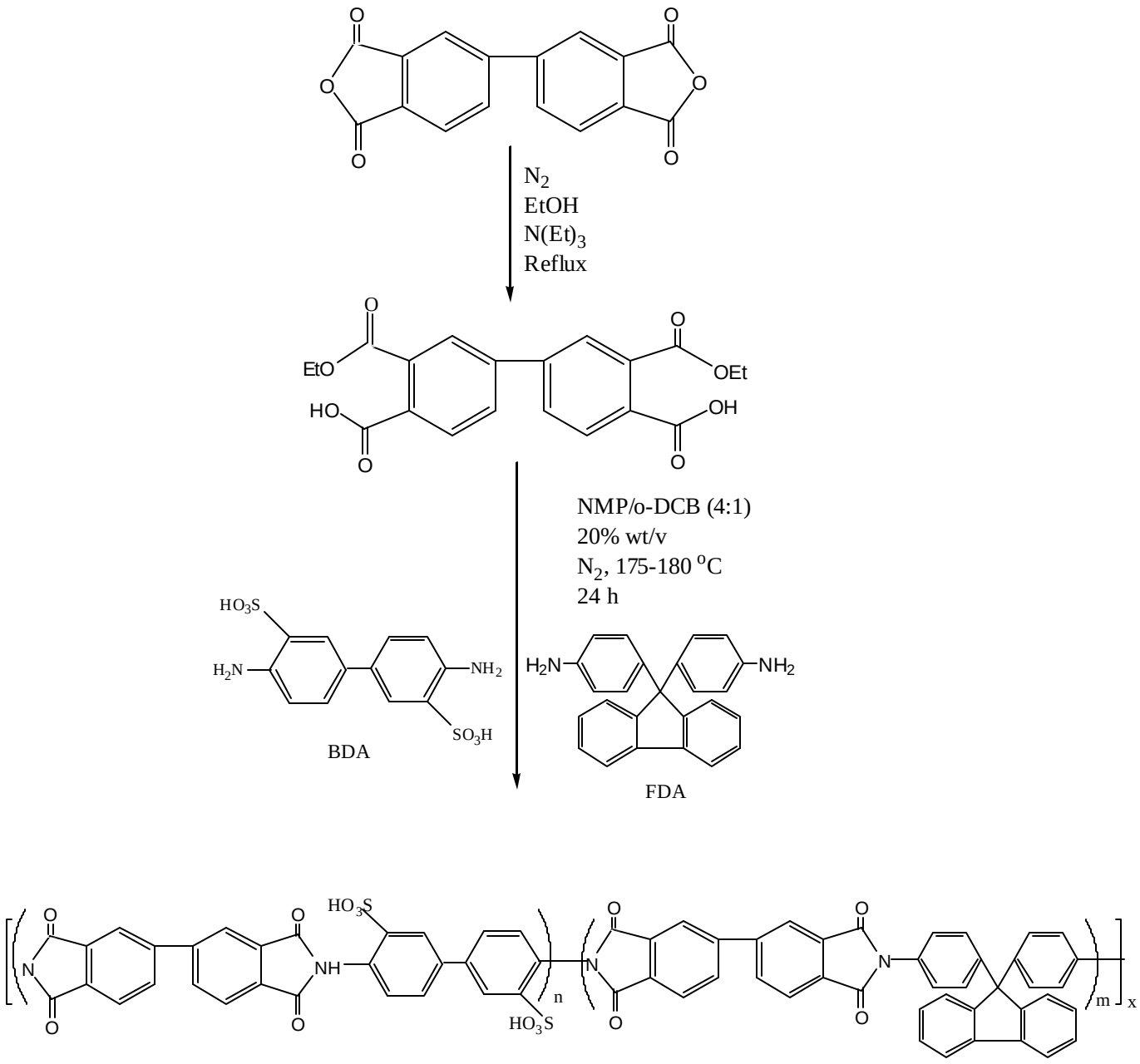

Scheme 3.3.1 Ester-acid route for sulfonated phthalic statistical copolyimides

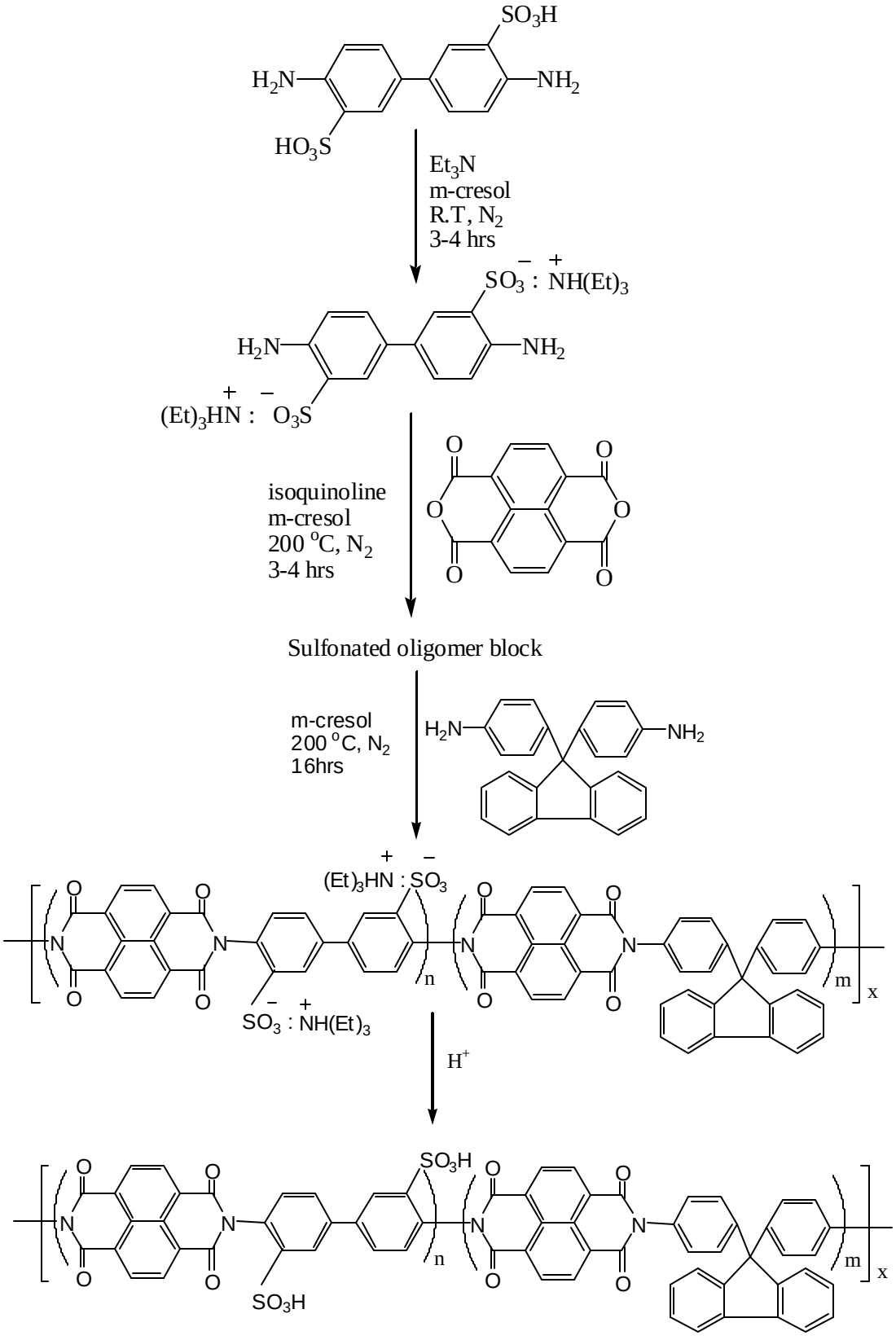

Scheme 3.3.1 One-step high temperature solution imidization of sulfonated napthalic statistical copolyimides

3.4 Characterization Methods

3.4.1 Nuclear Magnetic Resonance (NMR) Spectroscopy

Proton, Carbon 13 and Phosphorous 31 Nuclear Magnetic Resonance (^{1}H, ^{13}C and ^{31}P NMR) were used to obtain the chemical composition of the polymers and monomers synthesized. Samples were dissolved in deuterated solvents DMSO-d_6 or $CDCl_3$, at concentration of ~2 – 10% solid. NMR spectra were obtained on a Varian Unity Spectrometer operating at 400 MHz or 500 MHz. ^{1}H and ^{13}C spectra were referred to tetramethylsilane (TMS) at 0 ppm and ^{31}P NMR spectra were referred to $H_3\underline{P}O_4$ at 0 ppm.

3.4.2 High Performance Liquid Chromatography (HPLC)

High Performance Liquid Chromatography (HPLC) was utilized to aid the determination of monomer or intermediate purity. The reversed-phase HPLC analyses were conducted on a Vista 5500 with an C-18 (octadecyl or ODS). HPLC grade acetonitrile was used as mobile phase and methanol was used for amines and nitro-compounds. The injected sample volume was 10 µl and the flow rate of the mobile phase was 1 ml/min, UV detector (254 nm).

3.4.3 Fourier Transform Infrared (FTIR) Spectroscopy

FTIR was utilized to confirm the functional groups within both monomers and polymers. Measurements were conducted on a Nicolet Impact 400 FTIR Spectrometer on either KBr pellets with 1-5 wt% of monomer or on polymer thin films cast from DMAc or m-cresol solutions.

3.4.4 Gel Permeation Chromatography (GPC) or Size Exclusion Chromatography (SEC)

GPC measurements were used to determine molecular weight and molecular weight distributions of polymers. GPC was conducted with a Waters GPC/ALC 150C chromatogram equipped with a differential refractometer detector and an on-line differential viscometer detector (Viscotec 150R) coupled in parallel. TriSEC GPC Software V2.70e (Viscotek) was used to acquire and analyze the data. GPC

measurements were performed using an NMP (HPLC grade) mobile phase, containing 0.02 M P_2O_5, at a flow rate of 1.0 ml/min and an injection volume of 200 ìl with the polymer concentration of approximately 4 mg/ml. The stationary phase was crosslinked polystyrene gel (Waters ì styragel HT 10^2 Å, 10^3 Å and 10^4 Å, mean particle diameter 10 ìm) packed in three (7.8 mm I.D. x 30 cm) stainless steel columns. The column compartments, lines and detectors were maintained at a temperature of 60 ^oC during measurements. A series of polystyrene standards having narrow molecular weight distributions (Polymer Laboratory) were employed to generate a universal calibration curve. Number average molecular weight (Mn), weight average molecular weight (Mw) and polydispersity (Mw/Mn) were determined by using the universal calibration mentioned above.

3.4.5 Intrinsic Viscosity (IV)

Intrinsic viscosity measurements provided a qualitative measurement of molecular weight. Measurements were conducted using a Cannon- Ubbelohde viscometer at 25 oC in NMP or m-cresol. The reported values of intrinsic viscosity [η], were obtained by measuring specific viscosity $\eta_{sp} = (\eta/ \eta_0)-1$ and reduced viscosity $\eta_{red} = \ln(\eta/\eta_0)$ at four concentrations and extrapolating (η_{sp}/c) and (η_{red}/c) to zero concentration.

3.4.6 Thermogravimetric Analysis (TGA)

Prior to conducting TGA measurements, the polyimides were carefully dried under vacuum at elevated temperatures to remove residual solvent/moisture. Dynamic TGA was performed in either air or nitrogen to assess the thermal stability of sulfonated polyimide films. The samples were heated at a rate of 10 ^oC/min in a Perkin Elmer TGA7 instrument. The sample weight loss was measured as a function of temperature. The thermal stability of the polyimides was generally reported as the temperature at which 5% weight loss was observed.

3.4.7 Differential Scanning Calorimetry (DSC)

DSC was used to ascertain the thermal transition temperatures of the synthesized monomers and unsulfonated polyimide films. A Perkin-Elmer DSC 7 instrument was

programmed to heat the samples under nitrogen at a heating rate of 10 ^{o}C/min. First heat T_m values as the midpoint of the endotherm peak and second heat T_g values as the midpoint of the specific heat increase are reported.

3.4.8 Mass Spectroscopy (MS)

Mass spectroscopy analysis was conducted using a Fisons VG Quattro mass spectrometer to determine compound molecular weight.

3.4.9 Thin Layer Chromotography (TLC)

Thin layer chromatography is a valuable technique providing information on the completion of a reaction and the purity of synthesized monomers. TLC was therefore performed to determine the completion of reaction as well as the purity of the various compounds prepared in this research. A sealed developing chamber (a small bottle), a silica gel plate, an appropriate solvent, and a glass capillary tube previously heated while pulling from two ends to close one side were used.

3.4.10 Melting Point (m. p.) Measurements of Monomers by Capillary Method

The melting points of purified compounds were determined in a capillary tube with a Lab devices Melt-Temp II at a heating rate of no grater than 1 ^{o}C/min. Samples were ground before measuring and the formation of a meniscus was used to identify the beginning of the melt.

3.4.11 Solubility Tests

The solubility of various synthesized monomers and polyimides was determined using several commercial solvents. The completely dried monomer powder or polymeric film was mixed with a number of appropriate solvents including chloroform, methylene chloride, toluene, THF, NMP and DMAc, to give a concentration of 10 wt./vol. %. Then, the mixture was stirred at room temperature for 4-5 hours. Solubility was assessed by visual observation. “Soluble” samples remained in solution at R.T., whereas “insoluble” polyimides did not dissolve or precipitated out of solution.

3.4.12 Non-Aqueous Potentiometric Titration of Sulfonic Acids

Non-aqueous potentiometric titrations were employed to determine mili-equivalent weight of $-SO_3H$ groups in sulfonated five-membered ring polyimides. This value was then used to experimentally calculate Ion-Exchange Capacity (IEC, meq/g, miliequivalent of reactive $-SO_3H$ sites per gram of polymer) of the polyimide containing pendant sulfonic acid groups. Potentiometric titrations were performed using a MCI GTOS Automatic Titrator equipped with a standard calomel electrode and a reference electrode.

A typical sulfonated polyimide titration was conducted as follows:

Tetra methyl ammonium hydroxide (TMAH) was utilized as titrant for the titration of sulfonic acid groups in polyimides. The titrant, ~ 0.02 N was standardized with dry potassium hydrogen phthalate (KHP) immediately prior to titrating. Sulfonated polyimide membranes were previously dried at 150 ^{o}C before conducting the experiment and then they were completely dissolved in dimethyl acetamide (DMAc). The end-point was detected as the maximum of the first derivative for the potential versus volume of titrant used. The end point was then used to calculate the IEC (meq/g) of the polyimide membrane. The reported experimentally calculated IECs were the average of at least four titrated polyimide samples with similar weight.

3.4.13 Solvent-Cast Free Standing Films

Freestanding sulfonated five- and six-membered ring polyimide films were prepared by casting solutions of polymers dissolved either in DMAc (20 % wt/v) for five-membered polyimides or in m-cresol (5 % w/v) for six-membered polymers. About 2 g of polymer was dissolved in ~ 8 ml of DMAc (25 % w/v) or in ~ 40 ml of m-cresol (5% w/v) by stirring overnight. Prior to casting onto a glass substrate, polymer solutions were filtered to remove particles using a disposable syringe and Acrodisc filters having porosities of 0.45 and 0.22 μm.

Approximately 8 ml of each solution was filtered and cast in 3” diameter area on a clean glass plate placed on a hot plate. To confine the solution to this area, a 3’’ diameter stainless steel ring was used as a mold. The film was then heated gradually from room

temperature to 150 ^{o}C in 18 hours on a hot plate covered with a glass top under a nitrogen atmosphere supplied by a gas inlet. Using a programmable temperature controller (Omega CN2011), the hot plate temperature was gradually ramped up to provide heating according to the following schedule: 25 ^{o}C to 100 ^{o}C in 6 hours, at 100 ^{o}C for 3 hours, 100 ^{o}C to 150 ^{o}C in 6 hours, at 150 ^{o}C for 3 hours.

Following drying on a programmable hot plate under nitrogen, the high molecular weight films were peeled from the glass plate with the help of a drop of water. After re-placing the films loosely on the glass plate, they were then further dried under vacuum at 150 ^{o}C for 24 hours. The films were then used for characterization of the polymeric membranes

3.4.14 Spin-Cast Films

Very thin films in the micrometer thickness were obtained by spin casting on glass microscopic slides using a Headway Photo-resist Spinner (Model 1-EC101D-R485). The polymer solutions were prepared and filtered as explained above for free standing-films. Previously cleaned and dried glass slides were placed on the chuck of the spin-coating apparatus that holds the substrate with vacuum. The polyimide solutions were then applied onto the glass and the chuck was subsequently rotated at speeds ranging from 300 to 3,000 rpm, depending on the desired film thickness.

Spin-cast films were transferred to the lab in a desiccator and then immediately placed under nitrogen atmosphere supplied by a gas inlet and an outlet on a glass covered hot plate. Using a programmable temperature controller, films were generated after removing the solvent according to the same heating schedule as described in the previous section. Defect-free spin-cast thin polymer membranes were used for water uptake measurements.

3.4.15 Water Sorption

Water uptake was determined on polyimide thin films rigorously dried to a constant weight at 150 ^{o}C under vacuum for 24 hours and then immersed in water at room temperature as well as at various increasing temperatures up to 100 ^{o}C to study the effect of temperature on water sorption. The weight increase was monitored periodically using

an analytical balance until a constant weight percent of water uptake was found. The weight of the water absorbed by a given polyimide sample during periodic measurements was determined by taking the weight difference between the wet film and the dry film and dividing by the dry film weight.

3.4.16 Conductivity Measurements

Conductivity measurements were performed on membranes using the cell shown in Figure 3.3. This cell geometry was chosen to ensure that the membrane resistance dominated the response of the system. An impedance spectrum was recorded from 10MHz to 10Hz using a Solatron 1260 Impedance/Gain-Phase Analyzer. The resistance of the film was taken at the frequency, which produced the minimum imaginary response. All impedance measurements were performed at room temperature under full hydration conditions.

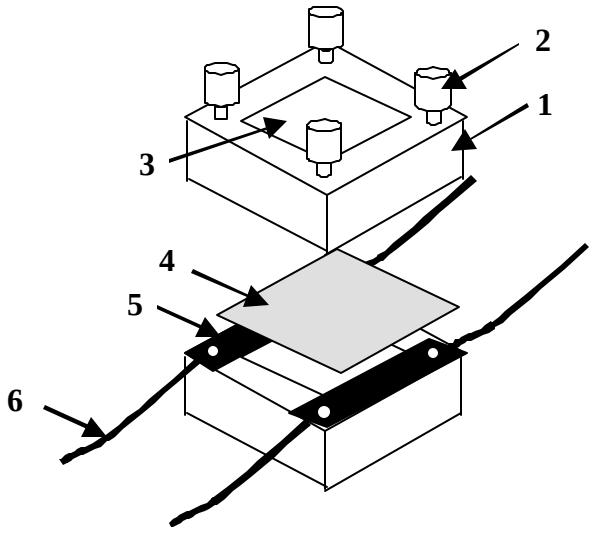

Legend
1. Teflon block
2. Thumbscrew
3. Open area to allow equilibration with environment
4. Membrane sample
5. Blackened Pt foil electrode
6. Pt lead

Figure 3.3 Conductivity Cell

CHAPTER 4. RESULTS and DISCUSSIONS

This chapter comprises three major sections. The first section will discuss the monomer synthesis involved in this research, including bis(3-aminophenyl)phenyl phosphine oxide (BAPPO), bis(3-aminophenoxy)phenyl phenyl phosphine oxide (s-BAPPPO), disulfonated 4,4'-bis(3-aminophenoxy)phenyl sulfone (s-DADPS), and six-membered bis(naphthalic anhydride) monomers such as bis(oxynaphthalic anhydride)phenyl phenyl phosphine oxide (NDA-PO) and bis(oxynaphthalic anhydride) phenyl sulfone (NDA-SO_2) and their intermediates.

The second section details the synthesis, molecular weight, thermal and structural characterization of several novel five- and six-membered ring polyimides which were targeted for their potential applications as proton ion-conducting polymer electrolyte membranes in fuel cells.

The third section of this chapter reports synthesis and characterization of several novel polyimides containing phosphineoxide [P(O)] or sulfone [$S(O_2)$] moieties in their repeat unit.

Several key characteristics including film formation, thermal stability, hydrolytic stability, water uptake *etc*. were studied for comparison with unsubstituted systems, and to elucidate the degree of ionic character/property relationship within the series. This chapter addresses the results of these experiments and the related knowledge that has been obtained from the data.

4.1 Monomer Synthesis and Characterization

4.1.1 Synthesis of Bis(3-aminophenyl)phenyl Phosphine Oxide (BAPPO)

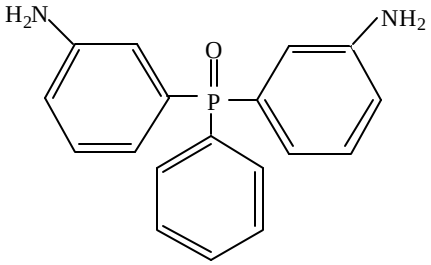

Bis(3-aminophenyl)phenyl phosphine oxide (BAPPO) monomer that requires two-step reaction was synthesized through the sequence shown in Scheme 4.1.1[(222)].

The first step is the preparation of bis(3-nitrophenyl)phenyl phosphine oxide intermediate, obtained via aromatic nucleophilic substitution reaction of the triphenyl phosphine oxide with $HNO_3/H2SO_4$ acid mixture at a very low temperature. The syntheses of dinitro intermediate (BNPPO) and diamine (BAPPO) monomer were presented earlier and may be found in section 3.2.3.1 and 3.2.3.2, respectively.

Nitration

The synthesis of this reaction starts with a three phenyl substituted phosphine oxide molecule, which is commercially available in large volume. Two of the phenyl groups are expected to undergo nitration. Since all the phenyl groups are identical, it is critical to experimental conditions are selective enough to avoid the occurance of trifunctional (or monofunctional) adducts to the final product. Scheme 4.1.2 presents three sequential nitration reactions that may occur during the nitration process of triphenyl phosphine oxide.

It was reasoned that the rates of reactions should follow the $R_{(1)}>R_{(2)}>R_{(3)}$ because of the induction effects and steric hindrance. However, the selectivity is small. Therefore, the reaction is conducted at low temperature to minimize the selectivity for reactions (1) and (2) and to minimize the formation of the by-product trinitro-compound by reaction (3). The stoichiometry was controlled at 1 mole:2 mole (triphenyl phosphine oxide : nitric acid).

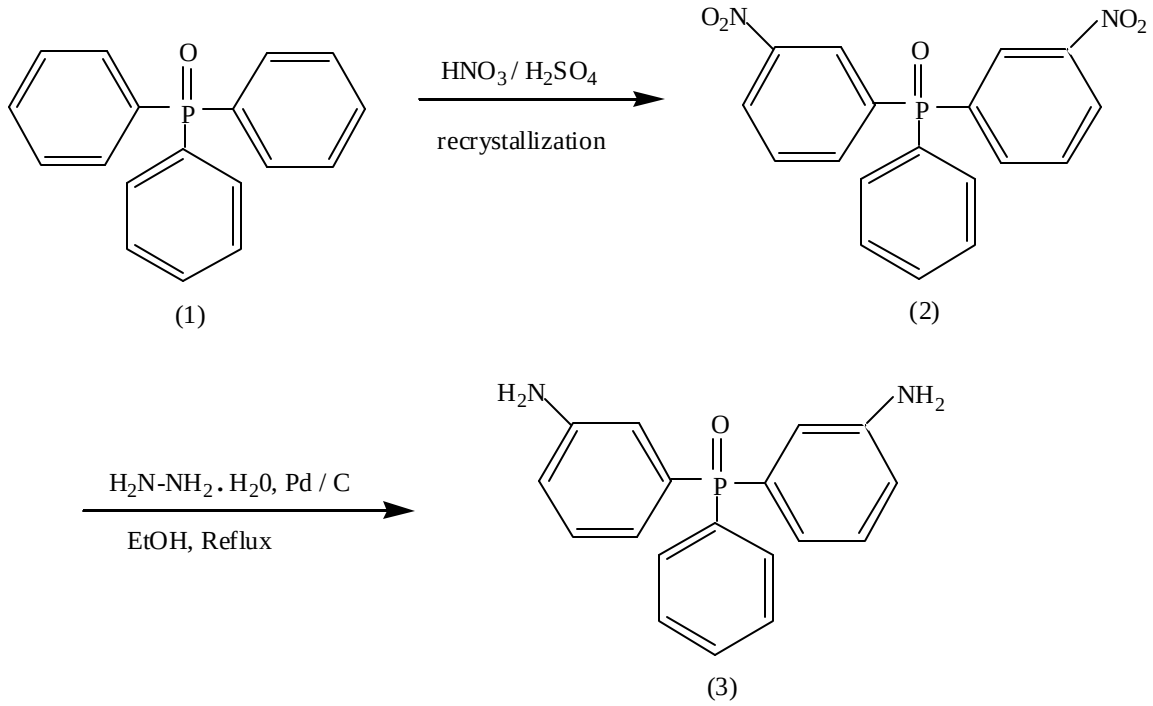

Scheme 4.1.1 Synthesis of Bis(3-aminophenyl)phenyl Phosphine Oxide (BAPPO)[222]

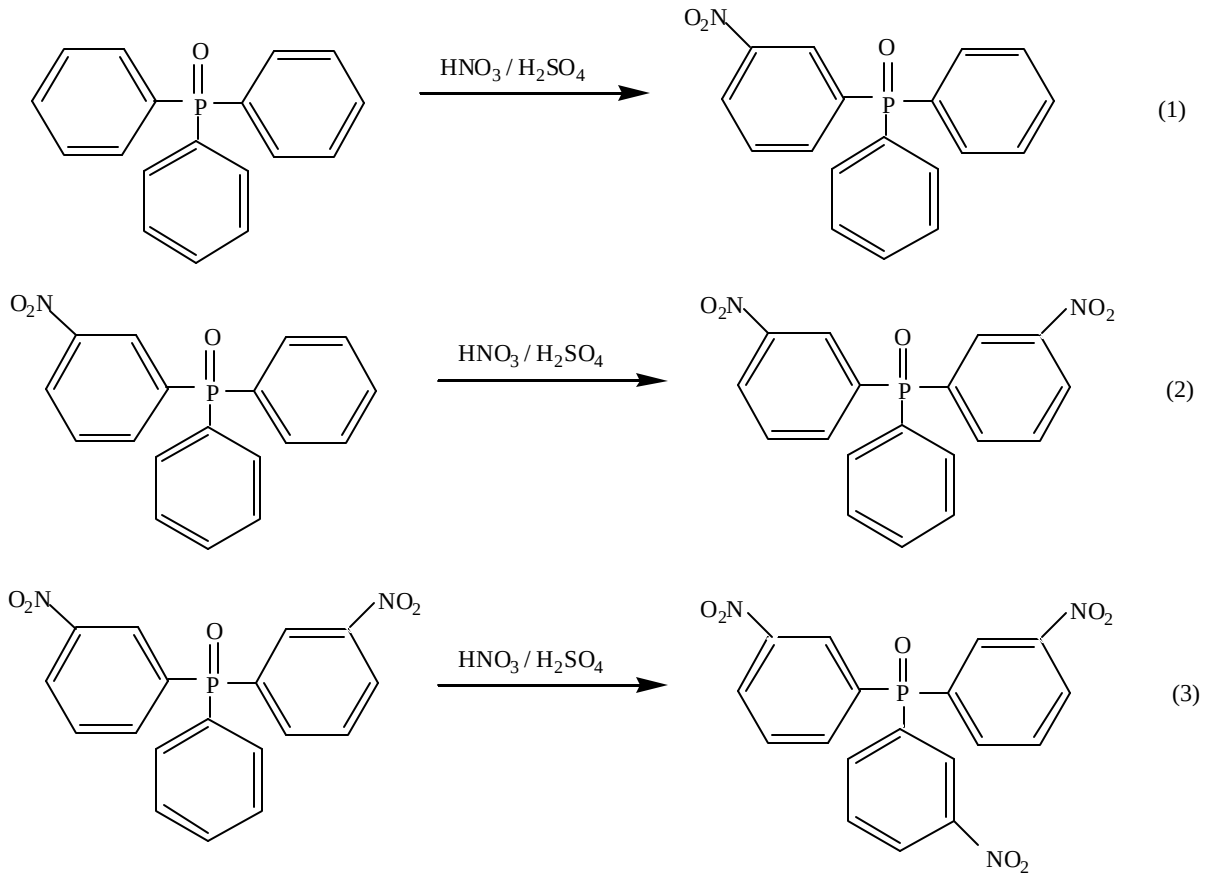

Scheme 4.1.2 Possible sequential nitration reactions of triphenyl phosphine oxide[222]

The most important thing in the nitration reaction of TPPO is that, the reaction temperature control is very critical. The ice bath was composed of ice, NaCl, and acetone to obtain a temperature of ~ (-10) – (-5) ^{o}C. A small amount of dry ice was added frequently and the addition of the acid mixture was very slowly to prevent heat build-up. Exact stoichiometric amount of fuming nitric acid (no excess) was used. The crude product was a viscous mass, because the significant number of impurities depressed the melting temperature. Therefore it was not washed with water directly, but rather washed by extraction with water/chloroform.

Purification of Bis(3-nitrophenyl)phenyl Phosphine Oxide (BNPPO)

The crude nitro compound was purified by recrystallization from a mixture of ethanol and water. The nitro compound was extensively purified and more than ten crystallizations were necessary to obtain nearly 100 % purity. The fundamental principle for purifying the material was the fact that the solubilities are in the order of mono- >di- >tri-nitro compound. The ratio of water and ethanol varied from 3:1 to 1:2 depending on the relative abundance of by products mono- and di-nitro compounds. A higher water/ethanol ratio is more efficient in eliminating tri-nitro (insoluble if the recrystallization liquid is saturated), while a lower one is more efficient for mono-nitro.

The obtained di-nitro compound, BNPPO, was a light yellow crystal with a melting point of 141-142 ^{o}C by capillary tube. Reverse phase HPLC showed no impurities. ^{31}P NMR (500 MHz, DMSO-d_6) showed a single peak (24.13 ppm) (Figure 4.1.1). ^{1}H NMR (400 MHz, DMSO-d_6) showed a matching chemical shift and integrations (Figure 4.1.2). The overall yield after recrystallization was 55 % (based on the theoretical yield).

Preparation of Bis(3-aminophenyl)phenyl Phosphine Oxide (BAPPO)

The di-nitro compound was reduced to the diamine with hydrazine as discussed in section 3.2.2.20. Compared to first step, formation of dinitro intermediate, the second step, reduction of dinitro compound was much more simple. Hydrazine monohydrate (9 times excess of the stoichiometric amount) was used as the reducing agent in the presence

of Pd/C catalyst.. Evolution of the gas from the mixture indicated the occurrence of the reaction. The completion of the reduction was monitored by TLC. The product was obtained with high purity >99% as detected by the elemental analysis, proton and phosphorous NMR spectroscopy techniques as shown in Figures 4.1.3 and 4.1.4. Mass spectroscopy data (Figure 4.1.5) was also consistent with the assigned structure. The molecular ion (M^+ =308) is visible, with a prominent (M^++1) peak, as it could be expected from a molecule containing one or several P atoms.

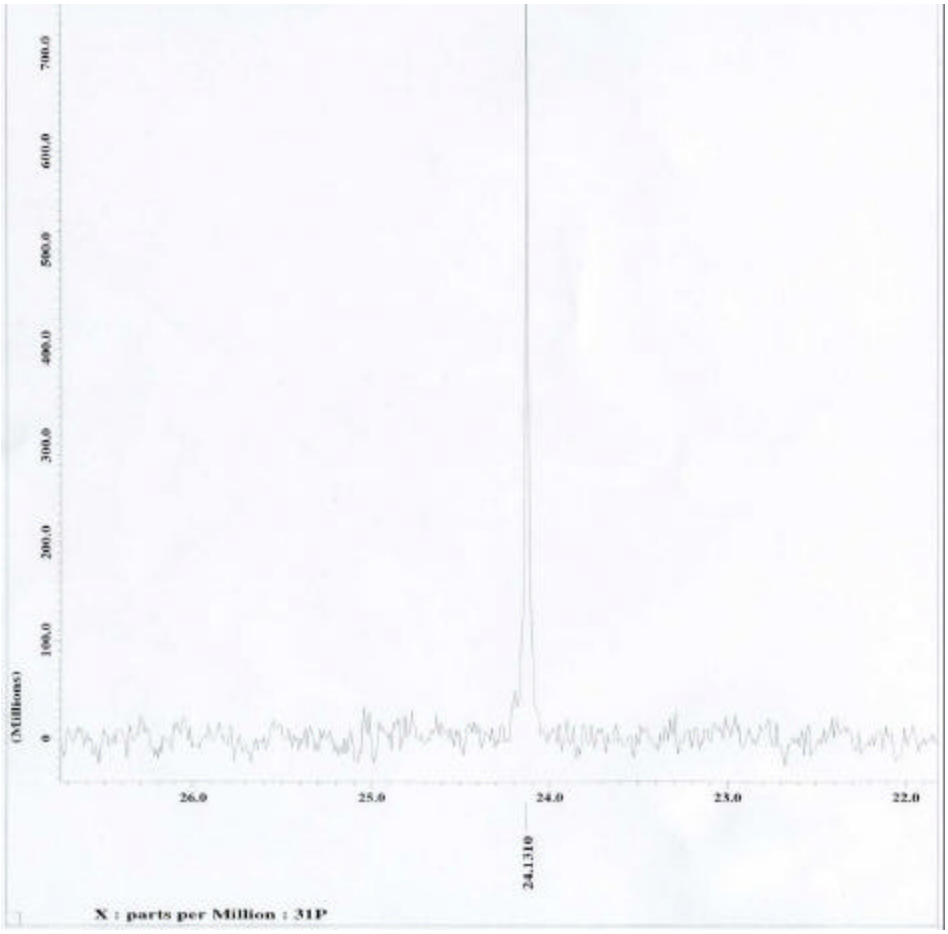

Figure 4.1.1 ^{31}P NMR spectrum of BNPPO

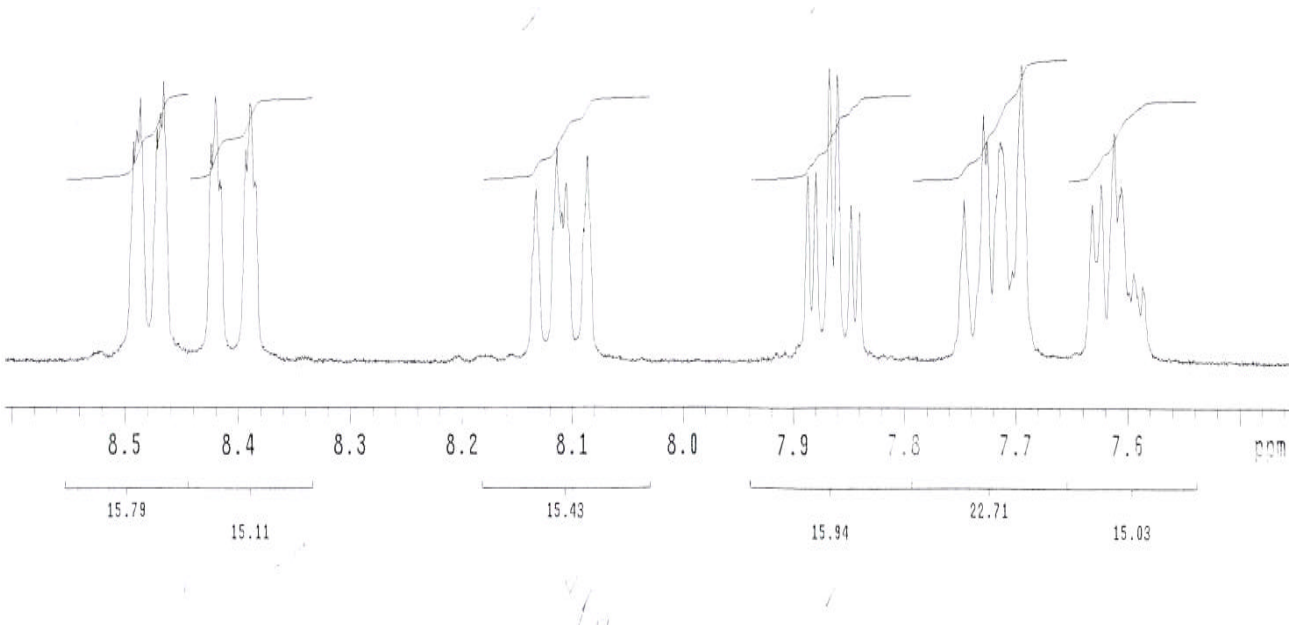

Figure 4.1.2 ^{1}H NMR spectrum of BNPPO

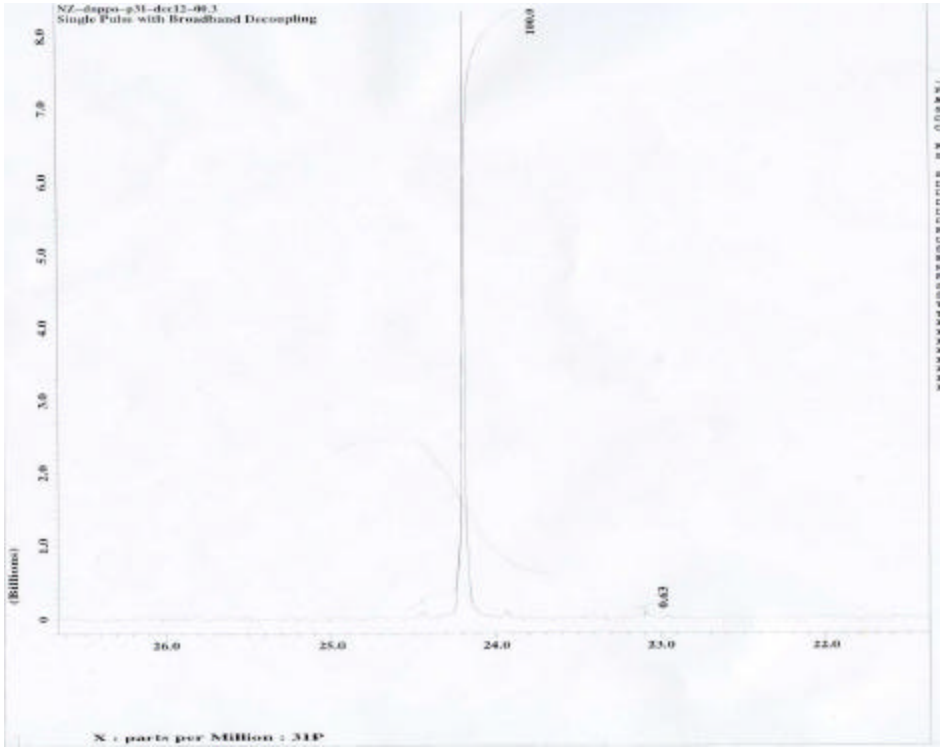

Figure 4.1.3 ^{1}P NMR spectrum of BAPPO

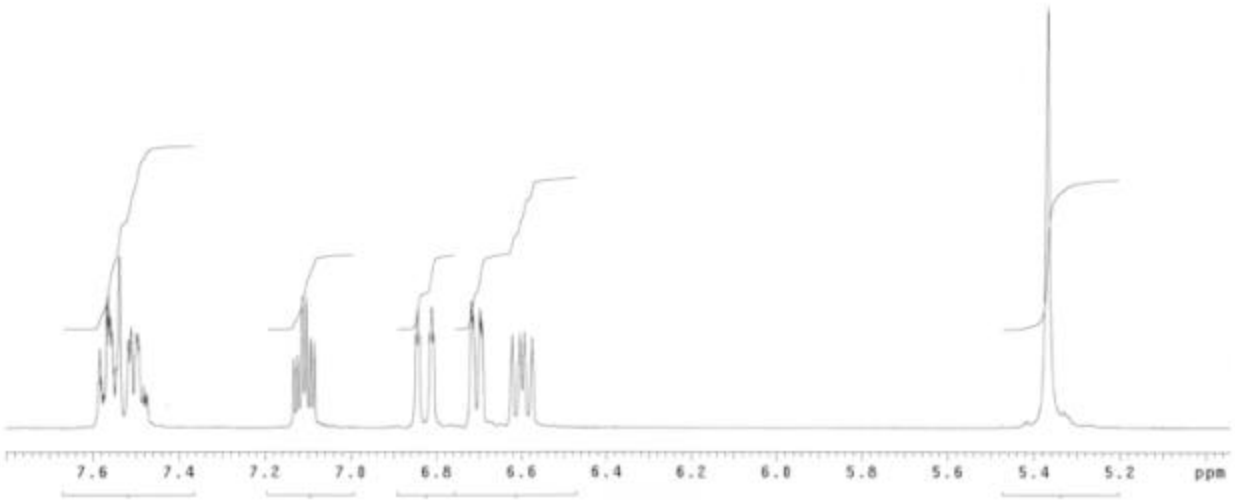

Figure 4.1.4 ^{1}H NMR spectrum of BAPPO

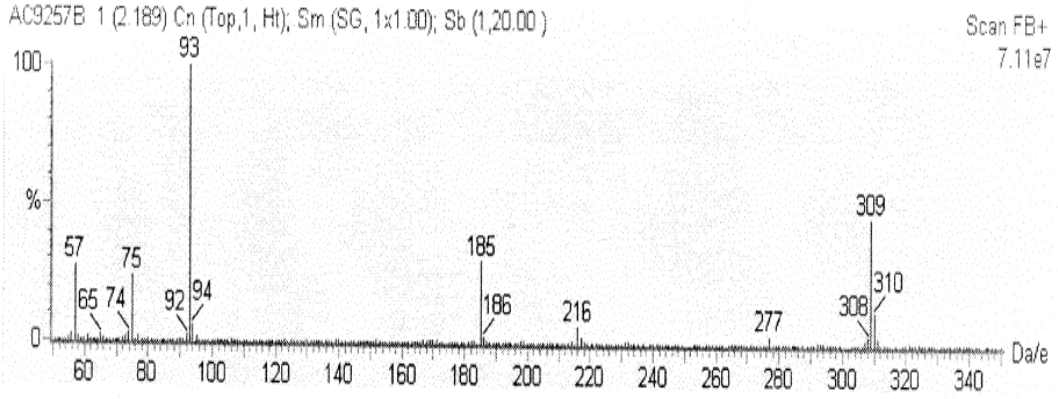

Figure 4.1.5 Mass spectrum of DAPPO

4.1.2 Synthesis of Sulfonated Bis(4-fluorophenyl) Phenyl Phosphine Oxide (s-BFPPO)

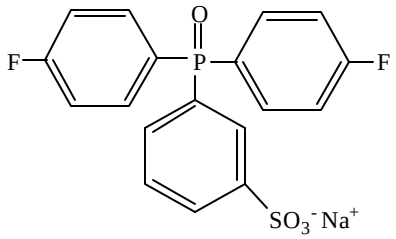

The synthesis of sulfonated bis(4-fluorophenyl) phenyl phosphine oxide (s-BAPPO) was presented in section 3.2.2.21.

Keeping in mind that this is a very exothermic reaction, stoichiometric ratio of the acid, temperature control and also the duration of the reaction are key factors in obtaining mono-sulfonated product with minimum amount of impurity (unreacted BFPPO and/or di- or tri- sulfonated BFPPO). Therefore, the temperature and the exact duration of the reaction solution at 90 ^{o}C were closely watched. Using of TLC to determine the completion of reaction was not very successful due to the oily character of the product in sulfonic acid solution. Thus, a small amount of reaction solution was dripped into ethyl acetate to be able see the completion of the reaction.

From TLC, it was seen that there was some un-reacted starting material, BFPPO. The product was then purified through silica gel column using methanol / ethyl acetate mixture as an eluent (BFPPO is soluble in ethyl acetate however, s-BFPPO is not soluble). The pure product was then obtained with 79% yield after removal of the solvent mixture and drying overnight at 130 ^{o}C under vacuum. (In some cases, the crude product was just stirred in excess of ethyl acetate overnight to remove any trace amount impurities and did not need to pass through the column)

The purity of the product was confirmed with TLC, ^{1}H (Figure 4.1.6) and ^{31}P NMR (Figure 4.1.7), elemental analysis and FAB mass spectroscopy (Figures 4.1.8).

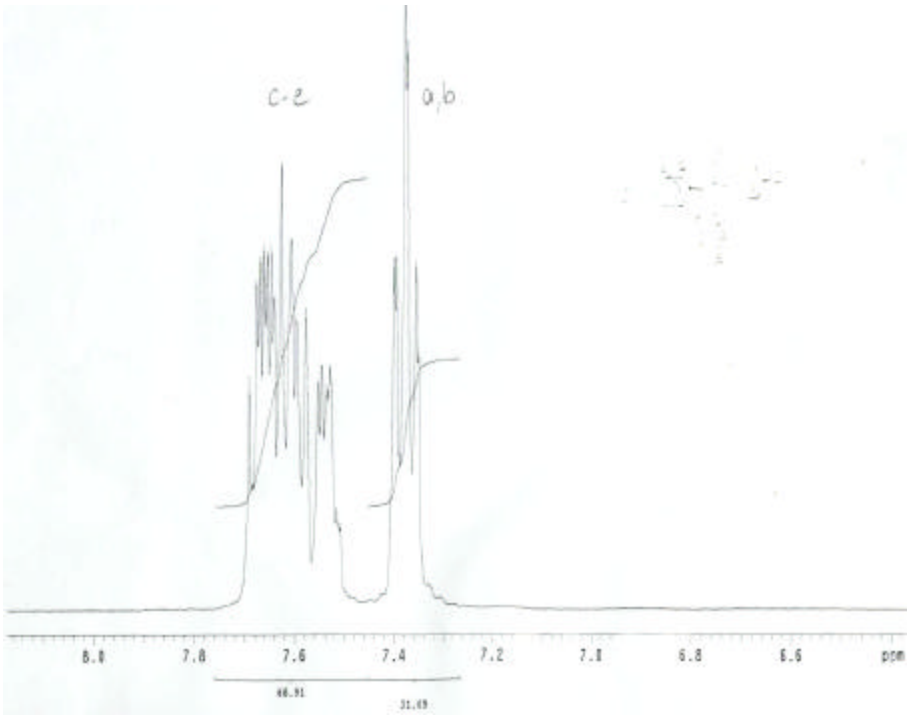

Figure 4.1.6 ^{1}H NMR spectrum of s-BFPPO *(solvent: DMSO-d_6)*

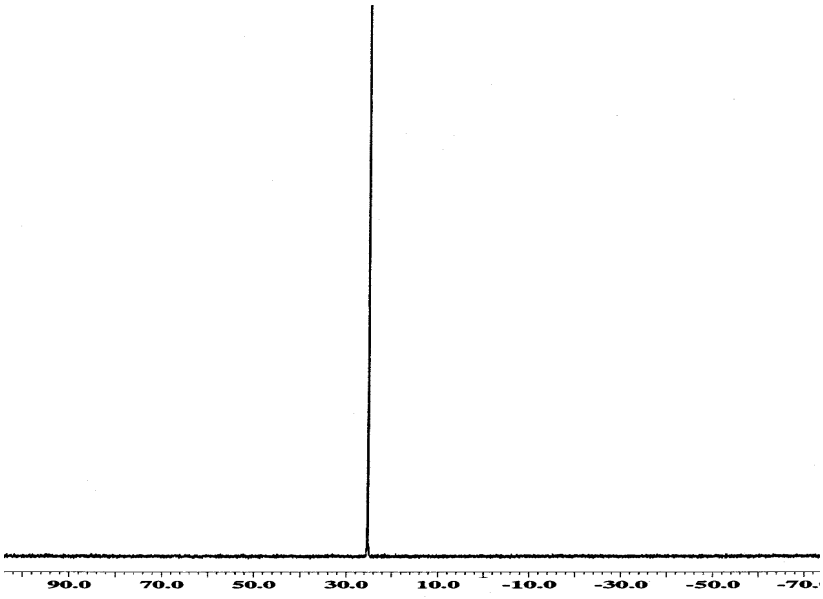

Figure 4.1.7 ^{31}P NMR spectrum of s-BFPPO *(solvent: DMSO-d_6)*

$C_{18}H_{12}F_2NaO_4PS$

Mol. Wt.: 416.31

C, 51.93; H, 2.91; F, 9.13; Na, 5.52; P, 7.44; S, 7.70

C, 52.15; H, 2.70; F, 9.44; Na, 5.52; P, 7.80; S, 8.02

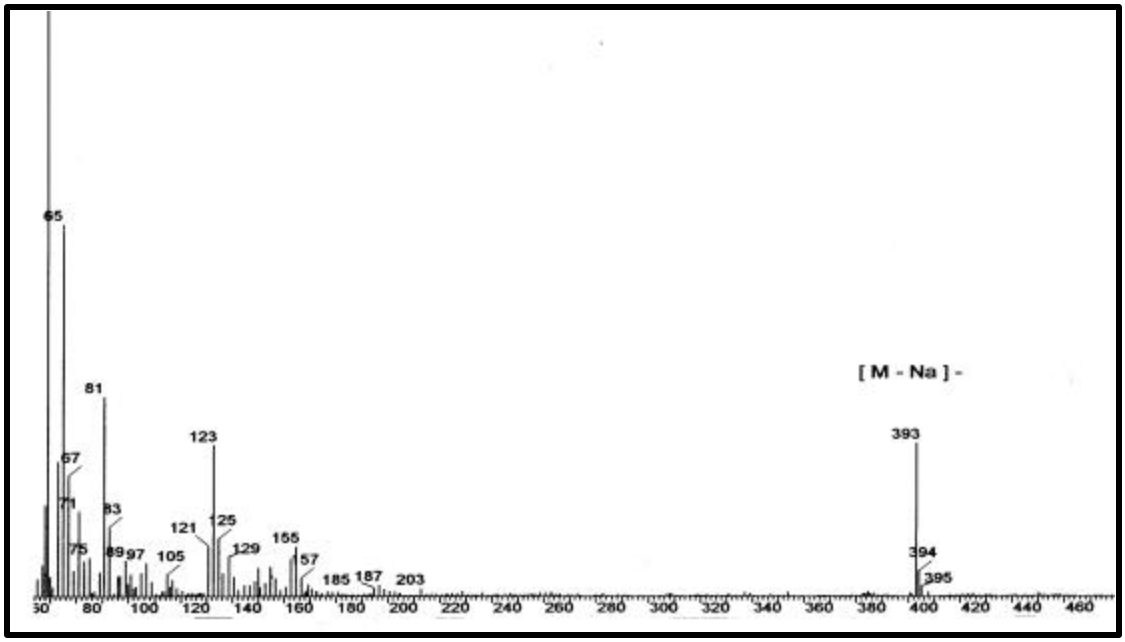

Figure 4.1.8 Elemental analysis data and Mass spectrum of s-BFPPO

4.1.3 Sulfonated Bis(3-aminophenoxy)phenyl sulfone (s-BAPPO)

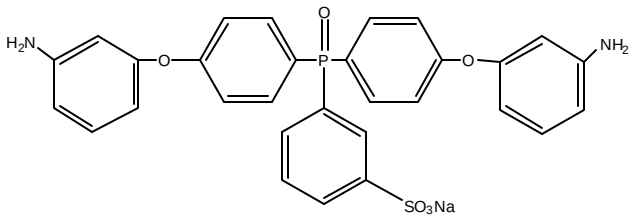

s-BAPPO was synthesized from the aromatic nucleophilic reaction of sulfonated bis(fluorophenyl) phenyl phosphine oxide (s-BFPPO) intermediate and *m*-aminophenol as a nucleophile in the presence of potassium carbonate (K_2CO_3). First, m-aminophenoxides were generated from the reaction of the *m*-aminophenol with the weak base, K_2CO_3 in DMAc at 135 ^oC removing the by-product water via the toluene azeotrope . Once the formation of potassium salt of the m-aminophenol was completed, the temperature was raised to 160 ^oC to essentially remove all the azeotropic solvent, toluene. Then, *m*-aminophenol was incorporated along with more DMAc and reaction was continued for 24 hours. The most difficult-to-remove impurity from this reaction is unreacted *m*-amino phenol if one uses the excess of it. In the first try of this reaction, the employment of column chromatography and/or dissolving the reaction product in minimum amount methanol and then precipitating in excess of ethylacetate was not successful to remove the excess of *m*-aminophenol, although m-aminophenol is soluble in ethylacetate and the product is not. The water extraction of *m*-aminophenol could not be employed, which is usually done for unsulfonated analogue of s-BAPPO, due the solubility of the product in water too. However, the same reaction with the exact stoichiometric amount of *m*-aminophenol did not cause the author extra effort for purification. The crude product was dissolved in very small amount of methanol and slowly precipitated in large amount of ethylacetate to remove the reaction solvent, DMAc, which is very difficult to be removed. One difference of this procedure from the previously published work[223] is that, the product was isolated from ethylacetate, instead of toluene, which gives sticky, dark brown precipitate.

However, the precipitation of the filtered reaction solution into ethylacetate gave a tan-color precipitate in powder form, which was much easier to work up with in further.

The pure product was obtained with 89 % yield and the molecular structure and purity of the Na-salt of sulfonated diamine monomer was confirmed by ^{1}H and ^{31}P NMR and FAB mass spectroscopy techniques such as those shown in Figures 4.1.10 and 4.1.11. There are 10 different aromatic protons are shown as H_1 and H_1 (7.89 and 7.8 ppm), H_2 and H_3 (7.52 ppm), H_4 (7.09 ppm), H_5 (7.0 ppm), H_6 (6.38 ppm), H_7 (6.23 ppm), H_8 and H_9 (6.21 ppm) and amine proton shows a peak at 5.28 as expected. The protons on the rings appear as higher multiplets , due to the coupling with phosphorus, which has a spin of ½. The protons have an integration ratio of 5 ring protons / 1 aromatic amine protons. The sole phosphorus shows a singlet at 26.3 ppm and the small side peaks equidistant on either side of the major phosphorus peak are side bands.

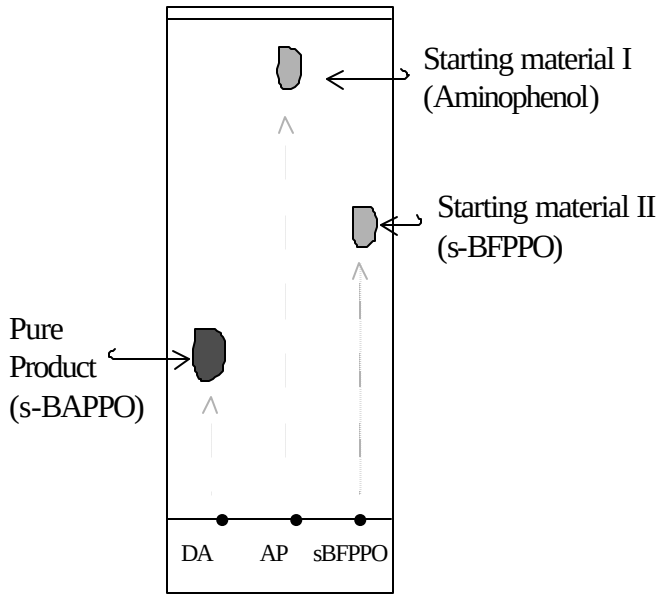

Figure 4.1.9 TLC of the purified diamine, DA (sBAPPO) and the starting materials, m-aminophenol (AP) and s-BFPPO in 25/75 (v/v) methanol/ethyl acetate mixture as an eluent

Table 4.1.1 Advancement of starting materials and their reaction products in thin layer chromatography purification solvents; ethyl acetate (EtAC), methanol (MeOH) and their mixtures. (S-BFPPO: sulfonated 4,4'-bis(fluoro phenyl) phosphine oxide; BFPPO: 4,4'-bis(fluoro phenyl) phosphine oxide; SBAPPO: sulfonated bis(3-aminophenyl)phenyl phosphine oxide; AP: 3-aminophenol) (x-insoluble, and + soluble)

	S_BFPPO	BFPPO	SBAPPO	AP
EtAc :	**x**	+ (*middle*)	**x**	+(*top*)
MeOH:	+ (*upper*)	+ (*upper*)	+ (*upper*)	+ (*upper*)
EtAc/MeOH: (1:1)	+ (*upper*)	+ (*upper*)	+ (upper)	+ (upper)
EtAc/MeOH: (7:3)	+ (*middle*)	+ *(upper*)	+ (*lower*)	+ (*upper*)

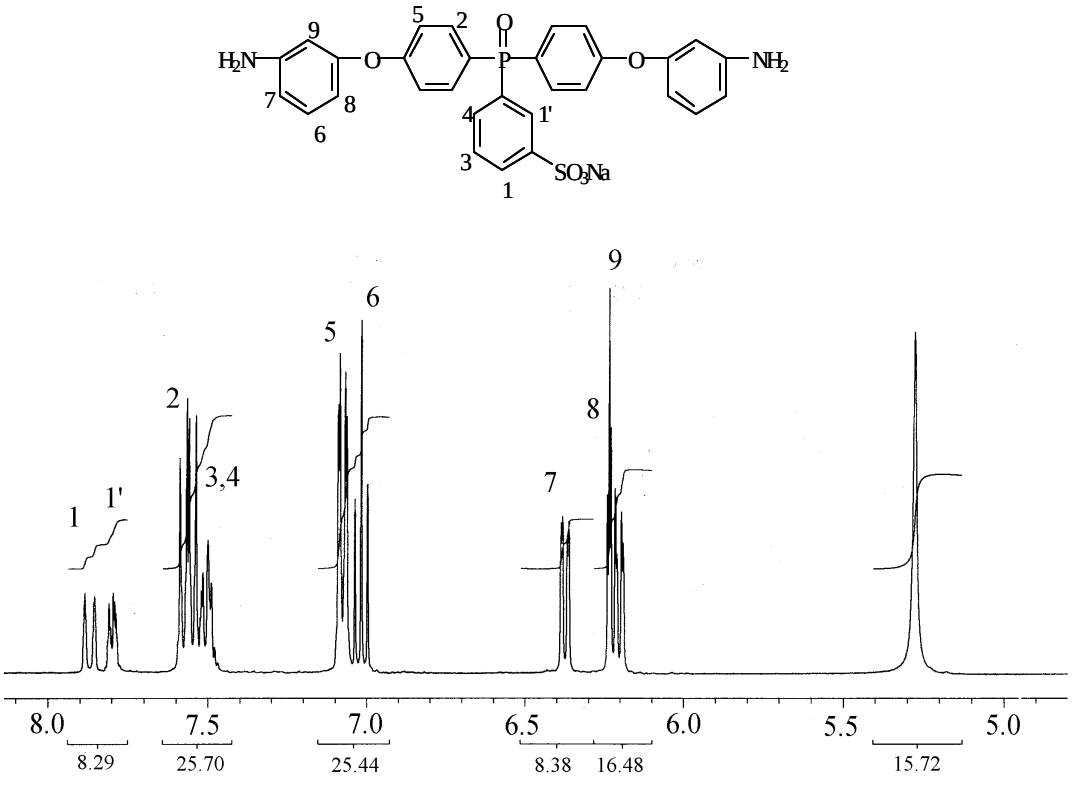

Figure 4.1.10 ^{1}H NMR of s-BAPPO in *d*-DMSO

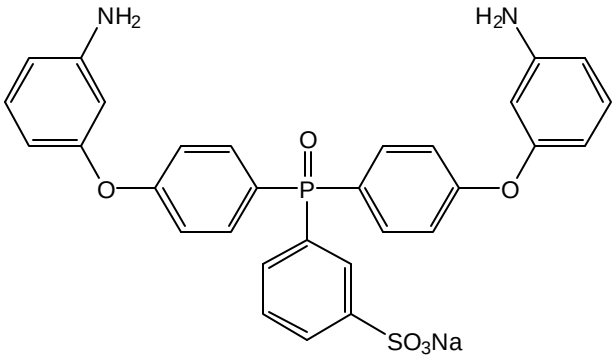

$C_{30}H_{24}N_2NaO_6PS$

Mol. Wt.: 594.55

C, 60.60; H, 4.07; N, 4.71; Na, 3.87; P, 5.21; S, 5.39

C, 61.32; H, 3.98; N, 4.46; Na, 4.11; P, 5.21; S, 5.76

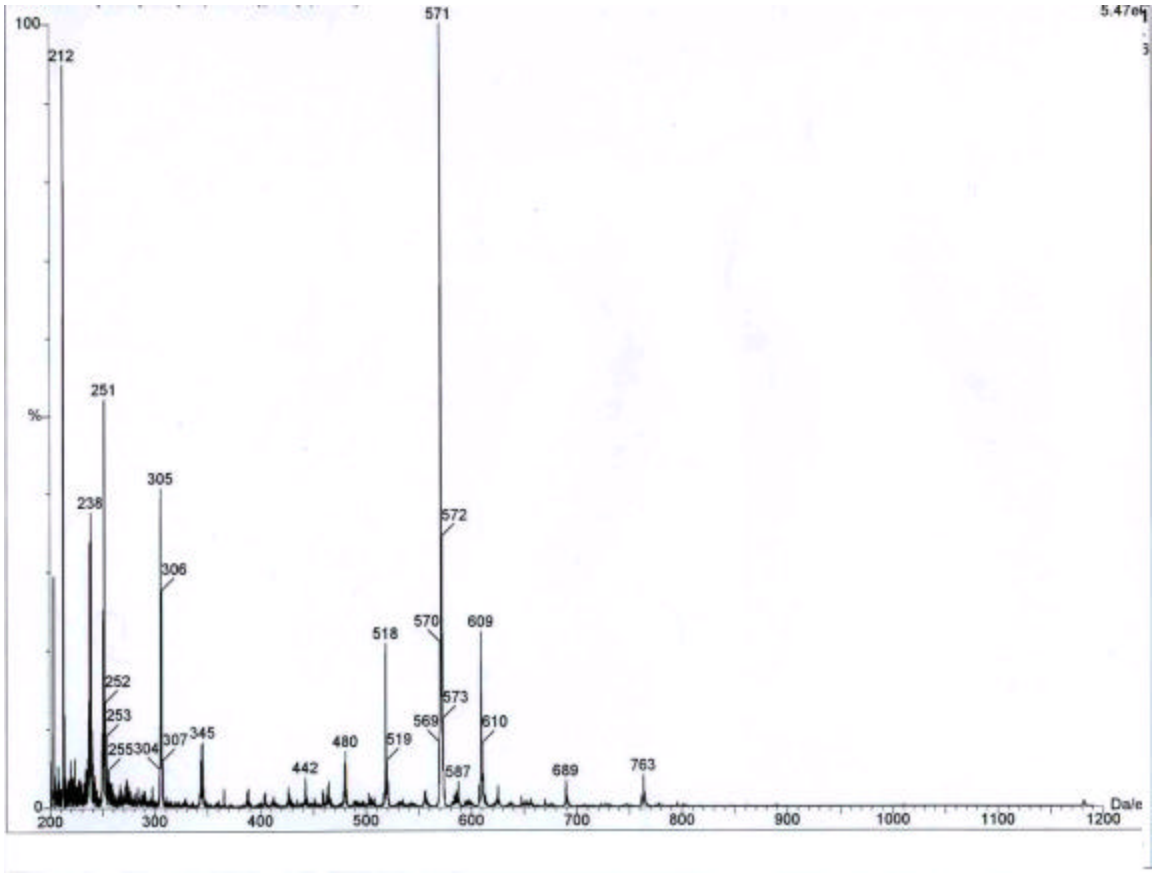

Figure 4.1.11 Elemental analysis and FAB^+ Mass Spectroscopy of s-BAPPO

4.1.4 Synthesis of Disulfonated 4,4'-dichlorodiphenyl sulfone (s-DCDPS)

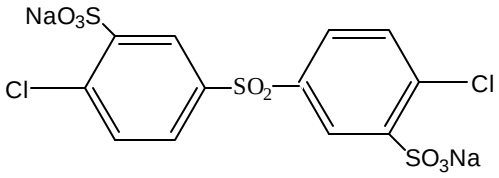

S-DCDPS intermediate was synthesized according to the published work from our research group[125]. Although the general reaction conditions for sulfonation of DCDPS was first described by Ueda and his coworkers[124], a modified procedure of s-DCDPS reported by our research group[4] provides more characterization details of the monomer's synthetic scheme as described in Scheme 3.2.5. The reported straightforward electrophilic substitution reaction procedure sulfonates the DCDPS meta to the sulfonyl group and ortho to the chlorine group, forming the di sulfonated monomer. It is then changed from the free acid form to its sodium salt form during neutralization and isolation, by "salting out", with excess of sodium chloride.

These reactions were conducted at 110 ^{o}C and afforded yields of ~90 % after recrystallization. Unlike the s-BFPPO, described in Section 4.1.2, s-DCDPS intermediate was easily purified by crystallization from 6:1 isopropanol:deionized water solution mixture and did not require the column chromatography. The melting temperatures of the sulfonated compounds couldn't be detected due to the decompositon of sulfonic acid moieties in their structure.

The anticipated molecular structure and the composition of the sulfonated monomer were confirmed by proton (^{1}H) and carbon (^{13}C) NMR in *d*-DMSO (Figure 4.1.12), as well as by infrared and elemental analysis techniques (Figure 4.1.13). The proton NMR spectra shows three different aromatic protons that appears at H_2 (7.43 ppm), H_3 (7.95 ppm), and H_5 (8.16 ppm)

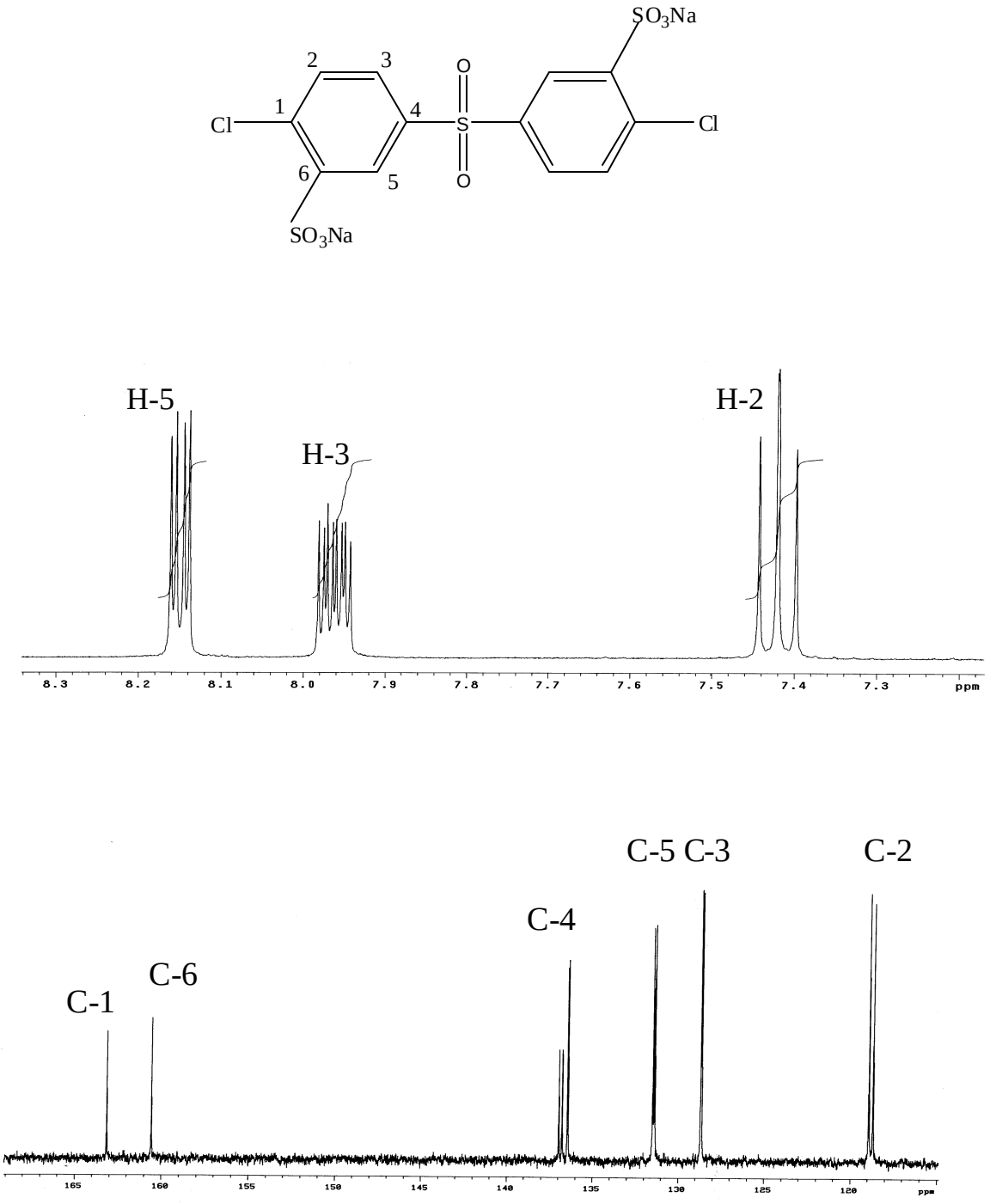

Figure 4.1.12 ^{1}H and ^{13}C NMR spectra of s-DCDPS (solvent: DMSO-d6)

$C_{12}H_6Cl_2Na_2O_8S_3$

Mol. Wt.: 491.25

Theoretical: C, 29.34 %; H, 1.23 %; Cl, 14.43 %; Na, 9.36 %; S, 19.58 %

Experimental: C, 30.03 %; H, 1.21 %; Cl, 14.27 %; Na, 9.45 %; S, 19.27 %

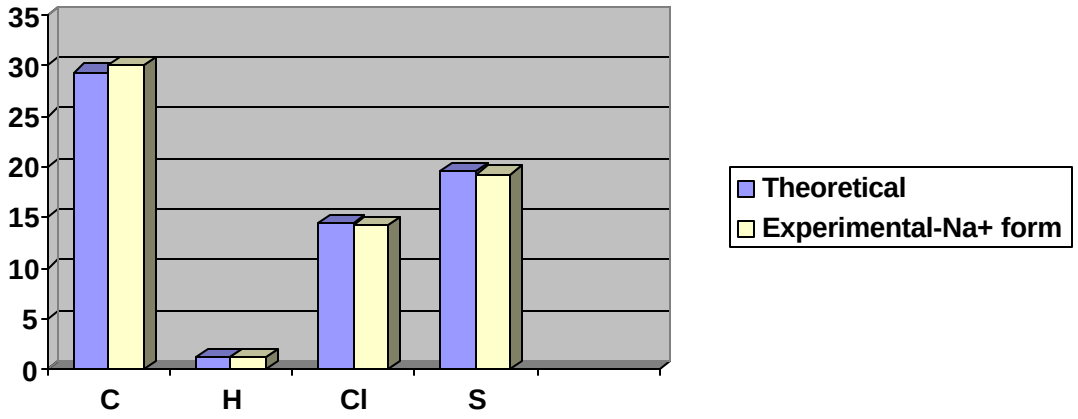

Figure 4.1.13 Elemental Analysis of s-DCDPS

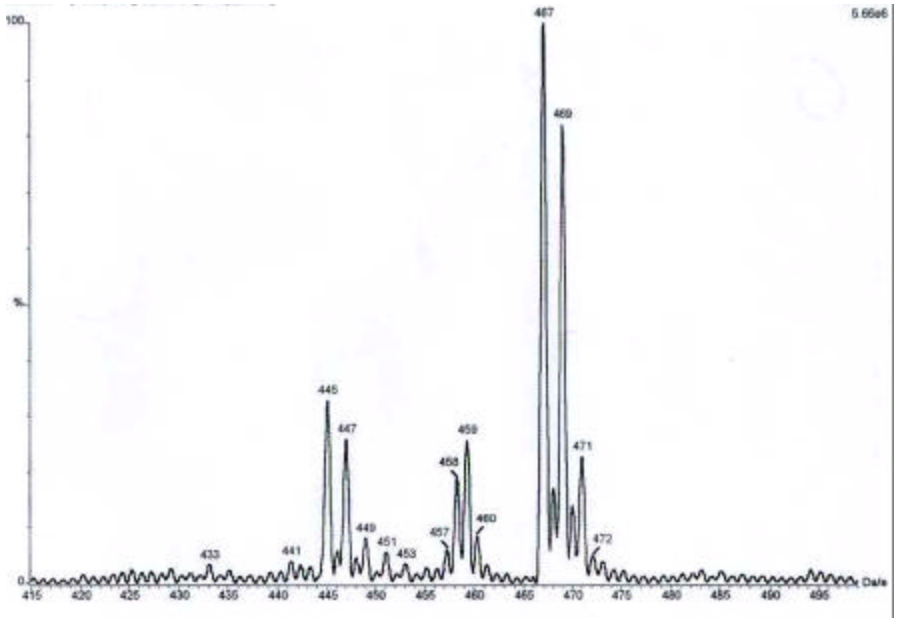

Figure 4.1.14 Mass Spectrum of s-DCDPS

4.1.5 Disulfonated 4,4'-bis(3-aminophenoxy)phenyl sulfone (s-DADPS)

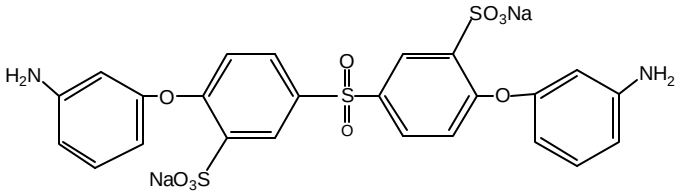

The synthesis of s-DADPS was similar to that of s-BAPPO, which is previously described in Section 4.1.3. The disulfonated DCDPS was synthesized via aromatic nucleophilic reaction chemistry using disulfonated dichlorodiphenyl sulfone (s-DCDPS) intermediate and *m*-aminophenol as a nucleophile in the presence of potassium carbonate (K_2CO_3). First, m-aminophenoxides were generated from the reaction of the *m*-aminophenol with the weak base, K_2CO_3 in DMAc at 135 ^oC removing the by-product water via the toluene azeotrope. Once the formation of potassium salt of the m-aminophenol was completed, the temperature was raised to 160 ^oC to essentially remove all the azeotropic solvent, toluene. S-DCDPS was then added into the flask along with more DMAc and reaction was continued for 24 hours at the refluxing temperature of the solvent as described in Section 3.2.2.23.

Unlike the s-BAPPO, described in Section 4.1.3, s-DADPS monomer was obtained with high purity after precipitating the reaction solution drop by drop into large amount of ethyl acetate. After repeating this process a couple of times, to remove or extract the DMAc from the product as much as possible, highly pure sulfonated diamine monomer was obtained with a yield of 92 %.

The anticipated molecular structure and the composition of the sulfonated monomer were confirmed by proton (^1H) NMR in *d*-DMSO (Figure 4.1.15), as well as by infrared, elemental analysis and mass spectroscopy techniques (Figure 4.1.16). The proton NMR spectra shows seven different aromatic ring protons that appears at H_1 (8.21 ppm), H_2 (7.79 ppm), H_3 (7.0 ppm), H_4 and H_5 (6.19 ppm), H_6 (6.88 ppm), and H_7 (6.39 ppm). Aromatic amine proton shows a peak at 5.33 ppm. The protons have an integration ratio of 7 ring protons/1 aromatic amine protons.

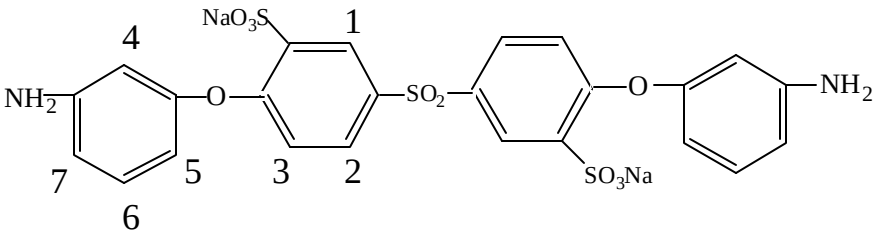

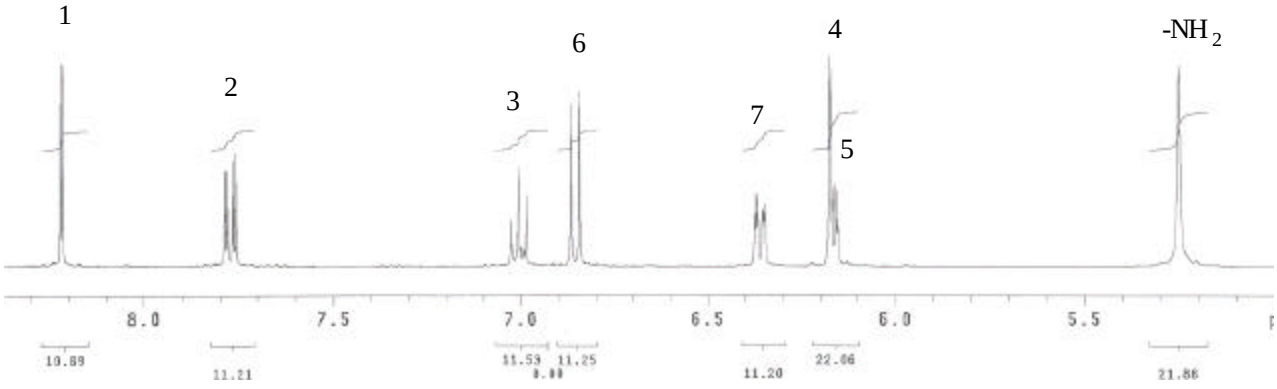

Figure 4.1.15 ^{1}H NMR of s-DADPS in DMSO-d6

$C_{24}H_{18}N_2Na_2O_{10}S_3$

Mol. Wt.: 636.58

Theoretical : C, 45.28 %; H, 2.85 %; N, 4.40 %; Na, 7.22 %; S, 15.11 %

Experimental: C, 45.52 %; H, 2.77 %; N, 4.32 %; Na, 7.28 %; S, 14.96 %

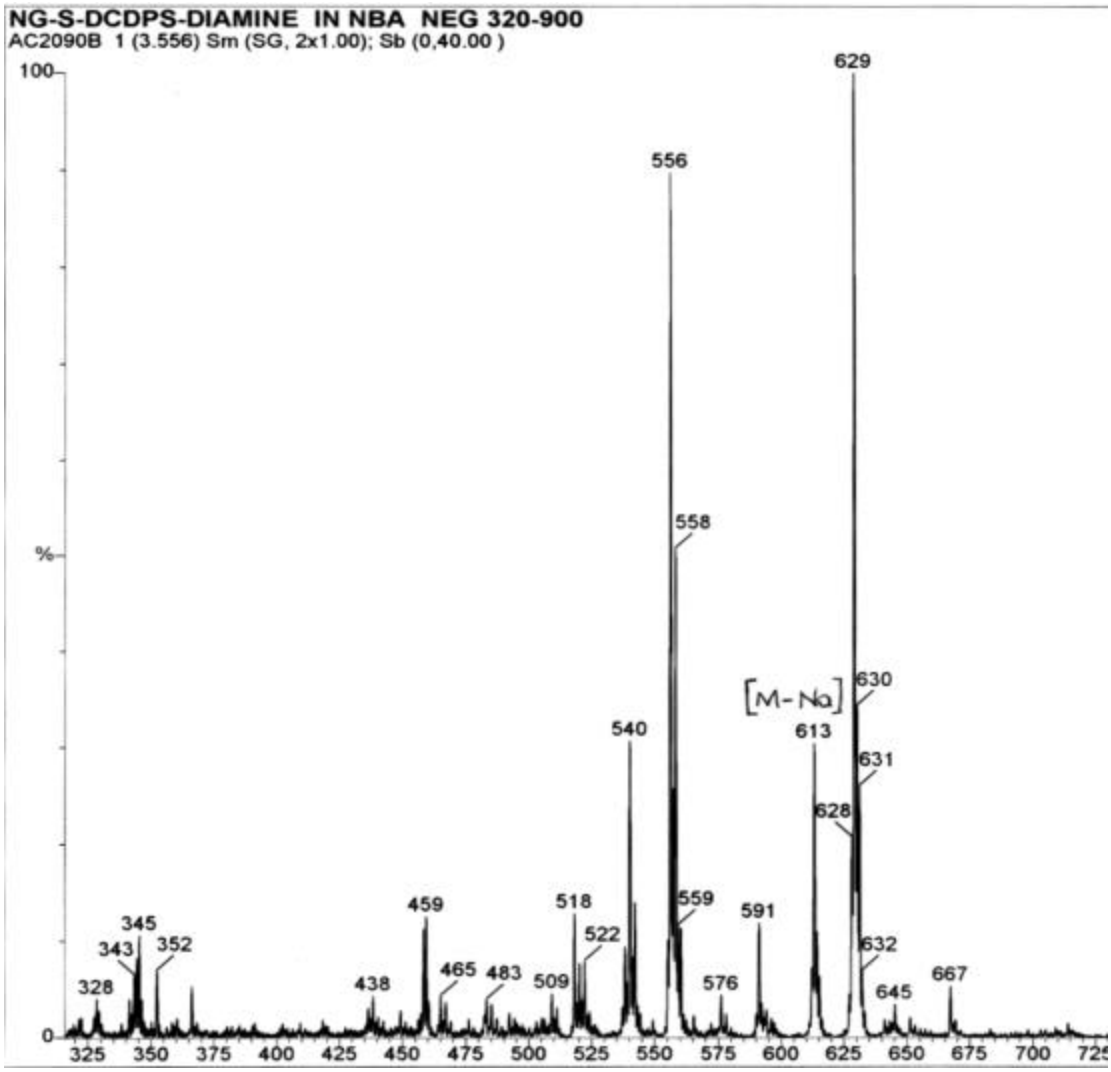

Figure 4.1.16 Elemental Analysis Data and Mass Spectroscopy of s-DADPS

4.1.6 Bis (4-hydroxyphenyl) phenyl phosphine oxide (BOHPPO)

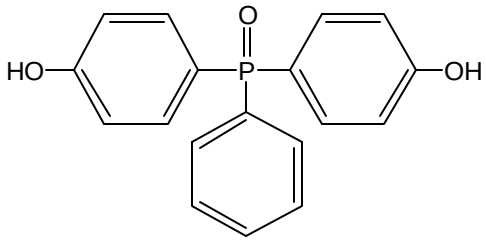

BOHPPO was synthesized according to the published procedure[226] in which BFPPO was hydrolyzed with five moles of potassium hydroxide at 135 ^{o}C for 10 hours to afford a yield of approximately 96 % of monomer grade material, after recrystallization in a methanol/water (1/5 vol/vol) mixture as discussed in Section 3.3.1. The melting point of the pure product was 237 ^{o}C. The chemical structure and purity of the material were confirmed using ^{1}H and ^{31}P NMR spectroscopy in *d*-DMSO (Figures 4.1.17 and 4.1.18) and inverse phase HPLC techniques. The integration of aromatic protons to the hydroxy peaks yielded a ratio of 13/2.

BOHPPO was used as a precursor in the synthesis of a novel six-membered ring bisnaphtahlic anhydride monomer to increase the solubility of its analogous monomer (naphthalene tetracarboxylic dianhydride) by incorporating flexible bridging units such as BOHPPO. The following section discusses the synthesis and basic characterization results of the

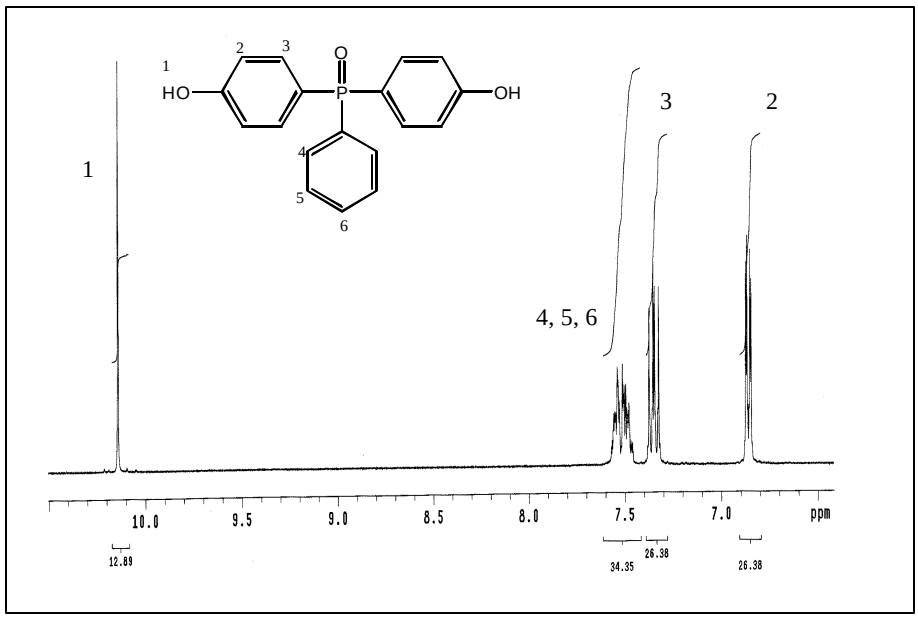

Figure 4.1.17 ^{1}H NMR of BOHPPO

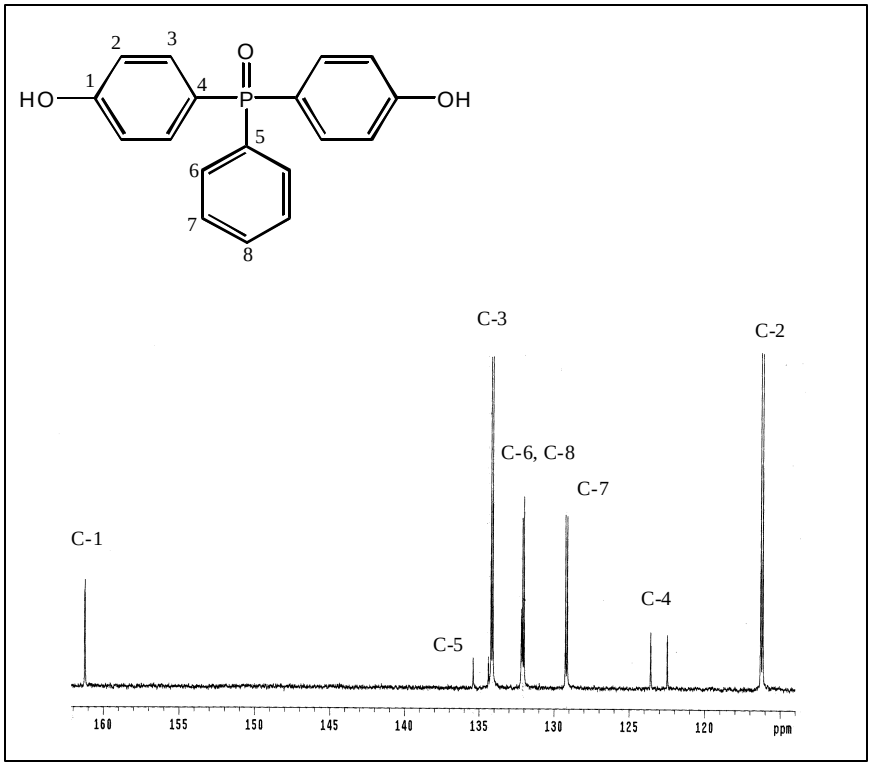

Figure 4.1.18 ^{13}C NMR of BOHPPO

4.1.7 4,4'-Bis(oxynaphthalic anhydride) phenyl phenyl phosphine oxide (NDA-PO)

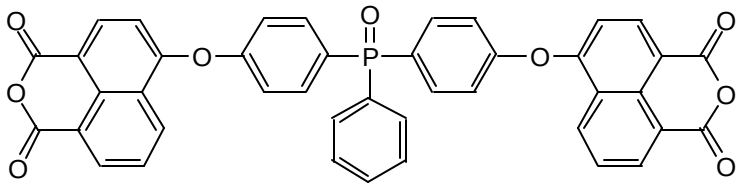

The above bis(oxyethernaphthalic anhydride) monomer (NDA-PO) was synthesized using one-pot two-step reaction procedure, utilizing nucleophilic aromatic substitution chemistry *via* the reaction of the bis-oxyphenolate (BOHPPO) and bromo-naphthalene dianhydride as described in Section 3.2.3.8. In the first step of the reaction, the biphenol was reacted with strong base, NaOH, in DMAc, at 135 ^{o}C removing the by-product water via the toluene azeotrope and forming the Na salt of bis-oxyphenolate-phenylphosphineoxide. The second step employed the reaction of the bisphenolate with the halide naphthalic anhydride at an elevated temperature, 160-164 ^{o}C for 24 hours. The reaction solution was filtered to remove the salt and precipitated by slowly adding into deionized water. The filtered and dried crude product usually contained impurities possibly one-side reacted phenolates and unreacted anhydride. The impurities, especially unreacted biphenols, were in higher percentages (>10 %) when all the reactants were added together and the reactions were conducted in one-step or even in two-step using K_2CO_3, weaker base, to deprotonate the biphenol. To remove unreacted biphenols, the crude product was redissolved in ice-cold 5 % NaOH solution, filtered to remove unsoluble part, and then precipitated with ice-cold 5 % HCl solution. The product was fully cyclized by drying at 170 ^{o}C under vacuum and the subsequently further crystallized several times from very concentrated toluene solution. The complete closure of the rings was necessary to increase the solubility of the monomer in toluene. The product yield was about 53 % after recrystallizations. (Calculated: C%: 71.79, H%: 3.28, P%: 4.42; Found: C%: 71.24, H%: 3.19, P%: 4.63)

The molecular structure of this material was confirmed using ^{1}H and ^{31}P NMR in DMSO-d_6. These spectra are shown below in Figures 4.1.19 and 4.1.20. 23 different

aromatic protons appear at H_1 (7.42 ppm), H_2 (7.96 ppm), H_3 (8.51 ppm), H_4 (8.64 ppm), H_5 (8.74 ppm).

These protons appear as higher multiplets, due to the coupling with phosphorus. The sole phosphorus shows a singlet at 29.4 ppm, and small side peaks equidistant on either side of major phosphorus peak are side bands. The melting of this monomer was 237 ^{o}C as depicted using DSC.

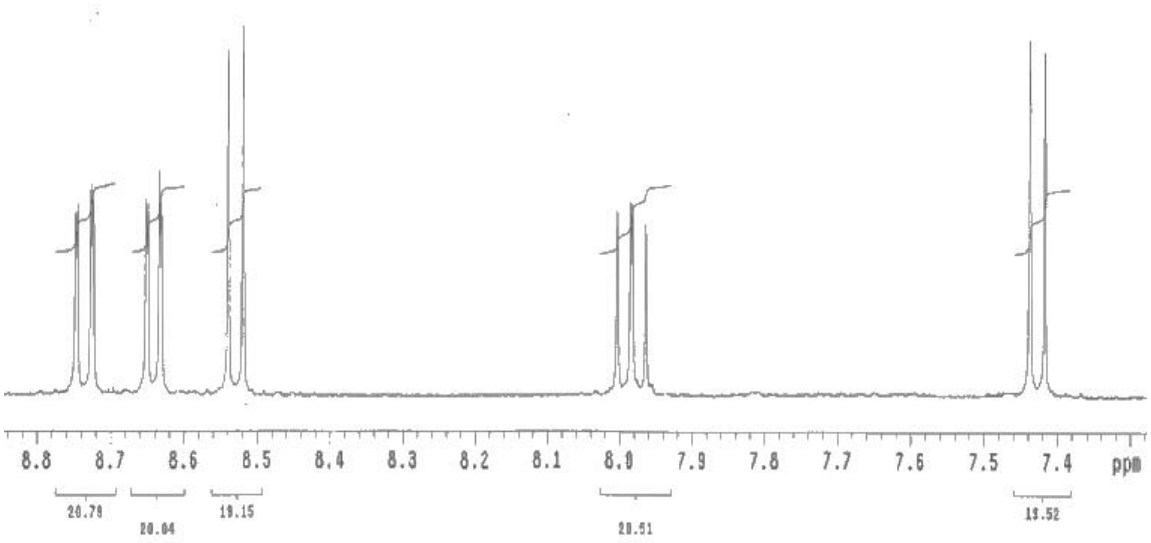

Figure 4.1.19 ^{1}H NMR Spectrum of NDA-PO

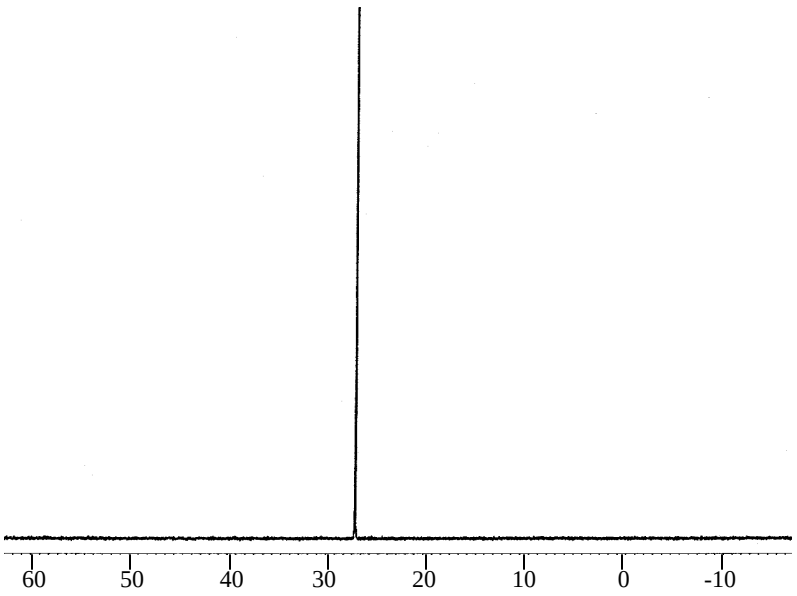

Figure 4.1.20 ^{31}P NMR Spectrum of NDA-PO

4.1.8 4,4'-Bis(oxynaphthalic anhydride) phenyl sulfone (NDA-SO_2)

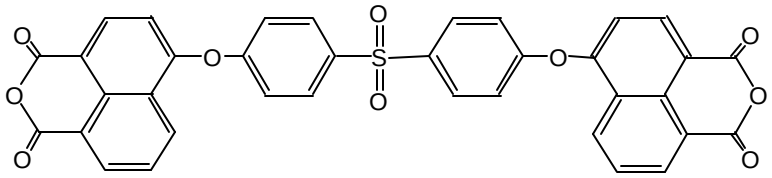

NDA-SO_2 six-membered dianhydride was synthesized in a similar manner to NDA-PO, except that commercially available 4,4'-Sulfonyldiphenol (SDP) was utilized as the biphenol starting material instead of BOHPPO as described in Section 3.2.3.9 and depicted in Scheme 3.2.3.3. The crude product was purified by precipitating with ice-cold 5 % HCl from an ice-cold alkali solution. It was subsequently further crystallized several times from very concentrated DMSO solution. The product yield was ~ 67 % after recrystallizations (Calculated: C%: 65.11, H%: 2.89, S%: 5.68; Found: C%: 65.58, H%: 2.93, S%: 5.38)

The molecular structure of this material was confirmed using ^{1}H NMR in DMSO-d_6. These spectra are shown below in Figures 4.1.21. Seven different aromatic protons appear at H_a (doublet, 8.31 ppm), H_b (doublet, 7.37 ppm), H_c (doublet, 8.53 ppm), H_d (triplet, 7.93 ppm), H_e (doublet, 8.64 ppm), H_f (doublet, 7.67 ppm), H_g (doublet, 7.47 ppm). The melting of this monomer was 250 ^{o}C by DSC (Figure 4.1.22).

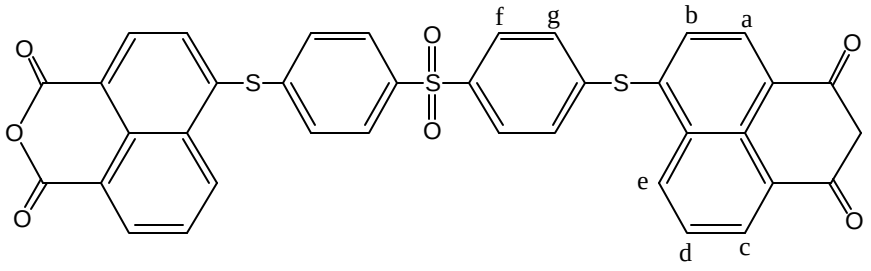

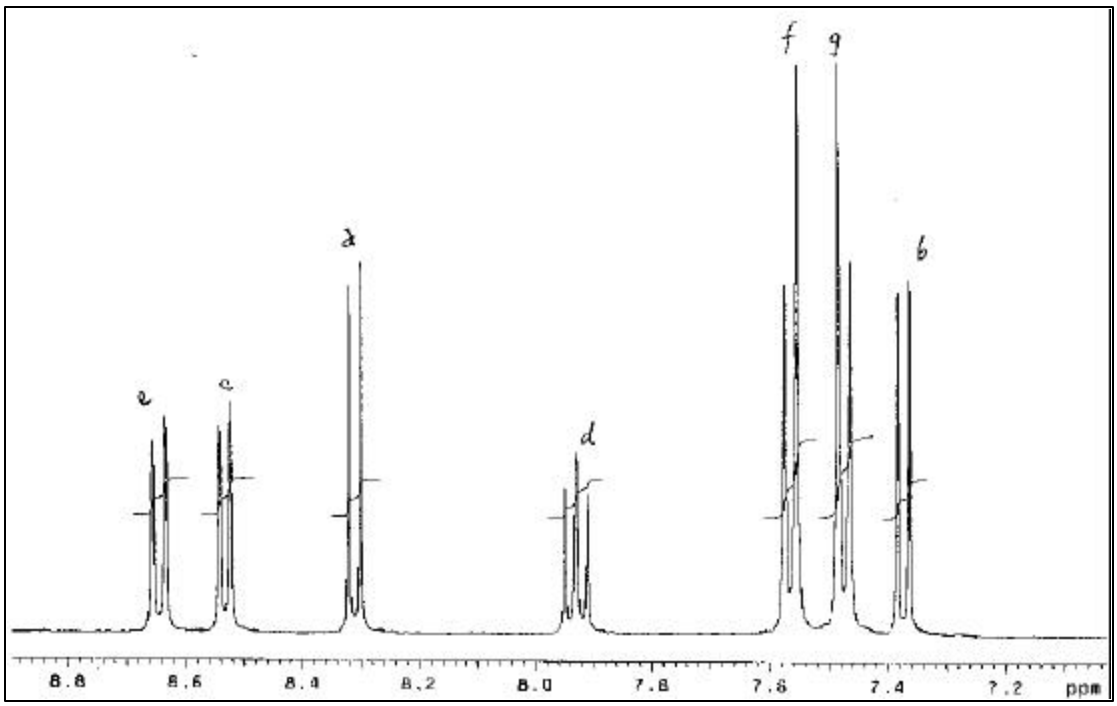

Figure 4.1.21 ^{1}H NMR Spectrum of NDA-SO_2

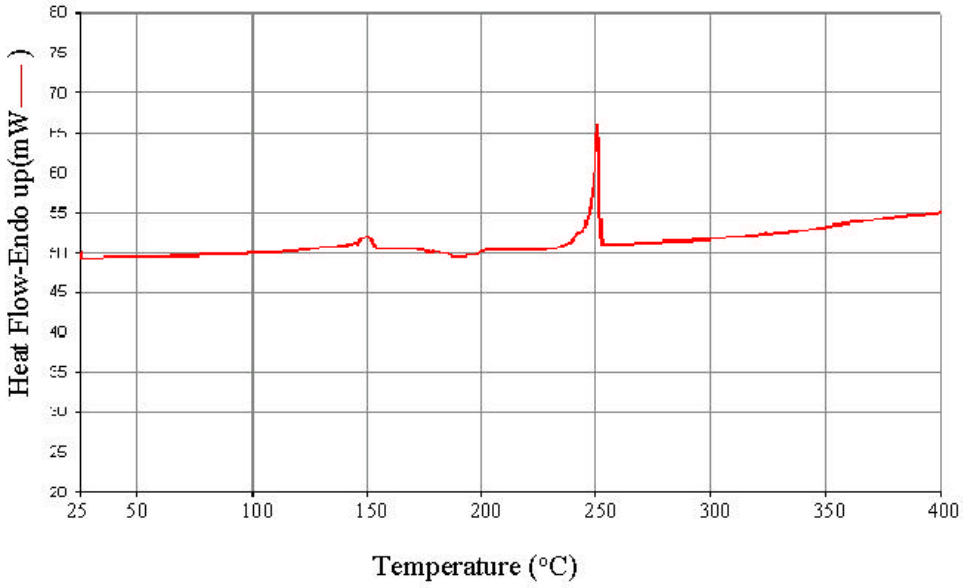

Figures 4.1.22 DSC thermogram of NDA-SO_2 (in nitrogen)

4.2 Polyimide Synthesis

4.2.1 Synthesis and Characterization of Sulfonated Phthalic Anhydride (Five-Membered Ring Polyimides)

Polyimides are well known for their excellent thermal and oxidative stability as well as excellent mechanical properties[227-229]. Due to their wide utility as matrix resins, coatings and adhesives for aerospace and microelectronic applications, a broad range of synthetic routes has been developed in an attempt to facilitate easier and more cost efficient syntheses.

The two most commonly used routes suitable for amorphous polyimide preparation are chemical and solution imidization. Both require the vigorous drying of commercially available solvents, since their water content can potentially upset the monomeric anhydride/diamine stoichiometry and lead to unpredictable lower molecular weights.

Our research group has been interested in developing improved polyimide material systems for some time[2,3,77,240-242]. In an effort to alleviate dianhydride water sensitivity, and subsequent hydrolysis, a method has been developed based on earlier work[227-229,243] which involves the pre-reaction of anhydride moieties with ethanol in the presence of a tertiary amine catalyst[241,242]. The ester-acids formed can be prepared in the presence of commercially available solvents and are very tolerant of water content in both solvents and reactants. Moreover, the ester-acids are more soluble in organic solvents. The factors necessary for the formation of high molecular weight amorphous polyimides via this route were recently reviewed by several different goups. It was shown

227. Feger, C., Khohasteh, M.M. and McGrath, J.E. (Eds.) *Polyimides: Materials, Chemistry and Characterizations*; Elsevier, **1989**.

228. Po*lyimides*, Wilson, D., Stenzenberger, H.D. and Hergenrother, P.M. (Eds.); Chapman and Hall: New York, **1990**.

229. Horie, K. and Yamashita, T., *Photosensitive Polyimides: Fundamentals and Applications*, Technomic, **1995**.

240. Tan, B. *Ph.D. Thesis*, Virginia Tech, **1997**.

241. Moy, T.M. *Ph.D Thesis*, Virginia Tech., **1993**.

242. Moy, T.M., DePorter, C.D. McGrath, J.E. *Polymer*, **1993**, 34(4), 819.

243. Ghosh, M.K., Mittal, K.L. (eds.) *Polyimides: Fundamentals and Applications*; Marcel Decker: **1996**.

that ester-acids are conveniently prepared from the monomeric dianhydrides in the presence of ethanol. At an elevated temperature, the dianhydride is formed along with the ethanol removal, followed by subsequent attack of an aryldiamine and finally cyclic imide formation.

The synthetic method usually used to prepare a series of sulfonated polyimides and their controls based on phthalic anhydrides was the ester-acid solution imidization route as shown in Scheme 4.2.1. This method was chosen, as discussed above, because it is known to afford fully imidized, hydrolytically stable polyimides[243]. Indeed, the benefits of using the ester-acid route were evident during this research: in almost all cases, fully imidized soluble high molecular weight polyimides were obtained.

A further advantage of this method was its simplicity. The reaction solvents did not have to be purified to remove trace amounts of water prior to use. A binary mixture of solvents was used for the reactions, NMP and o-DCB (4/1 vol/vol) with the o-DCB acting as an azeotroping agent. The system was found to be very effective in removing water during reaction as evidenced in the syntheses of all the polymers. Using 1 : 1 stoichiometry of the dianhydrides and the diamines, high molecular weights were obtained as judged by gel permeation chromatography (GPC) and intrinsic viscosity (IV).

A series of wholly imidized high molecular weight polyimides having controlled degrees of pendant sulfonic acid ($-SO_3H$) functionalities in their polymer backbones were prepared using various anhydrides and unsulfonated and sulfonated aromatic diamines[244]. The monomers utilized are depicted in Figure 4.2.1. All possible combinations of the anhydrides and the diamines were tried as long as they were soluble in reaction media. In most cases, unsulfonated homopolyimides were synthesized as a control to enable comparison of the physical properties.

In the first part of this dissertation research, commercially available dianhydrides and diamines were used due to their convenience, ready availability, and low cost. The monomers were chosen based on the literature review.

---

243. Meyer, G.W. *Ph.D. Thesis*, Virginia Tech, **1995**.; Meyer, G.W., McGrath, J.E. *US Patent*, 5,493,002 (to VPI and State University), **1996**; Meyer, G.W., Pak, S.J., Lee, Y.J., and McGrath, J.E. *Polymer* **1995** *36*(11), 2303; Meyer, G.W., Glass, T.E., Grubbs, H.J. and McGrath, J.E. *J. Polym. Sci. Part A: Polym. Chem*. **1995**, 33, 2141.

244. Gunduz, N. and McGrath, J.E. *Polym. Preprt., Am. Chem. Soc.* **2000** *41*(1), 182.

Since the aim of this research was to obtain highly sulfonated, fully cyclized, soluble, good film forming polymers, a series of high molecular weight homo- and co-polyimides having controlled degrees of pendant sulfonic acid groups were prepared. This section details the molecular weights and thermal characteristics of a number of sulfonated and unsulfonated five-member ring polyimides (phthalic anhydride-based), which will satisfy (some of) the requirements of proton-ion conducting membranes for fuel cell applications

Dianhydrides

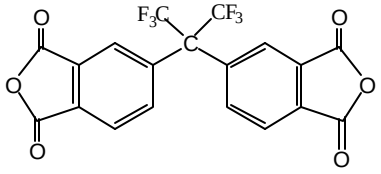

4,4′-hexafluoroisopropylidenebis (phthalic anhydride)
6FDA

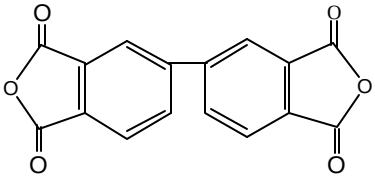

3,4,3 ′,4′-Biphenyltetracarboxylic dianhydride
BPDA

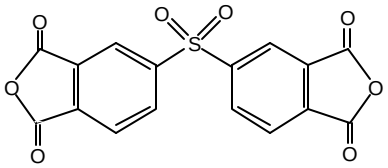

3,3′,4,4′-Biphenylsulfonetetracarboxylicdianhydride
BPSDA

Diamines

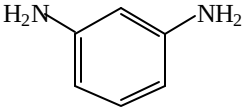

1,3-Phenylenediamine
m-PDA

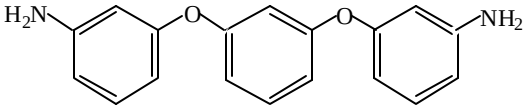

1,3-Bis(3-aminophenoxy)benzene
(APB)

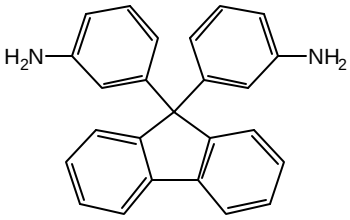

4,4'-(9-Fluorenylidene)dianyline
(FDA)

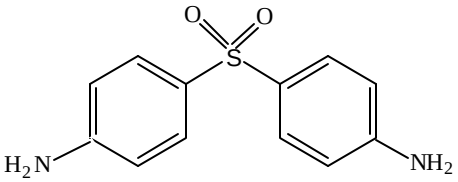

3,3'-Diaminodiphenyl sulfone
(*p*-DDS)

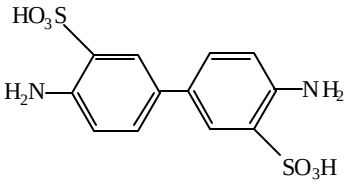

4,4'-diamino-2,2'-biphenyldisulfonic acid
BDA

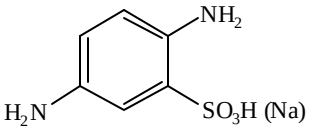

1,4-Diaminobenzene sulfonic acid
(pPDA-SO_3H)

Figure 4.2.1 Monomers used for synthesis of sulfonated five-membered ring polyimides

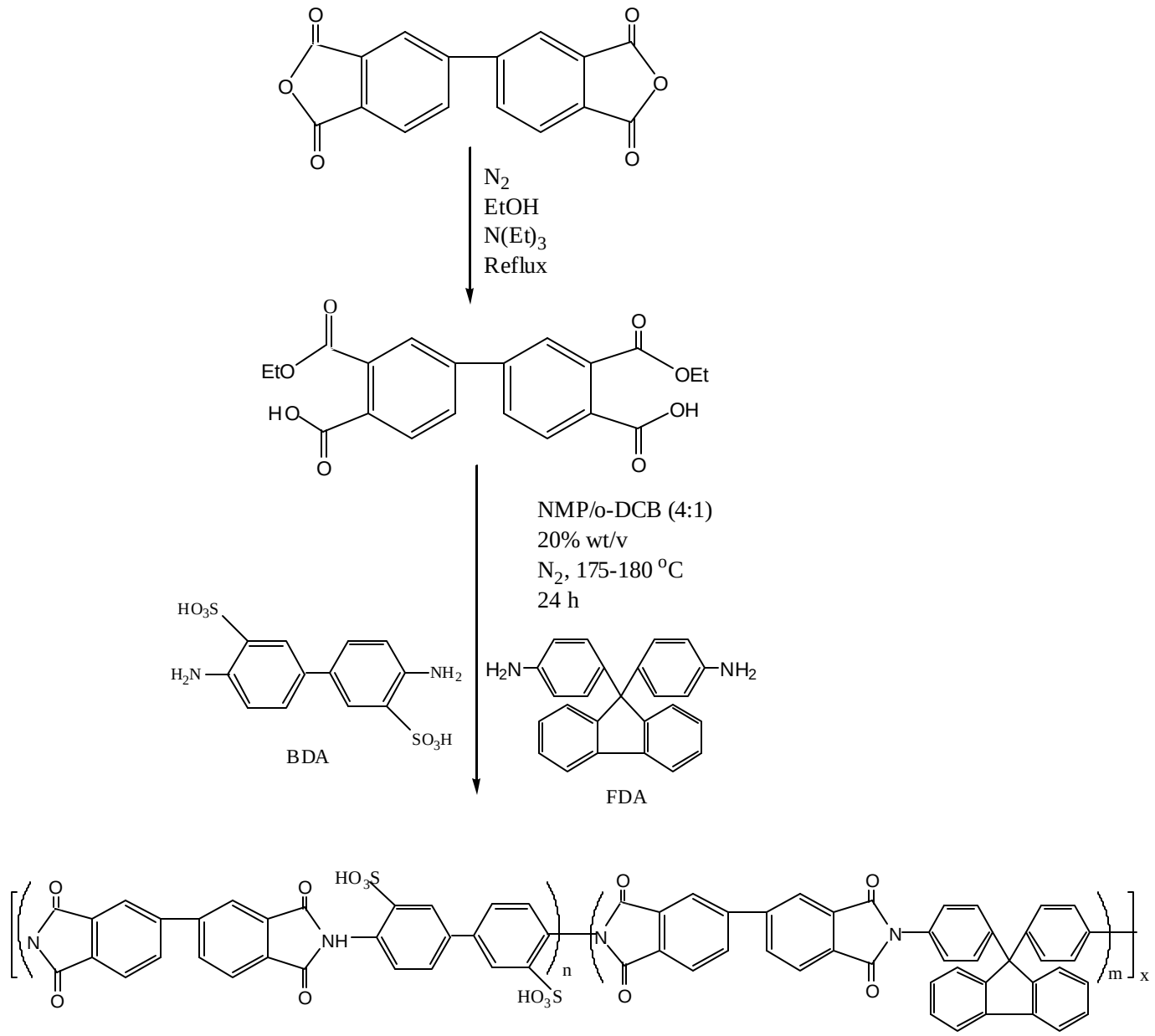

Scheme 4.2.1 Ester-acid route for sulfonated BPDA based polyimides

4.2.1.1 Hexafluoroisopropylidene Dianhydride (6FDA) Based Sulfonated Polyimides

Polyimides containing 6FDA were of interest due to their general properties of being rigid and having good solubility. The bulky structure of the two $-CF_3$ groups present in 6FDA and its kinked structure will hinder close packing between adjacent polymer chains. This monomer is also rigid due to the steric hindrance between fluorine atoms and aromatic protons ortho to the isopropylidene linkage which restricts free rotation of about $(CF_3)_2C-C(Ar)$ bond. In addition, 6FDA is known to impart solubility to polyimides.

Incorporation of p-PDA-SO_3H monomer in 6FDA-based polyimides was utilized as a strategy for increasing the polymer's hydrophilicity which is a must requirement to increase the water sorption in the polyimide membrane resulting in higher proton-ion conduction. Initial preparation of a copolyimide involved a mole ratio of 90:10 with respect to m-PDA:p-PDA-SO_3H. The ester acid solution imidization route was performed after rigorously purifying the monomers by vacuum sublimation (m-PDA) or drying under vacuum at 180 ^oC (6FDA). During the reaction, the increasing viscosity of the reaction mixture indicated the progress of the polymerization and imidization. The reaction solution remained clear during 24 hours. Furthermore, subsequent cooling to room temperature also resulted in a clear, viscous, dark brown solution. A fibrous polymer was obtained after precipitating the polymer solution into an excess amount of methanol.

To study the effect of degree of sulfonation, five additional copolyimides were prepared using 6FDA/m-PDA/p-PDA-SO_3H where the sulfonated diamine (p-PDA-SO_3H) content was increased to 25, 40, 50, 60, 75 and 90 mole % respectively. All the copolymerizations were conducted using the ester-acid solution imidization route in a similar manner, first forming the diester- diacid of the 6FDA and then incorporating the sulfonated diamine. In all cases, the sulfonated diamine monomer was allowed to oligomerize with the diester-diacid of the dianhydride for 2-3 hours, before the second, unsulfonated diamine was charged into the reaction flask. The idea behind this was that the sulfonated diamine having an electron-withdrawing —SO_3H group which is both

ortho- and meta- to the two amine groups might be a less reactive, weaker nucleophile than the unsulfonated diamine in attacking the carbonyl carbon of the dianhydride.

The solution imidization yielded identical results for each copolyimide trial: the materials were soluble both at imidization temperatures, and upon cooling. However, it was observed that increased sulfonic acid content, due to an increase of mole percent of sulfonated diamine incorporated, resulted in higher polymer solution viscosities.

It was observed that increase of sulfonation content, in other words, sulfonated monomer mole percent, increases the solubility. While unsulfonated copolymers of 6FDA-based polyimides, namely 6FDA/p-PDA/m-PDA having a mole % ratio of 80:20 with respect to p-PDA:m-PDA resulted in a cloudy solution upon cooling, which provided evidence for insolubility[245]. Even an increase of the kinked m-PDA content up to 40 % yielded identical results: small amounts of the materials were insoluble and precipitated upon cooling. However, in the case of sulfonated analogues of these 6FDA-based copolyimides, even with 90 mole % of p-PDA-SO_3H content completely soluble both at imidization temperatures and also upon cooling, were obtained.

Unsulfonated homopolyimide polymer based on 6FDA/m-PDA and completely sulfonated homopolyimide based on 6FDA/p-PDA-SO_3H were also prepared as controls by forming the ester-acid precursor, followed by the addition of diamine and then solution imidization.

The conversion of the poly(amic) acids to the fully cyclized polyimides were monitored by FTIR[246,248]. Cyclodehydration was confirmed by the appearance of absorption modes at approximately 1785, 1728, 1370, and 733 cm^{-1} due to the symmetric C=O, asymmetric C=O and C–N stretching, and ring deformation respectively as shown in Figure 4.2.2. These wavelengths correspond to previously reported imide ring

245. Dunson, D. *Ph.D Thesis*, May **2000**.

246. Woodard, M.H., Rogers, M.E., Brandom, D.K., Wilkes, G.L. and McGrath, J.E. *Polym. Prep*., 33 (2), 333 (**1992**).

247. Oishi, Y., Takado, H., Yoneyama, M., Kakimoto, M. and Imai, Y. *J. Polym. Sci.: Part A: Polym. Chem*., 28, 1763 (**1990**).

248. Silverstein, R.M., Bassler, G.C. and Morrill, T.C. "*Spectroscopic Identification of Organic Compounds*", 5th Edn., John Wiley & Sons, New York, (**1991**).

adsorptions[249]. Complete cyclization was also evident by the lack of amide C=O (1640 cm^{-1}) and N–H (1550 cm^{-1}) peaks.

Elemental analysis was also used to check if a proper amount of sulfonated and unsulfonated diamine monomers were incorporated into the polymer. Table 4.2.1 represents the calculated and experimental elemental analysis data for a couple of sulfonated polyimides from both series of sulfonated polyimides based on 6FDA/m-PDA and 6FDA/DDS.

Table 4.2.1 Elemental Analysis Results of Sulfonated Polyimide Polyimides

Polymer	Elemental analysis									
	C		H		F		N		S	
	calc.	found.	calc.	found.	calc.	found.	calc.	found.	calc.	found.
6FDA/m-PDA25	56.17	55.55	2.70	2.36	23.14	23.65	4.54	5.21	1.62	1.98
6FDA/m-PDA50	53.77	52.55	2.17	2.50	20.41	21.17	5.02	5.74	2.87	3.02
6FDA/DDS25	56.17	58.02	3.32	3.47	21.70	22.17	5.20	6.33	3.70	4.16
6FDA/DDS50	52.21	53.41	2.25	2.43	18.14	17.79	4.46	5.11	6.10	5.55

Since the main goal of this research was to prepare sulfonated high molecular weight polyimide membranes to be used as proton exchange membranes in fuel cells, only the film form of the polymers was of interest. Moreover, for all the polymers synthesized in this research, only one to one (1:1) stoichiometry with respect to the mole percent of dianhydride and the mole percent of the diamine(s) were used to be able to obtain maximum molecular weight, and thus, the author did not intend to use any endcapper, monofunctional monomer, to control the molecular weight of the polymers.

249. Arnold, C.A., Summers, J.D., Chen, Y.P. and McGrath, J.E. *Polymer*, 30, 986 (**1989**); Summers, J.D., Arnold, C.A., Chen, Y.P. and McGrath, J.E. *Polym. Prepr*. 27 (2), 403 (**1986**); Summers, J.D., *Ph.D Thesis*, Virginia Tech, 1987; Summers, J.D., Arnold, C.A. and McGrath, J.E. *Polym. Eng. Sci*., 29 (20) 1413, **1989**.

Since good film forming characteristics of these polymers is one of the critical needs of the proton-ion conducting membranes, synthesizing polymers with high molecular weights, to provide single piece, free-standing films, needed to be achieved. This was one of the immediate objectives of this research.

Film Formation

Free-standing sulfonated 6FDA-based polyimide membranes used in this study were prepared either by a solution casting method or by spin casting. First, the polymers were dissolved in DMAc affording about 20 % w/v concentrations, filtered using disposable syringe and Acrodisc glass filters, and then carefully cast onto a clean glass plate using a Doctor's blade. The film was then heated gradually from room temperature to 150 ^{o}C in 18 hours on a hot plate covered with a glass top under a nitrogen atmosphere supplied by a gas inlet. Using a programmable temperature controller (Omega CN2011), the hot plate temperature was gradually ramped up to provide heating according to the following schedule: 25 ^{o}C to 100 ^{o}C in 6 hours, at 100 ^{o}C for 3 hours, 100 ^{o}C to 150 ^{o}C in 6 hours, at 150 ^{o}C for 3 hours. The film was carefully peeled from the glass substrate under slowly running water, and kept in a beaker filled with deionized water to remove any extractable DMAc from the film. Finally, it was dried under vacuum at 150 ^{o}C for 24 hours. The film form of the polymers was used for all the characterizations unless otherwise mentioned.

Molecular weight characterization of the homopolymers and the copolymer series was conducted using gel permeation chromatography (GPC) and intrinsic viscosity (IV). Absolute molecular weight measurements from GPC were conducted with a Waters 2690 Separation Module equipped with a differential refractometer detector and an on-line differential viscometric detector (Viscotek T60A) coupled in parallel. NMP containing 0.02 M P_2O_5 was used as a mobile phase. Samples prepared to known concentrations (~ 4 mg/ml) were dissolved in the polar solvent NMP ((HPLC grade)) containing 0.02 M P_2O_5 and measurements were performed at 60 ^{o}C. Figure 4.2.3 shows a typical raw GPC chromatogram for a high molecular weight 50 % sulfonated 6FDA/m-PDA/p-PDA-SO_3H copolyimide. Intrinsic viscosities of the polymers were also measured in NMP at 25 ^{o}C using a Cannon Ubbelohde viscometer.

Tables 4.2.2 and 4.2.3 represent the molecular structures of the sulfonated 6FDA/m-PDA/p-PDA-SO_3H and 6FDA/DDS/p-PDA-SO_3H polyimides, and their molecular weight characterization data obtained from GPC and intrinsic viscosity. The very first column in the table indicates the composition of the polymer, the second one is the mole percent of the sulfonated diamine monomer, while the third is the composition ratio of unsulfonated to sulfonated block. For example, 6FDA/m-PDA-50 represents 6FDA-based copolyimide with m-PDA unsulfonated diamine monomer. Numbers next to the m-PDA (Table 4.2.2) and the DDS (Table 4.2.3) show their mole percent incorporation into the polymer backbone.

Very high molecular weight was obtained for the unsulfonated homopolymer 6FDA/m-PDA polyimide as indicated in Table 4.2.2. However, the molecular weights decreased with the increase of sulfonated diamine content in the polymer backbone. This may be due to the lower reactivity of the sulfonated diamines toward the carbonyl carbon of the dianhydride, as compared to the unsubstituted analogues. Electron-withdrawing SO_3H groups may decrease the basicity of the amine nitrogen and thus reduce its nucleophilic reactivity towards the carbonyl carbon resulting in lower molecular weight polymers.

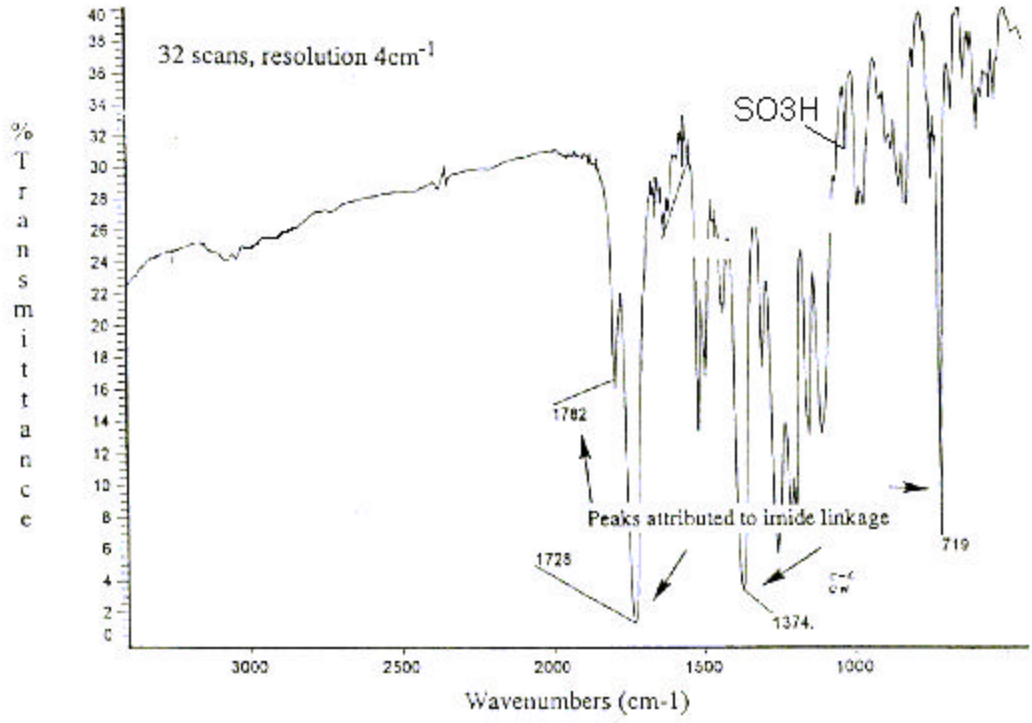

Figure 4.2.2 FTIR of High Molecular Weight 50 % Sulfonated 6FDA/m-PDA/p-PDA-SO_3H Showing Absorptions Due to Cyclic Imide Functionalities.

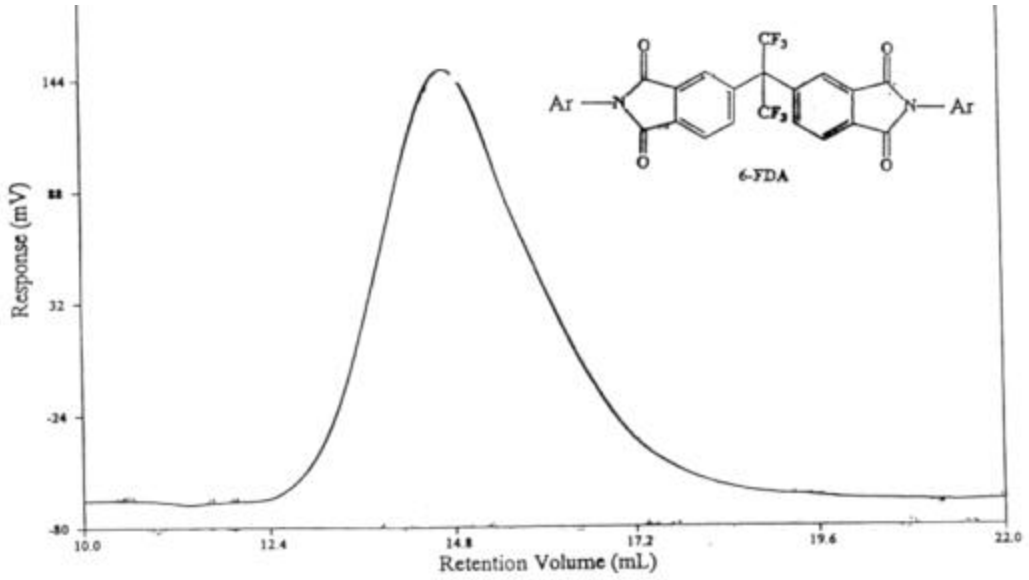

Figure 4.2.3 Typical Raw GPC Chromatogram Obtained for a High Molecular Weight 50 % Sulfonated 6FDA/m-PDA/p-PDA-SO_3H Copolyimide.

Table 4.2.2 Chemical Structure and Molecular Weight Characterization of the Sulfonated 6FDA/m-PDA -based Polymers in NMP

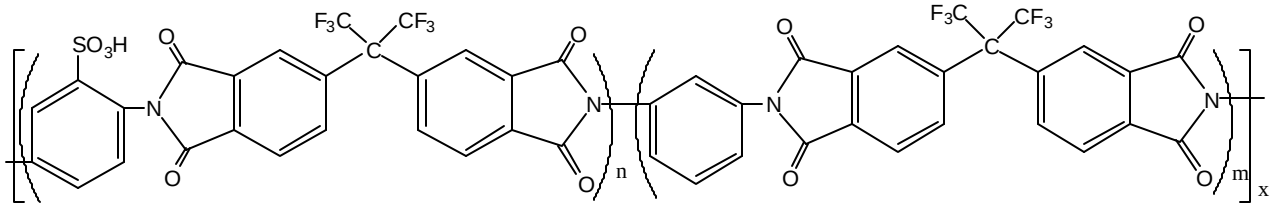

Polymer	Sulfonated diamine (mol %)	m/n	$\langle M_n \rangle \times 10^{-3}$ g/mol[a]	$\langle M_w \rangle \times 10^{-3}$ g/mol[a]	$\langle M_w \rangle / \langle M_n \rangle$[a]	[ç] (dL/g)
6FDA/mPDA-100	0	10/0	82	171	2.08	1.42
6FDA/mPDA-90	10	9/1	53	104	1.96	1.37
6FDA/mPDA-75	25	7.5/2.5	46	97	2.1	1.53
6FDA/mPDA-60	40	6/4	38	84	2.2	1.70
6FDA/mPDA-50	50	5/5	37	74	2.0	1.95
6FDA/mPDA-40	60	4/6	31	59	1.90	2.17
6FDA/mPDA-25	75	2.5/7.5	25	49	1.96	2.55
6FDA/mPDA-10	90	1/9	17	30	1.79	2.61
6FDA/mPDA-0	100	0/10	13	25	1.88	2.87

Table 4.2.3 Chemical Structure and Molecular Weight Characterization of the Sulfonated 6FDA/DDS-based Polymers in NMP

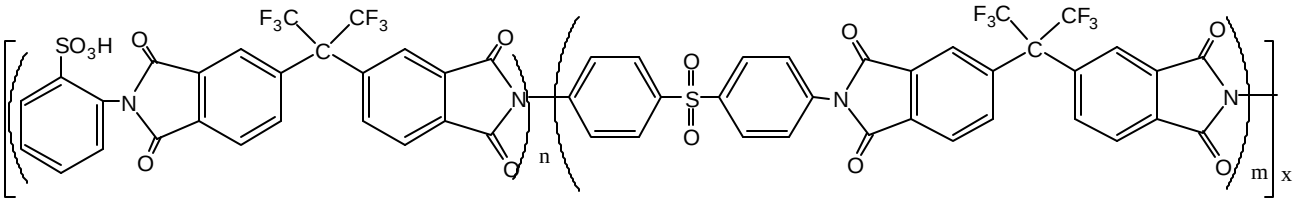

Polymer	m/n	Sulfonated Diamine Mol %	$<M_n>$ x 10^{-3} g/mol	$<M_w>$ x 10^{-3} g/mol	$<M_w>/<M_n>$	[ç] (dL/g)
6FDA/DDS-100	10/0	0.00	63	126	2.0	1.21
6FDA/DDS-90	9/1	10.00	51	103	2.02	1.22
6FDA/DDS-75	7.5/2.5	25.00	41	82	1.99	1.33
6FDA/DDS-60	6/4	40.00	37	74	1.99	1.54
6FDA/DDS-50	5/5	50.00	32	64	1.99	1.85
6FDA/DDS-40	4/6	60.00	29	61	2.1	2.17
6FDA/DDS-25	2.5/7.5	75.00	28	55	1.98	2.72
6FDA/DDS-10	10/90	90.00	23	46	1.99	2.88
6FDA/DDS-0	0/100	100.00	13	25	1.88	2.94

Thermal stability

The solution-cast polyimide membranes were thermally analyzed to study the effect of the degree of sulfonation on the thermal properties of sulfonated 6FDA-based polymers. The preliminary assessment of the thermooxidative stability of these polymers was evaluated by thermogravimetry using a Perkin-Elmer TGA7. The dynamic TGA scans were collected for about 10 mg of polyimide membranes from 30 to 800 ^{o}C in air at a heating rate of 10 ^{o}C/min as shown in Figure 4.2.4.

The primary factors that contribute to heat resistance of polymers are primary and secondary interactions, resonance stabilization, molecular symmetry and the mechanism of bond cleavage (21). As a class, unsulfonated polyimides based on both 6FDA/m-PDA and 6FDA/DDS show excellent resistance to thermal degradation as be judged by the 5 % weight loss which occurred above 500 ^{o}C. However, TGA thermograms of the sulfonated polyimides exhibited so-called "two-step" degradation. The first step in the degradation was attributed to the decomposition of sulfonic acid groups in the sulfonated block at around 350 ^{o}C. The second step was due to the decomposition of the polymer backbone above ca. 500 ^{o}C. Similar results were obtained for sodium-sulfonated polymers both within our research group[223,225] and in other research groups[250-252]. The TGA thermograms indicated that the initial weight losses were greater for polymers with higher sulfonation degrees. However, the onset temperature of the first weight loss temperature was independent of the degree of sulfonation (within +/- 2 ^{o}C) and was observed at about 285 ^{o}C.

It was obvious that the 5% weight loss temperature decreased as the content of ionic groups therein increased. Although, the amount of sulfonic acid groups introduced into the polymers significantly affected their thermal stability, all the polymers tested were stable up to 290 ^{o}C both in air and nitrogen atmosphere, indicating good thermal stability of the materials.

---

250. Bailly, C., Williams, D.J., Karasz, F.E., McKnight, *Polymer*, **1987**, *28*, 1987.

251. Noshay, A. and Robeson, L.M., *J. Appl. Polym. Sci*. **1976**, 20, 1885.

252. Jin, X., Bishop, M.T., Ellis, T.S. and Karasz, F.E., *Br.Polym. J*., **1985**, 17, 4.

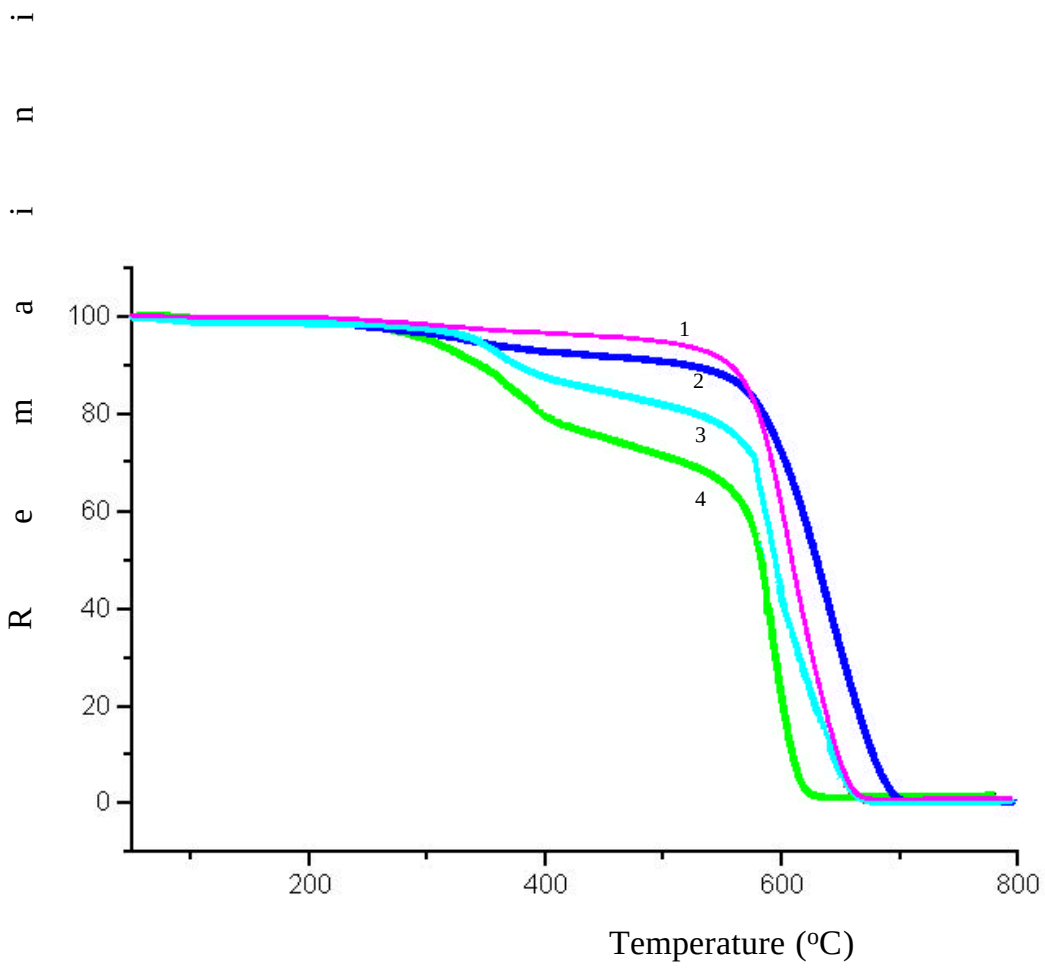

Figure 4.2.4 Thermogravimetric analysis of sulfonated 6FDA-based polyimides in air.

DSC scans were run at a heating rate of 10 °C/min in nitrogen. The control, unsulfonated 6FDA/m-PDA polyimide, yielded a T_g of 294 °C. Except for the 10% sulfonated 6FDA/m-PDA/p-PDA-SO_3H polyimide (Figure 4.2.5), no glass transition temperatures were observed for sulfonated copolymers in the temperature range of 30-320 °C. This indicated that the strong intermolecular interactions led to a stiffer polymer segment and the glass transition temperatures were higher than 320 °C. Compared to the unsulfonated control, the sulfonated polyimide having 10% pendant sulfonic acid functionality possessed a higher glass transition temperature (T_g). Although no T_g's were observed for polyimides having higher degrees of sulfonation to support this phenomenon, similar observations were made by others with different types of sulfonated polymers including s-PEEK[251,252], s-styrene[253], and carboxylic acid substituted

251. Wang, F., Chen, T. and Xu, *J.*, *Macromol. Chem. Phys.* 199, **1998,** 1421-1426

poly(ether ether)ketone[254]. It has been accepted that, besides chain rigidity of the polymer backbones, intermolecular interactions such as hydrogen bonding and ionomer effects are important factors in increasing the T_g of polymers[255]. For sulfonic acid-functionalized polyimides, based on two pairs of T_g values, it is fair to say that the introduction of pendant sulfonic acid groups increased intermolecular interaction through polar ionic sites and increased hindrance to chain rotation. These two factors resulted in the increase in T_g values.

As expected, incorporating in 6FDA containing polymers the much more rigid diaminodiphenylsulfone rather than m-phenylenediamine, produced much higher glass transition temperature materials (**294** ^{o}C for 6FDA/m-PDA compared to **353** ^{o}C for 6FDA/DDS; **301** ^{o}C for 10% sulf. 6FDA/m-PDA/PDA-SO_3H compared to **362** ^{o}C for 10% sulf. 6FDA/DDS/PDA-SO_3H).

The absence on any exothermic transition also suggests that sulfonated polyimides do not form sulfone groups by crosslinking reactions between pendant sulfonic acid groups and phenyl protons during heating.

252. Bailly, C., Williams, D.J., Karasz, F.E., MacKnight, W. *Polymer*, **1987**, *28*, 1987.

253. Shultz, A.R., personal communication.

254. Koch, T., Ritter, H., *Macromolecules* 28, **1995**, 4806.

255. Guiver, M.D., Robertson, G.P., and Feley, S., *Macromolecules* 28, **1996**, 7912.

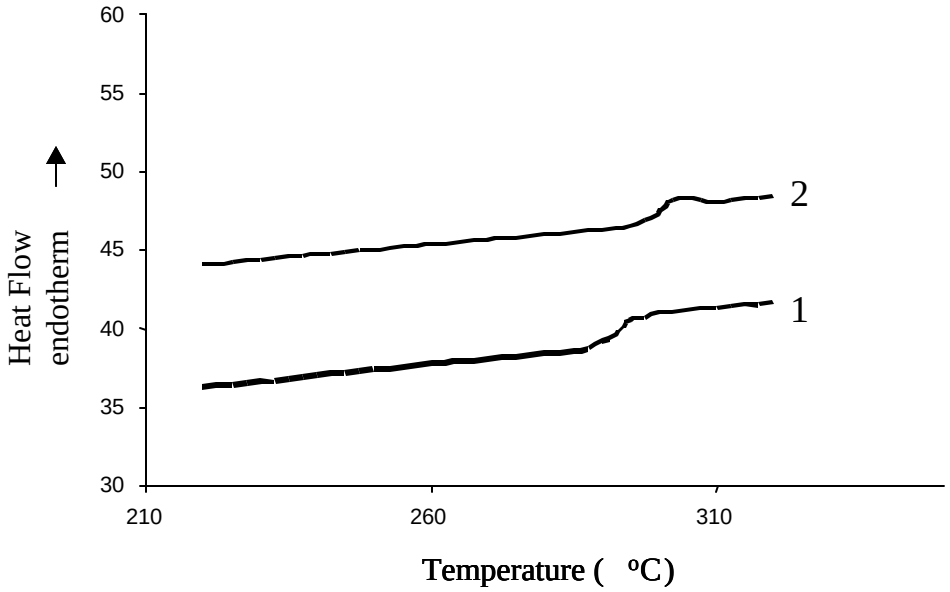

Figure 4.2.5 DSC of (1) 6FDA/m-PDA homopolymer and (2) 10 % sulfonated 6FDA/m-PDA/m-PDA-SO_3H copolymer (in nitrogen, heating rate =10 ^oC/min)

The successful introduction of the sulfonic acid groups was confirmed by the FT-IR spectra of sulfonated polyimides as compared to the control, (Figure 4.2.6), where the strong characteristic peak at 1030 cm^{-1} was assigned to the symmetric stretching of $-SO_3H$. In contrast, there was no peak at 1030 cm^{-1} for the unsubstituted control polyimide membrane prepared from 6FDA dianhydride and m-PDA diamine. The difference in the FTIR spectra indicates the presence of the $-SO_3H$ groups. One can calculate the degree of sulfonation from the peak area assigned to the sulfonic acid groups. If this peak area were properly calibrated, it could provide an analytical technique for measuring the degree of sulfonation[256]. However, other more direct methods, such as titration would appear more reliable[257].

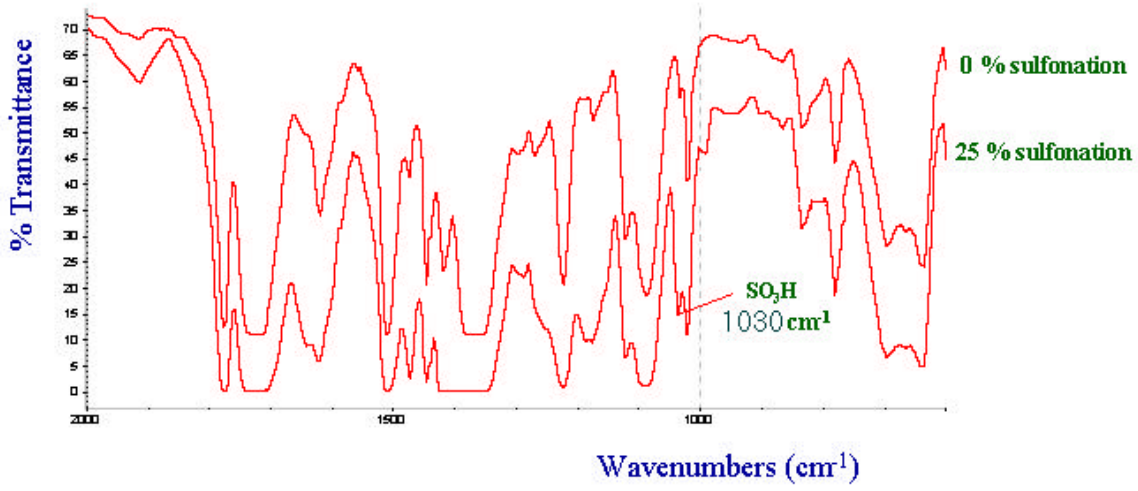

Figure 4.2.6 FT-IR Spectra of Non-Substituted Polyimide Control (top spectrum) and 25% Sulfonated 6FDA/DDS/m-PDA-SO_3H polyimide (bottom spectrum) membranes

256. Johnson, B.L., Tran, C., Yilgor, I., Igbal, M., Wightman, J.P., Lloyd, D.R. and McGrath, J.E., *ACS Polym. Prepr.*, **1983**, 24 (2), 31.

257. Jin, X., Bishop, M.T., Ellis, T.S. and Karasz, F.E., *British Polymer Journal*, Vol 17, No. 1, **1985**

Non-Aqueous Potentiometric Titrations of $-SO_3H$ Groups

The percent sulfonation of the polyimides was confirmed by non-aqueous potentiometric titration of sulfonic acid groups using tetrametyhlammonium hydroxide (TMAH) as a titrant at room temperature. The solution cast sulfonated polyimide membranes were first vacuum dried at 150 ^oC overnight, then dissolved by stirring in DMAc (~ 0.025 g/ 20ml) and then titrated with 0.05 N TMAH in isopropanol that was standardized with dry potassium hydrogen phthalate (KHP) immediately prior to titrating.

The end-point, detected as the maximum of the first derivative of the potential versus titrant volume, was used to calculate the mili-equivalent weight (meq) of available free $-SO_3H$ groups. Figure 4.2.7 shows one example of such a titration curve for 6FDA/DDS/p-PDA-SO_3H50.

It has been commonly recognized that potentiometric titration is a unique tool, one of the most important methods for investigating ion-exchange characteristics[258]. Since the inflection points of potentiometric titration curves for strong acidic and strong basic ion exchangers are obvious, the capacities of the ion-exchangers can be accurately determined from potentiometric titration curves[258]

In this dissertation work, the non-aqueous potentiometric titration method was employed to determine the content of proton-exchange groups ($-SO_3H$) quantitatively in sulfonated five-membered ring polyimides. This value was then used to calculate the Ion-Exchange Capacity (IEC, meq/g, milliequivalent of reactive $-SO_3H$ sites per gram of polymer) of the polyimides containing pendant sulfonic acid groups. Tables 4.2.4 and 4.2.5 represent theoretical and experimental (average of four titrations) IEC values of selected sulfonated 6FDA/m-PDA and 6FDA/DDS based polyimide membranes.

258. Son, W-K., Kim, S.H., Kim, T.I, *J. Polym. Sic. Part B: Polym. Physics*, Vol. 38, **2000**, 3181-88.

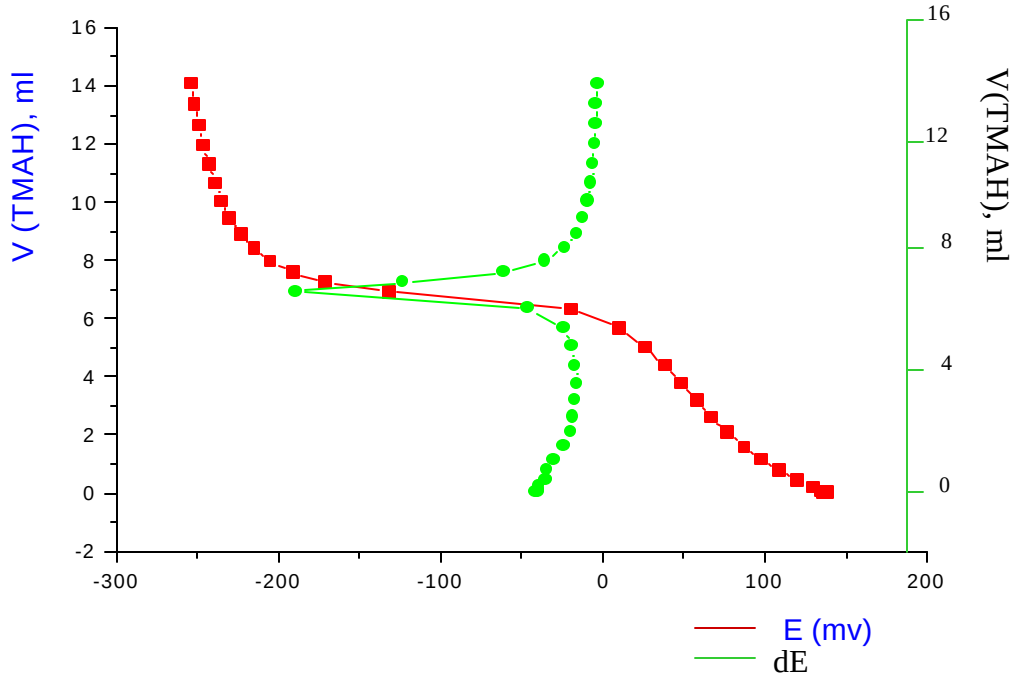

Figure 4.2.7.a Non-aqueous potentiometric titration of a 50 % sulfonated 6FDA/ DDS/ p-PDA-SO_3H polyimide membrane

As can be seen in Figure 4.2.7, only one sharp titration end point was observed indicating a reaction of the strong acid (-SO_3H) and the strong base (TMAH). Assuming that all of the sulfonated monomer was incorporated into the polymer chain, the theoretical ion exchange capacities (IEC) of the sulfonated 6FDA based polyimides in the range of 10-60 % were calculated using Equation 4.2.1. These theoretical IEC are tabulated for both 6FDA/m-PDA/p-PDA-SO_3H (Table 4.2.4) and 6FDA/DDS/p-PDA-SO_3H polyimides (Table 4.2.5). The results clearly indicate that there is a good agreement between the theoretical and experimental IEC values of the sulfonated polyimides that were tested. Furthermore, the above results also prove that the -SO_3H proton conductive groups could be introduced into the polyimide backbone via a sulfonated monomer without any of the side reactions that are often observed with post sulfonation methods[225]. Higher degrees of sulfonation (>60 %) were not tested due to the poor film forming characteristics of the highly sulfonated polyimides as was discussed earlier in this chapter.

Table 4.2.4 Theoretical and Experimental IEC Values of Selected Sulfonated 6FDA/m-PDA Based Polyimide Membranes.

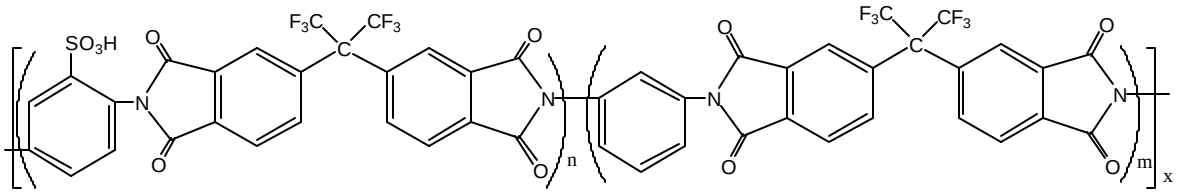

IEC (meq/g) 25 °C	% of Sulfonation [100 x n/ (n+m)])				
	10 %	**25 %**	**40 %**	**50 %**	**60%**
Calculated	0.193	0.46	0.727	0.896	1.06
Experimental*	0.187	0.51	0.721	0.890	1.11

Table 4.2.5 Theoretical and Experimental IEC Values of Selected Sulfonated 6FDA/DDS Based Polyimide Membranes.

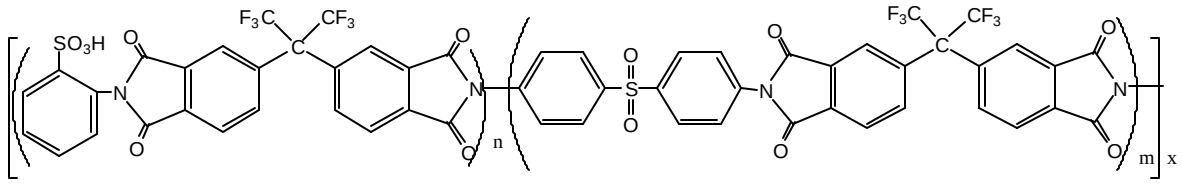

IEC (meq/g) 25 °C	% of Sulfonation [100 x (n/n+m)]				
	10 %	**25 %**	**40 %**	**50 %**	**60%**
Calculated	0.153	0.39	0.63	0.80	0.96
Experimental*	0.150	0.41	0.61	0.88	1.03

Film Formation Characteristics and Water Absorption of 6FDA-Based Sulfonated Polyimides

The primary objective was to determine the film-forming behavior of series of sulfonated and control 6FDA/m-PDA/p-PDA-SO_3H and 6FDA/DDS/p-PDA-SO_3H when cast from their polymeric solutions. Thin films of sulfonated and control 6FDA-based polyimides were made by solution casting or spin casting of 20 % wt/v solutions of the polymers in dimethylacetamide (DMAc). Initial film preparation attempts, which were conducted using N-methyl pyrrolidone (NMP) as the casting solvent, resulted in brittle films.

For thermal and mechanical characterizations, thicker films (in the range of 8-10 mil) were prepared using a doctor blade or a stainless steel mold. In all cases, glass plates were used as substrates. The polyimide solutions were either bladed directly onto the substrate, or a stainles-steel ring of approximately 3´´ diamater was placed on the plate and the solution was evenly poured into it. Using a programmable heating controller, the films were slowly dried under a slow nitrogen flow as described in the experimental section of this dissertation. Finally, they were vacuum dried at 150 ^{o}C for 24 hrs. In general, membranes which were made using the mold were not-bendable and had cracked in a few places around the edge during the drying process, presumably to relieve strain. The membranes prepared by the doctor b;ade technique had better mechanical properties.

The films obtained from the unsubstituted control polyimides, both 6FDA/m-PDA and 6FDA/DDS, produced very tough, bendable yellowish-light brown color films upon drying. Incorporation of low levels of sulfonated diamine monomer (up to 40 %) produced similar film characteristics when cast from ~20 % polymer solution in DMAc using a doctor blade. However, as the degree of sulfonation increased up to 60 %, although the films were not cracked during the drying process, they were less creasable and relatively more brittle than their lower level of sulfonation counterparts. The polyimide membranes having more than 60 % sulfonated diamine in their backbone showed brittle film characteristics. When attempts were made to fold these films to test for creasability, they cracked very easily. An increase in the level of sulfonation also caused an increase in the brown coloration in the dry films. Similar observations were also made by Jin *et al.* for s-PEEK polymers[257].

Incorporation of DDS as an un-substituted unit in 6FDA/DDS/p-PDA-SO_3H polymers produced less brittle, more creasable films as compared to the same level sulfonated 6FDA/m-PDA/p-PDA-SO_3H polymers. However, in all cases, brittleness increased as the level of sulfonation increased.

Since water-uptake measurements use the relative weight increase of the swollen films, they require, for correct comparisons, defect-free films of similar thickness. A small crack in a film, or uncomplete drying of the film may result in untrue water uptake values.

Spin-cast films were prepared using sulfonated and control 6FDA/m-PDA- and 6FDA/DDS-based polyimides. The first step involved dissolving the polymers in DMAc, and the second step was filtering the solutions through nylon syringe filters (0.45ìm porosites) to remove any undissolved particles to obtain films with minimal particle content.

The solutions were applied to 3 "by 3'', clean, dry glass plates, that were then rapidly spun on a spin-casting apparatus. After determining satisfactory spin rates for desired film thickness uniform films were achieved. Spin time for each sample was approximately 2 min. No protection from dust and/or humidity was afforded during spinning. After spin casting, the films were quickly placed under nitrogen on a hot plate and dried in a programmed manner. Following initial solvent removal, the films were kept under vacuum at 150 ^{o}C for 24 hours for subsequent drying. The film uniformity was assessed by both appearance and by quantitative thickness measurements using a micrometer.

The films prepared by spin casting were smooth, clear and of uniform thickness. Moreover, both 6FDA/m-PDA- and 6FDA/DDS-based sulfonated polyimide films prepared by spin casting were more flexible than the films obtained by solution casting. For example, while 75% sulfonated 6FDA/m-PDA/p-PDA-SO_3H polyimide prepared via solution casting using a doctor blade was somewhat brittle the same level sulfonated 6FDA/m-PDA-based polyimide films prepared via spin-coating exhibited creasible film characteristics. Similar observations were made for 6FDA/DDS-based sulfonated polyimides in which the film brittleness decreased with the formation of uniform micron-thick films.

The swelling in water was determined by measuring the water uptake at room temperature using the weight difference of the swollen to dry membrane, relative to the dry weight. The spin-cast films were dried under vacuum at least for 24 hours at 110 ^{o}C prior to the measurements and used for membrane swelling experiments in the following way: 3"-3" dry films were first weighed and then immersed in deionized water (at room temperature) until they reach equilibrium. The membranes were then wipe dried and quickly weighed again. The swelling degree [SW (%)] was determined using the following formula:

$$\text{SW (\%)} = \frac{M_{wet} - M_{dry}}{M_{dry}} \text{ x } 100$$

where M_{wet} and M_{dry} are the weight of the wet and dry membranes, respectively.Tables 4.2.6 and 4.2.7 represent film thickness and water uptakes [SW (%)] of the sulfonated films and their controls as reference. As it can be clearly seen from the tables, incorporation of the sulfonated phenylene diamine monomer containing pendant sulfonic acid ionic groups increased the hydrophilic character of both the 6FDA/m-PDA- and the 6FDA/DDS-based polymer backbones. Therefore, swelling of the sulfonated membranes, exceeded that of their controls. Increasing the diaminobenzenesulfonic acid monomer content from 10% to 90% increased the water uptake from about 7% to 34% in sulfonated 6FDA/m-PDA-based polyimides, and from 7% to 37% in sulfonated 6FDA/DDS-based polyimides. The water uptake increased linerally with increased sulfonation level in both 6FDA-based copolyimide series.

Table 4.2.6 Film thicknesses and water uptakes [SW (%)] of the sulfonated 6FDA/m-PDA/p-PDA-SO_3H

Polymer	Sulfonated Diamine Mol %	Thickness (mm)	SW* (%)
6FDA/m-PDA-100	0.00	0.037	2.0
6FDA/ m-PDA -90	10.00	0.036	4.8
6FDA/ m-PDA -75	25.00	0.034	9.1
6FDA/ m-PDA -60	40.00	0.035	15.9
6FDA/ m-PDA -50	50.00	0.035	19.3
6FDA/ m-PDA -40	60.00	0.034	23.8
6FDA/ m-PDA -25	75.00	0.033	28.4
6FDA/ m-PDA -10	90.00	0.032	33.7
6FDA/ m-PDA -0	100.00	0.032	—

(*) After 24 h immersion in water at R.T.
(—) Could not be measured due to its brittleness in water

Table 4.2.7.b Film thickness and water uptakes [SW (%)] of the sulfonated 6FDA/m-PDA/p-PDA-SO_3H

Polymer	Sulfonated Diamine Mol %	Thickness (mm)	SW* (%)
6FDA/DDS-100	0.00	0.033	1.8
6FDA/DDS-90	10.00	0.032	5.5
6FDA/DDS-75	25.00	0.030	10.1
6FDA/DDS-60	40.00	0.033	15.2
6FDA/DDS-50	50.00	0.029	18.8
6FDA/DDS-40	60.00	0.031	22.3
6FDA/DDS-25	75.00	0.030	29.1
6FDA/DDS-10	90.00	0.029	35.6
6FDA/DDS-0	100.00	0.028	41.2

(*) After 24 h immersion in water at R.T.

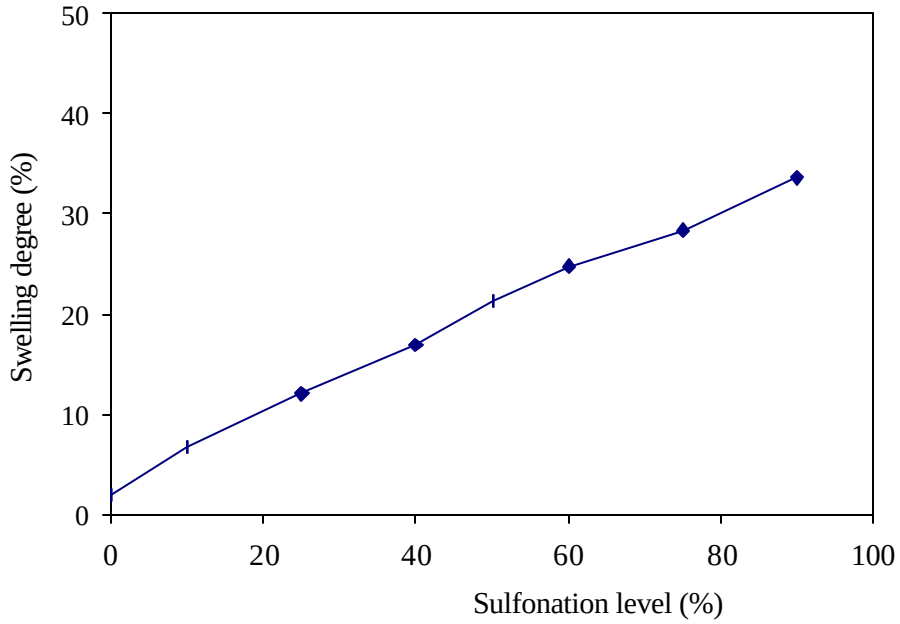

Figure 4.2.7 Swelling degree (%) vs. Sulfonation level (%) for 6FDA/m-PDA/p-PDA-SO_3H after 24 h immersion in water at R.T

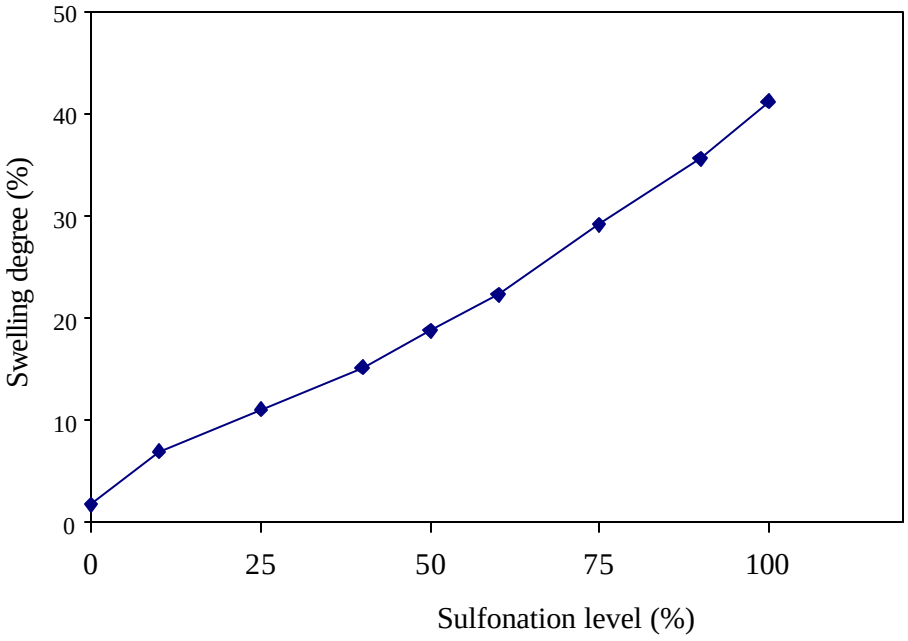

Figure 4.2.7 Swelling degree (%) vs. Sulfonation level (%) for 6FDA/DDS/p-PDA-SO_3H after 24 h immersion in water at R.T

4.2.1.2 Biphenyltetracarboxylic dianhydride (BPDA)-Based Sulfonated Polyimides

BPDA was of interest due to its rigid character that might provide the improved chemical and hydrolytic stability that are required in fuel cell conditions. However, due to the inherently rigid structure of BPDA, previous attempts to synthesize its sulfonated copolyimides using sulfonated diamine (p-PDA-SO_3H) and unsulfonated (m-PDA and DDS) comonomers were failed. The premature precipitation of the polyimides from solution during the reaction resulted in incomplete levels of cyclizations. On the other hand, synthesis of copolyimides of 6FDA with these diamines were successful. The structures and three-dimensional models of 6FDA and BPDA are shown in Figure 4.2.8[(3)]. Clearly, the 6FDA structure is much more bulky and bent than that of BPDA. This increases the solubility of 6FDA copolyimides over that of analogous BPDA copolyimides.

Sulfonated polyimides based on BPDA dianhydride, were expected to yield soluble polymers only with the proper diamines. Flexible diamines that were chosen to promote the solubility were 4,4 -(9-fluorenylidene)dianhydride (FDA), 1,3-bis(3-aminophenoxy)benzene (APB), and 4,4 -diamino-2,2 -biphenyldisulfonic acid (BDA).

The BDA monomer bearing two pendant ionic groups was employed as the source of the sulfonated unit that will provide proton conductivity. The disubstituted monomer was purified by refluxing in water for several hours and then dried in a vacuum oven at 120 ^{o}C for at least 24 hours prior to use[(259)].

Thermogravimetric analysis in air proved the complete dryness of the ionic monomer, which is very important in obtaining high molecular weight polymers. Figures 4.2.9 and 4.2.10 show the three-dimensional projection and TGA thermogram of disubstituted BDA after refluxing in water and drying under vacuum. Incorporation of a second, unsubstituted diamine provided the control of sulfonation level in the final polymer.

High molecular weight polyimides were obtained from an equimolar ratio of diamines and dianhydride using the one-pot ester-acid procedure by initially converting

259. Regis Mercier, *personal communications*.

the dianhydride to the diester-diacid derivative, followed by its reaction with sulfonated and unsulfonated aryl diamines. As mentioned in Part 4.2.1.2 of this chapter, the sulfonated diamine monomer was allowed to oligomerize with the diester-diacid of the dianhydride for 2-3 hours, before the second, unsulfonated diamine was charged into the reaction flask. By varying the mole ratio of sulfonated diamine to unsulfonated diamine, two

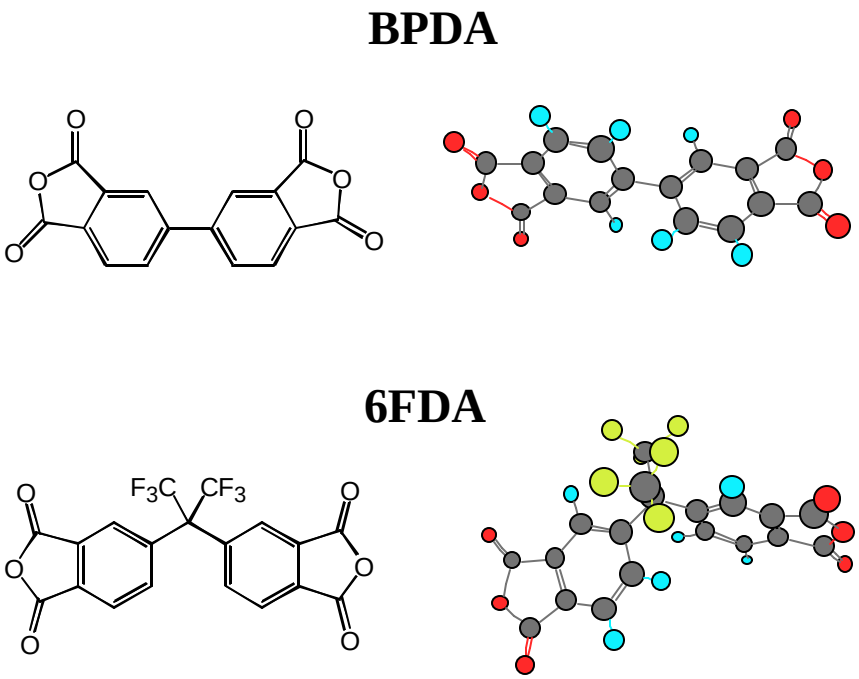

Figure 4.2.8 Three Dimensional Models of BPDA and 6FDA

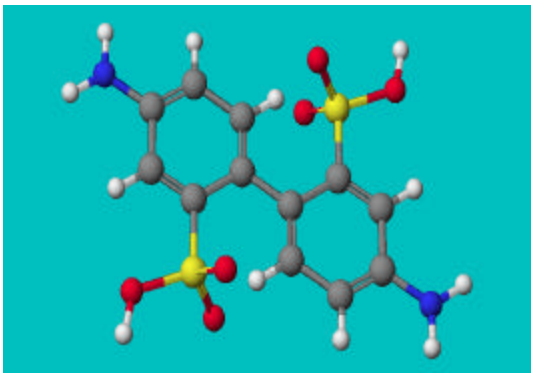

Figure 4.2.9 Three Dimensional Projection of Disubstituted BDA

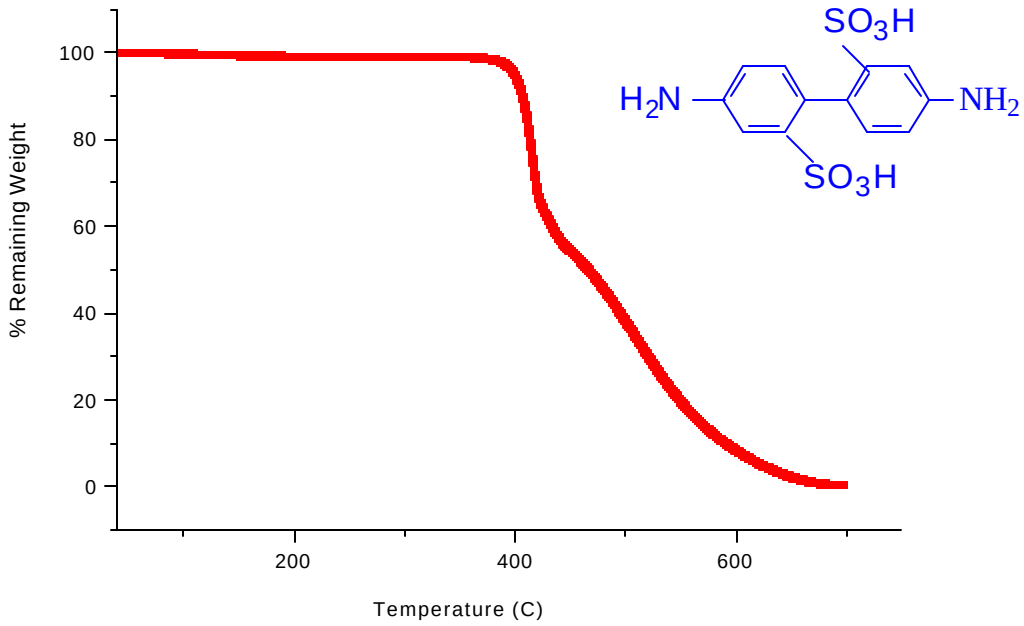

Figure 4.2.10 TGA of BDA in air at a heating rate of 2 ^{o}C/min from 40 to 150 ^{o}C and 10 ^{o}C/min from 150 to 700 ^{o}C

series of BPDA-based polyimides were synthesized at 0, 25, 40, 50, 60, 75 and finally 100 mol % of the BDA. The repeat units of sulfonated BPDA/FDA/BDA and BPDA/APB/BDA polyimides are given in Figure 4.2.11.

Unlike the sulfonated BPDA/m-PDA and BPDA/DDS systems, high temperature solution imidization of both sulfonated BPDA/FDA- and BPDA/APB-copolyimides yielded polymer solutions in which starting monomers and the growing polymer chain were soluble at imidization temperatures. BPDA/APB/BDA polymer solutions remained clear and stirable until they were cooled to ~ 60 ^{o}C. However, a more interesting polymer solution behavior was observed for BPDA/FDA/BDA systems. At the 15% solids level, their viscous polymerization mixtures set to a gel-like mass very quickly and remained unstirable when cooled down. This process was reversible as the gel could be dissolved by heating at ~120 ^{o}C, and reformed when it was removed from the heat to precipitate the solution. Therefore, the polymer solution was slowly dripped into 2-propanol while it was still hot, and reheated several times when gelation occurred. The gel-like mass formation upon cooling seemed to happen faster in solutions of highly sulfonated polymer. In general, higher polymer solution viscosities were observed with lower degrees of sulfonation yielding very fibrous polymers upon precipitation.

The recovered polymer yields were quantitative (>95 %). High molecular weights and unimodal molecular weight distributions with a polydispersity index of about two were obtained in each case, as expected for step-growth polymerizations. Intrinsic viscosities of the polymers were also determined in NMP at 25ºC. Molecular weight characterization results are summarized in Table 4.2.1.2.1 and Table 4.2.1.2.2 for BPDA/FDA/BDA and BPDA/APB/BDA polyimides respectively. It is always a possibility that the molecular weights obtained from GPC and intrinsic viscosities might be influenced by the sulfonated groups. This is no doubt related to enhanced intermolecular associations of the polymer backbones.

Except for the BPDA/APB homopolymer, flexible, clear and yellow-to-light brown films could be prepared by redissolving the control BPDA/FDA homopolyimide and the sulfonated copolymers in DMAC and casting from dilute polymer solutions (8-10 % w/v) directly onto 5" *by* 10" glass substrates at ambient temperature. The cast films were first carefully dried using infrared heat at increasing temperatures under a nitrogen

atmosphere, and then vacuum-dried at 150 ^{o}C for at least a day. By controlling the polymer solution concentration and the cast-film area (substrate area), similar film thicknessess (± 0.05 mm) were obtained. Sulfonated and control polyimide membranes were used for further characterization including structural, thermal, water uptake and hydrolytic stability measurements.

For each of the polymer series, high molecular weights were achieved as judged by GPC and intrinsic viscosity measurements as shown in Tables 4.2.8 and 4.2.9. Formation of tough, creasable films (of polymers with 0-60 % sulfonation level) was good evidence that fully imidized, high molecular weight polymers had been obtained. 75% and 90% sulfonated polymers gave rather brittle membranes. Fully sulfonated material (IEC=2.98 meq/g) was water soluble.

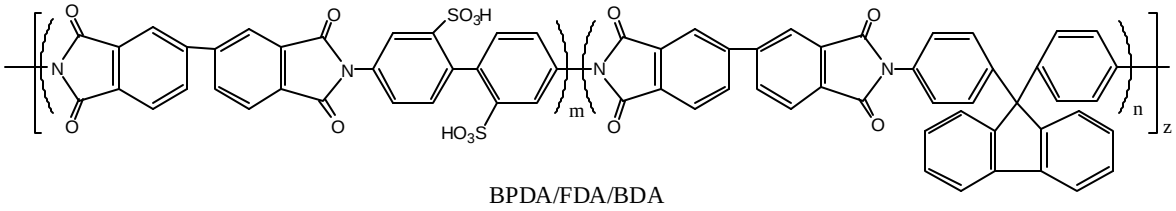

BPDA/FDA/BDA

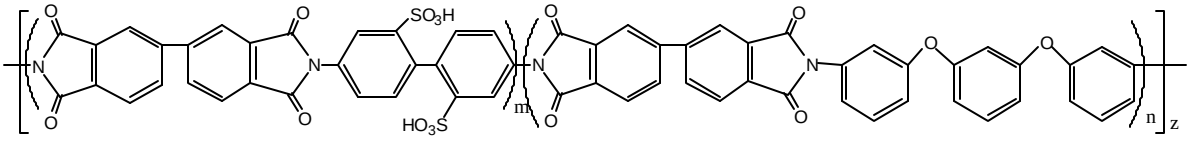

BPDA/APB/BDA

Figure 4.2.11 Chemical structures of sulfonated (1) BPDA/FDA/BDA and (2) BPDA/ DDS/BDA polyimides

Table 4.2.8 Molecular Weight Characterization of the Sulfonated BPDA/FDA- Based Polymers (a)-GPC, in NMP at 60 ^{o}C, 1µl/min; (b) intrinsic viscosity, in NMP at 30 ^{o}C

Polymer	**Sulfonated diamine (mol %)**	**n/m**	**$\langle M_n \rangle$x 10^{-3} g/mol**[a]	**$\langle M_w \rangle$x 10^{-3} g/mol**[a]	**$\langle M_w \rangle$ $\langle M_n \rangle$**[a]	**[ç]**[b] **dL/g)**
BPDA/FDA-100	0	10/0	39.5	82.9	2.1	0.92
BPDA/FDA-75	25	7.5/2.5	32.6	74.9	2.3	1.01
BPDA/FDA-60	40	6/4	29.9	62.8	2.1	1.41
BPDA/FDA-50	50	5/5	30.4	57.8	1.9	1.74
BPDA/FDA-40	60	4/6	23.3	41.9	1.8	1.93
BPDA/FDA-25	75	2.5/7.5	19.0	36.1	1.9	2.30
BPDA/FDA-0	100	0/10	6.2	16.1	2.6	2.55

Table 4.2.9 Molecular Weight Characterization of the Sulfonated BPDA/APB-Based Polymers (a)-GPC, in NMP at 60 ^{o}C, 1µl/min; (b) intrinsic viscosity, in NMP at 30 ^{o}C

Polymer	**Sulfonated diamine (mol %)**	**n/m**	**$<M_n>$x 10^{-3} g/mol**[a]	**$<M_w>$x 10^{-3} g/mol**[a]	**$<M_w>$ $<M_n>$**[a]	**[ç]**[b] **dL/g)**
BPDA/APB-100	0	10/0	52	113	2.1	0.94
BPDA/ APB-75	25	7.5/2.5	33	63	1.91	1.33
BPDA/ APB-60	40	6/4	31	78	2.5	1.47
BPDA/ APB-50	50	5/5	26	74	2.9	1.66
BPDA/ APB-40	60	4/6	14	37	2.6	1.90
BPDA/ APB-25	75	7.5/2.5	17	59	1.90	2.27
BPDA/ APB-0	100	0/10	6.2	16.1	2.6	2.55

FTIR spectra indicated the complete conversion of the poly(amic) acids to the fully cyclized polyimides. The appearance of absorption modes at ~ 1787 (symmetric C=O), ~1729 (asymmetric C=O), 1370 (C–N stretching) confirmed the cyclization (Figure 4.2.1.2). Furthermore, the successful introduction of the sulfonic acid groups through the disubstituted diamine was confirmed by the FT-IR spectrum where the characteristic peak at 1030 cm^{-1} was assigned to symmetric stretching of SO_3H. As shown in Figure 4.2.12, there is no peak at 1030 cm^{-1} for the unsubstituted control material prepared from BPDA and FDA. IR spectra were used to assess the levels of sulfonation, primarily on the basis of the $–SO_3H$ stretching frequency[260]. By calculating the ratio of the intensity of this stretching absorption, due to the sulfonic acid unit (A_{SO3H}), against an internal standard absorption such as that of the C=O ($A_{C=O}$) unit in the chain, the degrees of sulfonation in both series of BPDA-based polyimides were calculated. Elemental analysis was also used to check if a proper amount of sulfonated and unsulfonated diamine monomers were incorporated into the polymer. Figure 4.2.13 presents the degree of sulfonation results obtained from FTIR and elemental analysis.

260. Johnson, B.L., Tran, C., Yilgor, I., Igbal, M., Wightman, J.P., Lloyd, D.R. and McGrath, J.E., *ACS Polym. Prepr*., **1983**, 24 (2), 31.

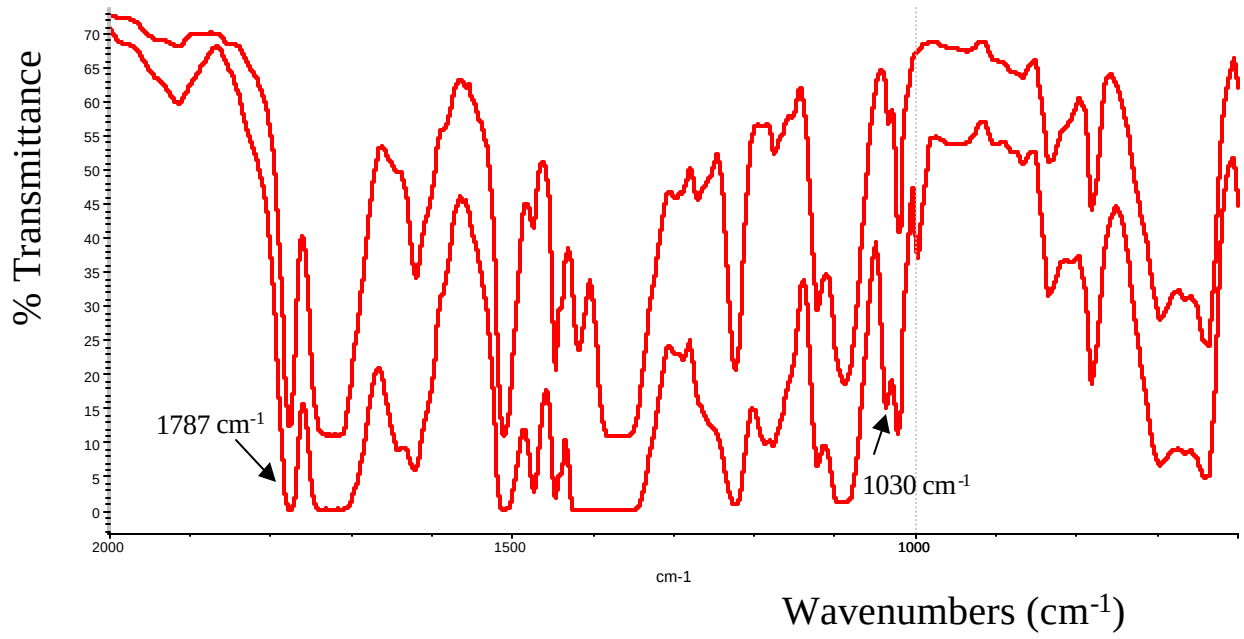

Figure 4.2.12 FTIR Spectra of (1) BPDA/FDA homopolymer
(2) BPDA/FDA/BDA copolymer

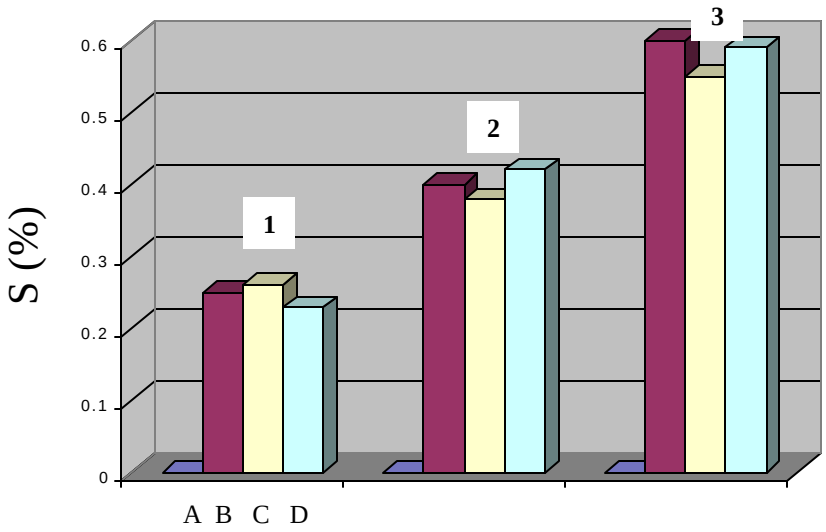

Figure 4.2.13 Degree of sulfonation calculated from (A) Control (no sulfonation), (B)Theory, (C) FTIR and (D) Elemental analysis for (1) 25 % sulfonated, (2) 40 % sulfonated, (3) 60 % sulfonated BPDA/FDA/BDA polyimides.

Non-Aqueous Potentiometric Titrations

Up to 1.5 $-SO_3H$ groups per repeating unit (75 mole % BDA) introduced into the BPDA-based substituted polymer chains, allowed high molecular weight, tough, film-forming materials.

Non-aqueous potentiometric titration, performed for all soluble sulfonated polyimides, was conveniently used to determine the content of proton-exchange groups ($—SO_3H$) quantitatively. The solution cast, well-dried sulfonated BPDA/FDA and BPDA/APB polyimide membranes were dissolved in DMAc and titrated by a standard tetramethyl ammonium hydroxide solution (~0.05N, in iso-propanol) at room temperature. When the samples are dissolved in solvents such as DMAc, NMP or DMSO or in other cases when the solvents consumes a certain volume of titrant during the titration, a volume correction for solvent is called for. This was effected by running a blank titration.

One sharp titration end point was observed in each case indicating a strong acid ($-SO_3H$) and base reaction. The TMAH volume required to neutralize all the acid functionalities was used to calculate the experimental ion exchange capacity (IEC, meq/g) of substituted BPDA/FDA and BPDA/APB at 25-60 mol % of the BDA Assuming that all of sulfonated monomer was incorporated into the polymer chain, the theoretical ion exchange capacity of the sulfonated films was calculated and found to be in good agreement with the experimental data as summarized in Tables 4.2.10 and 4.2.11.

Table 4.2.10 Ion Exchange Capacity of Sulfonated BPDA/FDA-Based Polyimides

n/m	IEC (meq/g)	
	Theory[a]	Titration[b]
25/75	0.82	0.90
40/60	1.32	1.27
50/50	1.65	1.63
60/40	1.99	2.05

Table 4.2.11 Ion Exchange Capacity of Sulfonated BPDA/APB-Based Polyimides

n/m	IEC (meq/g)	
	Theory[a]	Titration[b]
25/75	0.90	1.01
40/60	1.42	1.31
50/50	1.76	1.83
60/40	2.08	2.17

(a) Calculated from [1000/($MW_{sulf.\ block}$ x (mol% of sulf.block) + ($MW_{unsulf.\ block}$ x (mol% of unsulf. block))x 2 x mol % of sulf.

(b) Polymers were dissolved in DMAc, and titrated with TMAH at 25 ^{o}C

All the above results obtain from FTIR, elemental analysis, and non-aqueous titrations indicated that $-SO_3H$ proton conductive groups were successfully introduced into the polymer backbones via a sulfonated monomer without any complication, e.g. side reactions, which is usually the case with post-sulfonation of homopolymers[225].

The thermal stability of the $-SO_3H$ groups was investigated by a combination of non-aqueous potentiometric titration and intrinsic viscosity measurements. For this purpose, the 40% and 60 % sulfonated BPDA/FDA polyimide films were aged at increasing temperatures from 30 to 260 ^oC for an arbitrarily chosen short period of time (30 min) in a conventional air-oven. Aged films were then dissolved in DMAc and titrated with TMAH at room temperature. Table 4.2.12 summarizes the theoretical and experimental IEC values of aged films.

The free acid membrane is the form that would be of greatest interest in proton exchange membranes for fuel cells. After the short time aging, both copolyimide membranes were completely soluble in DMAc, indicating that no crosslinking was initiated upon keeping the films at temperatures up to 220 ^oC. Although the 40%-sulfonated BPDA/FDA/BDA polyimide was still soluble in DMAc upon aging at 240 ^oC, a small portion of the 60 %-sulfonated membrane remained insoluble after stirring for some time.

Moreover, as seen in Table 4.2.12 the table, the content of ionic groups was unchanged by the thermal aging. The stability of pendant ionic groups in the high molecular weight polymer backbone was significant; in fact, these polymeric ionomers showed much better stability than might have been expected from small molecule model experiments.

In this research, a further action was taken in proving the thermal stability of the ionic groups. Molecular weights of the sulfonated aged films were characterized indirectly via intrinsic viscosity measurements and compared with the intrinsic viscosity measurements before aging as shown in Table 4.2.13

The five-membered 40 and 60% sulfonated BPDA/FDA polymer structures were stable for 0.5 hour up to 220^oC in air, as proven by the stable IEC (Table 4.2.12) and intrinsic viscosity values (Table 4.2.13).

Table 4.2.12 Effect of Thermal Aging on Experimental IEC Values for 40 % and 60 % Sulfonated BPDA/FDA/BDA Polyimide Membranes

n/m / Aging Temp.	IEC (meq/g) [a]					
	Theory [b]	23 °C	100 °C	140 °C	180 °C	220 °C
40 / 60	1.42	1.39	1.47	1.38	1.45	1.48
60 / 40	1.76	1.80	1.83	1.71	1.69	1.81

(a) Polymer solutions (in DMAc) were titrated by TMAH after aging at each temperature for 30 min.
(b) Theory Value: Based on starting monomers mol %.

Table 4.2.13 Effect of Thermal Aging on Intrinsic Viscosity for 40 % and 60 % Sulfonated BPDA/FDA/BDA Polyimide Membranes (Intrinsic viscosity at RT in NMP solvent using a Ubbelohde viscometer)

n/m / Aging Temp.	Intrinsic Viscosity (dL/g) $[\eta]^{NMP}_{R.T}$				
	23 °C	100 °C	140 °C	180 °C	220 °C
40 / 60	1.01	1.09	1.1	1.03	1.00
60 / 40	0.95	0.91	0.89	0.92	0.97

Water Absorption of Sulfonated BPDA-Based Polyimides

The solution cast and vacuum-dried thin films (ca. 5 cm x 3 cm x $2x10^{-3}$ cm ± 0.002 mm) were swollen in deionized water at 25 ^{o}C and at 80 ^{o}C and weighed periodically until no more weight increase was observed (24 hours). Swollen weights were obtained by quickly wiping the samples with Kim-wipe tissue and weighing them carefully on a balance. The theoretical IEC (meq/g) values and swollen weights (SW) expressed as a percentage (pg. 213) were presented in Table 4.2.14 for BPDA/FDA/BDA polyimide films and in Table 4.2.15 for BPDA/APB/BDA films.

As expected, the general trend is an increase of swelling with an increase of ionic character of polymer backbone for these sulfonated BPDA based polyimides. The reported water uptake value of a commercially available poly(perfluorinated) polymer electrolyte membrane, Nafion™, is 37 wt% in its fully hydrated form. Therefore, the BPDA-based polyimides with a sulfonation level of 60 % to 70 % have water-uptakes similar to that of Nafion™ at room temperature. However, unlike the Nafion™, the water sorption of these polyimides were almost the same (±2 %) at 80 ^{o}C as at R.T. The same observation was made by Genies *et al.*[261] for sulfonated six membered ring polyimides. This will be discussed in Section 4.2.2 of this dissertation. Sulfonated polyimides, unlike the Nafion™, did not show any noticeable change in water absorption with increase of temperature. The hydrophilic nature of these sulfonated polyimides showed no enhancement in the temperature range R.T. to 80 ^{o}C.

261. Genies, C., Mercier, R., Sillion, B., Cornet, N., Gebel, G., Pineri, M. *Polymer* 42 **2000**, 359

Table 4.2.14 Water Uptakes [SW (%)] of the Sulfonated BPDA/FDA/BDA Polyimides

Polymer	Sulfonated diamine (mol %)	IEC (meq/g) (theory)	SW* (wt %)	SW** (wt %)	ë*[a] (H_2O mol./SO_3^-)
BPDA/FDA-100	0	0	2.17	2.41	-
BPDA/FDA-75	25	0.82	13.9	14.7	12.37
BPDA/FDA-60	40	1.32	19.2	20.5	10.62
BPDA/FDA-50	50	1.65	24.8	25.2	10.97
BPDA/FDA-40	60	1.99	31.7	33.1	11.63
BPDA/FDA-25	75	2.49	43.7	41.8	12.81
BPDA/FDA-0	100	3.32	WS	W.S	-

(*) after 24 h immersion at R.T.
(**) after 24 h immersion at 80 ^oC

Table 4.2.15 Water Uptakes [SW (%)] of the Sulfonated BPDA/FDA/BDA Polyimides

Polymer	Sulfonated diamine (mol %)	IEC (meq/g)	SW* (wt %)	SW** (wt %)	ë[a] (H_2O mol./SO_3^-)
BPDA/BDA-100[a]	0	0	-	-	-
BPDA/ BDA-75	25	0.90	12.8	14.2	10.27
BPDA/ BDA-60	40	1.42	20.3	20.5	10.43
BPDA/ BDA-50	50	1.75	24.1	23.6	9.95
BPDA/ BDA-40	60	2.08	33.2	32.8	11.53
BPDA/ BDA-25	75	2.56	41.7	42.5	11.76
BPDA/ BDA-0	100	3.32	WS	WS	-

(*) after 24 h immersion at R.T. (**) after 24 h immersion at 80 ^oC.
(a) calculated from [SW (g)/18 x IEC (eq/g)
(b) unable to cast the film due to gelation of polymer in DMAc
(WS) water soluble

Water uptake (SW %) of sulfonated BPDA/FDA/BDA membranes is plotted against their IEC (meq/g) in Figure 4.2.14.

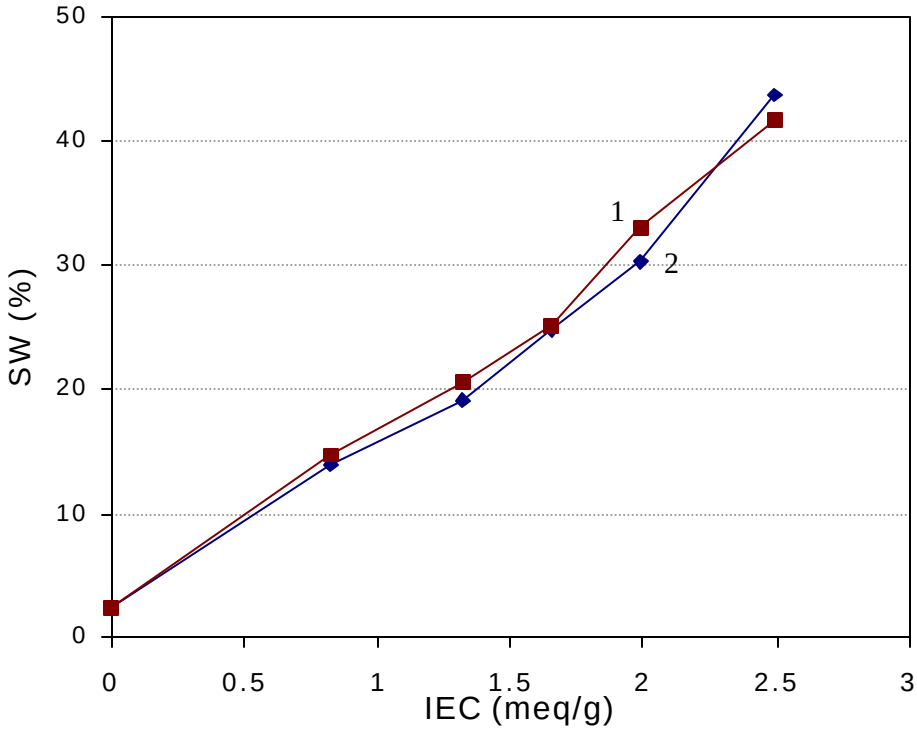

Figure 4.2.14 IEC (meq/g) *vs*. Water uptake (SW %) of sulfonated BPDA/FDA/BDA membranes at 25 ^{o}C (2), and at 80 ^{o}C (1).

Although all the films were immersed in deionized water for 24 hours, they had nearly reached their constant swollen weight much earlier. Especially the membranes having lower degrees of sulfonation (50 %) reached about 90% of their equilibrium swelling in less than four hours. On the other hand, polyimide films with higher degrees of sulfonation (60 %) reached less than 80% of their constant swollen weight in the same period of time. Overall, it was observed that membranes having higher degrees of sulfonation require longer times to equilibrate. Figure 4.2.15 shows the water uptake (SW %) as a function of the square rate of time for 40, 50 and 60 % sulfonated BPDA/FDA/BDA polyimide films.

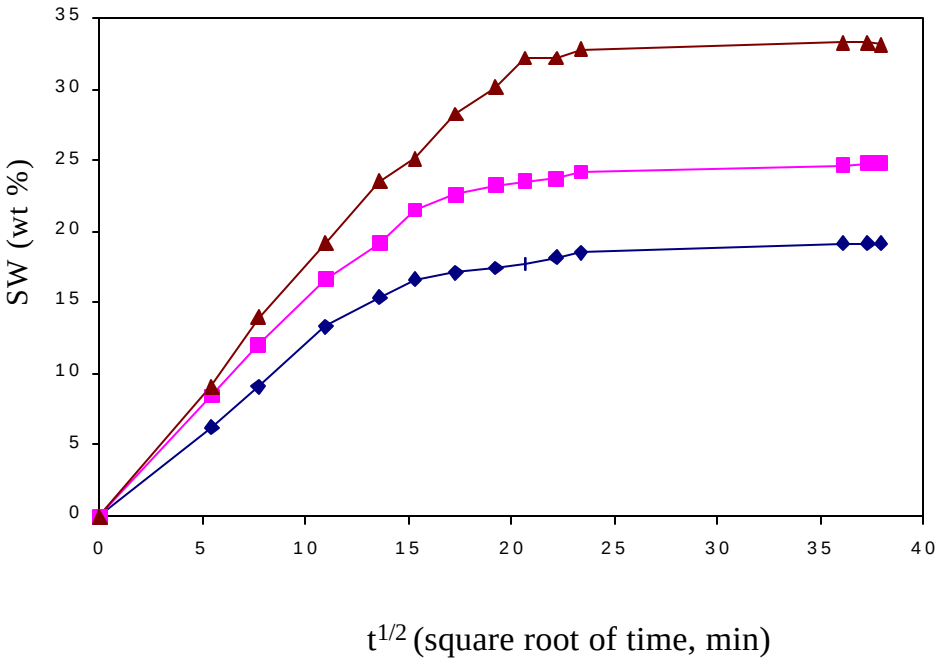

Figure 4.2.15 Water uptake (SW %) *vs*. $t^{1/2}$ (square root of time, min) for 40, 50 and 60 % sulfonated BPDA/FDA/BDA polyimide films for 40 (♦), 50 (■), and 60 (▲) %.

4.2.1.3 3,3',4,4'-Biphenyl Sulfone Tetracarboxylic Dianhydride (BPSDA) Based Sulfonated Polyimides

Sulfonated polyimides based on BPSDA were synthesized via high temperature solution imidization methods in NMP. The diamines, chosen in combination with BPSDA to yield soluble-film forming polyimides were 4,4 -(9-fluorenylidene) diamine (FDA), 1,3-bis(3-aminophenoxy) benzene (APB), and 4,4 -diamino-2,2 -biphenyldisulfonic acid (BDA).

High molecular weight polymers were obtained from an equimolar ratio of diamines and the BPSDA using the one-pot ester-acid procedure by initially converting the dianhydride to its diester-diacid derivative followed by the diester-diacid reaction with sulfonated and unsulfonated aryl diamines. As mentioned earlier, the sulfonated diamine monomer was allowed to oligomerize with the diester-diacid of the dianhydride for a few hours before the unsulfonated diamine was charged into the reaction flask. By varying the mole ratio of sulfonated diamine to unsulfonated diamine, two series of BPSDA-based polyimides were synthesized at 0, 25, 40, 50, 60 and 75 mol % of the BDA. The repeat units of sulfonated BPSDA/FDA/BDA and BPSDA/APB/BDA polyimides are given in Figure 4.2.16.

Homogenous, very viscous reaction solutions were obtained for all the polymers prepared. Furthermore, after subsequent cooling to room temperature, the polymer solutions stayed homogenous. Fibrous polymers were obtained upon precipitating the polymer solution in 2-propanol.

Films were prepared by redissolving the control BPSDA/FDA and BPSDA/APB homopolyimides and their sulfonated copolymers in DMAC and casting from very dilute polymer solutions (5 % w/v) directly onto 5" *by* 10" glass substrates. The cast films were first carefully dried by infrared heat at increasing temperatures under a nitrogen atmosphere, and then vacuum-dried at 150^{o}C for at least a day. By controlling the polymer solution concentration and the cast-film area (substrate area), similar film thicknesses (± 0.004mm) were obtained. Sulfonated and control polyimide membranes were used for further characterization including water uptake, structural, thermal and hydrolytic stability.

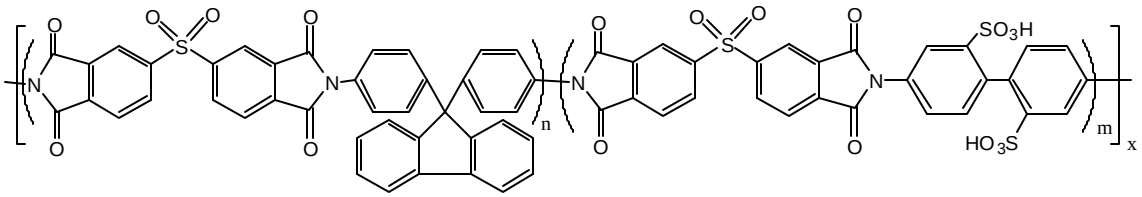

BPSDA/FDA/BDA

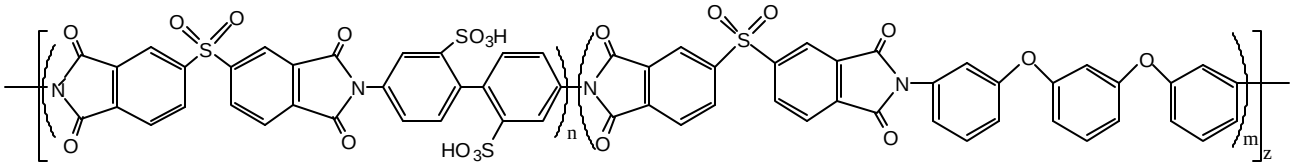

BPSDA/APB/BDA

Figure 4.2.16 Chemical structures of BPSDA-based sulfonated polyimides

Polymer Characterization

Figure 4.2.17 shows the ^{1}H NMR spectroscopy of 50 % sulfonated random copolyimide of BPSDA/FDA/BDA.

Infrared spectra of the cast films show absorbance characteristics of symmetric carbonyl stretching at 1785 cm^{-1} and C–N stretching at 1370 cm^{-1} indicating complete conversion of the poly(amic) acids to the fully cyclized polyimides (Figure 4.2.18).

Furthermore, the successful introduction of the sulfonic acid groups was indicated by the FTIR spectra where the characteristic peak at 1030 cm^{-1} was assigned to symmetric stretching of SO_3H. As shown in the figure, there is no related mode for the unsubstituted control film prepared from BPSDA and APB. This IR spectrum was used to assess the degree of sulfonation, primarily on the basis of the $–SO_3H$ stretching frequency. By calculating the ratio of this stretching frequency, absorption, due to the sulfonic acid unit (A_{SO3H}), to an internal standard absorption such as that of the C=O ($A_{C=O}$) unit along the chain, the degrees of sulfonation in both series of BPSDA-based polyimides were calculated. The ratio $A_{SO3H}/ A_{C=O}$ increases from the 1:0 APB:BDA to the 1:1 polymer and again on going to the 1:3 APB:BDA polymer. Figure 4.2.19 presents a plot of the theoretical ion exchange capacity (IEC, meq/g) of the sulfonated polymers against the degrees of sulfonation obtained from FTIR measurements. The almost linear plot of the theoretical IECs and the experimentally determined degrees of sulfonation levels once again confirmed the successful introduction of the sulfonic acid groups into the polymer backbone.

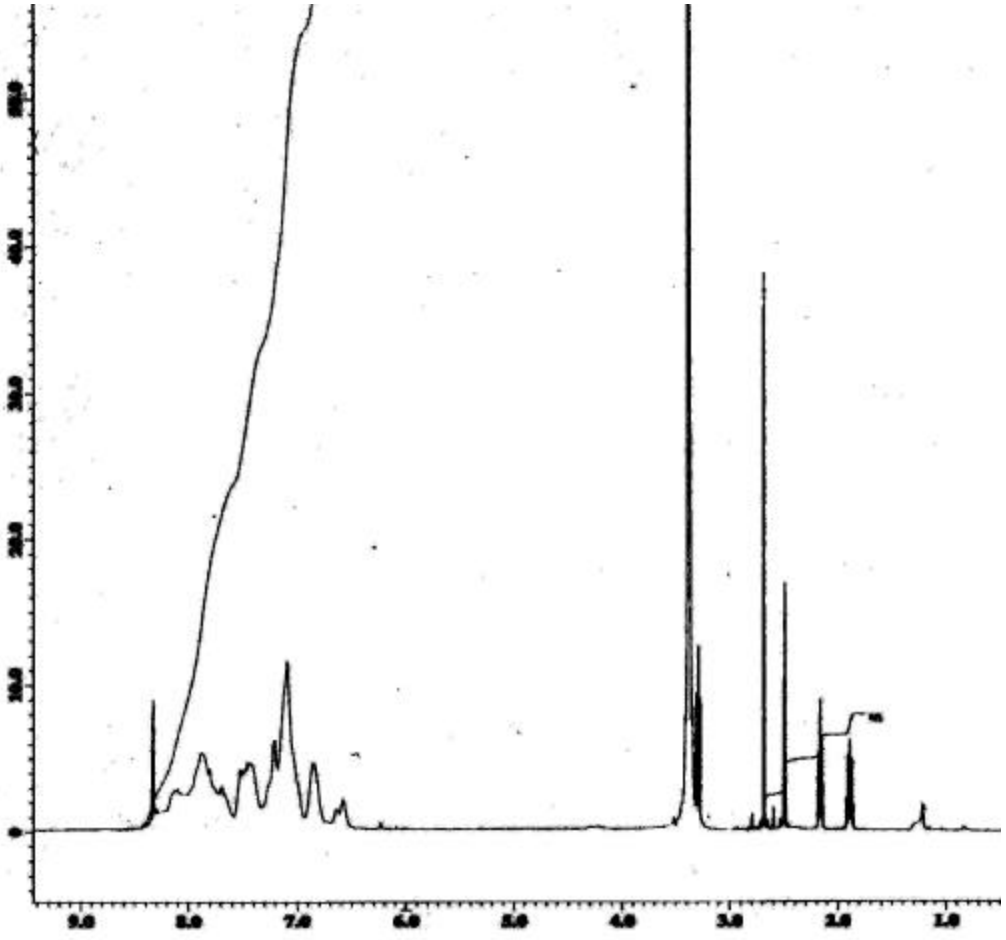

Figure 4.2.17 ^{1}H NMR spectroscopy of 50 % sulfonated random copolyimide of BPSDA/FDA/BDA.

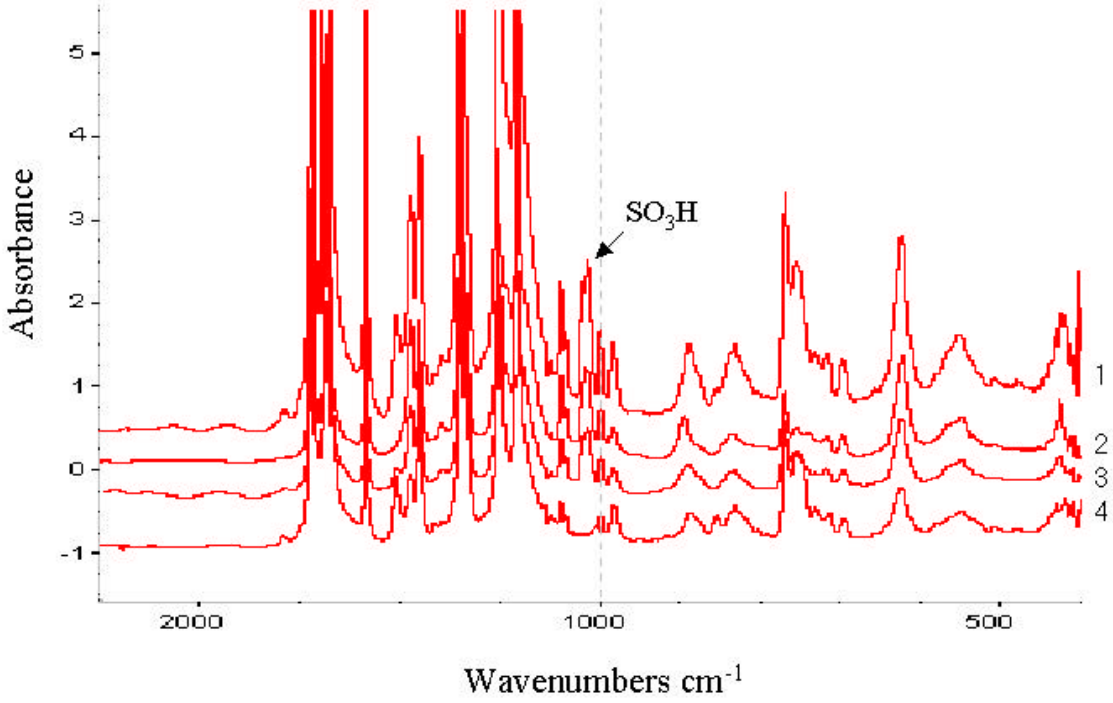

Figure 4.2.18 Infrared Spectrum of BPSDA/APB/BDA-Based Polyimide with APB:DAB ratio of 1:0 (spectrum 4), 3:1 (spectrum 3), 1:1 (spectrum 2) and 1:3 (spectrum 1)

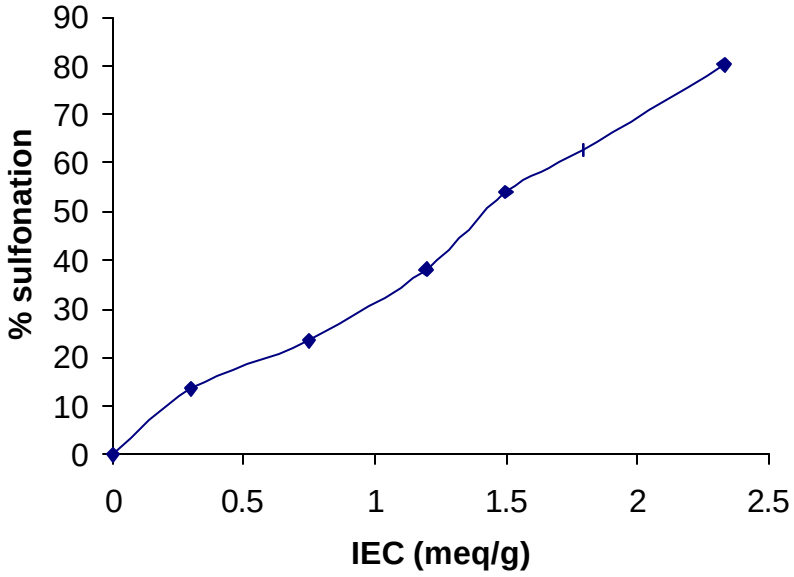

Figure 4.2.19 Plot of the degree of sulfonation data obtained from FTIR measurements (A_{SO_3H}/ $A_{C=O}$) against theoretical ion exchange capacity (IEC, meq/g) of BSDA/APB/BDA-based sulfonated polymers.

For both of the polymer series, high molecular weights were achieved as judged by intrinsic viscosity measurements (Tables 4.2.1.3.1 and 4.2.1.3.2) and good film forming characteristics. Inherent viscosities of these BPSDA-based random acid form sulfonated polymers in NMP ranged between 0.63 and 2.92 dL/g for the control homopolyimide and 75% sulfonated copolymer, respectively. The large increase in viscosity with increasing sulfonated diamine content, from control to 75% substituted copolymer, was probably not due to an increase of molecular weight but due to the increase of ion content of the polymer solution[262-263]. Increase in viscosity with increase of sulfonic acid content in the polymer backbone was also observed with other five-membered ring polymers and six-membered NDA-based polyimides in this study.

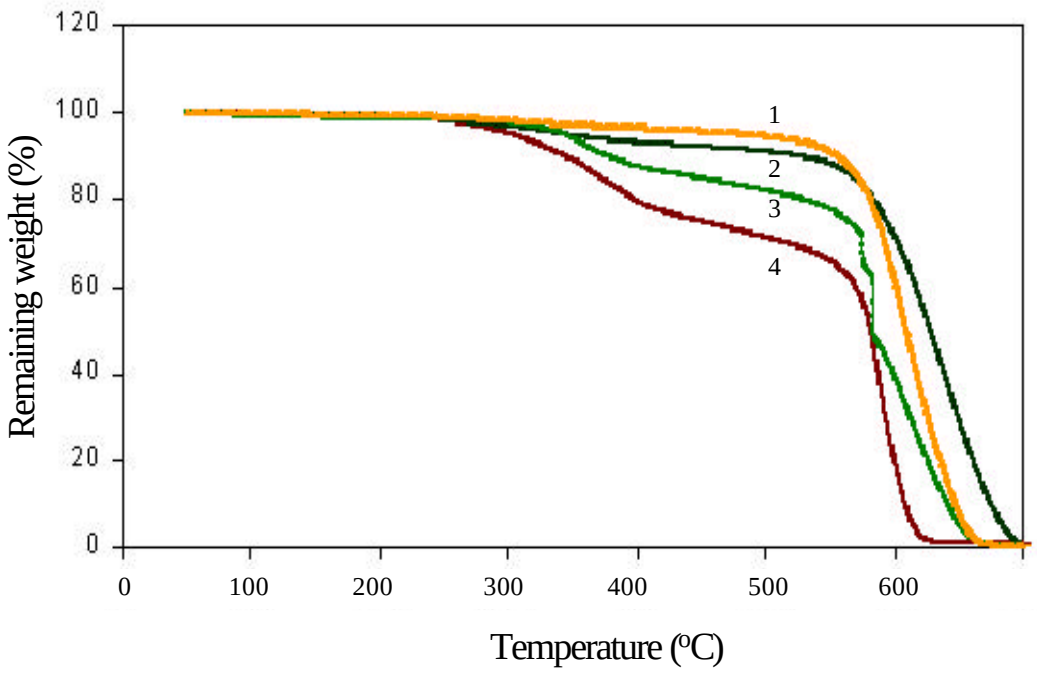

Figure 4.2.20 TGA thermograms of BSDA/APB/BDA polyimides
(1)- control ; (2)- 10 % ; (3) 25 % ; (4) 50 % sulfonation

262. Lundberg, R.D. and Makowski, H.S., J. Polym. Sci., Polym. Phys. Ed., 18, 1821 **1980**.

263. Kopitzke, R.W. *Ph.D. Thesis*, Florida Inst. Tech., Melbourne, Florida, May **1999**.

Table 4.2.1.3.1 Intrinsic Viscosity and Thermal Analysis of BPSDA/FDA/BDA-Based Sulfonated Polyimides

Polymer	Sulfonated diamine (mol %)	m/n	[ç][a] (dL/g)	5% weight loss in air[b] (^oC)	T_g[c] (^oC)
BPSDA/FDA-00	0	0/10	0.63	512	213
BPSDA/FDA-10	10	1/10	1.05	321	221
BPSDA/FDA-25	25	2.5/7.5	1.32	312	235
BPSDA/FDA-40	40	4/6	1.70	299	(n/o)
BPSDA/FDA-50	50	5/5	2.05	291	(n/o)
BPSDA/FDA-60	60	6/4	2.33	282	(n/o)
BPSDA/FDA-78	78	7.8/2.2	2.92	270	(n/o)

(a) NMP, 30 ^oC
(b) 10 ^oC/min in air
(c) 10 ^oC/min in nitrogen
(n/o) not observed

Table 4.2.1.3.2 Intrinsic Viscosity and Thermal Analysis of BPSDA/APB/BDA-Based Sulfonated Polyimides

Polymer	Sulfonated diamine (mol %)	n/m	[ç][a] (dL/g)	5% weight loss in air[b] (^{o}C)	T_g[c] (^{o}C)
BPSDA/APB-00	0	0/10	0.73	507	207
BPSDA/APB-25	25	2.5/7.5	1.47	319	224
BPSDA/APB-40	40	4/6	2.03	305	233
BPSDA/APB-50	50	5/5	2.21	294	241
BPSDA/APB-60	60	6/4	2.62	286	(n/o)
BPSDA/APB-75	75	7.5/2.5	2.84	279	(n/o)

(a) NMP, 30 ^{o}C
(b) 10 ^{o}C/min in air
(c) 10 ^{o}C/min in nitrogen
(n/o) not observed

Non-Aqueous Potentiometric Titrations

The level of pendant sulfonic acid (—SO_3H) incorporated into the polymer backbone was calculated via non-aqueous potentiometric titration measurements as described earlier. The solution-cast dry membranes were dissolved in DMAc and titrated by standard tetramethyl ammonium hydroxide solution (~0.05 N, in iso-propanol) at room temperature.The blank titration volume for pure DMAc was subtracted from the end-point volume of the samples. The results were presented as ion exchange capacity, IEC (meq g^{-1}) of the corresponding polymer. As mentioned earlier, higher the degree of sulfonation, higher the IEC value, which is required, and in general, indication of high proton conductivity in fuel cells.

Assuming that all of the sulfonated monomer was incorporated into the polymer chain, the theoretical ion exchange capacity of the sulfonated films was calculated and found to be in good agreement with experimental data obtained from potentiometric titration. The results are summarized in Table 4.2.1.3.3 for the BSDA/FDA/BDA membranes and in Table 4.2.1.3.4 for the BSDA/APB/BDA membranes.

Table 4.2.1.3.3 Theoretical and Experimental IEC Values for Sulfonated Polyimides of BPSDA/FDA/BDA

% Sulfonation [100 x (m/n+m)]	IEC (meq /g) (25 C)	
	Theoretical*	Experimental**
10	0.299	0.303
25	0.748	0.757
40	1.197	1.181
50	1.497	1.483
60	1.794	1.802

***** 1000 x 2 x % of sulfonation/[$MW_{sulf.\ block}$ x (% of sulf.block) + $MW_{unsulf.\ block}$ x (% of unsulfonated block)]

****** Polymers were dissolved in DMAc, titrated with TMAH at 25 ^{o}C

Table 4.2.1.3.4 Theoretical and Experimental IEC Values for Sulfonated Polyimides of BPSDA/APB/BDA

% Sulfonation [100 x (m/n+m)]	IEC (meq /g) (25 C)	
	Theoretical*	Experimental**
25	0.791	0.807
40	1.246	1.232
50	1.541	1.62
60	1.831	1.858
75	2.255	2.185

* 1000 x 2 x % of sulfonation/[$MW_{sulf.\ block}$ x (% of sulf.block) + $MW_{unsulf.\ block}$ x (% of unsulfonated block)]

** Polymers were dissolved in DMAc, titrated with TMAH at 25 ^{o}C

The stability of $-SO_3H$ groups was investigated by combination of non-aqueous potentiometric titration and intrinsic viscosity measurements. For this purpose, the 25%, 40% and 60% sulfonated BPSDA/FDA/BDA and BPSDA/APB/BDA polyimide films were aged at increasing temperatures from 30 to 220 ^oC for an arbitrarily chosen short period of time (30 min) in a conventional air-oven. Aged films were then redissolved in DMAc and titrated with TMAH at room temperature. Table 4.2.1.3.5 and Table 4.2.1.3.6 summarize the theoretical and experimental IEC values of aged films of BPSDA-based sulfonated polyimides.

Exposing the various levels of sulfonated polymers to temperatures as high as 220 ^oC did not alter the molecular structure, as one might expect from model small molecule experiments[264]. The aged copolymer films remained soluble in DMAc. Quantitative characterization of the sulfonic acid structures, ionic equivalent measurements showed stable IEC values up to 220 ^oC in air. Moreover, simple intrinsic viscosity measurements of aged films remained constant indicating good thermal stability of free sulfonic acid groups.

264. McGrath, J.E., *Polycondensation,* **2000**, Tokyo Institute of Technology, Tokyo, Japan

Table 4.2.1.3.5 Theoretical and Experimental IEC Values of Aged Films of Sulfonated Polyimides of BPSDA/FDA/BDA

n/m / aging temp.	IEC (meq/g)				
	Theory**	**23 °C**	**100 °C**	**140 °C**	**220 °C**
25/75	0.748	0.757	1.751	1.760	0.738
40/60	1.197	1.181	1.214	1.189	1.205
60/40	1.794	1.802	1.810	1.813	1.786

Table 4.2.1.3.6 Theoretical and Experimental IEC Values of Aged Films of Sulfonated Polyimides of BPSDA/APB/BDA

n/m / aging temp.	IEC (meq/g)				
	Theory**	**23 °C**	**100 °C**	**140 °C**	**220 °C**
25/75	0.791	0.807	0.812	0.820	0.816
40/60	1.246	1.232	1.230	1.858	2.185
60/40	1.831	1.858	1.867	1.824	1.821

* Polymer solutions (in DMAc) were titrated by TMAH after aging at each temp. for 30 min in air

** Theory Value: Based on starting monomers mol %

Water Absorption of Sulfonated BPSDA-Based Polyimides

The solution cast and vacuum-dried thin films (ca. 5 cm x 3 cm x 0.020 ± 0.005 mm) were weighed, swollen in deionized water at 25 ^{o}C and weighed periodically until no-more weight increase was observed (24 hours). Swollen weights were obtained by quickly wiping the samples with Kim-wipe tissue and weighing them carefully on a balance. The theoretical IEC (meq/g) values, water uptake [100 x (swollen wt.-dry wt.)/dry wt.] and the number of water molecules per ionic group (ë) are presented in Table 4.2.1.3.7 for BPSDA/FDA/BDA polyimide films and in Table 4.2.1.3.8 for BPSDA/APB/BDA films.

As expected, an increase of swelling with an increase of ionic character of the polymer backbone was observed for the sulfonated BPSDA based polyimides. For example, the water uptake observed at room temperature for the sulfonated polyimides varied from ~ 5% to ~44 % for theoretical IEC values varying from 0.30 to 2.25 meq g^{-1}. High water uptake of these ionic membranes would be advantageous for high proton conductivity through the membranes.

The number of water molecules per $-SO_3H$ group (ë), however, didn't change with the increase of ionic equivalency of the membranes. This indicates a saturation of each ion domain with ~11 water molecules (Figure 4.2.21). Unlike the perfluorosulfonated polymer membranes, in which ë increases with increase of IEC, almost constant ë values have also been reported in literature for sulfonated polyimides[265]. Similar ë values are also found in the present study for six-membered polyimides. This will be discussed in more detail in Section 4.2.2.

One of the required characteristics of proton-exchange membranes is that they should have good hydrolytic stability in a fuel cell working environment. Although it was possible to cast flexible films from high viscosity solutions at low polymer concentration for the control homopolyimide and the 10-50 % sulfonated copolymers of both series, the 75 % sulfonated BPSDA/ABP/BDA polyimide film was less flexible. Bending the latter film to test its flexibility of the film resulted in cracks. Moreover, it was found that soaking the films containing > 40% sulfonic acid groups in DI water or even exposing

265. Genies, C., Mercier, R., Sillion, B., Cornet, N., Gebel, G., Pineri, M. *Polymer* 42 **2000**, 359.

them to ambient atmosphere caused brittleness. Freshly-cast and dry films didn't show any embrittlement or considerably less embrittlement (highly sulfonated copolyimide films). Membranes that were kept in a vacuum oven for drying at 110 ^{o}C for more than a week didn't show brittleness. Control solution-cast membranes of BPSDA/FDA and BPSDA/APB homopolyimides did not turn brittle after soaking them in water for several days.

Increase of ionic groups in the polymer resulted in increased brittleness in soaked membranes. It was obvious that sulfonated polyimide membranes were undergoing hydrolytic decomposition resulting in lowered molecular weight and increasing brittleness. As compared to the unsulfonated analogues, the sulfonated polyimides were more susceptible to hydrolytic degradation. The presence of hydrophilic sulfonic acid groups which increase the water uptake of the polymer may affect the susceptibility of the polymer to hydrolysis in several ways[263].

Table 4.2.1.3.7 Water Uptake and Ion Exchange Capacity Values of Sulfonated BPSDA/FDA/BDA Polyimide Membranes

Polymer	Sulfonated diamine (mol %)	IEC[a] (meq/g)	Water Uptake[b] (%w/w)	ë[b] (H_2O molecules/ SO_3^-)
BPSDA/FDA-00	-0-	-0-	1.5	–
BPSDA/FDA-10	10	0.299	5.2	11.6
BPSDA/FDA-25	25	0.748	14.2	12.5
BPSDA/FDA-40	40	1.197	20.5	11.4
BPSDA/FDA-50	50	1.497	25.0	11.1
BPSDA/FDA-60	60	1.794	33.2	11.3
BPSDA/FDA-75	75	2.243	43.6	13.3

(a) Theory Value: Based on starting monomers mol %
(b) Soaked in dionized water at room temperature for 24 hrs

Table 4.2.1.3.8 Water Uptake and Ion Exchange Capacity Values of Sulfonated BPSDA/APB/BDA Polyimide Membranes

Polymer	Sulfonated diamine (mol %)	IEC[a] (meq/g)	Water[b] uptake (%w/w)	ë[b] (H_2O mol./SO_3^-)
BPSDA/APB-00	-0-	-0-	1.7	–
BPSDA/APB-25	25	0.791	13.4	11.3
BPSDA/APB-40	40	1.246	19.1	10.2
BPSDA/APB-50	50	1.541	24.7	10.7
BPSDA/APB-60	60	1.831	30.2	11.0
BPSDA/APB-75	75	2.255	47.2 [c]	14.0[c]

(a) Theory Value: Based on starting monomers mol %
(b) Soaked in dionized water at room temperature for 24 hrs
(c) May have error due to embrittlement of the film in water

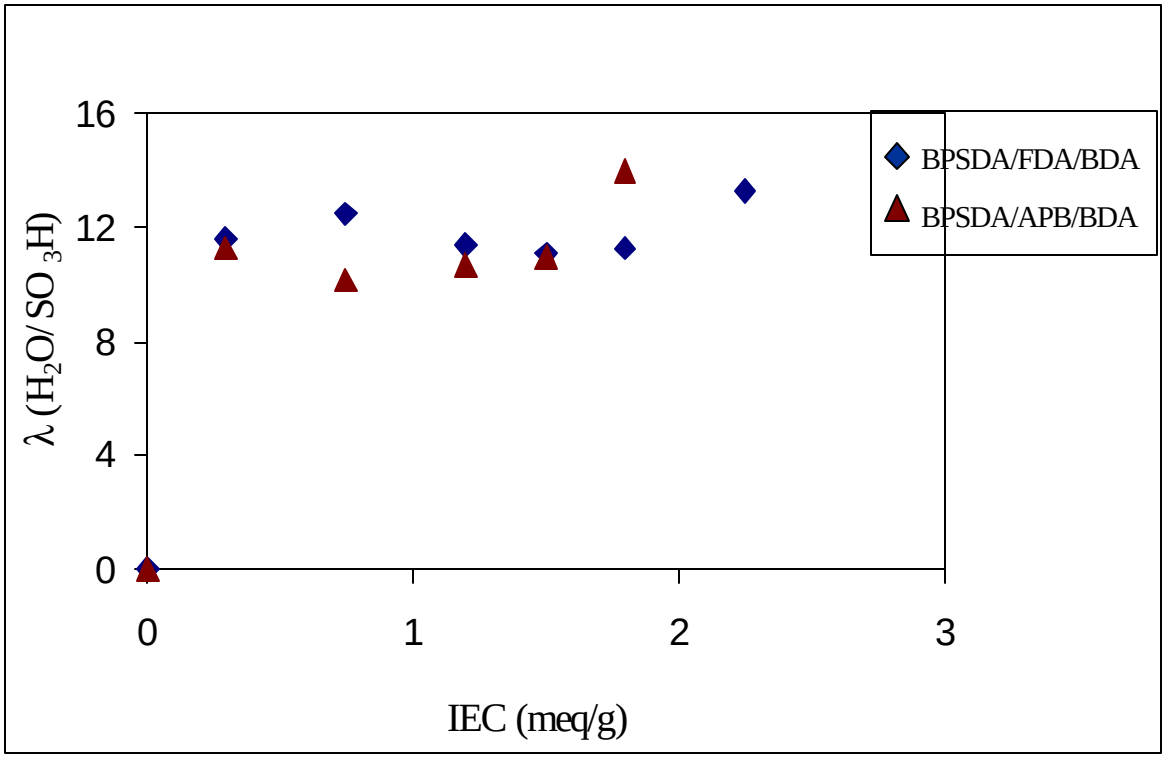

Figure 4.2.21 The number of water molecules absorbed per ionic group) plotted versus the theoretical IEC for BPSDA-based sulfonated polyimides.

4.2.2 Synthesis and Characterization of Sulfonated Six-Membered Ring Polyimides

In the first part of this section, commercially available 1,4,5,8-naphthalene tetracarboxylic dianhydride (NDA) is reacted with some commercially available sulfonated and unsulfonated diamines to synthesize series of polyimides with controlled levels of sulfonation. The monomers utilized are depicted in Figure 4.2.2.1. Although several other diamines, both sulfonated and unsulfonated, were tested to form soluble sulfonated six-membered ring polyimides, all of the trials resulted in precipitation of oligomers under reaction conditions, at an early stage (in several hours) of the imidization process.

Previous studies [266] found that six-membered ring anhydrides, especially highly rigid 1,4,5,8-naphthalene tetracarboxylic dianhydrides are less reactive towards aromatic amines, and do not dissolve and react with them in both protic and aprotic solvents below 140 ^{o}C. Therefore, a one-step high temperature polycondensation method in m-cresol was used, instead of the two-step process that was described in Section 4.1.1 (Scheme 4.2.1) for five-membered sulfonated polyimides.

Since the goal of this research was to obtain highly sulfonated, fully cyclized, soluble, good film forming polymers, a series of high molecular weight homo- and co-polyimides having controlled degrees of pendant sulfonic acid groups were prepared using 1,4,5,8-naphthalene dianhydride and wholly aromatic diamines, namely 4,4'-(9-fluorenylidene) dianiline (FDA), 1,3-bis(3-aminophenoxy) benzene (APB), and 4,4'-diamino-2,2'-biphenyldisulfonic acid (BDA) (Figure 4.2.2.1). The latter diamine (BDA) was used in various molar amounts (10-100 mol %) as a sulfonic acid source in the polyimide backbones.

The second part of this section details the molecular weight, thermal and film forming characteristics of the synthesized sulfonated and unsulfonated six-membered

266. Rusanov, A.L. and Bulycheva, E.G. *Polyimides and Other High Temperature Polymers*, Abadie, M.J.M. and Sillion, B. (eds.), Elsevier, **1991**, p. 125-149; Mercier, R. *French Papent;* Ponomarev, I.I., Nikol'skii, O.G., Volkova, Y.A., and Zakharov, A.V., *Polymer Science*, Ser. A, Vol. 36, No. 9, **1994**, 1185.

ring polyimides. Also, the characteristics of the sulfonated six-membered ring polyimides as proton-ion conducting membranes for fuel cell applications.

4.2.2.1 1,4,5,8-Naphthalene Tetracarboxylic Dianhydride (NDA)-Based Sulfonated Polyimides

The one-step high-temperature polycondensation method was used to synthesize two series of homo- and copolyimides of six membered naphthalene dianhydride because of 1) the insolubility of the starting dianhydride monomer and resulting polyimide oligomers in polar aprotic solvents such as NMP and 2) the low reactivity of six membered anhydride towards aromatic amines.

The synthesis was carried out in a phenolic medium, m-cresol, in the presence of isoquinoline as a catalyst. The reaction proceeded at 200 ^{o}C for about 20 hours in nitrogen atmosphere.

Preliminary trials of NDA reaction with the sulfonated and unsulfonated diamines m-PDA-SO_3H, m-PDA, ODA, DDS resulted in precipitation during the cyclization process. Sulfonated polyimides based on NDA were expected to yield soluble polymers with the proper diamines. Flexible diamines that were chosen to promote the solubility were 4,4 -(9-fluorenylidene)dianiline (FDA) and 1,3-bis(3-aminophenoxy)benzene (APB). Indeed, the solubility of the resulting polymers was greatly improved by the introduction of bulky groups (FDA) and flexible phenylene ether bonds (APB).

The commercially available disulfonated diamine, 4,4 -diamino-2,2 -biphenyl-disulfonic acid (BDA) was chosen as the sulfonic acid source. It was obtained with 76% purity (> 25 % water) (dark purple) and purified by refluxing in water for several hours (off-white). Since the disubstituted diamine absorbs quite a bit water, the pure monomer was dried at 120 ^{o}C under vacuum for at least 48 hours and was kept under vacuum at 60 ^{o}C when it was not in use. The complete dryness of the monomer which is crucial for obtaining high molecular weight polymers, was checked by thermogravimetric analysis under nitrogen as shown in Figure 4.1.2.3. All other monomers used in this section (Figure 4.2.2.1) were dried for at least 16 hours under vacuum. The solvent, m-cresol, was freshly distilled from P_2O_5 under reduced pressure.

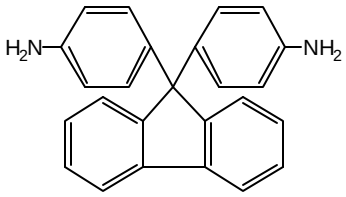

4,4'-(9-Fluorenylidene) dianyline (FDA)

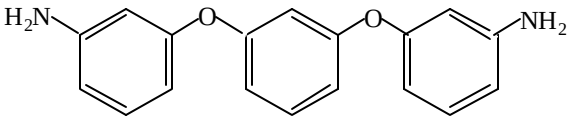

1,3-Bis(3-aminophenoxy) benzene (APB)

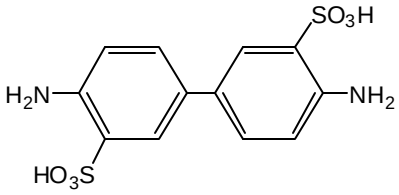

4,4'-diamino-2,2'-biphenyldisulfonic acid

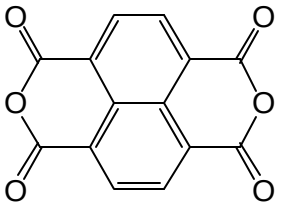

1,4,5,8-Napthalene tetracarboxylic dianhydride(NDA)

Figure 4.2.2.1 Monomers utilized for the syntheses of sulfonated six-membered polyimides

A number of unsuccessful polymerization reactions were done prior to finding the conditions necessary for synthesizing high molecular weight polymers. A discussion of these unsuccessful reaction is instructive. During the development of a synthetic procedure for obtaining copolymer containing the sulfonated diamine (BDA) fragments, it was found that the BDA was almost insoluble in m-cresol and did not react with the naphthalene dianhydride (NDA) monomer even at refluxing conditions of m-cresol (~205 ^{o}C). This behavior was most probably caused by the formation of a stable salt from the SO_3^- and NH_3^+ groups[267]. The incorporation of a tertiary amine resulted in the formation of a tertiary amine-sulfonate (Figure 4.2.2.2) salt, which made the sulfonated diamine not only soluble in m-cresol but also made the $-NH_2$ groups available to react with the carbons of the dianhydride.

After complete dissolution of the sulfonated diamine salt in m-cresol, naphthalene dianhydride was charged into the flask with a few ml of m-cresol to afford a solids concentration of 8-10 % w/v. At this stage, isoquinoline (2.2 times excess of anhydride) was added as a catalyst, and the reaction flask was immersed into a salt-bath and the temperature was raised to 200 ^{o}C. In the first part of this imidization process, the content of the flask was stirred at this temperature under a fast-flow of nitrogen for 3-4 hours allowing pre-oligomerization of the sulfonated diamine with the dianhydride.

Finally, a calculated amount of unsulfonated diamine (FDA or APB) (1.02 moles of 1:1 combined diamines per 1.00 moles of dianhydride) was added along with a wash solution of m-cresol, and the reaction was continued at 200 ^{o}C for ~20 hours. Scheme 4.2.2.1 shows the reaction procedure for a naphthalene dianhydride based sulfonated NDA/FDA/BDApolyimide.

Water formed during the imidization process was continuously removed with a stream of nitrogen. The reaction viscosity increased noticeably after 3-4 hours of the reaction, indicating the progress of polymerization and imidization.

267. Ponomarev, I.I., Nikol'skii, O.G., Volkova, Y.A., and Zakharov, A.V., *Polymer Science*, Ser. A, Vol. 36, No. 9, **1994**, 1185.

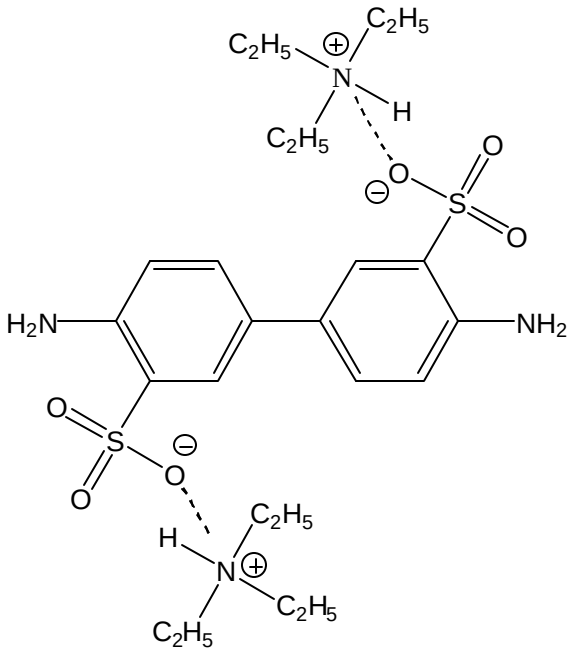

Figure 4.2.2.2 Formation of tertiary amine-sulfonate in m-cresol

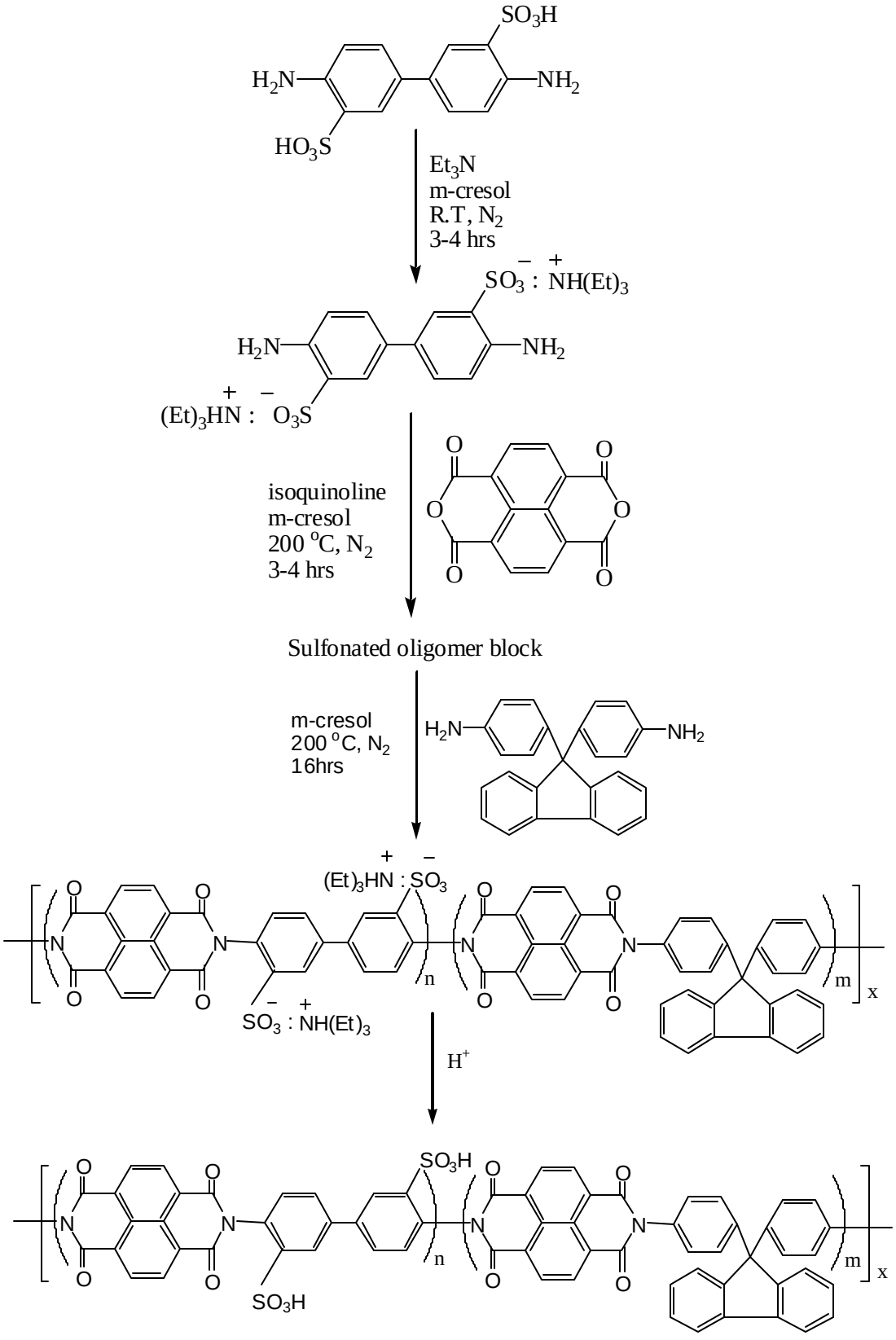

Scheme 4.2.2.1 One-step high temperature solution imidization of sulfonated NDA/FDA/BDA polyimides

At the end of reaction, the polymer solution was cooled down to about 80 ^{o}C and precipitated by very slowly dripping it into an excess amount of isopropanol in a high-speed blender. In some cases, viscous polymer solutions were diluted with more m-cresol prior to isolation. Since m-cresol is a very high boiling solvent (b.p. 205 ^{o}C / 760 mmHg), extra effort was given to remove the solvent from the polymer. Isolated polymers were washed with an excess of isoproponal, and then kept in a large amount of water at ~ 60 ^{o}C overnight to extract any left-over m-cresol from the bulk polymer. Finally, the polymers were first air dried for several hours and then vacuum dried at increasing temperatures up to 160 ^{o}C for at least 24 hours.

Except for the reaction of NDA with APB, completely homogenous, dark brown and very viscous reaction solutions were obtained for all the polymers prepared. Furthermore, after subsequent cooling to room temperature, the polymer solutions stayed homogenous. In the case of the reaction of NDA/APB, however, the oligomer precipitated under reaction conditions to form a cloudy, heterogeneous gel-like mass. Since it could only be obtained as an oligomeric material, it did not precipitate from isopropanol. Therefore, further characterization of the control polyimide of NDA/APB/BDA was not pursued. On the other hand, the reaction of the NDA/FDA control polyimide continued homogenously, forming a very viscous polymer solution upon cooling. The diluted and precipitated polymer solution yielded black polymer beads (every single drop stayed as it was in isopropanol). These beads couldn't be dissolved again in m-cresol to prepare a film. Thus, the control NDA/FDA polyimide was cast from the viscous reaction solution for thermal characterizations.

Sulfonated copolyimides based on NDA/FDA and NDA/ABP were prepared in a wide range of sulfonation levels from 10 –100 mol% using the disubstituted BDA monomer. All of the copolymerizations were conducted using the direct one-step high temperature solution imidization route, using equimolar mixtures of the monomers in m-cresol in the presence of triethylamine as a solubilization agent and isoquinoline as a catalyst. In all cases, yellow fibrous polymers were obtained upon precipitation into 2-propanol. The polymers were washed with 2-propanol and then stirred in hot H_2O (~ 60 ^{o}C) overnight to extract residual m-cresol. In all cases, the recovered polymer yields were nearly quantitative (>93 %).

Film Preparation

Series of tough, creasible polymeric membranes were prepared with essentially controlled thicknesses in the range of 0.025-0.030 mm. The sulfonated NDA/FDA/BDA and NDA/APB/BDA polymers were redissolved in m-cresol (<5 % wt/v) at ~40 ^{o}C and cast directly onto clean 5" *by* 10" glass substrates. They were first slowly dried under infrared heat at increasing temperatures under a nitrogen atmosphere, and then vacuum-dried at 160^{o}C for at least a day. By controlling the polymer solution concentration and the cast-film area (substrate area), similar film thickness (± % 5) was obtained. In all cases, tough, creasible membranes were obtained which ranged in color from light brown to dark brown. The intensity of the color increased with sulfonation. The membranes were immersed in 0.1 M H_2SO4 solution for 2 hours to acidify all the sulfonated groups, were washed with an excess of water and finally were vacuum dried at 100 ^{o}C for at least 12 hours. Solution cast-membranes of the sulfonated polyimides were used for characterization.

Polymer Characterization

^{1}H NMR, ^{13}C NMR and FTIR spectroscopy were used to confirm the chemical structures of the sulfonated polyimides.

The FTIR spectra given in Figure 4.2.2.3 indicate the completion of reaction which is shown by the characteristic naphthalenic imide absorptions of a fully cyclized polyimide. The appearance of absorption modes at ~ 1719 cm^{-1} (symmetric C=O), ~1680 cm^{-1} (asymmetric C=O), and 1345 cm^{-1} (C–N stretching) confirms the cyclization. Furthermore, the successful introduction of the sulfonic acid groups through the incorporation of the disubstituted diamine is confirmed by the FTIR spectra which exhibit the characteristic peak at 1030 cm^{-1} that is assigned to symmetric stretching of $-SO_3H$. As seen from the spectra, intensity of the $-SO_3H$ stretching increased with the increase of the sulfonation level from 40 to 100 %.

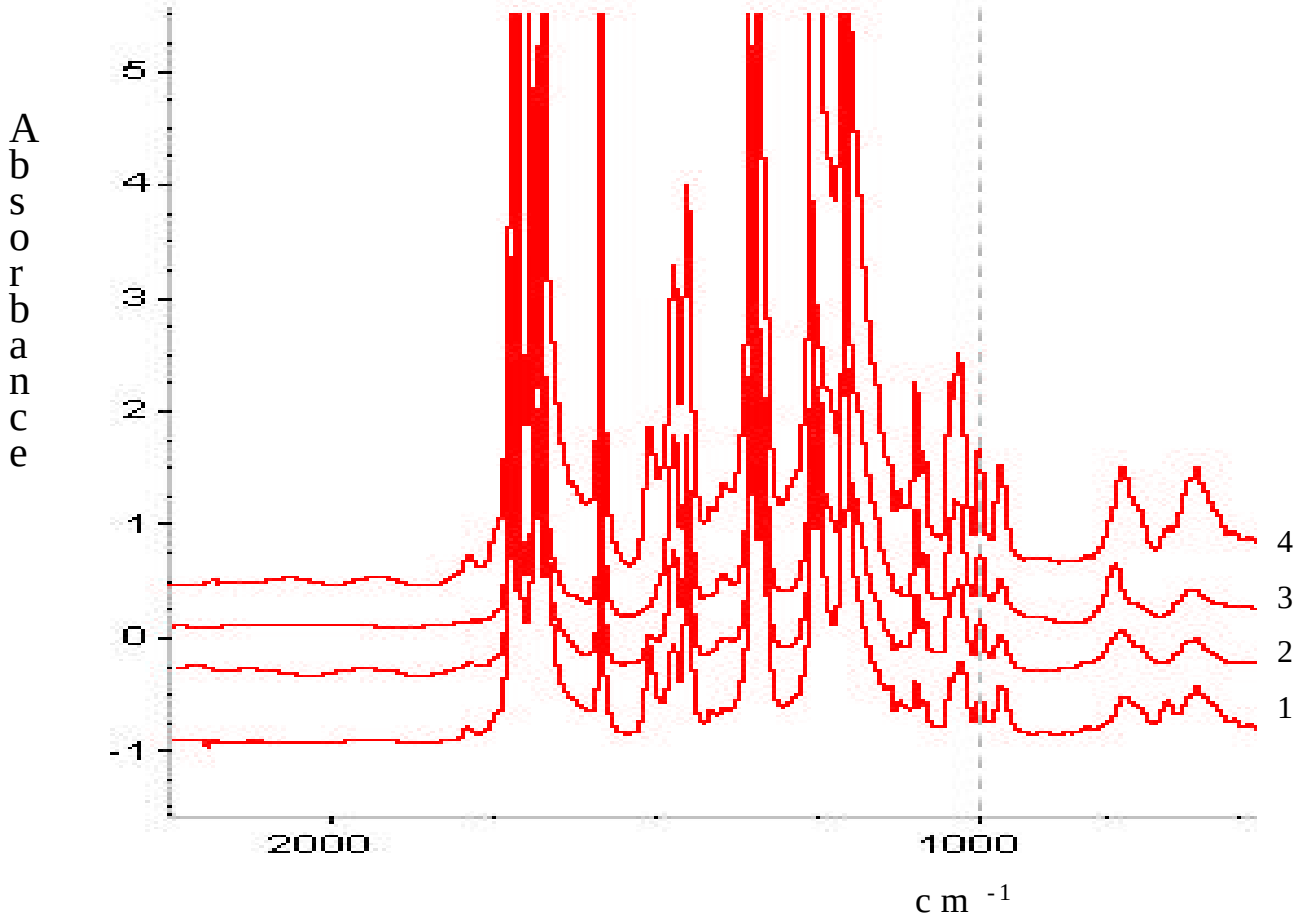

Figure 4.2.2.3 FTIR spectra of (1) 40 %, (2) 60 %, (3) 75 %, (4) 100 % sulfonated NDA/APB/BDA polyimide membranes

Intrinsic Viscosity Measurements

The inherent viscosities of the bulk polymers in their triethylamine-sulfonate salt form were determined in m-cresol using 0.5 g/dL polymer solution at 25ºC in a Ubbelohde dilution viscometer. The inherent viscosities of polymer membranes in their free acid form were measured at 0.1 g/dL in m-cresol. The results are summarized in Table 4.2.2.1.

In general, the triethylamine-salt form of the sulfonated polyimides gave high inherent viscosities measured on 0.5 g/dL polymer solutions suggesting that very high molecular weights were obtained. Similar high inherent viscosity values in m-cresol were observed by Litt et.al. [(268)] with similar types of sulfonated polymer. In general, the inherent viscosities of the sulfonated polymers decreased with an increased degree of sulfonation. This result may indirectly suggest that lower molecular weights were obtained with an increase of ionic character in the polymer backbone.

It is worth mentioning that the inherent viscosity of a given sulfonated polymer measured at 0.1 g/dL is much lower than the inherent viscosity measured at 0.5 g/dL. The inherent viscosity data plotted against concentration for a 25% sulfonated NDA/FDA/BDA polymer gave an almost linear relationship as seen in Figure 4.2.2.4. No polyelectrolyte effect was observed in m-cresol by the triethylammonium form. Similar results were observed in the literature[(269)] and were explained by the low dielectric constant of the m-cresol and also by the large triethylammonium moieties. The use of large hydrophobic counterions (triethylammonium) which do not favor the polymer aggregation, masked the ionic character of the polymer and avoided or minimized the effect of electrostatic interactions.

On the other hand, the inherent viscosities of the free-acid form of the polymers measured on 0.1 g /dL polymer solutions in m-cresol were between 1.62 – 4.23 dL/g. Higher η_{inh} values were obtained for polymers with higher degrees of sulfonation (or higher IEC values). These results clearly indicate that the polymer chain aggregate due to electrostatic interactions[(266)] between pendant ionic $-SO_3H$ groups. The [η] of sulfonated

268. Litt, M. *Personal Communications*, ACS Meeting in Washington, DC, **2000**.

269. Binning G., Quate, C.F. Gerber C., Atomic Force Microscope. *Phys. Rev. Lett.* **1986**;56:930-3.

NDA/FDA/BDA polymers against corresponding IEC (meq/g) values were plotted in Figure 4.2.2.5.

Table 4.2.2.1 The repeat unit and inherent viscosities of sulfonated NDA/FDA based polyimides

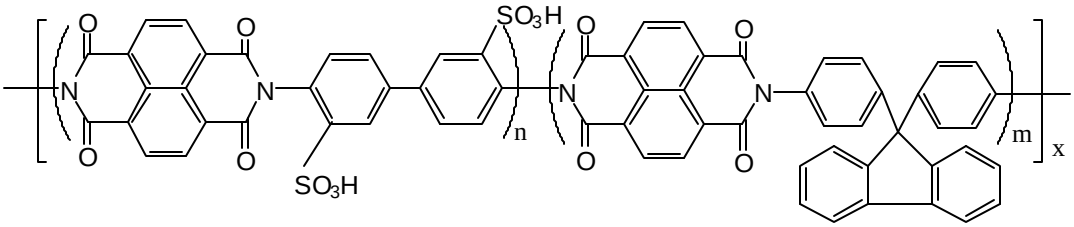

NDA/FDA/BDA

Polymer	Sulfonated diamine (mol %)	m/n (FDA/BDA)	η_{inh} [a] (dL/ g)	η_{inh} [b] (dL/g)
NDA/FDA-00	0	10/0	–	–
NDA/FDA-25	25	7.5/2.5	4.1	1.74
NDA/FDA-40	40	6/4	4.2	2.11
NDA/FDA-50	50	5/5	4.2	2.50
NDA/FDA-60	60	4/6	3.8	3.03
NDA/FDA-75	75	2.5/7.5	4.1	3.45
NDA/FDA-90	90	1 0/90	3.9	3.94
NDA/FDA-100	100	0/10	3.7	4.23

(a) triethylamine-sulfonate salt of the polymer, measured at a concentration of 0.5 g/dL in m-cresolat 25 ^{o}C

(b) acid form of the polymer, measured at a concentration of 0.1 g/dL in m-cresol at 25 ^{o}C

(–) not measured.

Table 4.2.2.2 The repeat unit and inherent viscosities of sulfonated NDA/APB based polyimides

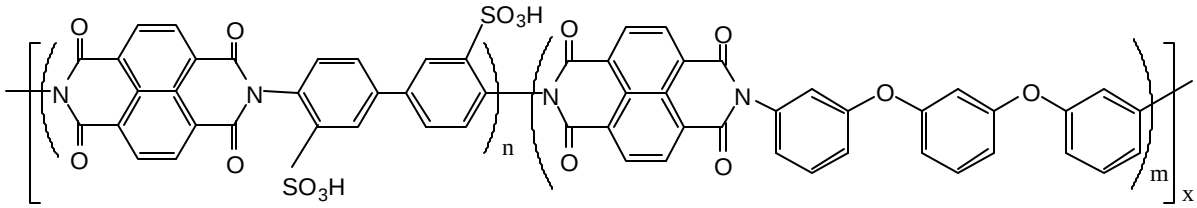

NDA/APB/BDA

Polymer	Sulfonated diamine (mol %)	m/n (FDA/BDA)	ζ_{inh} [a] (dL/ g)	ζ_{inh} [b] (dL /g)
NDA/APB-00	0	10/0	4.3	–
NDA/APB-25	25	7.5/2.5	4.1	1.62
NDA/APB-40	40	6/4	4.1	1.96
NDA/APB-50	50	5/5	4.2	2.36
NDA/APB-60	60	4/6	4.1	2.80
NDA/APB-75	75	2.5/7.5	3.9	3.34
NDA/APB-90	90	1 0/90	3.7	3.77
NDA/APB-100	100	0/10	0.18[c]	4.11

(a) triethylamine-sulfonate salt of the polymer, measured in m-cresol at a concentration of 0.5 g/dL at 25 ^{o}C

(b) acid form of the polymer, measured in m-cresol at a concentration of 0.1 g/dL at 25 ^{o}C

(c) precipitated during polymerization

(–) not measured.

Figure 4.2.2.4 The inherent viscosity plotted against concentration for a 25% sulfonated NDA/FDA/BDA solution in m-cresol at 25 ^{o}C

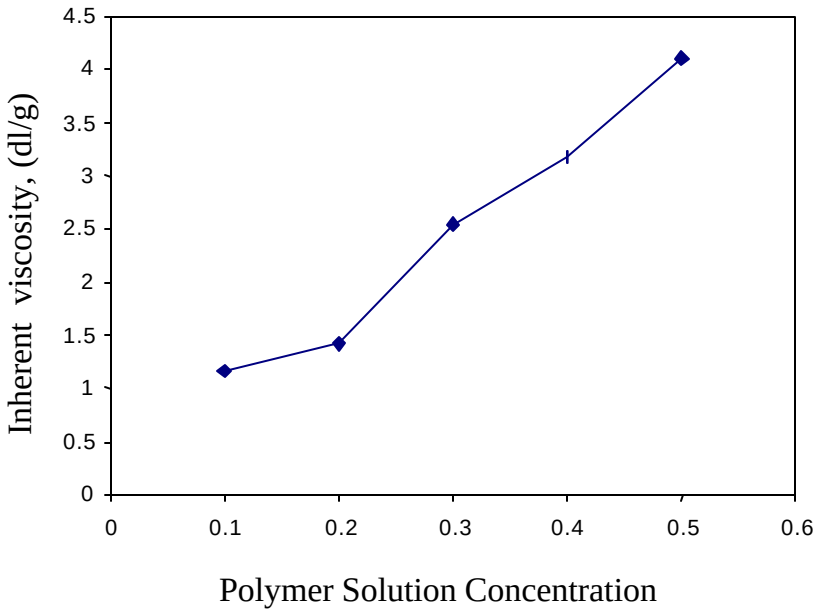

Figure 4.2.2.5 Inherent viscosity (concentration of 0.1 g dl^{-1} in m-cresol at 25 ^{o}C) and theoretical IEC (meq/g) plotted against % sulfonation for sulfonated (25-100%) for NDA/FDA/BDA polymers

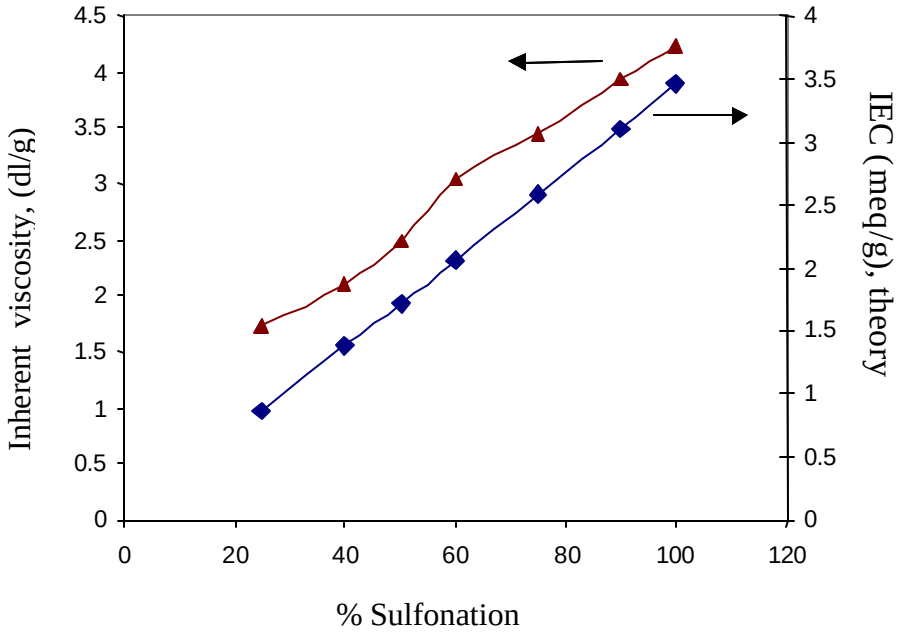

Other molecular weight measurements, such as GPC could not be performed on these sulfonated polymers due to adsorption of the polymer chains on the gel packing. However, the fact that highly fibrous materials were isolated and tough membranes were formed by solution casting allowed us to believe that these sulfonated polyimides have very high molecular weights. This belief was reinforced by the high observed inherent viscosity values as was discussed earlier.

Thermal stability

The solution-cast polyimide membranes were thermally analyzed to study the effect of degree of sulfonation on the thermal properties of sulfonated NDA-based polymers. The preliminary assessment of the thermooxidative stability of these polymers was evaluated by thermogravimetry using a Perkin-Elmer TGA7. The dynamic TGA scans were collected for about 10 mg polyimide membranes from 30 to 800 ^{o}C in air at a heating rate of 10 ^{o}C/min as shown in Figure 4.2.2.6. Before collecting the runs, samples were dried in the TGA furnace from 30-210 ^{o}C at 5 ^{o}C/min to remove any trace amount of absorbed water and solvent.

Except for the unsulfonated control NDA/FDA polymer, all the thermograms of the sulfonated polyimide films exhibited a two-step degradation behavior. The first weight loss, observed between 300 and 400 ^{o}C, corresponds to desulfonation in the sulfonated block, and the second weight loss, observed at a temperature higher than 450 ^{o}C corresponds to the polymer backbone degradation. After extracting the solvent with hot water and properly drying the membranes in a vacuum oven and finally in the TGA furnace, all the sulfonated polymer membranes exhibited thermal stability up to 250 ^{o}C in both inert nitrogen and air atmosphere. This temperature, below which the sulfonic acid groups are stable, is far above the required temperature (150 ^{o}C) for polymer electrolyte membranes in fuel cells.

The TGA thermograms indicated that the initial weight losses were steeper for polymers with higher sulfonation degrees. Furthermore, the weight loss temperature of the sulfonated polyimides decreased and the weight loss temperature range broadened with increasing sulfonation levels for both the free acid and the salt forms (Figure

4.2.2.8). However, the onset of the initial weight loss temperature was independent of the degree of sulfonation.

Although the amount of sulfonic acid groups introduced into the polymers significantly affected their thermal stability, *e.g*. the 5% weight loss temperature decreased as the content of the ionic groups therein increased all the polymers tested were stable up to 250 ^{o}C both in air and nitrogen atmosphere. Thermogravimetric curves of NDA based copolyimides containing sulfonated and unsulfonated diamines also indicated that the temperature at which weight losses due to desulfonation was observed was independent of the unsulfonated diamine structure.

By replacing the bulky diamine, FDA, with the flexible diamine containing phenylether bonds, APB, no change was observed in the onset temperature of the first weight drop, or in the temperature the 5% weight loss temperature at the same degree of sulfonation. Tables 4.2.2.3 and 4.2.2.4 represent thermogravimetric analysis results and IEC (meq/g) values of NDA based sulfonated polyimide membranes.

Weight loss data in dTGA curves of the sulfonated polymers in their acid form were used to calculate their degrees of sulfonation. Experimental (TGA) and theoretical (based on mol % of sulfonated diamine) sulfonation values are also presented in Table 4.2.2.3 for NDA/FDA/BDA membranes and in Table 4.2.2.4 for NDA/APB/BDA membranes.

Two weight loss steps were observed for sulfonated polyimides, which were reflected by two broad peaks in dTGA in two separate temperature ranges. Unsubstituted NDA/FDA/BDA homo-polymer had high thermal stability showing 5 % weight loss at 543 ^{o}C due to decomposition of the polymer backbone. On the other hand, the initial weight loss of the 40% sulfonated polymers starts at around 310 ^{o}C and shows its 5 % weight loss at ~355 ^{o}C which is believed to be due to the splitting off of the sulfonic acid groups. Similar observations were observed for s-polyetherether ketones[273], s-polysulfones[274], s-poly(aryleneether) sulfone[225,272].

In all the TGA runs of the completely dry samples, the weight loss of the sulfonated polymers were larger than that of their control unsulfonated analogues at a given

273. Zaidi, S.M.J. et al., *Journal of Membrane Science* 173 (**2000**) 17-34.

274. O'Gara, J.F., Williams, D.J., Macnight, W.J., Karasz, F.E., *J. Polym. Sci. B: Polym. Phys*. 25 (**1987**) 1519.

temperature. For all the NDA/APB/BDA and NDA/FDA/BDA polyimide films tested, there was a greater decomposition in the sulfonated derivatives than in the unsubstituted polymers. In general, the onset temperature of the polymers showed no dependence on the degree of sulfonation and observed to be at around 300 ± 5 ^{o}C. This indicates that polymer membranes are thermally stable up to 300 ^{o}C, and therefore they will be stable enough within conceivable temperature range of polymer electrolyte fuel cell conditions.

The degree of sulfonate groups in polymers were also evaluated by the mass loss measurements by thermogravimetric analysis. The fist peak of the derivatives of TGA curves (dTGA) was conveniently used to determine the percent of weight loss.

Theoretical weight losses (%) were calculated assuming that the splitting-off of a sulfonic acid groups releases one SO_3H molecule, using the formula below:

$$[(\text{Degree of Sulfonation, mol\%}) \times (MW_{SO3H})/ (MW_{\text{repeat unit}})] \times 100 \times 2^{a}.$$

Similar experimental and theoretical values were obtained for both series of polymers. For example, dTGA curves of the 40 % sulfonated NDA/APB/BDA polyimide membrane (0.8 ionic groups per repeat unit) showed a mass loss of 6.43 % as compared to the theoretical mass loss value of 5.88 %. This result is a good indication of the thermal degradation of all the sulfonic acid groups in the first step at ~ 300 ^{o}C. Tables 4.2.2.3 and 4.2.2.4 summarize the degree of sulfonation results in terms of percent weight loss obtained from the TGA measurements.

a) Number "2" represents the two moles of SO_3H group per repeat unit

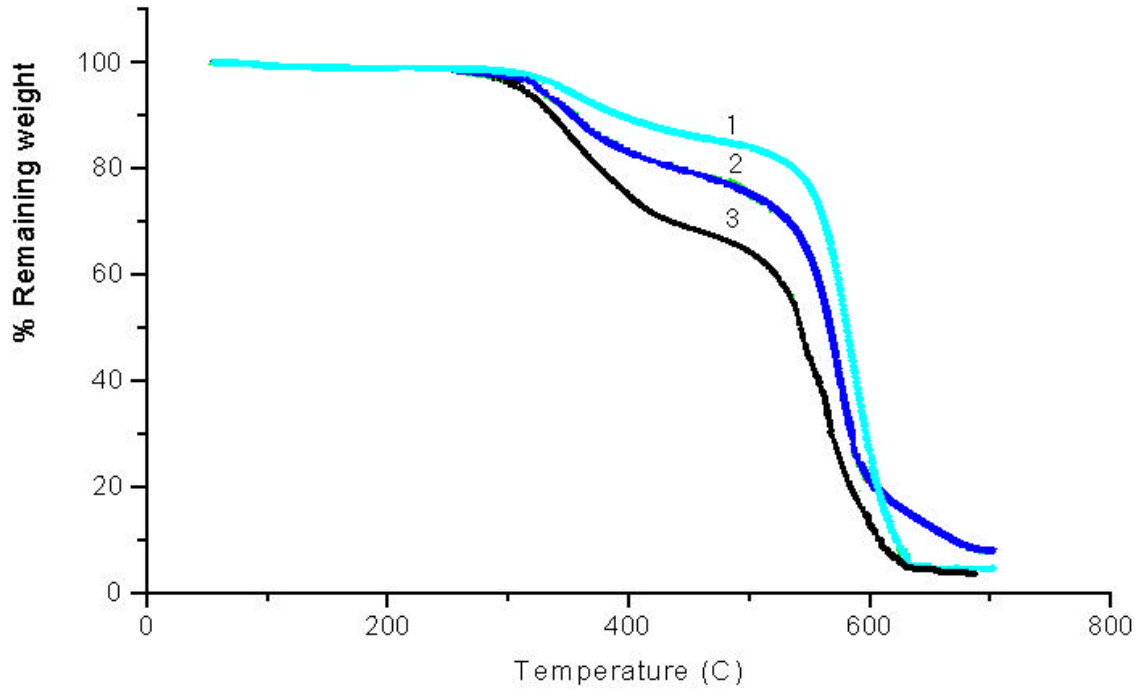

Figure 4.2.2.7 TGA Thermograms of Sulfonated NDA/FDA/BDA Polyimide Membranes (1) D.S.= 25% ; (2) D.S.= 40 % ; (3)D.S.= 60 %

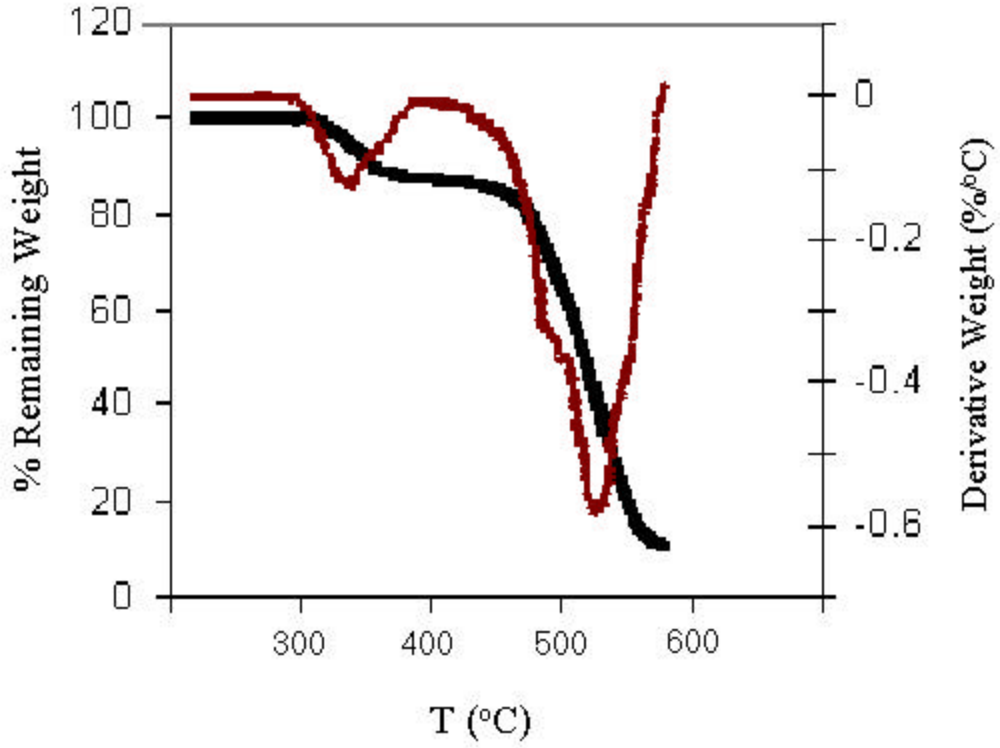

Figure 4.2.2.8 TGA and dTGA Thermograms of a 40 %Sulfonated NDA/APB/BDA Polyimide Membrane.

Table 4.2.2.3 Thermal Characterization of Sulfonated NDA/FDA/BDA Polyimides by dynamic TGA in air

Polymer	**Sulfonated diamine (mol %)**	**5% weight loss[a] temp. (^{o}C)**	**Weight loss (theoretical) (wt %)**	**Weight loss *by* TGA (wt%)**
NDA/FDA-00 [b]	0	543	–	–
NDA/FDA-25	25	366	3.75	3.18
NDA/FDA-40	40	353	6.00	7.70
NDA/FDA-50	50	347	7.50	8.11
NDA/FDA-60	60	338	9.00	10.45
NDA/FDA-75	75	328	11.25	13.23
NDA/FDA-90	90	323	13.50	16.31
NDA/FDA-100	100	313	15.00	18.55

(a) 10 ^{o}C/min in air, previously dried in TGA furnace up to 210 ^{o}C
(b) Bulk polymer beads

Table 4.2.2.4 Thermal Characterization of Sulfonated NDA/APB/BDA Polyimides by dynamic TGA in air

Polymer	Sulfonated Diamine (mol %)	5% weight loss[a] temp. (^{o}C)	Weight loss theoretical (wt %)	Weight loss *by* TGA (wt%)
NDA/APB-00 [b]	0	–	–	–
NDA/APB-25	25	364	3.68	4.70
NDA/APB-40	40	354	5.88	6.43
NDA/APB-50	50	345	7.35	7.98
NDA/APB-60	60	337	8.82	9.35
NDA/APB-75	75	330	11.03	13.11
NDA/APB-90	90	320	13.24	14.50
NDA/APB-100	100	313	14.80	16.67

(a) 10 ^{o}C/min in air, previously dried in TGA furnace up to 210 ^{o}C
(b) Unsulfonated oligomer, precipitated during the polymerization.

Water Uptake Measurements

Swelling measurements were conducted at room temperature and at 80 ^{o}C. The equilibrium water contents in the films were determined gravimetrically by periodically weighing the swollen membranes until until they reached constant weights (after 24 hr. immersion). The water uptake results were calculated as both weight % and as the number of water molecules absorbed per ionic group (ë). Table 4.2.2.5 and Table 4.2.2.6 represent the data determined at room temperature for the two series of polymers. Theoretical ion exchange capacities are also tabulated.

The water uptakes observed at room temperature for the sulfonated polyimides varied from ~15 to 43 % for IEC values varying from 0.875 to 3.13 meq g^{-1}. In general, the weight increase (%) from absorbed water did not seem to depend on the nature of the unsulfonated diamine. For example, by replacing the bulky diamine, FDA, with the flexible diamine, APB, the water uptake varied ± ~ 4% for the polymers having the same level of sulfonation. However, it may not be completely correct to compare the water uptakes on a weight % basis. The unit masses differ in the polymer series[(265)]. A better way to compare the absorptions of the water of two series of sulfonated polymers is to compare the number of water molecules associated with a single ionic group. Therefore, water sorptions of the membranes were also calculated as the number of water molecules per ionic group (ë) using the formula[(265)] below:

where $n(H_2O)$ is the number of moles of water molecules, $n(SO_3^-)$ is the number of

$$ë = \frac{n(H_2O)}{n(SO_3^-)} = \frac{SW}{18 \text{ x } IEC}$$

moles of sulfonic acid groups. SW is the weight of water absorbed per gram of polymer, IEC is the ion-exchange capacity (eq g^{-1}) and 18 corresponds to the weight of one mole of water (18 g mol^{-1}).

For both of the NDA-based sulfonated polymer series, the percent of water uptake increases as the ionic character (the number of pendant $-SO_3H$ sites) increases in a given polymer structure. On the other hand, the total number of water molecules absorbed per ionic group (ë) remained almost constant (10.5 ± 3 H_2O molecules/SO_3^- group)

(Figure 3.2.2.9). This result suggests that the absorbed water is mainly located in the hydrophilic domains[265]. An almost constant ë value for a given polymer structure also indicates the saturation of ionic domains with 10-14 water molecules. Genies *et al*. found similar ë values for their sulfonated five-and six- membered polyimides. However, these findings are different from those found for typical ionomer membranes like perfluorosulfonated polymer membranes, radiation-grafted membranes, or even sulfonated arylene ether sulfones[225]. For example, in Nafion, as IEC increases, the ë value increases significantly, and for critical IEC, the ë value diverges due to membrane dissolution. In the case of sulfonated polyimides, the fact that ë values are constant is surprising and could be explained by a specific morphology of membranes related to their preparation. It was explained in the literature[265] that the solvent used for preparing the solution-cast films, and the drying temperature of films, which remains lower than the T_g of these polymers are important parameters for the polymer morphology.

Similar ë values between different polymer structures do not indicate significant differences. Moreover, these values obtained in this part for NDA-based polyimides are very close to the ë numbers obtained for sulfonated phthalic polyimides, e.g. BPSDA-based polyimides in Section 4.2.1.2 (ë = ~11values).

Although having large values of IEC, the conductivity values of sulfonated polyimides are rather low compared to typical proton exchange membranes (0.12 S/cm for IEC=0.91 meq/g) and bisphenol based polyarylene ethers (0.11 S/cm for IEC=1.5 meq/g polymer and 0.17 S/cm for IEC=2.2 meq/g polymer). For example, the 40 % sulfonated polyimide NDA/FDA-40 with an IEC= 1.38 meq g^{-1} has a conductivity of 0.06 S/cm at 25 ^{o}C.

Table 4.2.2.5 Water Uptake and Ion Exchange Capacity Values of Sulfonated NDA/FDA/BDA Polyimide Membranes

Polymer	Sulfonated diamine (mol %)	IEC (meq/g)	Water uptake[a] (%w/w)	ë[a] (H_2O mol./SO_3^-)
NDA/FDA-00	-0-	-0-	–	–
NDA/FDA-25	25	0.86	19.2	12.4
NDA/FDA-40	40	1.38	25.4	10.23
NDA/FDA-50	50	1.72	35.1	11.4
NDA/FDA-60	60	2.06	40.7	11.0
NDA/FDA-75	75	2.58	51.0	11.0
NDA/FDA-90	90	3.10	58.3	10.5
NDA/FDA-100[b]	100	3.47	42.5	7.5

(a) measured after 24 h immersion in D.I. water at 25 ^oC.
(b) did not reach equilibrium due to partial solubility in water

Table 4.2.2.6 Water Uptake and Ion Exchange Capacity Values of Sulfonated NDA/APB/BDA Polyimide Membranes

Polymer	Sulfonated diamine (mol %)	IEC (meq/g)	Water[a] uptake (%w/w)	ë (H_2O mol./SO_3^-)
NDA/APB-00	0	0	–	–
NDA/APB-25	25	0.875	15.4	10.8
NDA/APB-40	40	1.40	24.0	10.5
NDA/APB-50	50	1.75	32.1	11.2
NDA/APB-60	60	2.10	39	13.6
NDA/APB-75	75	2.62	47.5	11.0
NDA/APB-90	90	3.13	55.1	10.8
NDA/APB-100[b]	100	3.47	42.5	7.5

(a) measured after 24 h immersion in D.I. water at 25 ^oC.
(b) did not reach equilibrium due to partial solubility in water

Genies *et al.* published comparable ë values for their sulfonated phthalic (ë= ~12.5) and naphthalic polyimides (ë= ~13.2)[265] with various levels of sulfonation. As compared to perfluorinated ionomeric membranes (0.12 S/cm for IEC=0.91 meq/g), low proton conductivity values (25°C) were also observed for the fully hydrated acid form membranes of sulfonated polyimides (1.3×10^{-3} S/cm for IEC=0.96 meq/g). This is possibly due to the fact that the ë values are constant and not dependent on the IEC of the polymer. In some cases, the ionic conductivity reached a threshold at an IEC higher than 1.3 meq/g[265]. It was stated that this observation confirmed a relationship between the water swelling and the conductivity through the concept of ionic domain percolation. For low IEC values, the conductivity is limited by the lack of connection between the ionic domains. By increasing the IEC, the ionic domains are more and more inter-connected, and above the percolation threshold the level of interconnection is large enough to be no longer the limiting parameter for the diffusion process. Therefore, the ionic conductivity increases up to a maximum value because the ion concentration is constant in the ionic domains (constant ë value) and the ion mobility in the ionic domains is expected to be identical for all samples. The most important criteria is then the ionic phase volume fraction that varies only slightly with IEC for large IEC values[265].

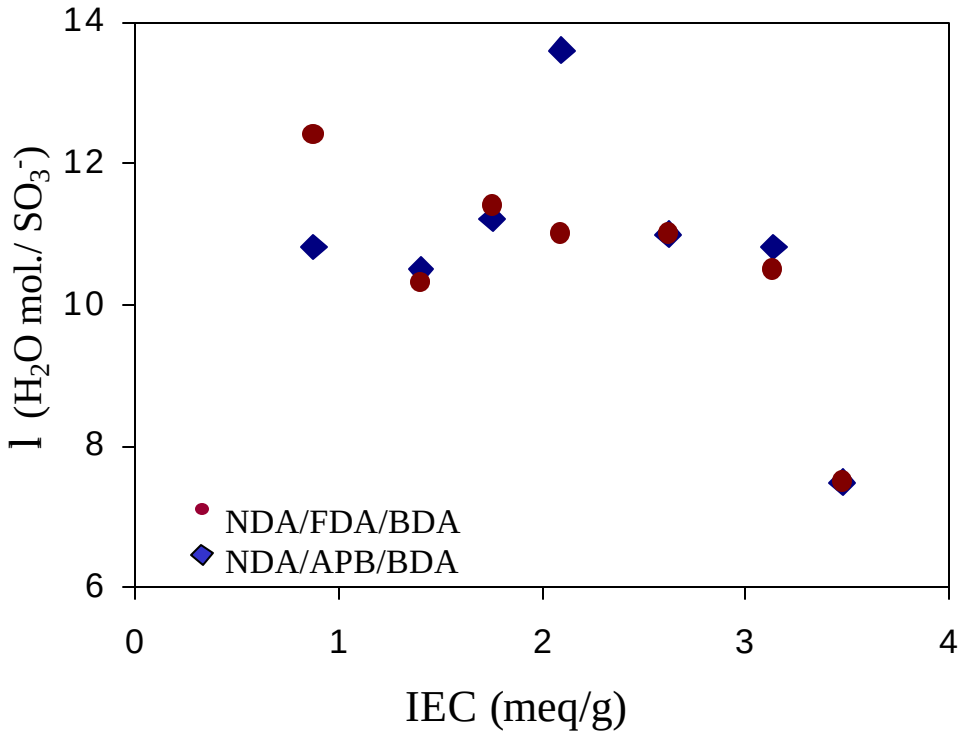

Figure 4.2.2.9 λ (H_2O molecules/SO_3^-) vs. IEC (meq/g) for NDA/FDA/BDA and NDA/APB/BDA polyimide membranes

AFM Study

Tapping mode phase imaging is a relatively new atomic force microscopy (AFM) technique[270] and has been in use for less than two decades. It can differentiate between areas with different properties regardless of their topographical nature[271]. The phase angle is defined as the phase lag of the cantilever oscillation relative to the piezo-driving signal sent to the cantilever. Its value depends on the energy dissipated in the tapping interaction of the probe and with the specimen.

Tapping mode AFM images of sulfonated NDA/FDA/BDA films were recorded at room temperature. Figure 4.2.2.10 shows an example of 1 ìm-wide height and phase images of a dry 75 % sulfonated NDA/FDA/BDA film. A feature common to all of the sulfonated NDA membranes was that no phase separations between the sulfonic acid-rich ionic regions and the unsulfonated polymer blocks were observed. Since all of these sulfonated polyimides are random copolymers and the pendant sulfonic acid groups are actually on the polymer backbone, in other words, not separated or branched away from the hydrophobic imide backbone, no ionic-cluster like structure formation was observed. Unlike the sulfonated polyimides, perfluoro-sulfonate cation exchage membranes have hydrophilic-hydrophobic regions proved using tapping mode phase imaging[272].

270. Binning G., Quate, C.F. Gerber C., Atomic Force Microscope. *Phys. Rev. Lett.* **1986**; 56:930-3.

271. Howard A.J., Rye R.R., Houston J.E., Nanomechanical Basis For Imaging Soft Materials with Tapping Mode Atomic Phase Microspcopy, *J. Appl. Phys*. **1996**;79:1885-90.

272. James, P.J., McMaster, T.J., Newton, J.M. and Miles, M.J., *Polymer* 41 **(2000)** 4223-4231.

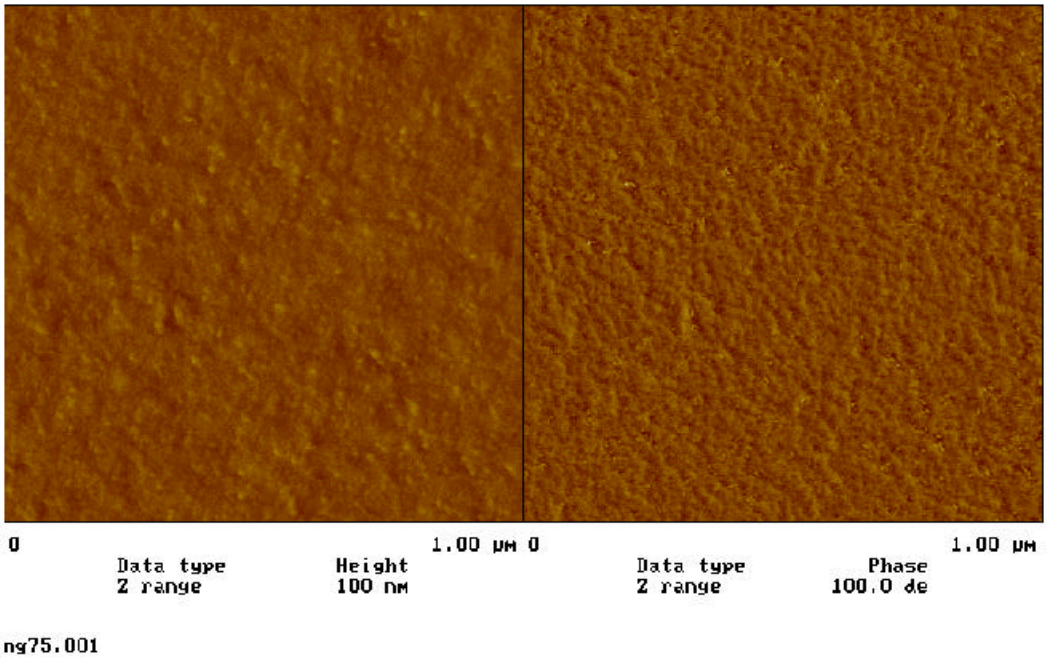

Figure 4.2.2.10 Tapping mode, 1 ìm wide height and phase images of a dry 75 % sulfonated NDA/FDA/BDA film

Sulfonated films were dehydrated in a vacuum oven at 120 ^{o}C for at least 12 hours and were first imaged as “dry”. Then, they were swollen with room temperature de-ionized water for 24 hours and imaged again as “wet”. Figures 4.2.2.11 and 4.2.2.12 show the AFM tapping mode, 1 ìm wide phase images of 40 % and 75 % sulfonated dry and wet NDA/FDA/BDA films, respectively. As it can be seen from the images, the morphologies of the films were changed by just soaking them in water. The phase image contrast increased with water uptake as the hydrophilic sulphonic acid groups incorporated water and became more easily distinguished from the hydrophobic regions. The corresponding height images of the dry and wet membranes didn’t show any appreciable change. It was difficult to distinguish any difference between the dry and swollen forms in this respect.

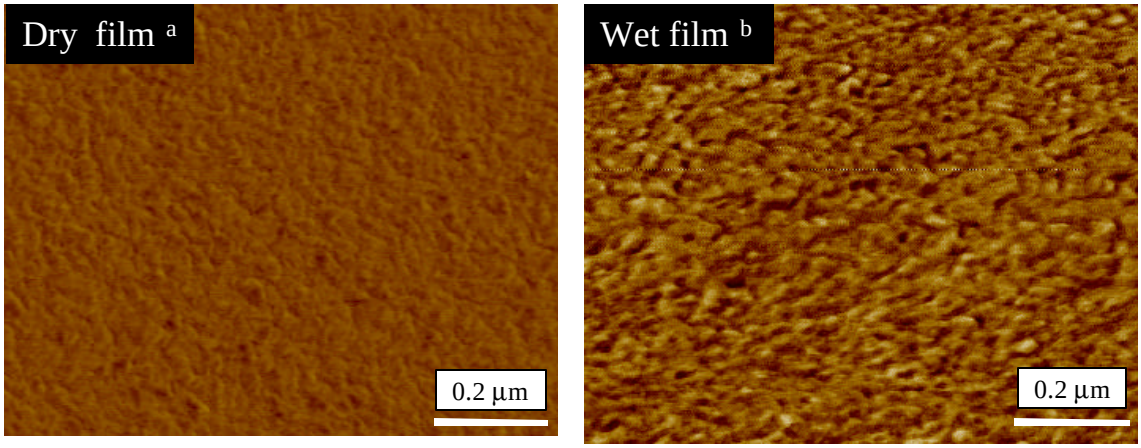

Figure 4.2.2.11 Tapping mode, 1 ìm wide phase images of 40 % sulfonated dry and wet NDA/FDA/BDA films (a) dried at 120 ^{o}C overnight (b) soaked in water(25 ^{o}C) for 24 hours (Z range = 30^{o}).

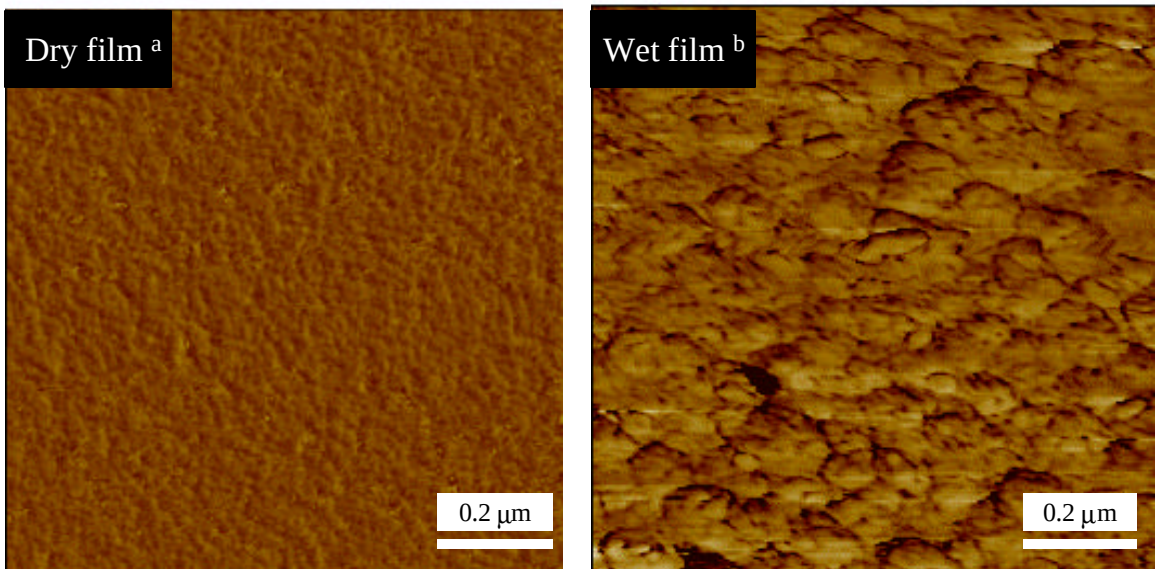

Figure 4.2.2.12 Tapping mode, 1 ìm wide phase images of 75 % sulfonated dry and wet NDA/FDA/BDA films (a) dried at 120 ^{o}C overnight (b) soaked in water (25 ^{o}C) for 24 hours (Z range = 50^{o}).

4.2.3 Sulfone [–(SO_2)–] and Phosphine Oxide [–(PO)–] Containing Diamines and Their Sulfonated Polyimides

Three sulfonated and unsulfonated diamines, namely disulfonated-4,4'-bis(3-amino phenoxy) phenyl sulfone (s-DADPS), sulfonated-bis(3-aminophenoxy)phenyl phosphine oxide (s-BAPPPO) and bis(3-aminophenyl) phenyl phosphine oxide (BAPPO) containing either phosphine oxide or sulfone moieties were synthesized as described in detail in the experimental section and in the first part of this chapter. The former diamine, s-DADPS, was synthesized for the first time in this research while the last two diamines had been previously synthesized in our research group[224, 225]. The synthesis of sulfone [–(SO_2)–] and phosphine oxide [–(PO)–] containing diamines and their related polyimides were of interest for two reasons. The first reason was that by using these sulfonated or unsulfonated diamines containing flexible *meta* –oxyether linkages as in (s-DADPS) and (s-BAPPPO) might increase the solubility and flexible chain conformations in naphthalene-based polyimides. The second reason was that incorporation of these monomers into the polymer backbone might show an additional interesting feature of extensive hydrogen bonding[264] between the O=S=O and P=O and pendant sulfonic acid (–SO_3H) groups as indicated in Figure 4.2.3.1.

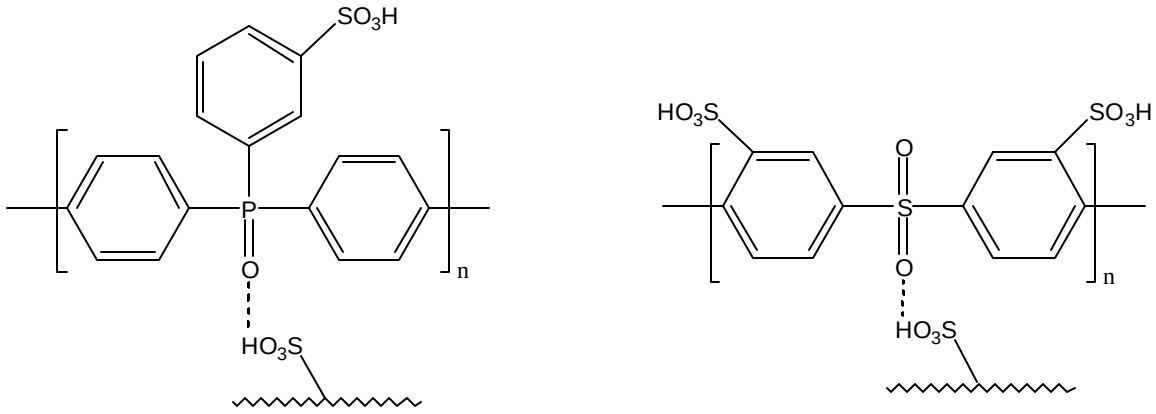

Figure 4.2.3.1 H-Bonding in (O=S=O) and (P=O) Containing Sulfonated PIs

This might also allow efficient dispersion of inorganic acid additives, which could permit the utilization of these ion conductor proton exchange membranes at temperatures well above 100 ^{o}C, where the conversion of hydrogen or direct methanol fuel cells is known to be much more efficient[(264)].

The objective of this part of the dissertation was the synthesis and full characterization of the above diamines, and use of these diamines in their corresponding polyimide syntheses. The preparation, characterization and preliminary evaluations of new phthalic copolyimides will be discussed in following section.

4.2.3.1 Disulfonated 4,4'-Bis(3-aminophenoxy)phenyl Sulfone (s-DADPS)-Containing BPDA-Based Sulfonated Polyimides

The novel 4,4'-Bis(3-aminophenoxy)phenyl Sulfone (s-DADPS) diamine monomer bearing two pendant sodium-sulfonate groups *meta* to the sulfone and *ortho* to the oxy-ether moieties was synthesized via aromatic nucleophilic reaction chemistry as described in Section 3.2.2.23 and characterized as discussed in Section 4.1.4. Using this disulfonated diamine (s-DADPS), and an unsulfonated diamine (APB), a series of BPDA-based polyimides was prepared. Once again, the approach of incorporation of ionic groups into the polymer backbone using a sulfonated monomer allowed us to control both sulfonation level and ionic group distribution.

All of the random copolyimides of BPDA/APB/s-DADPS were prepared using the high temperature ester-acid solution imidization procedure in an NMP/o-DCB solvent mixture. The BPDA dianhydride was converted to its diester-diacid derivative using an EtOH/Et_3N mixture and was then reacted with the aryl diamines, in equimolar ratio, at 180 ^{o}C for 24 hours. The s-DADPS monomer was allowed to react with the diester-diacid of the BPDA for oligomerization for a few hours before the APB was charged into the reaction flask. By varying the mole ratio of s-DADPS : APB, a series of copolyimides was synthesized having 10, 25, 40, 50 60, 75 and 100 mol % of the s-DADPS

Homogenous solutions having high solution viscosities were observed during the reactions. These viscous polymer solutions were poured into 2-propanol and gave fibrous

yellow to light brown color precipitates. The precipitated polyimides were collected by filtration, washed and dried at 160 ^{o}C under vacuum for 24 hours.

Structures of the BPDA/s-DADPS/APB and BPDA/s-DADPPO/APB polyimides are shown in Figure 4.2.3.4.

Film Preparation

Membranes of the BPDA-based sulfonated polyimides were obtained by casting their 8-10 % w/v polymer solutions in DMAc on 5" by 10" glass substrates at ~30 ^{o}C. The cast membranes were first slowly dried using infrared heat at increasing temperatures under a nitrogen atmosphere, and were then vacuum-dried at 150 ^{o}C for 24 hours. The dried membrane films were released from their glass plate supports by immersion in dionized water at room temperature. This series of tough sulfonated BPDA/s-DADPS/APB-based polyimide films were prepared with controlled thicknesses of 0.030-0.040 mm. The membranes were acidified with 1 M H_2SO_4 solution for 24 hours and then rinsed with an excess of water. Finally they were dried overnight at 100 ^{o}C under vacuum.

The film formation of the control unsulfonated polyimide was not successful. At the 10 % solids level the BPDA/APB-based unsulfonated control polyimide did not dissolve completely in DMAc. The polymer solution became cloudy (first the upper part of the mixture) in a couple of hours of stirring, its viscosity increased and then the mixture slowly set to an opaque –color unstirrable gel-like mass overnight. This process was irreversible; the gel could not be dissolved by heating at ~60 ^{o}C or by diluting with more solvent. For thermal characterizations the control polyimide was used as synthesized in bulk. The cast membranes of the sulfonated membranes were used in their thermal characterizations. It was obvious that incorporation of the sulfonated diamine into the polymide backbone increased its solubility in polar aprotic solvents.

Polymer Characterization

Figure 4.2.3.2 shows the ^{1}H NMR spectrum of the 40 % sulfonated random copolyimide of BPDA/s-DADPS/APB in DMSO-d_6.

Infrared spectra of the sulfonated polyimide membranes revealed absorption bands at 1788 cm^{-1}, 1370 cm^{-1} and at 1030 cm^{-1}, that were assigned to symmetric carbonyl stretching (C=O), C–N stretching and symmetric O=S=O stretching, respectively complete conversion of the poly(amic) acids to the fully cyclized polyimides was thereby confirmed (Figure 4.2.3.3).

FTIR, being very sensitive to the SO_3 absorption is a unique tool for calculating the level of sulfonation in the final polymers. A simple ratio of the SO_3 stretching absorption intensity to an internal standard absorption is very important and useful in quantitative analysis of the degree of sulfonation of these polyimides. Therefore, FTIR studies were extensively used in this research to determine the sulfonated imide block content (Figure 4.2.3.4).

As is seen in the Figure 4.2.3.3, there is no related absorption mode at 1030 cm^{-1} for the unsubstituted control polymer prepared from BPDA and APB. These IR spectra were used to assess the level of sulfonation, primarily on the basis of the absorption intensity at the $–SO_3H$ stretching frequency. By calculating the ratio of this stretching frequency due to absorption intensity by the sulfonic acid unit (A_{SO3H}), against an internal standard absorption intensity of the C=O ($A_{C=O}$) unit, the degrees of sulfonation in both series of BPDA-based polyimides were calculated. The ratio of A_{SO3H}/ $A_{C=O}$ increases from the 10:1 APB: s-DADPS to the 4:1 APB:s-DADPS and again on going to the 1:4 APB:s-DADPS polyimide.

Figures 4.2.3.5 and 4.2.3.6 present FTIR data results for the copolyimide BPDA/s-DADPS/APB and BPDA/s-DADPPO/APB, respectively. The rather good correlation of experimental (FTIR) mol% sulfonated diamine and theoretical (based on monomer feed) mole % sulfonated diamine values indicates good incorporation of the sulfonated diamines in both both series of copolyimides.

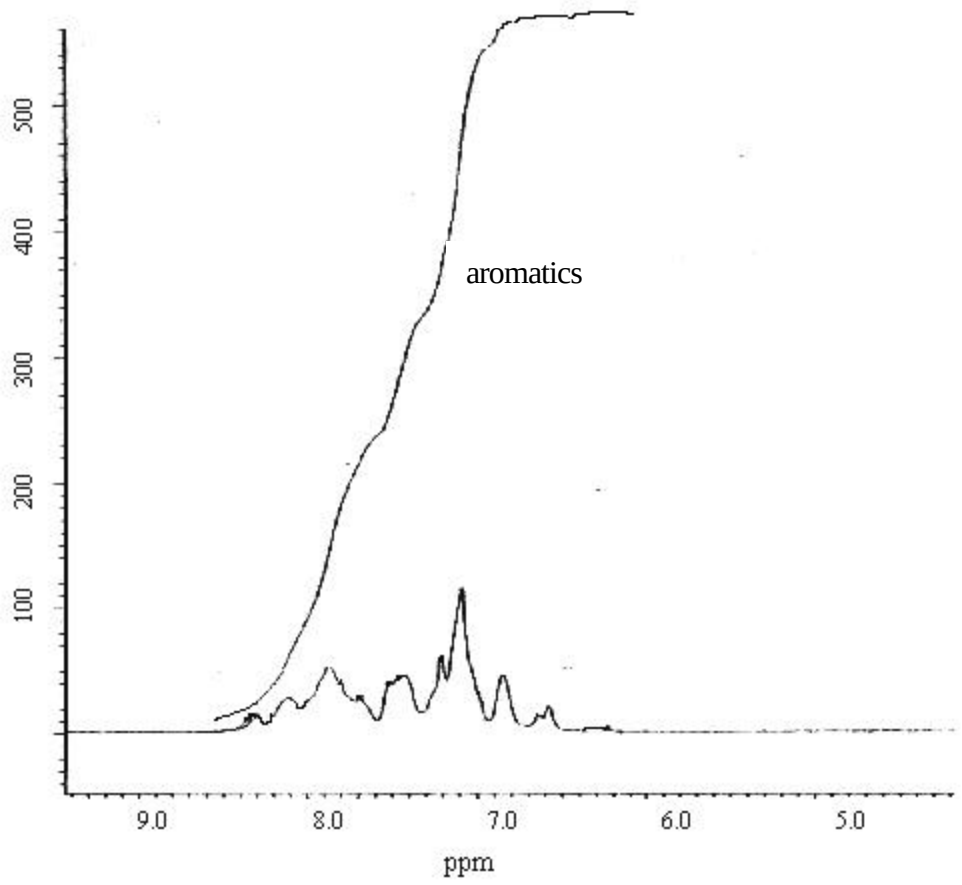

Figure 4.2.3.2 ^{1}H NMR spectrum of 40 % sulfonated random copolyimide of BPDA/s-DADPS/APB in DMSO-d_6.

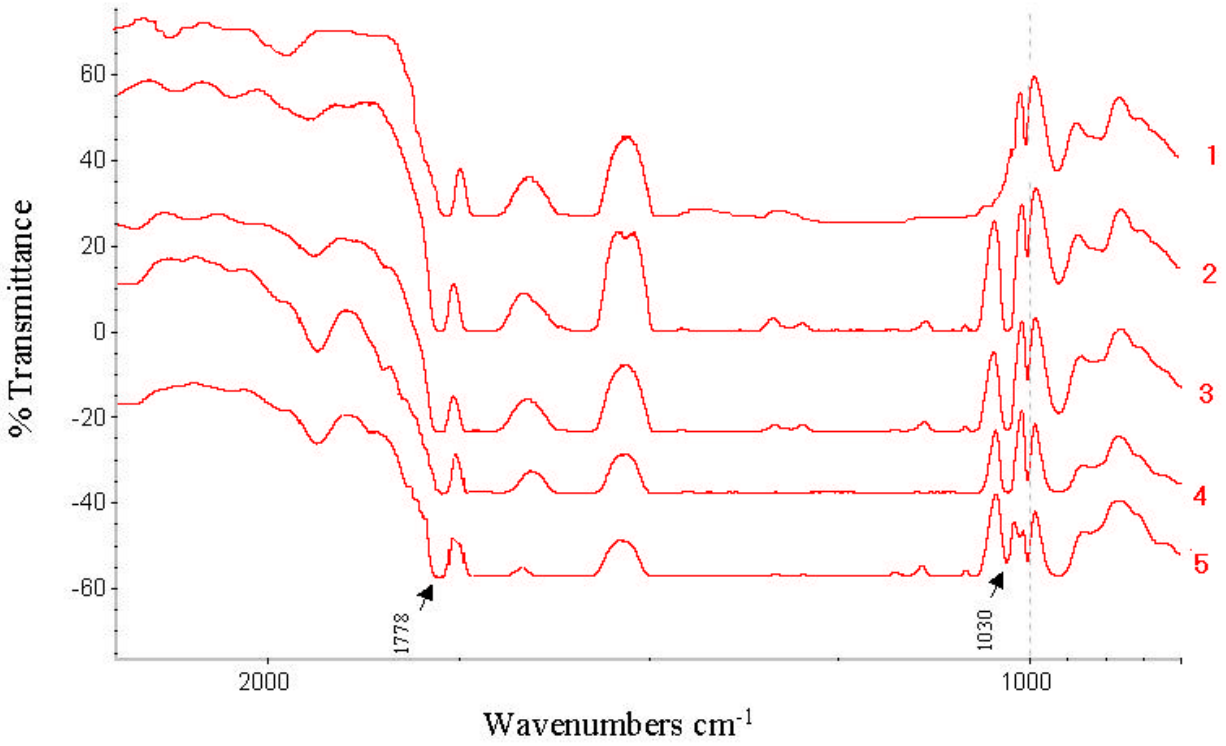

Figure 4.2.3.3 FTIR spectra showing the effect of level of sulfonation on relative peak intensities of BPDA/s-DADPS/APB polyimides (**1**) control (D.S.=0) (**2**) 60 % sulfonated (D.S.=0.6), (**3**) 40 % sulfonated (D.S.=0.4), (**4**) 25 % sulfonated (D.S.=0.25), (**5**) 10 % sulfonated (D.S.=0.6).

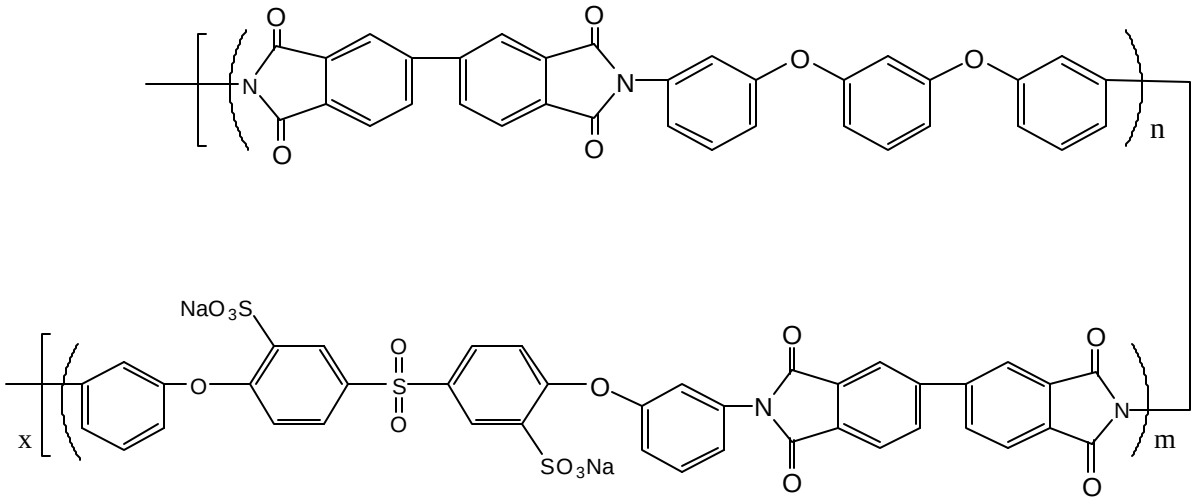

BPDA/s-DADPS/APB

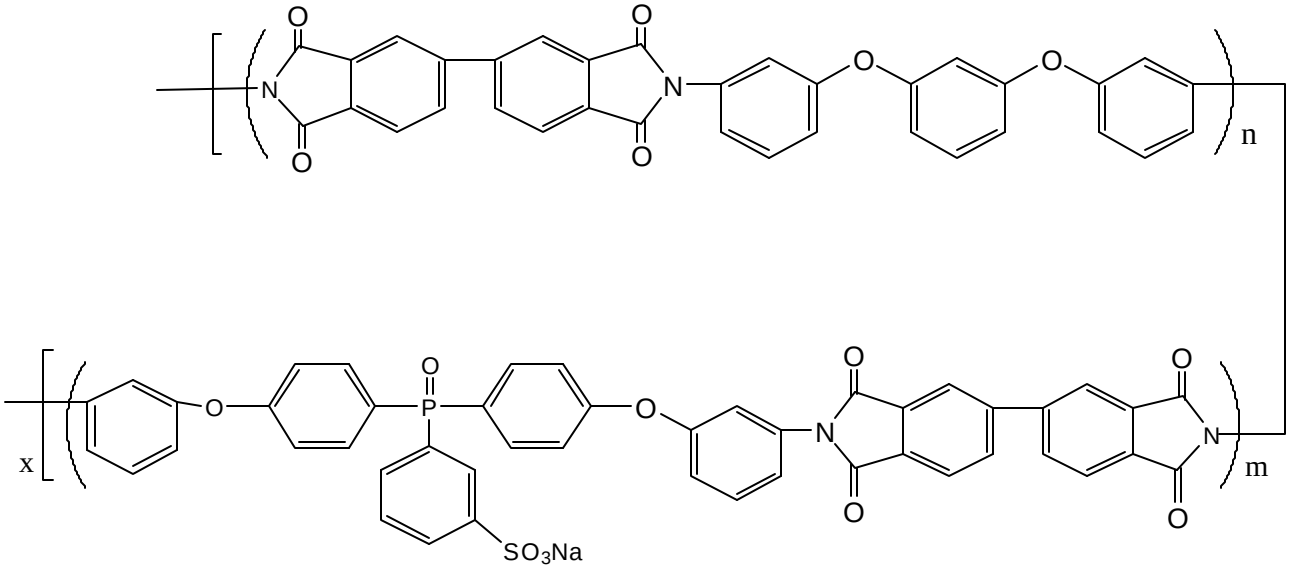

BPDA/s-DADPPO/APB

Figure 4.2.3.4 Repeat Units of Sulfonated PBDA/s-DADPS/APB and BPDA/s-DADPPO/APB Polyimides

mol% SO_3H (theory)	IEC(meq/g) (theory)	mol% SO_3H (FTIR)	IEC(meq /g) (FTIR)
0	0	0	0
10	0.341	10.8	0.368
25	0.784	23.4	0.7338
40	1.161	41.27	1.194
60	1.583	62.53	1.65
75	1.852	73.92	1.825
100	2.230	97.32	2.17

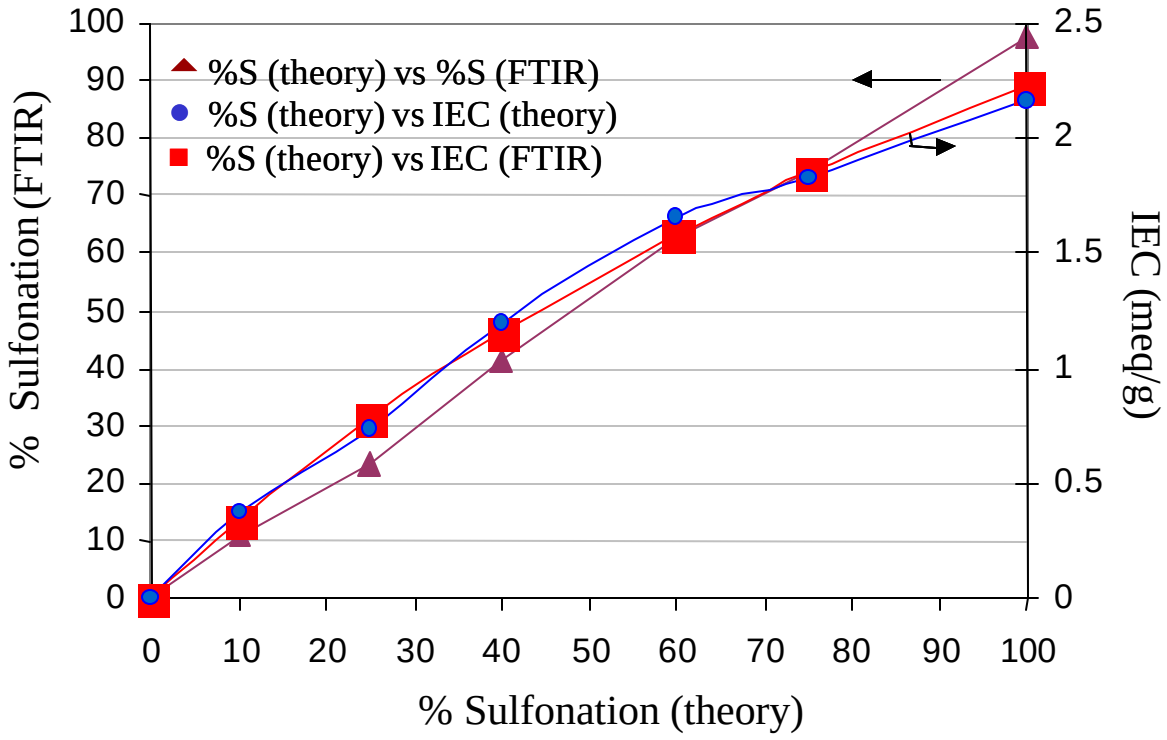

Figure 4.2.3.5 Plots of mol % Sulfonation (theory) vs mol % Sulfonation (FTIR) (▲); % Sulfonation (theory) vs IEC (theory) (●) and % Sulfonation (theory) vs IEC (FTIR) (■) for BPDA/s-DADPS/APB polymers

mol% SO_3H (theory)	IEC (meq/g) (theory)	mol% SO_3H (FTIR)	IEC (meq/g) (FTIR)
0	0	0	0
10	0.172	11.3	0.194
25	0.43	23.7	0.4076
40	0.688	41.1	0.707
60	1.032	59.5	1.023
75	1.29	77	1.324
100	1.72	98.3	1.69

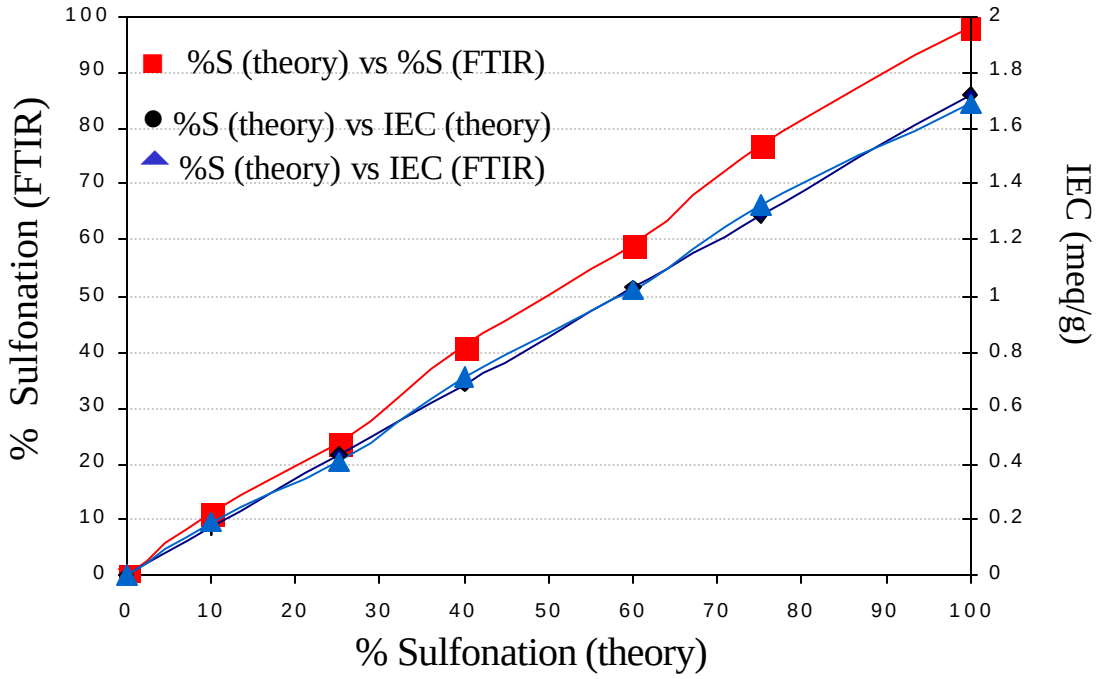

Figure 4.2.3.6 Plots of mol % Sulfonation (theory) vs mol % Sulfonation (FTIR) (■); % Sulfonation (theory) vs IEC (theory) (●) and % Sulfonation (theory) vs IEC (FTIR) (▲) for BPDA/s-DADPPO/APB polymers

Inherent viscosity values of the polyimide membranes were determined at 0.1 g/dL in NMP at 30 ^{o}C. These are presented along with their thermal analysis 5 % wt. Loss temperature (TGA) and glass transition temperature, T_g (DSC) in Table 4.2.3.1 and Table 4.2.3.2. The inherent viscosities increased with the increases of sulfonation, in other words, ionic character, in the polymers from 0.83 dL/g for unsulfonated polyimide to 4.3 dL/g for the sulfonated homopolymer BPDA/s-DADPS-100 and to 3.7 dL/g for the sulfonated homopolymer BPDA/s-DADPPO-100. This large increase of viscosity in these ionomers is probably not due to an increase of molecular weight of the polymers but due to an increase of intermolecular polymer chain aggregation with an increase of ionic character. Unlike the large triethylammonium hydrophobic counterion which does not favor the polymer aggregation in sulfonated polyimides as discussed in Section 4.2.2, the inherent viscosity behaviors of the sodium-sulfonate as well as the free acid form of the ionic polymers clearly suggest indicate the polymer aggregation due to electrostatic interactions between pendant ionic $-SO_3H$ groups. The large hydrophobic triethylammonium moieties used in the napthalenic polyimide solutions masked the ionic character of the polymer and avoided or minimized the effect of electrostatic interactions. Enhanced inherent viscosity with increased sulfonation has been noted in solutions of Na-sulfonate poly(arylene ether sulfone) [272] was observed in the literature. The ς_{inh} of the present sulfonated BPDA/s-DADPPO/ APB and BPDA/s-DADPPO/APB polymers are plotted against their corresponding IEC (meq/g) values in Figure 4.2.3.7

272. Feng Wang, Michael Hickner, Qing Ji, William Harrison, Jeffrey Mecham, Thomas A. Zawodzinski, and James E. McGrath, Synthesis of Highly Sulfonated Poly(arylene ether sulfone) Random (Statistical) Copolymers Via Direct Polymerization, *in publication*, **2001**.

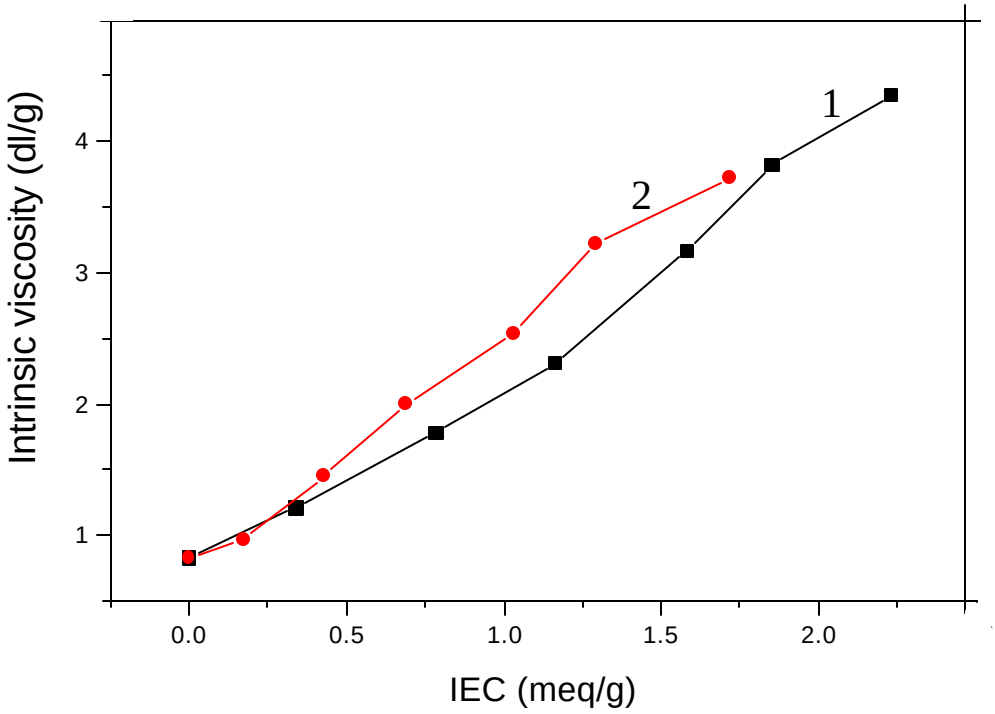

Figure 4.2.3.7 The effect of IEC (meq/g) on η_{inh} of (1) BPDA/s-DADPS/ APB and (2) BPDA/s-DADPPO/ APB polymers

The thermal stability of the polyimide membranes was studied using a Perkin-Elmer TGA-7 apparatus (in air, at a heating rate of 10 ^{o}C/min) and the glass transition temperature was measured in a Perkin-Elmer DSC-7 (in nitrogen, at a heating rate of 10 ^{o}C/min). All the sulfonated polymers are highly hygroscopic and readily absorb moisture.

It was particularly important that the sulfonated polyimide samples be completely dry. Otherwise, preliminary weight loss (at around 100 ^{o}C) in a TGA run of a sample would cause a significant error in determining the true degradation weight losses. Furthermore, the change in the heat capacity at T_g becomes very small as sulfonation is increased. Although most plasticized water would be lost below T_g, it was advisable to remove it prior to the DSC T_g scan. In order to eliminate an initial weight drop due to the loss of water or residual solvent, each film was dried in the TGA furnace by heating up to 180 ^{o}C at 5 ^{o}C/min prior to an actual TGA run.

Example thermogravimetric curves for the control-unsulfonated BPDA/APB polymer (a), and for a 40 % sulfonated BPDA/s-DADPS/APB polymer having 0.8 SO_3Na groups per repeat unit (b) is represented in Figure 4.2.3.8.

The derivative TGA curves (dTGA) (%/T) were calculated from the mass loss [% remaining mass at T_2 ($\%m_2$) - % remaining mass at T_1 ($\%m_1$)] and temperature (T_2-T_1). Example dTGA curves for unsulfonated and 40 % sulfonated BPDA/s-DADPS/APB are also plotted in Figure 4.2.3.8. The 5% weight loss in air was readily determined from the continuous curves.

Two weight loss steps were observed for sulfonated polyimides, which was reflected by two broad peaks in dTGA in two separate temperature ranges. As it can be clearly seen from the mass loss curves, the unsubstituted polymer has high thermal stability showing a 5 % weight loss temperature of ~ 541 ^{o}C due to decomposition of the polymer backbone. On the other hand, the initial weight loss of the 40% sulfonated polymer starts at around 270 ^{o}C and shows its 5 % weight loss at ~298 ^{o}C; this is believed to be due to the splitting off of the sulfonic acid groups. Similar observations were reported for s-polyetherether ketones[273], s-polysulfones[274], and s-poly(aryleneether)

273. Zaidi, S.M.J. et al., Journal of Membrane Science 173 (2000) 17-34.

274. O'Gara, J.F., Williams, D.J., Macnight, W.J., Karasz, F.E., J. Polym. Sci. B: Polym. Phys. 25 (1987) 1519.

sulfone[225,272]. The maximum wt. loss rate corresponding to the sulfonic acid decomposition, was found to be at ~ 326 ± 3 ^{o}C in the dTGA curves for all the sulfonated polymers.

In all of the TGA runs of the completely dry samples, the weight losses of the sulfonated polymers were larger than those of their control unsulfonated analogues at a given temperature. For all the BPDA/s-DADPS/APB and BPDA/s-DADPPO/APB polyimide films tested, there was a greater decomposition in the sulfonated derivatives than in the unsubstituted polymers. The weight loss onset temperature of the polymers showed no dependence on the degree of sulfonation and was observed to be at 270 ± 4 ^{o}C. This indicates that the polymer membranes are thermally stable up to 270 ^{o}C, and thus will be stable enough within the conceivable temperature range of polymer electrolyte fuel cell conditions.

The concentrations of sulfonate groups in the polymers were also evaluated by the mass loss measurements by thermogravimetric analysis. The initial dTGA peak area used to determine the percent of weight loss (Figure 4.2.3.8-b).

Theoretical weight losses (%) were calculated assuming that the splitting-off of a sulfonic acid groups releases one SO_3H molecule, using the formula below:

$$[(\text{Degree of Sulfonation, mol\%}) \times (MW_{SO3H})/ (MW_{\text{repeat unit}})] \times 100 \times 2^{a}.$$

Comparable experimental and theoretical values were obtained for both series of polymers. For example, the dTGA curve of the 40 % sulfonated BPDA/s-DADPS/APB polyimide (0.8 ionic groups per repeat unit) showed a mass loss of 6.43% as compared to the theoretical mass loss value of 5.69%. This result is a good indication of the thermal degradation loss of all the sulfonic acid groups in the first step at ~ 300 ^{o}C. Tables 4.2.3.3 and 4.2.3.4 summarize the calculated and observed (TGA) weight losses for the polyimides in the $-SO_3H$ decomposition temperature ragion. Figures 4.2.3.9 and 4.2.3.10 show the plots of mol percent of s-DADPS monomer versus weight loss by TGA due to sulfonic acid decomposition for BPDA/s-DADPS-based polyimide membranes.

a) Number "2" represents the two moles of SO_3H per repeat unit

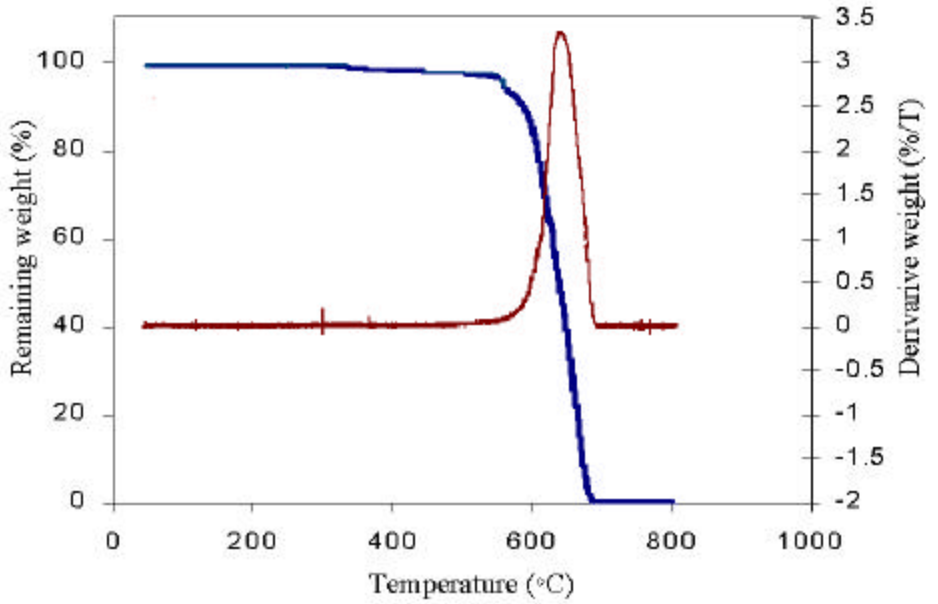

(a)

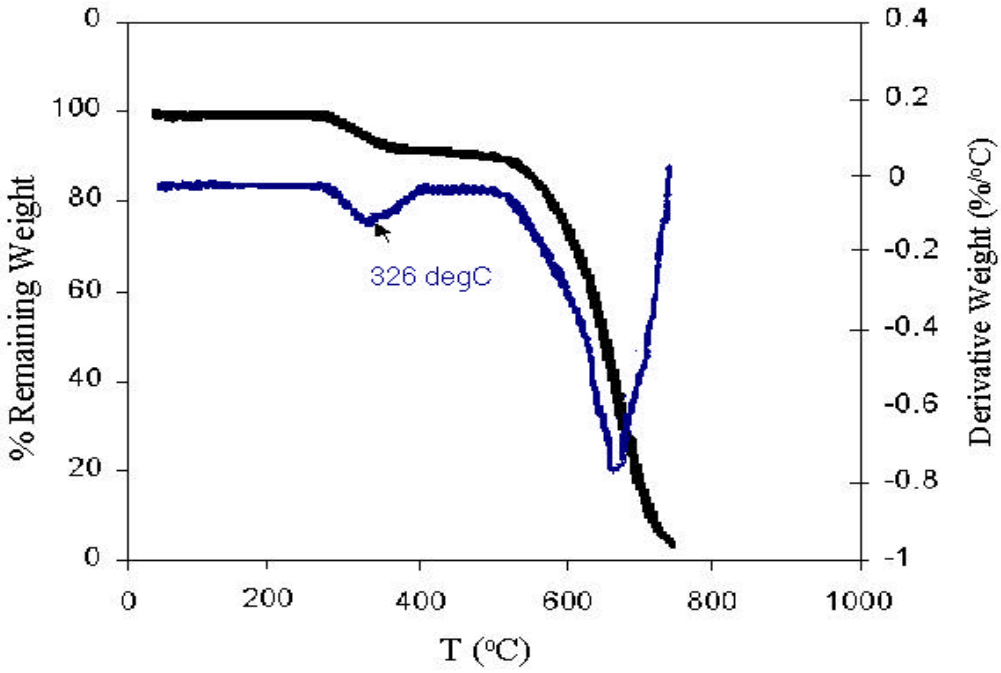

(b)

Figure 4.2.3.8 Thermogravimetric curves (TGA and dTGA) for (a) Control BPDA/APB polyimide (b) 40% sulfonated BPDA/s-DADPS/APB polyimide

Table 4.2.3.1 Inherent Viscosity and Thermal Analysis of BPDA/s-DADPS/APB-Based Sulfonated Polyimides

Polymer	Sulfonated diamine (mol %)	m/n	ζ_{inh}[a] dL/g)	5% weight loss in air[b] (^oC)	T_g[c] (^oC)
BPDA/s-DADPS-00	0	0/10	0.83	541	201
BPDA/s-DADPS-10	10	1/10	1.21	319	212
BPDA/s-DADPS-25	25	2.5/7.5	1.78	310	226
BPDA/s-DADPS-40	40	4/6	2.31	298	242
BPDA/s-DADPS-60	50	6/4	3.17	287	n/o
BPDA/s-DADPS-75	60	7.5/2.5	3.82	272	n/o
BPDA/s-DADPS-100	100	10/0	4.35	260	n/o

(a) NMP, at 0.1 g/dL cont. in NMP 30 ^oC (b) 10 ^oC/min in air
(c) 10 ^oC/min in nitrogen (n/o) not observed

Table 4.2.3.2 Inherent Viscosity and Thermal Analysis of BPDA/s-DADPS/APB-Based Sulfonated Polyimides

Polymer	Sulfonated diamine (mol %)	m/n	ζ_{inh}[a] dL/g)	5% weight loss in air[b] (^oC)	T_g[c] (^oC)
BPDA/s-DADPPO-00	0	0/10	0.83	541	201
BPDA/s-DADPPO-10	10	1/10	0.97	317	208
BPDA/s-DADPPO-25	25	2.5/7.5	1.45	320	222
BPDA/s-DADPPO-40	40	4/6	2.00	296	224
BPDA/s-DADPPO-60	60	6/4	2.54	283	238
BPDA/s-DADPPO-75	75	7.5/2.5	3.22	270	n/o
BPDA/s-DADPPO-100	75	10/0	3.72	257	n/o

(a) NMP, at 0.1 g/dL cont. in NMP 30 ^oC (b) 10 ^oC/min in air
(c) 10 ^oC/min in nitrogen (n/o) not observed

Table 4.2.3.3 Calculated and observed (TGA; 10 ^{o}C/min in air) weight losses for BPDA/s-DADPS/APB Polyimides in the $-SO_3H$ decomposition region.

Polymer	**s-DADPS (mol %)**	**Weight loss (theory) wt %**	**Weight loss *by* TGA, wt%**
BPDA/s-DADPS-00	-0-	-0-	-0-
BPDA/s-DADPS-10	10	1.44	2.73
BPDA/s-DADPS-25	25	3.56	4.21
BPDA/s-DADPS-40	40	5.69	6.43
BPDA/s-DADPS-60	60	8.54	10.37
BPDA/s-DADPS-75	75	10.67	12.66
BPDA/s-DADPS-100	100	14.22	15.78

Table 4.2.3.4 Calculated and observed (TGA; 10 ^{o}C/min in air) weight losses for BPDA/s-DADPPO/APB Polyimides in the $-SO_3H$ decomposition region.

Polymer	**s-DADPS (mol %)**	**Weight loss (theory) wt %**	**Weight loss *by* TGA, wt%**
BPDA/s-DADPPO-00	0	-0-	-0-
BPDA/s-DADPPO-10	10	0.74	2.13
BPDA/s-DADPPO-25	25	1.83	2.66
BPDA/s-DADPPO-40	40	2.93	3.20
BPDA/s-DADPPO-60	60	4.41	5.57
BPDA/s-DADPPO-75	75	5.51	7.05
BPDA/s-DADPPO-100	100	7.34	8.75

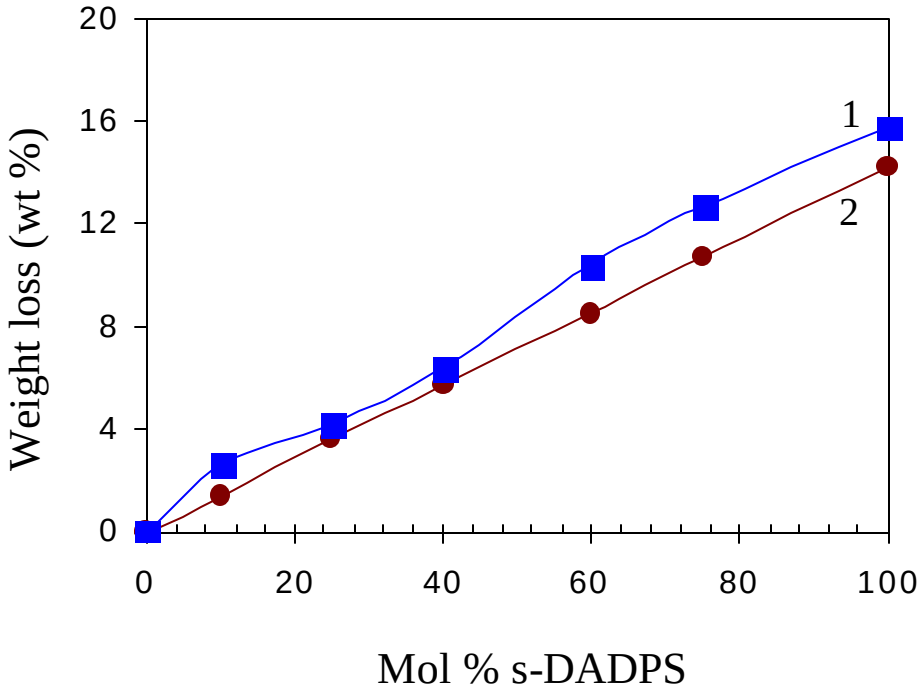

Figure 4.2.3.9 Weight loss by due to sulfonic acid group decomposition for BPDA/s-DADPS/APB Polyimides (TGA in air, 10 ^{o}C/min)

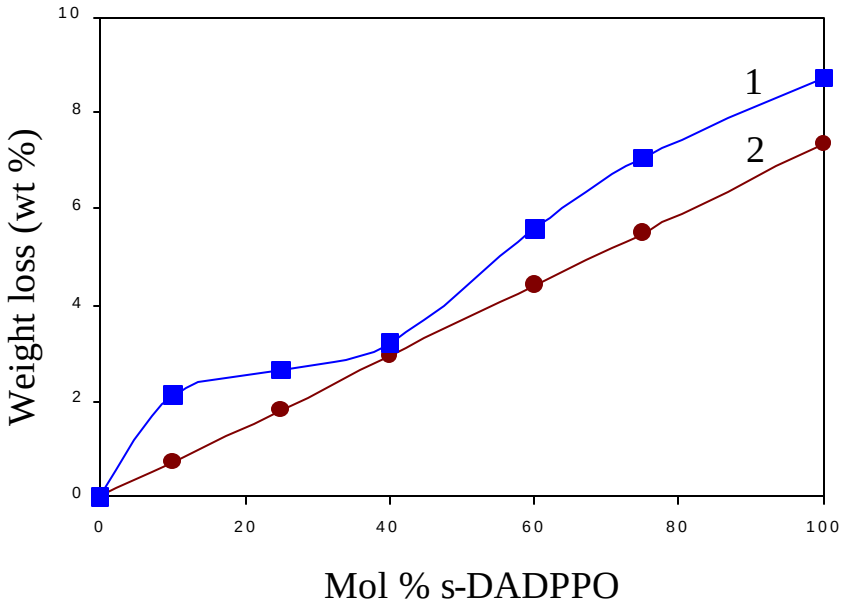

Figure 4.2.3.10 Weight loss due to sulfonic acid decomposition for BPDA/s-DADPPO/APB Polyimides (TGA in air, 10 ^{o}C/min)

Softening temperatures of the polymers were also tested using a Perkin-Elmer DSC under nitrogen atmosphere (Figure 4.2.3.11). The glass-transition temperature (T_g) was calculated at the intersection of the tangents to the corresponding DSC curve. Homopolymer of BPDA/APB and 10 % sulfonated BPDA/s-DADPS polyimide chain mobility were weak showing small changes in the heat capacity at T_g. The obvious result from the DSC measurements is that the glass transition temperature of the sulfonated polymers shifted to higher values from 201 ^oC for control unsubstituted BPDA/APB to 242 ^oC for 40% sulfonated BPDA/s-DADPS/APB polymer and 238 ^oC for 60 % sulfonated BPDA/s-DADPPO/APB polyimide. The plots of the sulfonation level (based on mol % of the sulfonated diamine monomers) versus the observed glass transition temperatures gave a linear relationship for both of the polymer series (Figure 4.2.3.12). No T_g was observed by DSC for the higher level of sulfonated polymers.

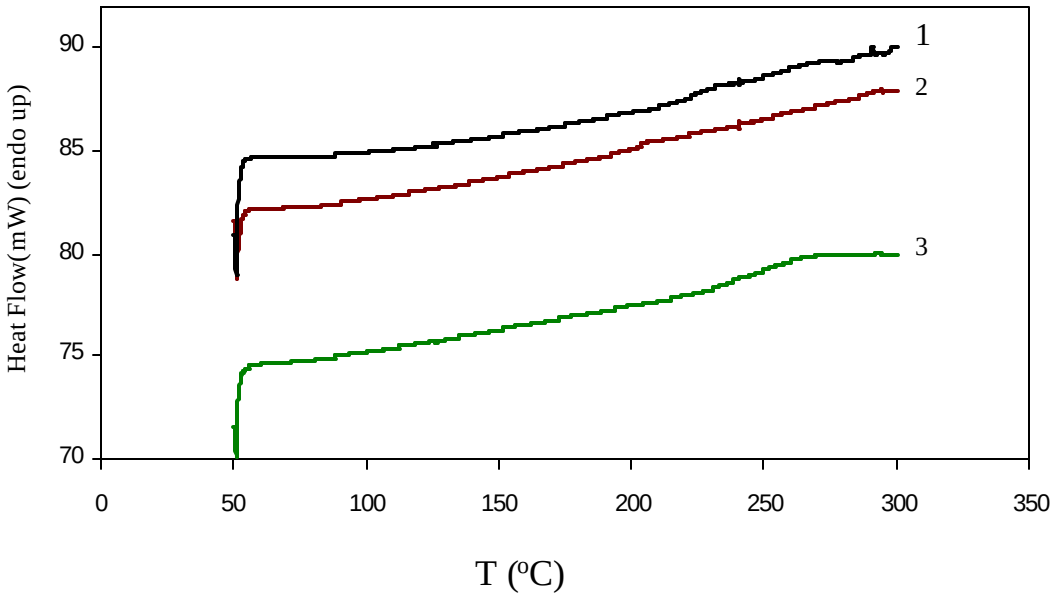

Figure 4.2.3.11 DSC of BPDA/s-DADPS/APB polyimides,
1) D.S= 25%
2) D.S= 0 %
3) D.S= 40%

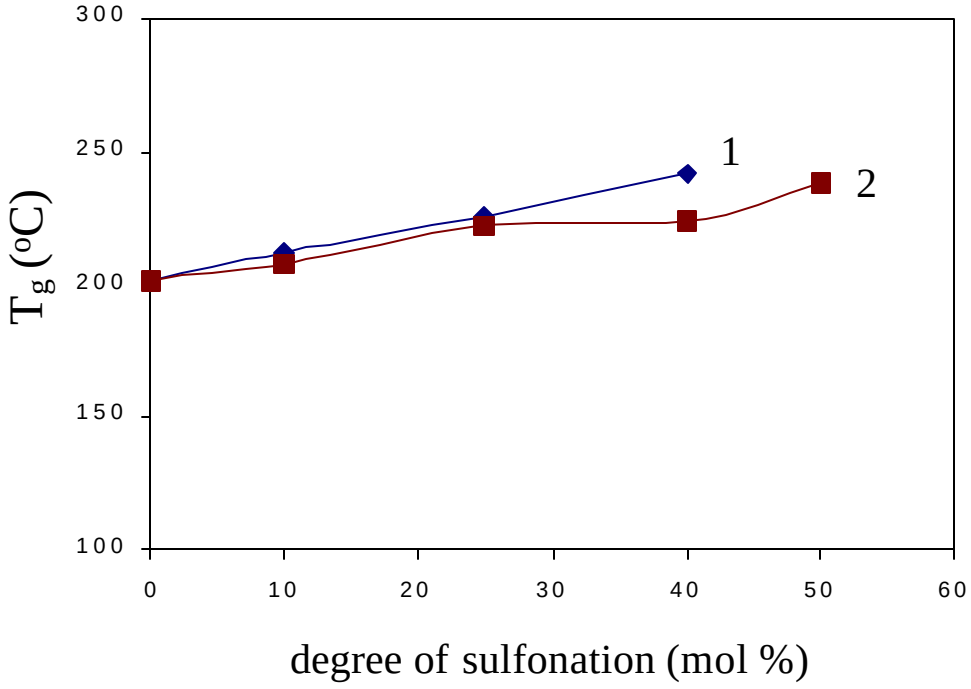

Figure 4.2.3.12 Effect of Sulfonation on Glass Transition Temperature [Tg (^{o}C)] for
1) BPDA/s-DADPS/APB
2) BPDA/s-DADPPO/APB

Water Uptake and Conductivity

The principal purpose of synthesizing sulfonated aromatic polyimides is to provide novel hydrophilic membranes that will conduct proton ions in fuel cells. The main purpose of incorporation of ionic sulfonic acid groups is to enhance the acidity and hydrophilicty of the polymer. As discussed in the literature review of this dissertation, the amount of absorbed water increases with increases in sulfonation of the polyimide, facilitates proton transfer, and thereby increases the conductivity of an electrolyte membrane.

In this research, the enhancement of hydrophilicity by incorporating sulfonated monomer into the backbone was followed by water absorption of the polyimides as a function of the degree of sulfonation or ion exchange capacity. For that purpose, ~ 1 gr samples of polymer films were freshly dried at 110 ^{o}C under vacuum for 24 hours and then immersed in D.I. water at room temperature until no more weight change was observed (24 hours). The wet films were blotted dry with tissue paper and weighed immediately. The weight gain of absorbed water was first calculated as the percent increase in the dry membrane weight and then converted to units of water molecules absorbed per sulfonic acid site [$\lambda = n($(H_2O molecules)/SO_3H]. The conductivity of fully hydrated membranes were obtained at room temperature via impedance measurements.

Table 4.2.3.5 summarizes the water absorption and conductivity data for the BPDA/s-DADPS/APB polyimide membrane films. The fully hydrated BPDA/s-DADPS-25 film was very though and easy to work with. Manipulation of the fully hydrated BPDA/s-DADPS-10 and BPDA/s-DADPS-25 films without the breakage was possible. However, the fully hydrated BPDA/s-DADPS-60 and BPDA/s-DADPS-75 films were very brittle and attempts to assemble them in the conductivity cell were unsuccessful.

The water uptakes observed at room temperature for the sulfonated BPDA/s-DADPS/APB polyimides varied from ~6 to 55 % for IEC values varying from 0.341 to 1.85 meq g^{-1}. The water uptake of BPDA/s-DADPPO/APB polyimide membranes varied from 4.2 % (w/w) for 10 % sulfonated polymer (0.172 meq/g) to 43.6 % (w/w) for 75 % sulfonated polymer (IEC= 1.29 meq/g). Although the incorporation of monosulfonated diamine monomer into the polymer backbone resulted in lower water uptakes, the number of water molecules per ionic site (SO_3^-) gave similar results as compared to the

BPDA/s-DADPS-based polyimides bearing two sulfonic acid groups per repeat unit. Interestingly, although λ stays almost constant, the conductivity increases with the increase of ionic character of the polymer (Figure 4.2.3.13).

Table 4.2.3.5 Water Uptake and Ion Exchange Capacity Values of Sulfonated BPDA/s-DADPS/APB Polyimide Membranes

Polymer	**s-DADPS (mol %)**	**IEC (meq/g) (theory)**	**Water Uptake[a] (%w/w)**	**Ë[b] (H_2O mol. /SO_3H)**	**Conductivity[c] x 10^{-2} (S/cm)**
BPDA/s-DADPS-00	-0-	-0-	d	d	-
BPDA/s-DADPS-10	10	0.341	6.2	12.12	0.4
BPDA/s-DADPS-25	25	0.784	15.9	13.52	0.7
BPDA/s-DADPS-40	40	1.161	28.5	16.36	1.5
BPDA/s-DADPS-60	60	1.583	37.7	15.87	–
BPDA/s-DADPS-75	75	1.852	55.5	16.59	–
BPDA/s-DADPS-100	100	2.230	W.S	W.S	W.S

(a) 25 °C, from wet weight and dry weight data.
(b) Calculated from water uptake and mol % s-DADPS
(c) Conductivity measurements at 25 °C.
(d) Couldn't cast the film due to the insolubility and gelation of the polymer in DMAc

Table 4.2.3.6 Water Uptake and Ion Exchange Capacity Values of Sulfonated BPDA/s-DADPPO/APB Polyimide Membranes

Polymer	s-DADPPO (mol %)	IEC (meq/g) (theory)	Water Uptake[a] (%w/w)	ë[b] (H_2O mol. /SO_3^-)	Conductivity[c] x 10^{-2} (S/cm)
BPDA/s-DADPPO-00	-0-	-0-	d	d	d
BPDA/s-DADPPO-10	10	0.17	4.2	10.2	0.27
BPDA/s-DADPPO-25	25	0.43	10.3	12.45	0.45
BPDA/s-DADPPO-40	40	0.69	20.7	13.36	0.92
BPDA/s-DADPPO-60	60	1.03	31.2	12.87	–
BPDA/s-DADPPO-75	75	1.29	43.6	13.65	–
BPDA/s-DADPPO-100	100	1.72	W.S	W.S	W.S

(a) 25 ^oC, from wet weight and dry weight data.
(b) Calculated from water uptake and mol % s-DADPS
(c) Conductivity measurements at 25 ^oC.
(d) Couldn't cast the film due to the insolubility and gelation of the polymer in DMAc

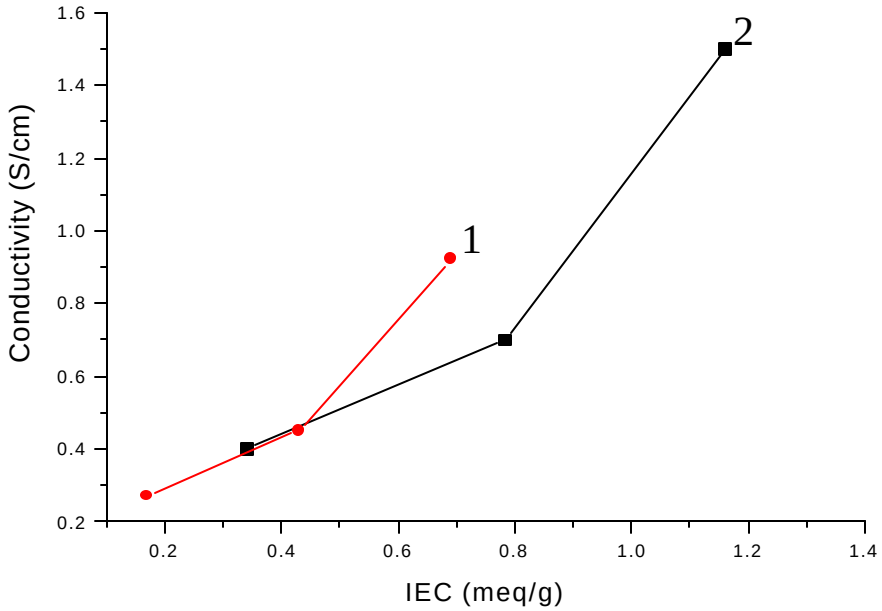

Figure 4.2.3.13 Effect of IEC (meq/g) on conductivity (S/cm) for

1- BPDA/s-DADPPO/APB polyimide membranes
2- BPDA/s-DADPS/APB polyimide membranes

CHAPTER 5. CONCLUSIONS

The primary objectives of this research were to synthesize a series of pendant sulfonic acid group bearing wholly aromatic five- and six-membered ring polyimides, characterize them as polymer electrolyte proton exchange membranes by investigating their film forming characteristics, thermal and hydrolytical stability, ion-exchange capacity, water uptake and conductivity. Particular emphasis was given to tailoring the physical properties by systematic variations of monomer structure and degree of sulfonation based on mole percent of sulfonated diamine, to meet the requirements for proton-exchange membranes in fuel cells.

The ester-acid high temperature solution imidization method was utilized for the phthalic anhydride based polyimides, while the one-step direct imidization method was employed for the napthalic-based polyimides. In all cases, an equimolar ratio of diamines and dianhydride were used to obtain high molecular weight polyimides with controlled degree of sulfonation. Although the sulfonated five membered polymers are soluble in polar aprotic solvents such as NMP, DMSO and DMAc, the six-membered sulfonated polyimides could only be prepared using strong acids or phenolic solvents such as m-cresol due to the rigidity of the polymer backbone. Solubility of polymers was enhanced with an incorporation of a sulfonated diamine monomer.

In general, the unsubstituted control polyimides produced very tough, bendable yellowish-light brown color films upon drying. Incorporation of a low level of sulfonated diamine monomer (up to 40 %) produced similar film characteristics when cast from ~20 % polymer solution in DMAc for phthalic polyimides and from ~5 % polymer solutions in m-cresol for naphthalic polyimides using a doctor blade. However, as the degree of sulfonation increased up to 60 %, although the films were not cracked during the drying process, they were less creasable and relatively more brittle than their lower level of sulfonation counterparts. The polyimide membranes having more than 60 % sulfonated diamine in their backbone showed brittle film characteristics. When attempts were made to fold these films to test for creasability, they cracked very easily. An increase in the level of sulfonation also caused an increase in the brown coloration in the dry films. Similar observations were also made by Jin *et al.* for s-PEEK polymers[257].

Incorporation of controlled degree of pendant sulfonic group(s) bearing monomer into the polymer backbone improved the ionic character, hydrophilicity of the polymer, resulting in an increase of water absorption, which is critical for proton conductivity in fuel cells. The hydrolytic stability of the polyimides generally decreased with degree of sulfonation. The six-membered ring systems showed good hydrolytic stability up to 60 % sulfonation level, which is superior as compared to the sulfonated five-membered systems. Pendant sulfonic acid groups being directly on the polymer chain increased susceptibility to degradation by decyclizing the imide structure and resulting in lowering the molecular weight and embrittlement in polymer membrane. Development of the sulfonated six-membered ring systems with an improved solubility that has been initiated in this dissertation remains a worthwhile future research.

Two main weight loss steps were observed in the TGA thermograms for all the sulfonated block copolymers. The first weight loss between 300-400 ^{o}C was due to the decomposition of sulfonic acid groups, and the second weight loss was due to the degradation of polymer chain around 500 ^{o}C. The thermal degradation and stability tests of the solution-cast membranes indicated that introduction of SO_3H groups into polyimide structure significantly decreased the thermal stability due to the desulfonation at around 300 ^{o}C in the ionic block. Although 5% weight loss temperature decreased with sulfonation content, the onset of first weight loss step, in general, was independent of sulfonic acid content and way above the thermal stability requirement of membranes in fuel cells. At the same time, T_g also increased with ionic character reflecting an increased intermolecular association through polar ionic sites. TGA thermograms were successfully used to determine degree of sulfonation in polymers and closely matched with the theory, based on mol percent of sulfonated diamine content in polymer.

Non-aqueous potentiometric titrations were also employed for five-membered systems to calculate degree of sulfonation. Solvent solubility and potentiometric acid-base titrations of air-oven aged films confirmed the thermal stability of sulfonic acid groups up to 220 ^{o}C indicating no degradation nor branching or crosslinking occurring.

Sulfonated statistical copolymers prepared in this research were different compared to Nafion, perfluorinated ionomer, in their swelling behavior, swollen

morphology and conductivity. For example, in contrast the Nafion, the water uptake of sulfonated polyimides did not increase with temperature.

The NDA-based sulfonated polymer series, the percent of water uptake increasesd as the ionic character (the number of pendant $-SO_3H$ sites) increased in a given polymer structure. On the other hand, the total number of water molecules absorbed per ionic group (ë) remained almost constant (10.5 ± 3 H_2O molecules/SO_3^- group). This result suggests that the absorbed water is mainly located in the hydrophilic domains[265]. An almost constant ë value for a given polymer structure also indicates the saturation of ionic domains with 10-14 water molecules. Similar ë values for sulfonated five-and six-membered polyimides were founf in the literature.

On the other hand, in Nafion, as IEC increases, the ë value increases significantly, and for critical IEC, the ë value diverges due to membrane dissolution. In the case of sulfonated polyimides, the fact that ë values are constant is surprising and could be explained by a specific morphology of membranes related to their preparation. It was explained in the literature[265] that the solvent used for preparing the solution-cast films, and the drying temperature of films, which remains lower than the T_g of these polymers are important parameters for the polymer morphology.

Similar ë values between different polymer structures do not indicate significant differences. Moreover, these values obtained in this part for NDA-based polyimides are very close to the ë numbers obtained for sulfonated phthalic polyimides, e.g. BPSDA-based polyimides in Section 4.2.1.2 (ë = ~11values).

Although having large values of IEC, the conductivity values of sulfonated polyimides are rather low compared to typical proton exchange membranes (0.12 S/cm for IEC=0.91 meq/g) and bisphenol based polyarylene ethers (0.11 S/cm for IEC=1.5 meq/g polymer and 0.17 S/cm for IEC=2.2 meq/g polymer). For example, the 40 % sulfonated polyimide NDA/FDA-40 with an IEC= 1.38 meq g^{-1} has a conductivity of 0.06 S/cm at 25 ^oC.

AFM results of polyimide membranes did not indicated the presence of separate hydrophilic and hydrophobic domains in dry state. The less effective separation of the aqueous phase compared to Nafion may be due to the immobilized or poorer associatation of anionic counter ions ($-SO_3^-$). Small water molecules, however, on the

sulfonis acid sites were detected for water-swollen membranes. Finally, the room temperature proton conductivity in sulfonated polyimide aromatic membranes were about a magnitude lower than that of Nafion.

VITA

Nazan Gunduz, daughter of Huriye Kaptan and Kenan Kaptan, was born on January 1, 1971 in Izmir, Turkey. She graduated from Suphi Koyuncuoglu High School in July of 1988, and began her undergraduate studies at Ege University as Chemistry major, receiving her B.S. degree in July of 1992. On May 19th, 1994, she married Irfan Gunduz in Izmir. On May 19th, 1997, she gave a birth to her precious daughter, Erin Ilge Gunduz.

In September of 1993, she was accepted as a graduate teaching/research assistant at Akdeniz University, Antalya, in the Department of Chemistry where she developed an interest in polymer science during her a short period of time stay there. In February of 1994, Nazan took a nationwide exam to continue her graduate studies overseas. As a result of her success, she received a scholarship from the Ministry of Education of Turkey and came to the United States.

In the fall of 1995, Nazan began her graduate studies in the Department of Chemistry at Virginia Polytechnic Institute and State University under the supervision of Professor James E. McGrath. Her M.S. research focused on the synthesis and photopolymerization of novel dimethacrylates on which, she received the Best Master Thesis award from Virginia Tech. After receiving her Master of Science degree in June of 1998, she was accepted at the same university in order to work towards her goal of obtaining a Ph.D. Her graduate research efforts at Virginia Tech under the guidance of Dr. James E. McGrath focused primarily on the design and synthesis and characterization of novel polyimide membranes with controlled degree of sulfonation for proton exchange membranes in fuel cells.

She has accepted a advanced product technologist position in the High Performance Polymers Unit at the General Electric Company, GE Plastic, in Mt. Vernon, Indiana.